

**INSIGHTS INTO THE DESIGN AND SYNTHESIS OF
ARTIFICIAL ENZYMES**

A Thesis Presented by

Matilda Jane Bingham

In Partial Fulfilment of the Requirements
for the Award of the Degree of

DOCTOR OF PHILOSOPHY

OF THE

UNIVERSITY OF LONDON

Christopher Ingold Laboratories
Department of Chemistry
University College London
London WC1H OAJ

December 1999

ProQuest Number: 10630747

All rights reserved

INFORMATION TO ALL USERS

The quality of this reproduction is dependent upon the quality of the copy submitted.

In the unlikely event that the author did not send a complete manuscript and there are missing pages, these will be noted. Also, if material had to be removed, a note will indicate the deletion.



ProQuest 10630747

Published by ProQuest LLC (2017). Copyright of the Dissertation is held by the Author.

All rights reserved.

This work is protected against unauthorized copying under Title 17, United States Code
Microform Edition © ProQuest LLC.

ProQuest LLC.
789 East Eisenhower Parkway
P.O. Box 1346
Ann Arbor, MI 48106 – 1346

ABSTRACT

This thesis is divided into three parts.

The first part is an introduction to the design and synthesis of artificial enzymes and details some of the more recent developments in this area, with an emphasis on emerging 'selection approaches' to artificial enzymes. The introduction concludes with a short review on the synthesis of artificial receptors using dynamic combinatorial libraries (DCLs), and discusses the relevance of such a strategy in the design and synthesis of artificial enzymes.

The second part is a discussion of our investigations into the design and synthesis of an artificial enzyme which is able to induce selectivity in the acid catalysed ring opening reaction of α -pinene oxide to afford *trans*-carveol as the major product. The research is based on the molecular imprinting approach to artificial enzymes and begins with the synthesis of polystyrene-divinylbenzene molecularly imprinted polymers (MIPs), using the crude transition state analogue (1*R*, 5*R*)-*trans*-carvyl amine as the imprint molecule. Binding studies confirmed the successful imprinting of a range of MIPs with various crosslinker to monomer ratios and loadings. The influence of the MIPs on the product distribution of the ring opening reaction of α -pinene oxide was investigated.

The development and synthesis of a second generation transition state analogue (TSA), *N*-methyl isonipecotic acid *N*-oxide is then described. The TSA was used in molecular modelling studies to select three tri-peptide 'functional monomers' which established favourable binding interactions with the ligand TSA. The peptides were synthesised and pulsed field gradient NMR experiments were used to study the change in the observed rate of translational diffusion on complex formation between the TSA and the three tri-peptides.

Research into the development of polyacrylamides as MIPs is then presented. Binding studies were carried out to establish the effectiveness of imprinting of a range of polyacrylamide MIPs.

Part three is an account of the experimental work and procedures used throughout this work.

CONTENTS

	Page
Abstract	1
Contents	2
Acknowledgements	6
Abbreviations	7
Part 1. Introduction	
Chapter 1. Progress in the design and synthesis of artificial enzymes	9
1.0 Transition state theory	10
1.1 The design approach	15
1.1.0 Cyclodextrins as enzyme mimics	16
1.1.1 Cyclophane enzyme mimics	19
1.1.2 Reversibly self-assembled dimers	21
1.2 The transition state analogue (TSA)-selection approach	23
1.2.0 Catalytic antibodies	24
1.2.1 Molecularly imprinted polymers	30
1.2.2 Imprinting an artificial proteinase	36
1.2.3 Bioimprinting	37
1.3 Catalytic activity-selection approaches	38
1.3.0 Combinatorial polymers as enzyme mimics	39
1.3.1 Combinatorially developed peptide catalysts	41
1.3.2 <i>In vitro</i> evolution	42
1.3.3 Screening methods for the identification of catalysts in combinatorial mixtures	44
1.4 Dynamic Combinatorial Libraries	45
1.5 Conclusions	50

Part 2. Results and Discussion

Chapter 1. Insights into the design and synthesis of artificial enzymes	53
Chapter 2. Polystyrene divinylbenzene MIPs	54
2.0 Choice of the polymer system and the imprint molecule	54
2.1 Synthesis of the imprint molecule	56
2.2 Synthesis of the polymers	57
2.3 Polymer regeneration	61
2.4 Binding studies	62
2.5 Synthesis of the reference polymer	73
2.6 Competitive binding studies	75
Chapter 3. Reactions of the imprinted polymers with α -pinene oxide	80
3.0 Model studies with <i>p</i> -tolenesulfonic acid	80
3.1 Reactions of the MIPs with α -pinene oxide in toluene	81
3.2 Reactions of the MIPs with α -pinene oxide in methanol	83
3.3 Reactions of the MIPs with α -pinene oxide in DMF	85
3.4 Inhibition studies	87
3.5 Conclusions	88
Chapter 4. Transition state analogue development	93
Chapter 5. Molecular modelling	98
Chapter 6. Synthesis of TSA and tri-peptides	107
6.0 Synthesis of imprint molecule	107
6.1 Synthesis of tri-peptides	108
Chapter 7. NMR studies	110
7.0 Diffusion edited NMR	110
7.1 Diffusion measurements	116
Chapter 8. Polyacrylamide molecularly imprinted polymers	125
8.0 TSA selection and synthesis	125
8.1 Synthesis and selection of the functional monomer, crosslinker and monomer	126
8.2 Studies on a model catalytic system	127

8.3 The pre-organised complex	128
8.4 Synthesis of polyacrylamide MIPs	130
8.5 Polymer regeneration and binding studies	131
8.6 Reactions of the polyacrylamide MIPs	133
8.7 Conclusions	133
Chapter 9. Conclusions and perspectives for future research	135

Part 3. Experimental

Chapter 1. General experimental	139
Chapter 2. Synthesis and analysis of polystyrene-divinylbenzene MIPs	141
2.1 Synthesis of the imprint molecule	141
2.2 Synthesis of the polystyrene-divinylbenzene MIPs	145
2.3 Binding studies of the polystyrene-divinylbenzene MIPs	148
2.4 Synthesis of the blank polystyrene	160
Chapter 3. Reactions of the polystyrene-divinylbenzene polymers	165
3.1 Solution reactions of <i>p</i> -toluenesulfonic acid with α -pinene oxide	165
3.2 Reactions of the polystyrene-divinylbenzene MIPs with α -pinene oxide	172
Chapter 4. Molecular modelling	178
Chapter 5. Synthesis of the transition state analogue	179
Chapter 6. Synthesis of the tri-peptides	182
Chapter 7. Synthesis and analysis of the polyacrylamide MIPs	192
7.1 Synthesis of the imprint molecule	192
7.2 Synthesis of the cross-linkers and monomers	194
7.3 Synthesis of the polyacrylamide MIPs	196
7.4 Binding studies on the polyacrylamide MIPs	200
Chapter 8. Reactions of the polyacrylamide polymers	207
8.1 Solution reactions of <i>N</i> -(2-methyl)-propanoyl glycine with α -pinene oxide.	207

8.2 Reactions of polyacrylamide MIP [G]	208
Chapter 9. NMR studies	210
9.1 Diffusion edited NMR: The test system	210
9.2 Diffusion measurements at pD 5	210
9.3 Diffusion measurements at pD 7	211
Appendix 1 Competitive binding study data	213
Appendix 2 Molecular modelling libraries	216
Appendix 3 NMR diffusion experiments: pulse program	221
References	223

ACKNOWLEDGEMENTS

I would like to thank my supervisor Prof. Willie Motherwell, for his inspiration, enthusiasm and encouragement over the last three years.

I thank my two proof readers Catherine and Mike for all their diligence in the face of my terrible typing and for their useful advice. My PhD has encompassed a range of subjects, which would not have been possible without the help of many experienced collaborators: I would like to thank Dr Stephen Garland and Dr Mike Tennant at SB for all their help with the molecular modelling, Dr John Darker for his advice on peptide synthesis, Dr Yvan Six for his help with the polymer binding studies and Dr Abil Aliev, for his enthusiasm in getting the NMR diffusion measurements running in house. I also thank the technical staff at UCL for all their help; Jill Maxwell and Jorge for NMR, Mike Cocksedge for mass spectra and Alan Stores for microanalysis. Last, but not least I would like to thank my sponsors Quest without whom none of this would have been possible

As to all those in the lab. There are so many I would like to thank. My special thanks goes to Catherine, my fellow imprinter for all her friendship advice and encouragement and in the face of polymers. I would also like to thank all the post docs in the lab for their advice over the years especially Pierre and Santi who have always had the time to answer questions. Similarly thanks goes to Robyn who seems to spend most of the day doing things for other people for which I'm very grateful. For making the lab a friendly place I'd also like to thank Matt, Marta, Ray, Mike, Rosa, Lynda, Oliver, Yvan, Martin, and all the others too numerous to mention.

There is a life outside the lab and I'd like to thank all those people who have shared weekends in the sun, and in the rain, in south London. Special thanks to Clare and Lucy, I'll be sad to leave you both, and to all the Bob crowd: the band of course, Chris, Steve, Milli and Dave, James and everyone else who I can't possibly name here. I hope to keep in touch with you all for a long time even if many of you do all disappear off to Australia. I'd also like to thank Mike, who has become an important part of my life these last few months, for his love and support whilst writing this thesis.

Finally, I'd like to thank my family, Mum, Dad, Celia and Chloe, for their love and their endless support. I would like to dedicate this thesis to them.

ABBREVIATIONS

Ac	acetyl
ACD	available chemicals directory
Aib	α -aminoisobutyric acid
AIBN	azo bis-isobutyronitrile
Ala	alanine
aq	aqueous
Ar	aryl
Arg	arginine
b	broad
Boc	tertiary butoxycarbonyl
<i>t</i> -Bu	tertiary butyl
CI	chemical ionisation
CBz	benzoyloxycarbonyl
conc	concentrated
d	doublet
dd	double doublet
DCL	dynamic combinatorial library
DCM	dichloromethane
DEPT	distortionless enhancement by polarisation transfer
DIAD	diisopropyl azodicarboxylate
DIC	<i>N,N'</i> -diisopropylcarbodiimide
DMF	dimethyl formamide
DMSO	dimethyl sulfoxide
ee	enantiomeric excess
EI	electron impact
equiv	molar equivalents
Et	ethyl
FAB	fast atom bombardment
GC	gas chromatography
HPLC	high performance liquid chromatography
h	hour

IR	infrared
J	coupling constant
Lys	lysine
m	multiplet
Me	methyl
Min	minutes
MIP	molecularly imprinted polymer
NMR	nuclear magnetic resonance
Pfb	2,2,4,6,7-pentamethyldihydrobenzofuran-5-sulfonyl
Ph	phenyl
Phe	phenylalanine
ppm	parts per million
q	quartet
R _f	retention factor
r.t.	room temperature
s	singlet
satd	saturated
t	triplet
tert	tertiary
TFA	trifluoroacetic acid
THF	tetrahydrofuran
TLC	thin layer chromatography
Ts	<i>para</i> -toluenesulfonyl
TSA	transition state analogue
UV	ultraviolet
VCL	virtual combinatorial library
w	weak
w/v	weight by volume

Part 1. INTRODUCTION

Chapter 1. PROGRESS IN THE DESIGN AND SYNTHESIS OF ARTIFICIAL ENZYMES

Enzymes catalyse reactions with remarkable regio and stereoselectivity under very mild conditions. They are a source of inspiration to chemists, demonstrating what could be achieved with a full understanding of the underlying principles of the subject and have long provided a stimulus for research into synthetic equivalents. The basic principle behind enzyme catalysis: molecular recognition and stabilisation of the transition state of a reaction, was originally proposed by Pauling over 50 years ago¹. However, despite some impressive advances in the field of artificial enzymes, chemists have yet to put this theory into practice to produce a synthetic equivalent which can rival enzymes in rate acceleration, turnover and specificity.

Enzymes have had billions of years to evolve into the sophisticated three-dimensional structures of today. As chemists, we need to concentrate this period to a feasible timescale for research. In recognition of this fact, recent developments in the field of artificial enzymes have moved away from the rational design and multistep synthesis of complex molecules and have tended to focus on selection approaches. Advances in the fields of molecular biology, biochemistry and more recently combinatorial and polymer chemistry have all furnished unique and often co-operative solutions to the synthesis of artificial enzymes, and it is the aim of this introduction to discuss some of the more recent and diverse approaches taken by organic chemists towards the creation of effective enzyme mimics.

In general the different approaches can be divided into three categories;

The 'design approach'. A host molecule is designed with salient functionality (often also present in the natural enzyme counterpart) which is expected to be involved in catalysis of the chosen reaction. Catalytic cyclodextrins are one such example.

The 'transition state analogue-selection approach'. A library of hosts is generated in the presence of a transition state analogue (TSA) and the best host is then selected from the library. This latter approach has been employed with considerable success in the field of catalytic antibodies and has more recently inspired the process of 'molecular imprinting'.

The 'catalytic activity-selection approach'. This takes advantage of the combinatorial chemistry revolution: a library of possible catalysts is generated and screened directly for enzyme-like activity.

Although a review on enzyme mimics would not be complete without mention of the more established enzyme mimics such as cyclodextrins and catalytic antibodies. They represent review articles in their own right^{2,3} and only selected examples will be discussed here. This introduction will instead concentrate on less developed areas and will conclude with a discussion of some of the more recent developments in 'selection approaches' towards artificial receptors. In particular, dynamic combinatorial libraries (DCLs) and related research will be described with reference to possible applications in the field of enzyme mimics.

1.0 TRANSITION STATE THEORY

The currently accepted view is that catalysis rests on the enzymes ability to stabilize the transition state of a reaction relative to that of the ground state. This principle is illustrated overleaf (Figure 1) for a unimolecular example where the enzyme-substrate complex is stabilised relative to the free species in solution. The activation barrier to reaction is represented by the difference ΔG_{cat} and ΔG_{uncat} for the enzyme catalysed and the uncatalysed reactions respectively.

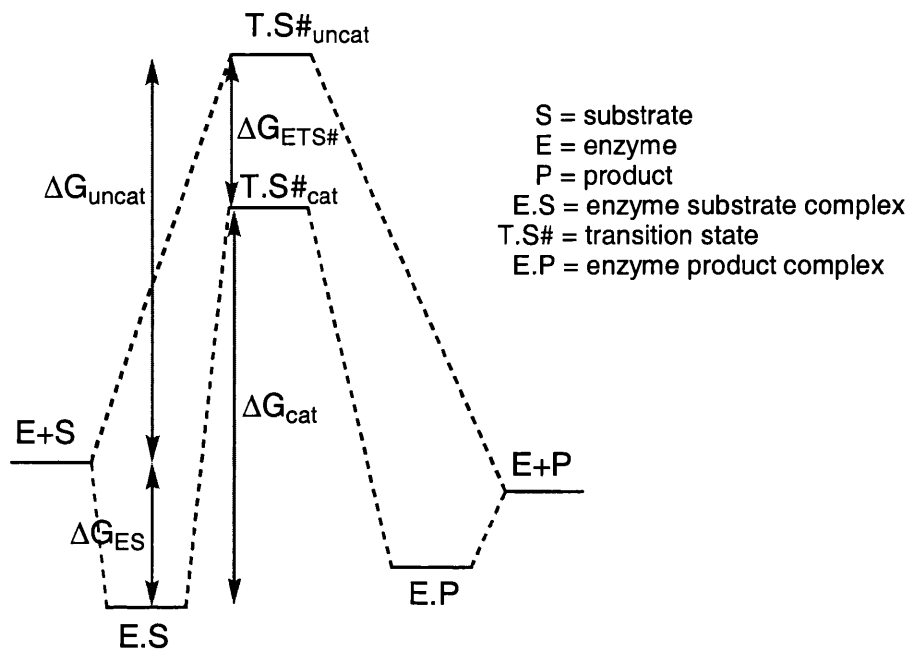
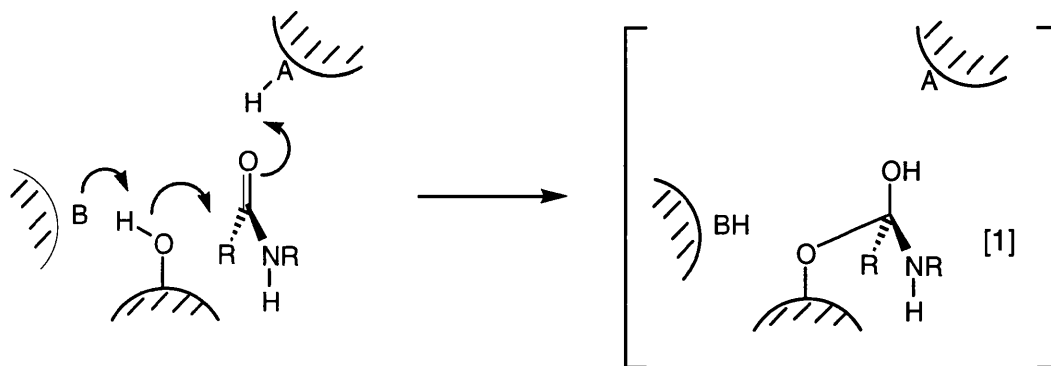


Figure 1

It is clear from this picture that for catalysis to work the difference $\Delta G_{ETS\#}$ must be larger than ΔG_{ES} . In other words, the enzyme must stabilise the transition state of the reaction more than it stabilises the ground state of the substrate⁴. For true catalysis, a system also needs to exhibit turnover. If the product binds to the enzyme significantly stronger than it binds to the substrate ($E.S < E.P$) then product inhibition of the reaction can result. In this case substrate binding can be beneficial. The most important consequences of this picture of enzyme action are that design of an enzyme mimic must consider not only transition state binding relative to substrate binding; the active site must be designed such that product release is a thermodynamically favourable process.

The discussion above is a simplification of the real situation since enzyme catalysis of a transformation often involves an alternative reaction pathway from that of the noncatalysed process, usually taking advantage of the enzymes ability to reduce the molecularity of multistep sequences. The situation also becomes more complicated for bimolecular processes and reactions involving covalent enzyme-bound intermediates⁴, such as the intermediate [1], invoked in the initial step of the mechanism for amide bond cleavage by serine proteases (Scheme 1).



Schematic representation of the first step: an acylation reaction, in a serine protease amide bond cleavage reaction.

Scheme 1

In these more complex systems, application of the above model of transition state stabilisation is less straightforward, however, the discussion is adequate to understand the basic principle behind many of the various approaches to artificial enzymes.

Perhaps the biggest obstacle to the synthesis of enzyme mimics is that in order to design an artificial enzyme it is necessary to understand *how* enzymes achieve this selective binding of the transition state. Many studies have been carried out in attempts to quantify the contributions of the many weak intermolecular forces involved. In general the overall binding is a product of electrostatic, hydrogen bonding, hydrophobic and Van der Waals influences⁵. Since enzymes operate in water, desolvation effects and the resulting entropy changes are also important factors^{6,7}.

Hydrogen bonding and electrostatic interactions contribute significantly to the binding affinity between the substrate or transition state and the enzyme, although, since enzymes operate in water, the contribution of these effects is greatly moderated by solvation. In fact, in some cases, desolvation of both the polar group on the ligand and the complementary group in the enzyme may cost as much in enthalpy as is gained by bringing the two groups together⁵. Many studies into the influence of hydrogen bonding in particular have been carried out, in an attempt to quantify the energy difference gained upon the formation of a ligand-host hydrogen bond in water⁸⁻¹⁰. The value for a neutral-neutral hydrogen bond has been generally found to be in the order of 1.5kcal mol⁻¹, which represents a perhaps surprisingly modest energy gain. As a result it has

been suggested that such interactions “may play less of a role in enhancing association of the correct ligand than they do in creating a penalty for binding the wrong ligand, ie., in determining ligand specificity”⁵.

In contrast, the contribution of charged hydrogen bonds to binding enthalpy is more significant. This difference between neutral and charged hydrogen bonding is elegantly illustrated by comparison of the two model receptors [2] and [3] for glutaric acid (Figure 2).

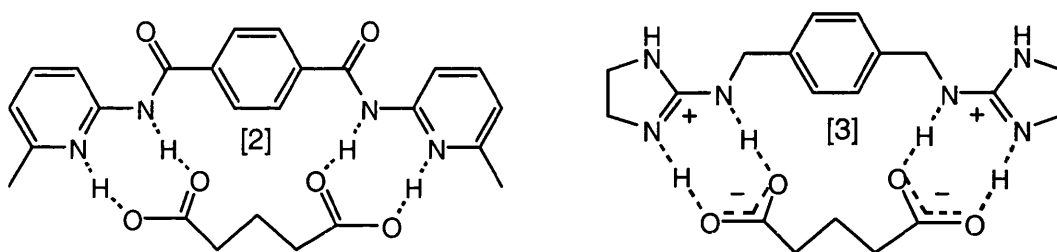


Figure 2

Both receptors create the same number of hydrogen bonds with glutaric acid, however, the neutral diamide [2] binds glutaric acid strongly in chloroform ($K_{\text{ass}} = 60\,000\text{M}^{-1}$) but not in DMSO¹², whilst the receptor [3] which incorporates two charged electrostatic hydrogen bond interactions is almost as good a receptor in DMSO ($K_{\text{ass}} = 50\,000\text{M}^{-1}$) containing 5% THF and binding is still measurable in the presence of 25% water¹³. In quantitative terms, the presence of a charged hydrogen bond has been estimated to contribute up to 4.7kcal mol^{-1} to the stability of an enzyme-ligand interaction¹¹.

More recently the importance of the hydrophobic effect in selective binding has been highlighted¹¹. This stabilising influence arises from the transfer of a hydrophobic surface out of water and into contact with a complementary hydrophobic region of a ligand or receptor. The driving force behind this favourable interaction is the beneficial change in free energy as ordered water molecules surrounding the hydrophobic surfaces are released into bulk solvent. The importance of this phenomenon has been emphasised in a recent review into molecular recognition in drug design¹¹. A range of examples where hydrophobic interactions play an important role in binding are discussed. Most

importantly, the concept of an “induced fit” in which the receptor undergoes a conformational change in order to optimise hydrophobic interactions with the ligand is emphasised.

An example is the interactions involved in the complexes of inhibitors [4] and [5] with the matrix metalloproteinase stromelysin¹⁴. Replacement of the *N*-methyl amide group in [4] by a phenyl ring [5] (Figure 5) was accompanied by an unexpected conformational shift of a loop in stromelysin which allowed an unexpected Leu residue to bind to the hydrophobic benzhydryl moiety. This elegantly demonstrates the inherent flexibility of enzymes, which are able to undergo conformational change in order to accomplish binding.

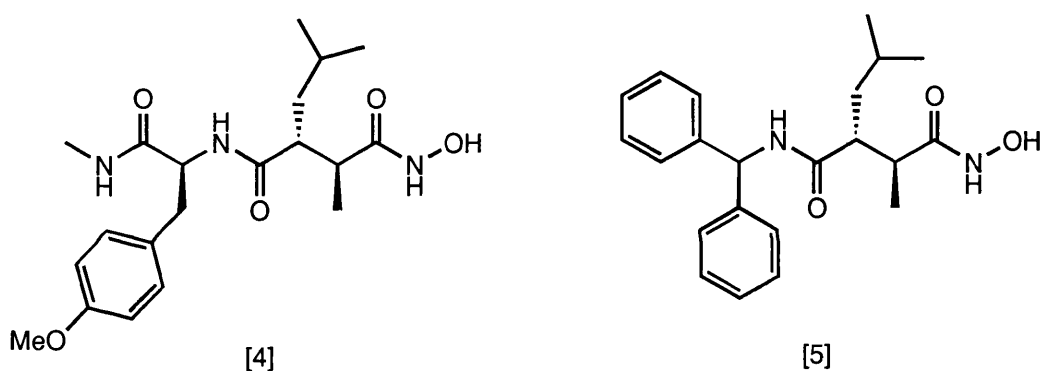


Figure 3

All the above effects, as well as π -stacking and Van der Waals interactions^{15,5}, involve binding between discrete ligand and receptor moieties. Perhaps the most difficult binding effects to understand are those interactions at the catalytic centre of the enzyme site between the transition state and the host. This is because the system, and hence the bonding interactions, are dynamic in nature. It is these binding phenomena, termed “dynamic binding” interactions, which distinguish between an active artificial enzyme and a synthetic receptor. To revisit the acyl transfer step in the serine proteases discussed earlier, Kirby¹⁶ has used this example to illustrate the concept of dynamic binding. The transition state for this step is illustrated in Figure 5 below in which at least six bonds are being made and broken.

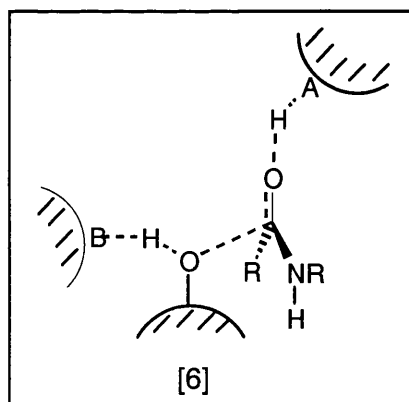


Figure 5

Although the exact nature of the transition state is unknown the important feature is that the “binding” of this transition state by the enzyme involves more than ordinary molecular recognition. The partially formed covalent bonds at the reaction centre represent “dynamic” binding interactions which have no conveniently modelled ground state counterpart. It can also be expected that these interactions must make a major contribution to transition state binding and stabilisation, not least because they clearly represent a difference between substrate and transition state recognition.

All the factors described above contribute to the overall binding of the transition state. Despite the many reviews available on the factors which influence molecular recognition and binding in enzyme systems¹⁷, the practical application of these hypotheses remains the true test of our understanding. It is thus of pertinent interest to investigate the design and synthesis of artificial enzymes since this will hopefully also lead to a better understanding of molecular recognition itself.

1.1 THE ‘DESIGN APPROACH’

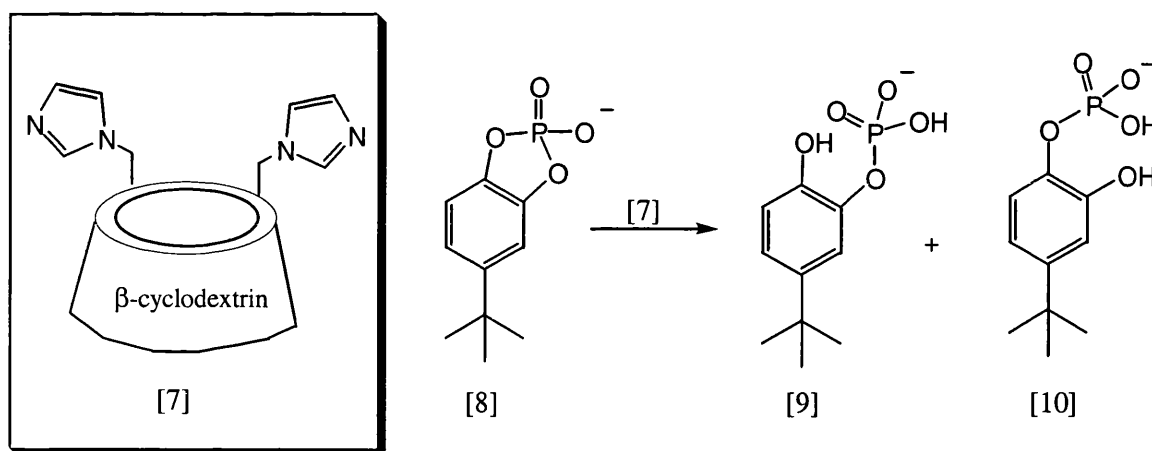
The traditional approach to enzyme mimics has focused on the *de novo* design of macromolecular receptors with appropriately placed functional groups. These catalytic groups are usually chosen to mimic the amino acid residues known to be involved in the enzyme catalysed reaction. The realisation of ideas in such a process can be an arduous

affair and although there are some impressive successes (*vide infra*), efficient catalysis rivalling enzyme rate accelerations still seems a long way down the line.

1.1.0 Cyclodextrins as enzyme mimics

One of the most prodigious aspects of enzyme mechanism is the functional group co-operation often displayed in the active site. The electrostatic environment in the binding site maintains the delicate balance of pK_a s required for the various groups to participate catalytically. In particular, histidine is often able to function as both an acid and base in simultaneous bi or multifunctional catalysis. Intrigued by the challenge of imitating this phenomenon Breslow *et al* chose to mimic the enzyme ribonuclease A^{18a,b}. This enzyme uses His12 and His119 as it's principle catalytic groups in the hydrolysis of RNA.

To mimic this enzyme two imidazole rings were attached to the primary face of β -Cyclodextrin as depicted below in Scheme 2.

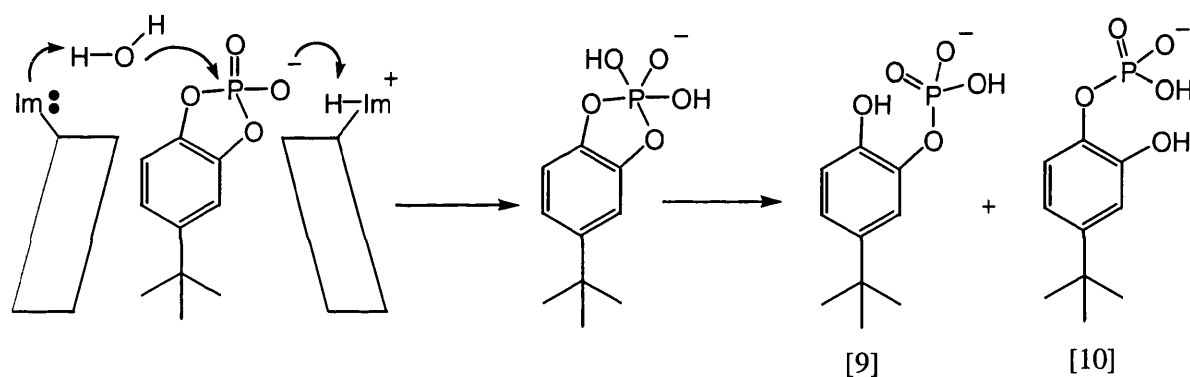


Scheme 2

This mimic [7] catalyses the hydrolysis of the cyclic phosphate [8] with a k_{cat} $120 \times 10^{-5} \cdot s^{-1}$ compared to k_{uncat} $1 \times 10^{-5} \cdot s^{-1}$ for the uncatalysed reaction and shows greater than 99:1 selectivity for [9]. This is in comparison to the solution reaction with NaOH which gives a 1:1 mixture of both products. Isotope effects showed that the two catalytic groups were operating simultaneously and the pH rate profile, which was almost

identical to the enzyme itself^{18a}, shows that one imidazole functions in its protonated form whilst the other is unprotonated.

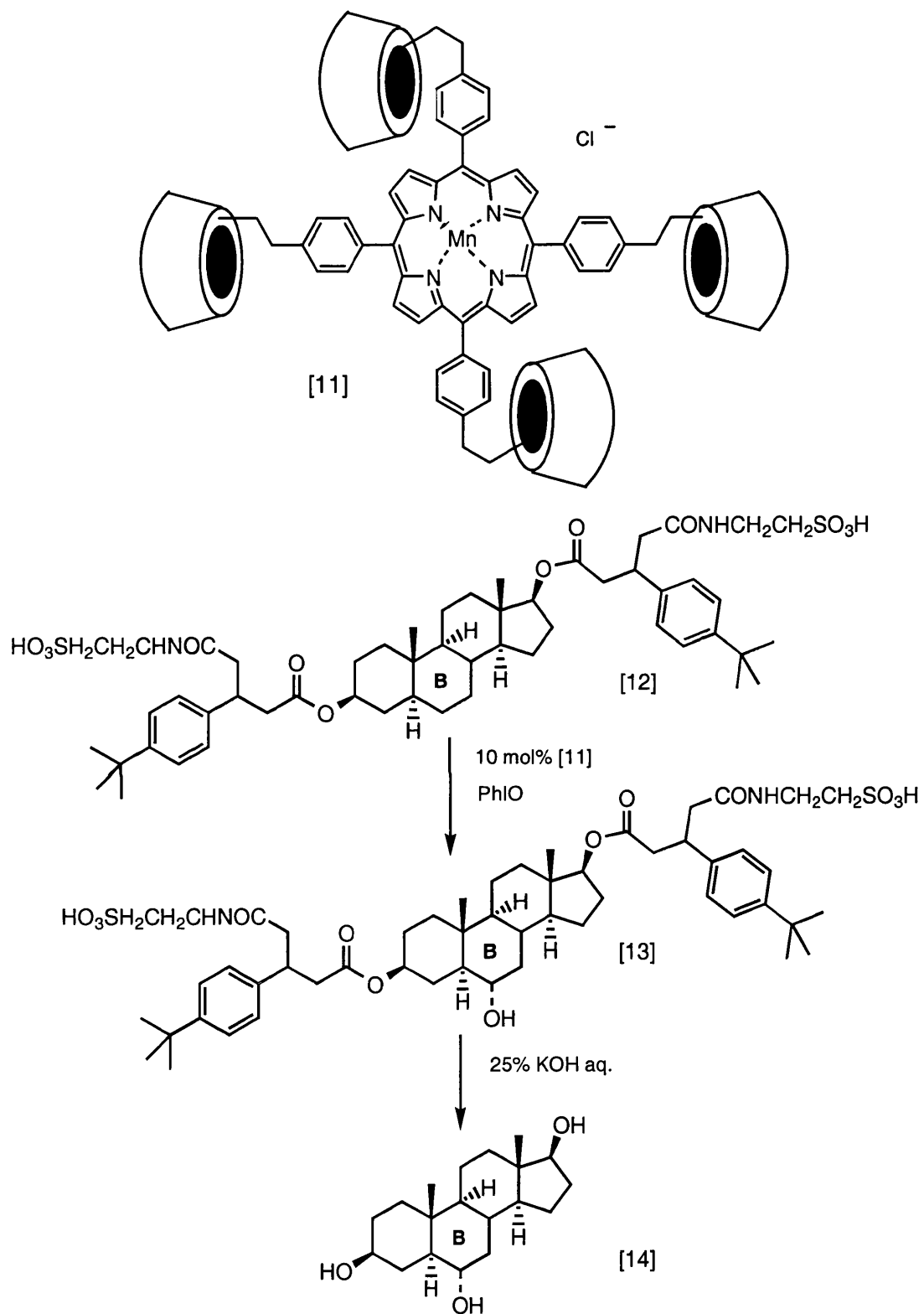
The relative positioning of the imidazole groups on the ring of the β -cyclodextrin was found to be crucial. Only when the imidazole groups were attached to adjacent sugars was a single product [9] detected. This regioisomer of β -cyclodextrin was not only more selective but it also gave the fastest rate of hydrolysis and displayed the strongest binding to the substrate [8]. Importantly, this result gave information about the mechanism involved since the imidazolium ion in this isomer would be better placed to protonate the phosphate anionic oxygen which it can reach better than the other catalyst isomers (Scheme 3).



Scheme 3

This, coupled with the evidence that the imidazoles function simultaneously allowed the group to postulate that the mechanism was as depicted (Scheme 3) and was the same as used by the enzyme, ribonuclease itself².

The use of cyclodextrins as enzyme mimics has been extended to incorporate dimers and trimers of cyclodextrins, as well as a range of transition metal complexes^{2,19}. An example demonstrating both these features is the cytochrome P450 mimic [11]²⁰. This mimic is capable of selectively oxidising the 6-CH₂ position in the B-ring of steroid derivative [12] (Scheme 4).



Scheme 4

Molecular modelling indicated that the two *tert*-butylphenyl groups in the substrate [12] bind into two trans β -CD rings of [11] thus placing the steroid B-ring directly above the

porphyrin ring. The reaction is carried out with 10mol % of catalyst [11] and iodobenzene as co-oxidant. The ester groups are hydrolysed *in situ* to afford 40% of the oxidised product [14] along with unreacted starting material. This yield corresponds to at least 4 turnovers and although this may be considered modest, the example nevertheless demonstrates the power of using designed binding constraints to influence the selectivity of a reaction.

1.1.1 Cyclophane enzyme mimics

Another impressive application of the design approach is Diederich's pyruvate oxidase mimic.

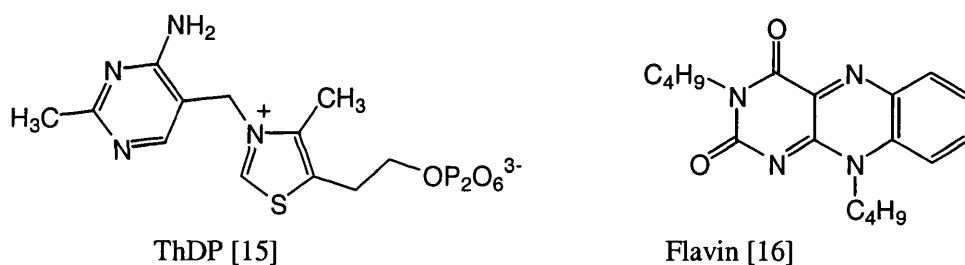
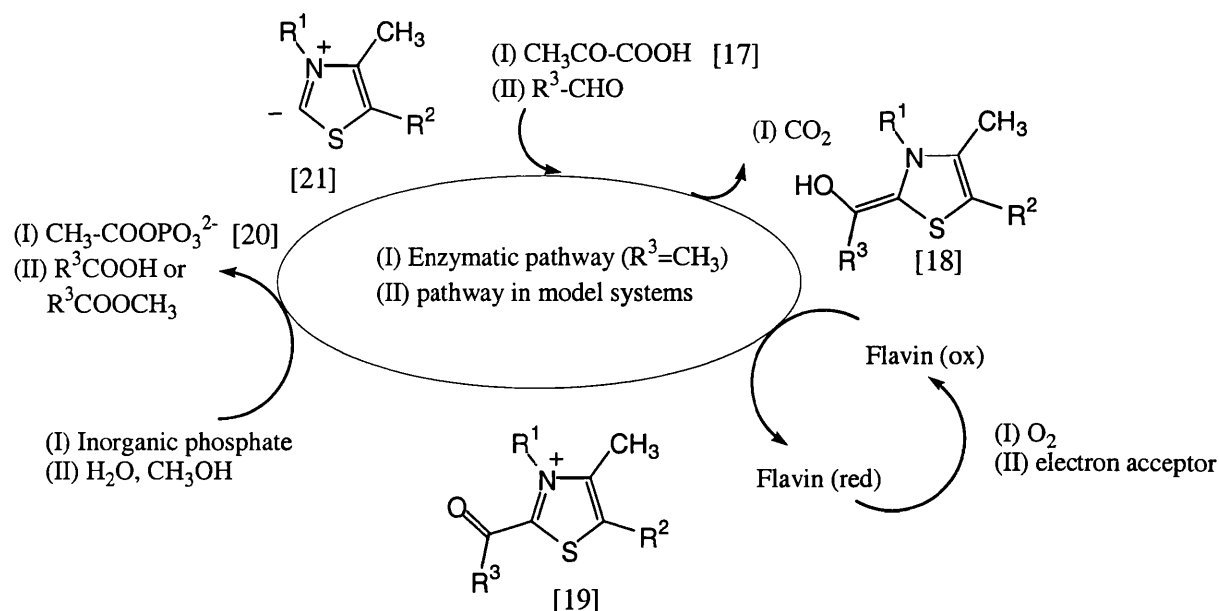


Figure 6

Pyruvate oxidase employs two co-factors ThDP [15] and Flavin [16] (Figure 6) to catalyse the transformation of pyruvate [17] to acetyl phosphate [20] (Scheme 5). The thiazolium group of ThDP forms an activated aldehyde [18] which is oxidised by the flavin to give an electrophilic intermediate [19]. This is then attacked by the inorganic phosphate nucleophile to release the product and regenerate the thiazolium ylide [21] (Scheme 5). In an analogous fashion aldehydes are oxidised by either water or alcohols to carboxylic acids or esters respectively by simple thiazolium ions in the presence of flavin.



Scheme 5

Diederich's pyruvate oxidase mimic [22] combines a well defined binding site with both the flavin and thiazolium groups attached covalently^{21a,b} (Figure 7). The proximity of the groups to the binding site and the intramolecularity of the oxidation step was expected to improve catalysis relative to previous two component systems²². It should also mimic the situation in the enzyme where the cofactors are bound in the enzyme active site thus increasing the effective molarity of the reagents.

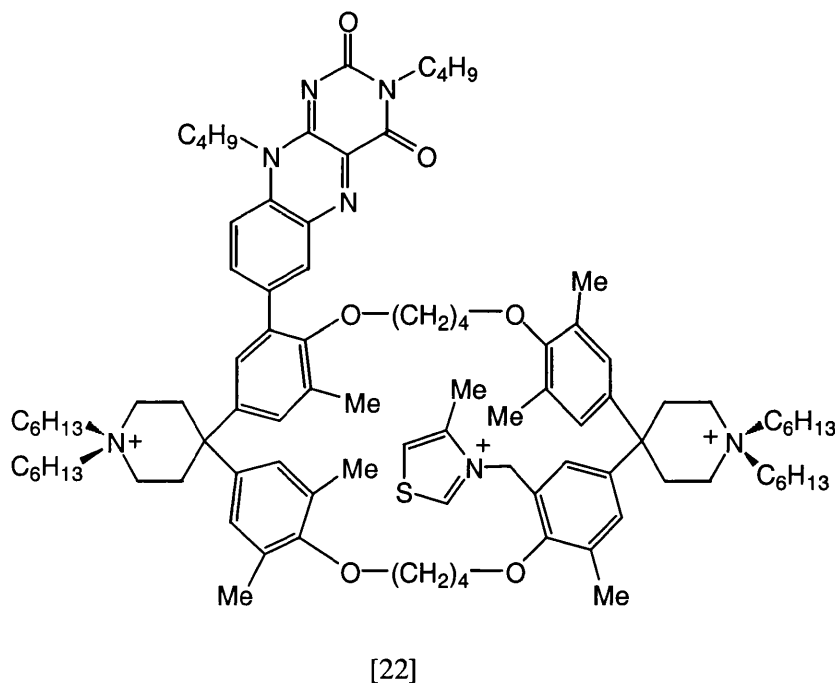
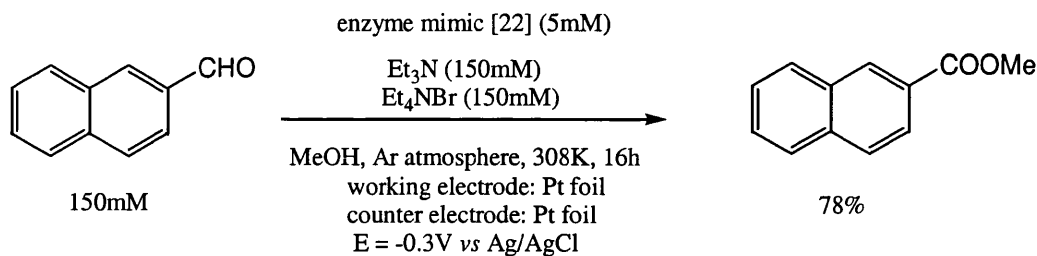


Figure 7

The transformation of naphthalene-2-carbaldehyde [23] to methyl naphthalene-2-carboxylate [24] in basic methanol is indeed catalysed by [22] with a k_{cat} 0.22s^{-1} (Scheme 6). In order to demonstrate true catalysis the attached flavin derivative needs to be reoxidised *in situ*. This was achieved by regeneration at a working electrode potential of -0.3V vs Ag/AgCl . Under these conditions the enzyme mimic [22] is able to act catalytically on a truly preparative scale with a turnover of up to 100 catalytic cycles.

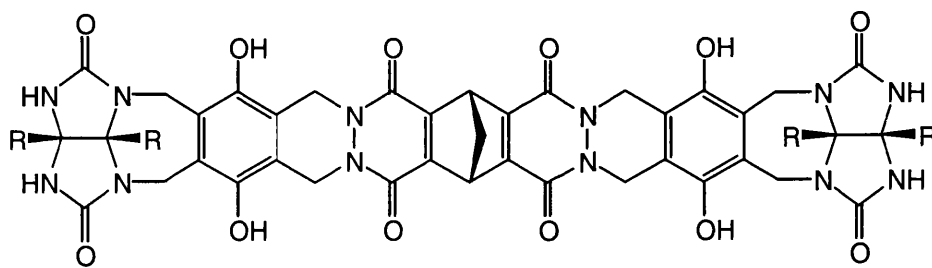


Scheme 6

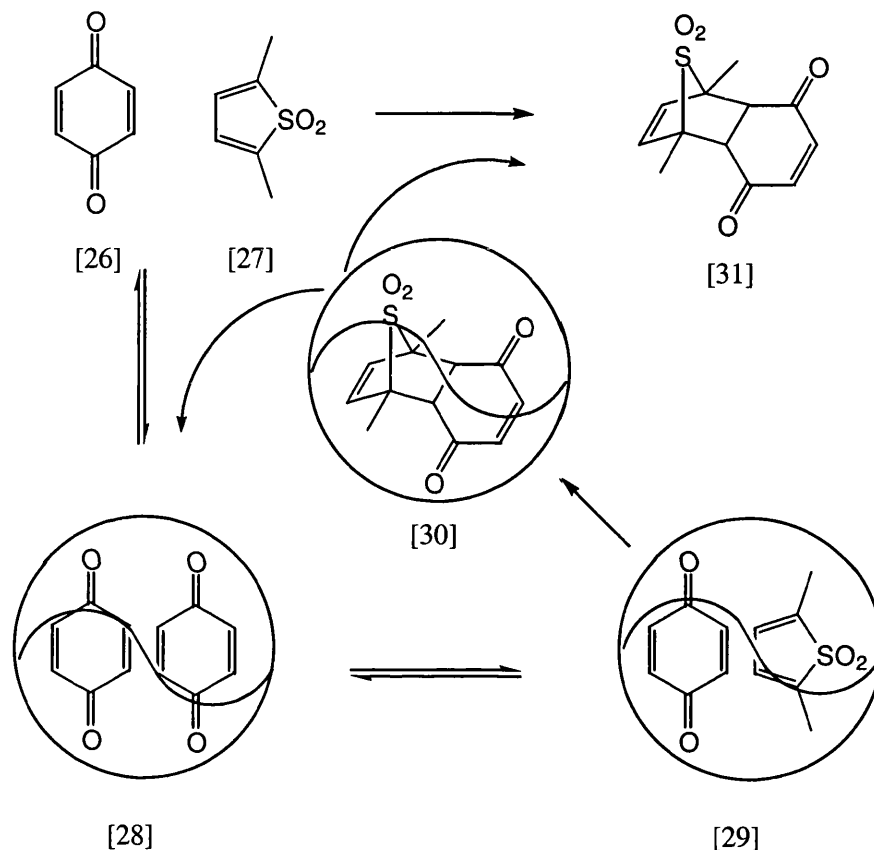
1.1.2 Reversibly self-assembled dimers as enzyme mimics.

In a different approach, Rebek *et al* have investigated the influence of a designed binding cavity on the rate of reaction²³. In this case, no catalytic groups are required. Furthermore, although a Diels Alderase is known²⁴, no natural enzyme catalyst is available for synthetic applications as yet. This is important, since the desirability of designing artificial enzymes for reactions which have no convenient natural enzyme equivalent is evident.

Rebek and co-workers have carried out much research into the synthesis of reversibly self-assembled dimers²⁵. The multiring structure [25] (Scheme 7) exists as a hydrogen-bonded dimer in organic solvents and adopts a pseudo spherical structure (described as a ‘hydroxy-softball’) which is able to form and dissipate on a timescale of milliseconds. This dynamic behaviour, coupled with the microenvironment provided by the ‘softball’ led Rebek *et al* to investigate the catalytic potential of [25] towards the Diels Alder reaction of thiophene dioxide [27] and benzoquinone [26] (Scheme 7).



R = 4-*n*-heptylphenyl [25]



Scheme 7

Earlier attempts at Diels alder catalysis for a different reaction were hindered by product binding, necessitating stoichiometric amounts of host²⁶. However, in this case, binding studies with product [31] showed that the adduct is an unwelcome guest and is driven out of the cavity by benzoquinone. This strong preference for benzoquinone is also a problem since the resting state of the species in solution is [28]. However, true catalysis and turnover were observed in the desired Diels Alder transformation when compared to a reference reaction in the presence of an isomer of [25] unable to form a dimer.

That the reaction was taking place in the capsule was confirmed by the addition of the competitive inhibitor [32], known to be an excellent guest for the ‘softball’ [25] (Figure 8).

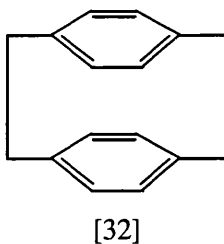


Figure 8

Many other examples of designed hosts have been reported²⁷, including several inorganic based examples such as the porphyrin trimers of Sanders *et al*^{28a,b}.

1.2 THE ‘TRANSITION STATE ANALOGUE - SELECTION APPROACH’.

The traditional approach to enzyme mimics is the design approach described above. Whilst this has furnished us with much information on the recognition processes involved in binding and the criteria required for successful catalysis, the realisation of a project from original conception to experimental studies on an enzyme mimic can be a long and laborious process. A case in point is Diederich’s pyruvate oxidase mimic (Section 1.1.1) which required an 18 step synthesis of the host [22]. In an attempt to move away from this linear approach, several techniques have been developed which make use of a selection strategy. This allows for the simultaneous screening of a wide range of possible candidates thus significantly reducing the time required and hopefully allowing for the detection of better hosts.

The earliest examples of a selection approach chose affinity for a transition state analogue (TSA) as their screening criteria. The logic behind this is that any macromolecule which shows strong binding to a molecule resembling the transition

state of a reaction, should also bind to and stabilise the real transition state. As this stabilisation of the transition state is the basis behind enzyme catalysis, the hosts selected should behave as enzyme mimics for the chosen transformation.

More recently it has been recognised that TSA binding in itself may not be enough to obtain the rate accelerations needed to rival enzyme catalysis. Nowadays, the incorporation of catalytic groups in the host is often a designed aspect of the selection process and it is this, in combination with the TSA host selection, which has led to some of the most impressive advances described below.

1.2.0 Catalytic antibodies.

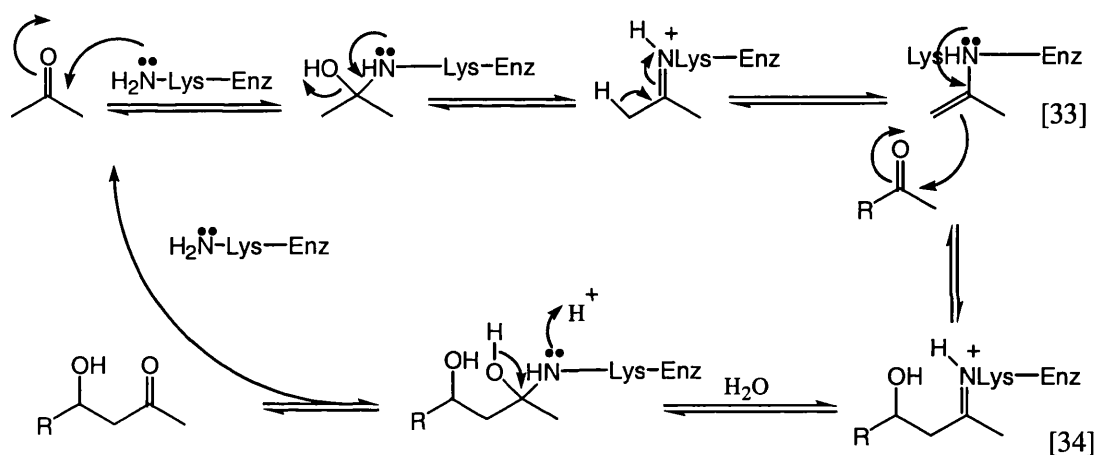
The most established application of the above TSA selection strategy is in the field of catalytic antibodies, pioneered by Lerner²⁹ and Schultz³⁰ in the mid eighties. The immune system generates a natural library of hosts, known as antibodies, in response to the introduction of a foreign molecule into the bloodstream. Advances in molecular biology techniques, notably the process of isolating monoclonal antibodies, allow the selection of a chosen antibody library member on the basis of function.

Traditionally, catalytic antibody technology focussed on a purist TSA approach: the TSA was designed, synthesised and used as a hapten[#] in immunisation. The desired monoclonal antibody was then selected from the polyclonal population on the basis of binding affinity to the TSA. Early efforts produced a range of successes in various synthetic transformations, affording artificial antibody catalysts for ester hydrolysis^{29,31}, the Diels alder reaction³¹, cationic cyclisations³²⁻³⁴, cyclopropanation³⁵, elimination reactions³⁶, the oxy-Cope rearrangement³⁷ and an allylic sulfoxide-sulfonate rearrangement³⁸, amongst others. However, rate accelerations always fell short of the enzyme catalysed equivalents. Furthermore, detailed mechanistic investigations often revealed that a mechanism other than that originally assumed for the design of the TSA was involved³⁹. This has important consequences. Since the selection event is based on binding to the TSA and not on the basis of catalytic activity, the antibody selected may

not be the best catalyst. The transition state is after all, not a real discrete entity and any TSA can only be expected to be an approximation of the true charge distribution required.

In the last few years there have been significant advances in the field of catalytic antibodies using the process of “reactive immunisation”. In this method, the selection criteria are changed from simple binding to chemical reactivity. Illustrative examples are the antibody aldolases 38C2 and 33F12⁴⁰.

The natural aldolase mechanism was known to operate as shown below in Scheme 8⁴¹.



Scheme 8

A lysine residue in the enzyme active site forms a covalently bound intermediate with the substrate. Initial attack by the lysine amino group affords a carbinolamine which eliminates water to give a Schiff base imine. This can tautomerise to give an enamine [33] capable of reacting with a further equivalent of the carbonyl substrate to give the Schiff base [34]. Hydrolysis with water furnishes the aldol product and regenerates the active lysine group of the enzyme to complete the catalytic cycle. Lerner *at al* reasoned that if their selection criteria was the ability to form an enamine intermediate such as [33], then the antibodies chosen should hopefully act as artificial aldolases with a similar

A hapten is a small molecule attached to a carrier protein which is used to stimulate the immune response.

mechanism. The challenge was then experimental; how to observe the covalently bound antibody intermediate.

The enamine intermediate [37] of the 1,3 diketone [35] (Scheme 9) is a vinylogous amide due to the presence of the β -carbonyl group. This vinylogous amide [37] has a strong ultraviolet absorption outside the range of the protein (316nm). The rationale was thus to generate a library of antibodies against diketone [35] and select successful candidates on the basis of their ability to absorb in this region.

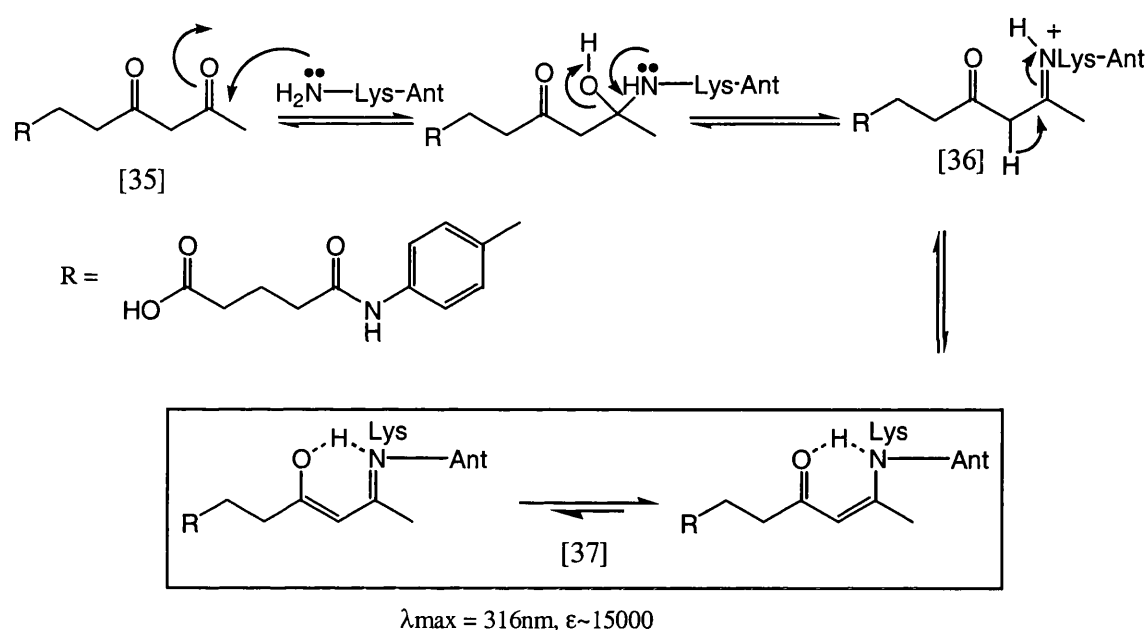
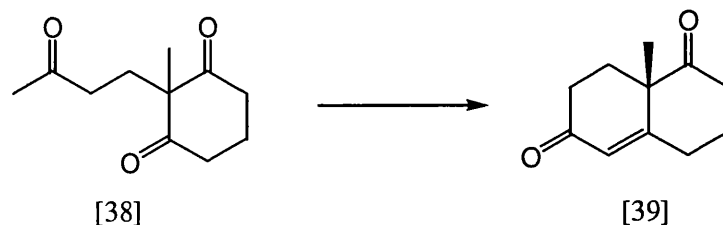


Figure 11

Two catalytic antibodies isolated in this manner, 38C2 and 33F12 were broad in scope, catalysing over 100 different aldol additions involving aldehyde-aldehyde, ketone-aldehyde and ketone-ketone transformations. The example below of the formation of the (*S*)-Weiland-Mischler ketone [38] operates with a rate acceleration of $k_{\text{cat}}/k_{\text{uncat}} 3.6 \times 10^6$ and affords an enantiomeric excess (ee) of >95% (Scheme 10).

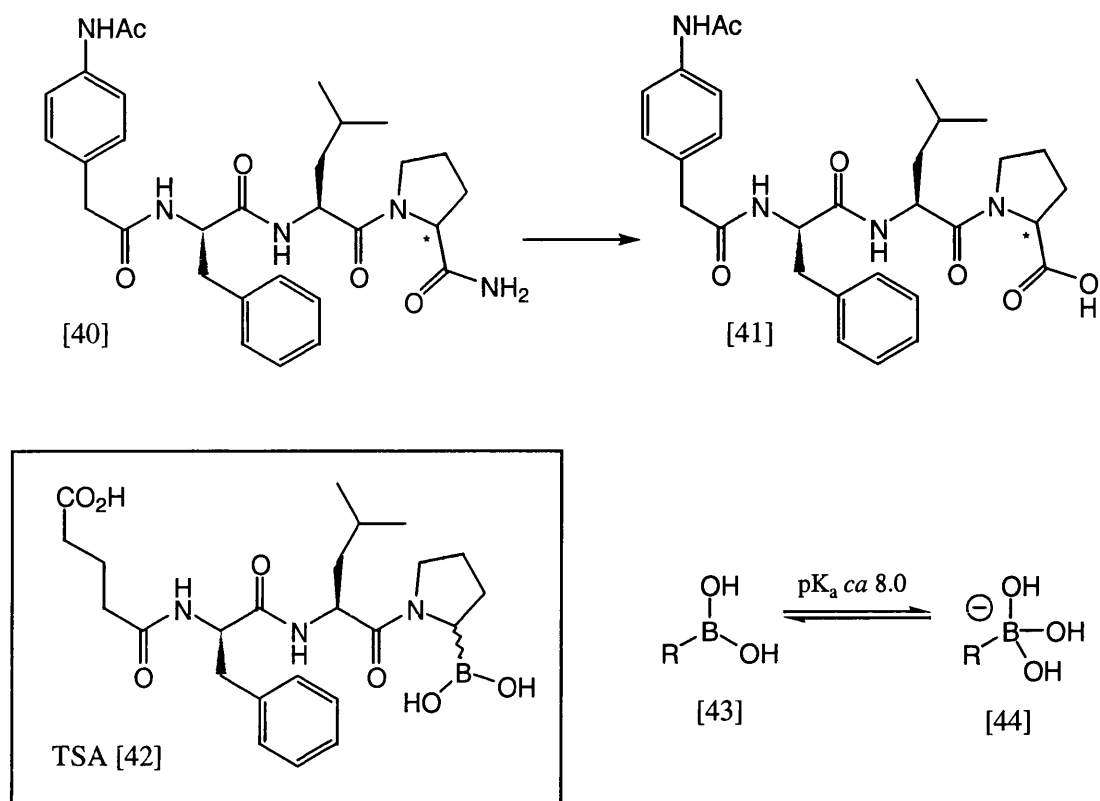


Scheme 10

Not only do these catalytic antibodies accept a wider range of substrates than their natural enzyme counterparts, the catalytic turnover achieved by these antibodies is within 10 times that of the natural enzyme for the optimal substrates of each.

The mechanism of action was shown to be the same as for the natural aldolase. This is significant since the mechanism involves a nucleophilic lysine residue, a group which would usually be protonated at physiological pH. The origin of catalytic activity in the antibody is believed to derive from a greatly perturbed lysine residue in the binding pocket. Cloning and sequencing of the 33F12 genes allowed the group to obtain enough material for an X-Ray crystal structure. This indicated that the active Lys residue is contained in a hydrophobic pocket which may explain its enhanced nucleophilicity.

In a very recent example, which employs a novel selection method involving construction of a Fab* library, Janda *et al* have reported the isolation of a catalytic antibody for primary amide bond hydrolysis⁴² (Scheme 11).



Scheme 11

The hapten chosen for immunisation [42] contains a boronic acid group which is in equilibrium with the tetrahedral hydrate [44] (Scheme 11). This latter substrate is expected to mimic the transition state for the addition of water to a carbonyl centre. Moreover, the boronic Lewis acid hapten could form this tetrahedral intermediate by a covalent interaction with a complementary Lewis base or serine hydroxyl in the antibody binding site. This immobilising interaction was used as a basis for the screening protocol.

* The Fab fragment is the antigen binding domain of an antibody.

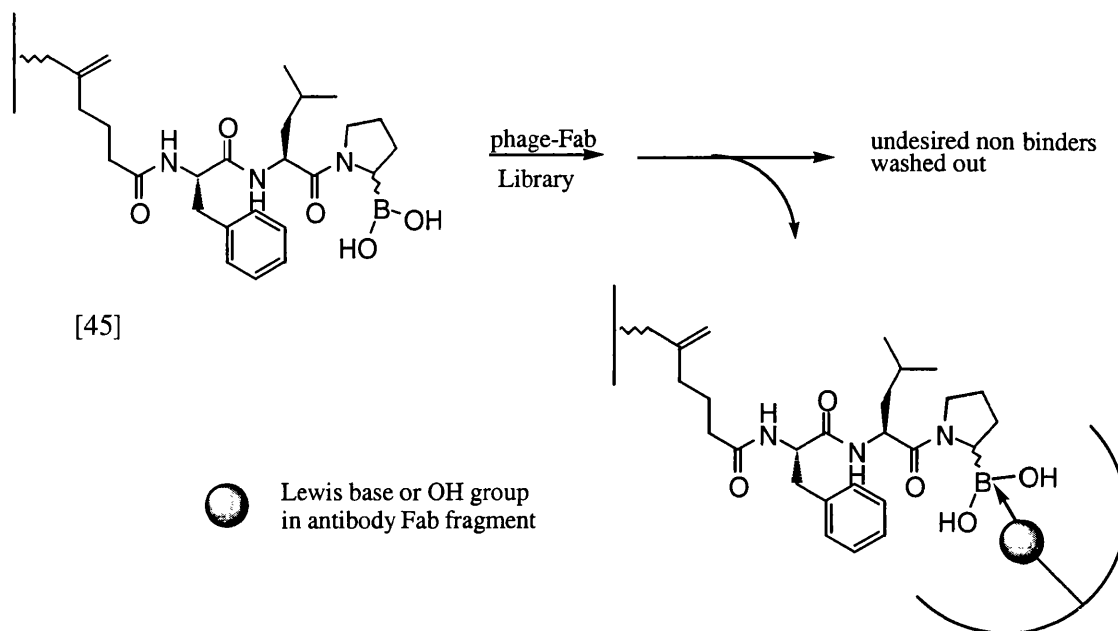


Figure 9

Immunisation and subsequent manipulation produced a Fab library expressed on phages which was exposed to immobilised hapten [45] and incubated. After washing off the non bound Fab library members the selected candidates could be isolated by washing with acid, since at pH 2.2 the equilibrium of the boronic acid groups should be shifted towards the free acid (Figure 9). Isolated library members were then amplified and tested for catalysis. The Fab fragment BL-25, isolated in this manner reduces the half life of the primary amide [40] (Scheme 11) from ca 17.5 years to 3.9h which is greater than two orders of magnitude higher than for a catalytic antibody elicited using a phosphinate TSA. Studies into the mechanism used in the antibody are still in their early stages, although preliminary results suggest that the catalytic power of BL-25 is derived from transition state stabilisation of the anionic tetrahedral intermediate⁴².

Notwithstanding these impressive achievements there remain some problems with the catalytic antibody technology. The necessity of using mice to generate the antibodies is undesirable, although advances in *in vitro* immunisation methods⁴³ may render this less of an issue. Furthermore, the molecular biology techniques involved are highly specialised. The isolation of a monoclonal antibody is very time consuming process and, once a catalytic antibody is found, it can be a process of many months (to years) before the structure of the active site is characterised.

1.2.1 *Molecularly Imprinted Polymers.*

Catalytic molecularly imprinted polymers represent a much younger field than their biological counterparts; catalytic antibodies. The basic concepts underlying both subjects are very similar. Molecular Imprinting⁴⁴ is a polymerisation technique which produces macroporous polymers with binding sites which can selectively rebind the molecule with which they were 'imprinted'. If this 'imprint' molecule is a TSA, then the resulting molecularly imprinted polymer's (MIPs), should behave as artificial enzymes for the reaction chosen.

The process of molecular imprinting is outlined below (Figure 10). In the first step monomers containing functional groups which interact with the imprint molecule, are pre-organised around the imprint molecule [48]. A mixture of monomer and cross-linker is then co-polymerised around this imprint molecule-monomer complex in a radical polymerisation process, to form a macroporous polymer which contains sites at which the imprint molecule is bound [49]. Finally, the imprint molecule is removed from the polymer to leave well defined, shape specific cavities which are spatially and functionally compatible with the imprint molecule [50].

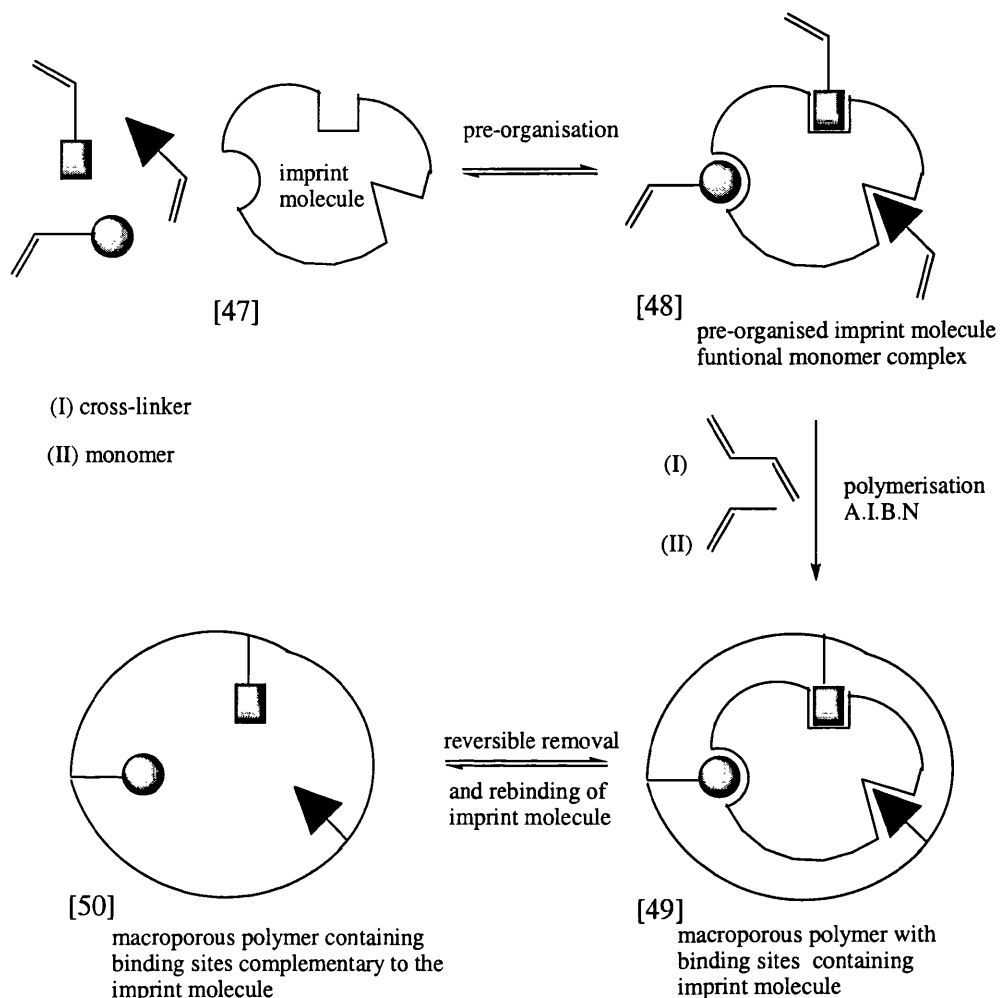


Figure 10

The interactions between the imprint molecule and the functional monomers can be either covalent or non-covalent. In the latter case the description pre-organisation can be a slight misnomer, since the combination of weak intermolecular forces involved lead rather to a dynamic associated complex in constant exchange with solution. This, along with other factors (part 2), defines the inherent heterogeneity of the molecular recognition sites produced in the polymer. This has proved to be one of the major sticking points in catalytic applications of MIPs. Despite this drawback, the manifest stability of MIPs when compared to natural enzymes or other artificial analogues, means the realisation of catalytic MIPs remains a desirable goal.

Several successes have been reported exploiting the molecular imprinting technique, however, the scope of catalytic MIPs remains relatively limited. Table 1 contains a comprehensive list of MIPs which have been applied catalytically as artificial enzymes.

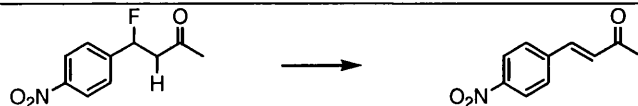
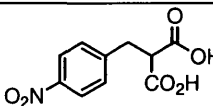

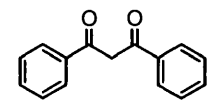

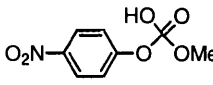
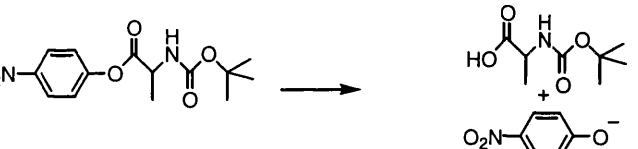
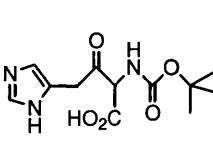
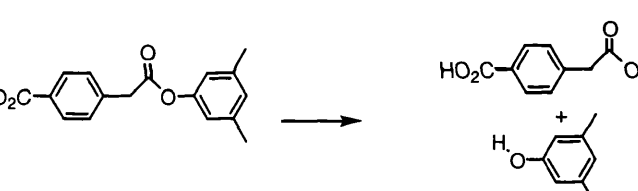
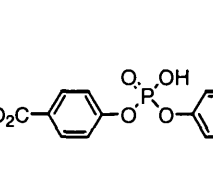
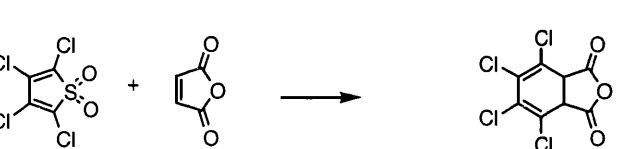
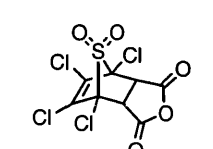

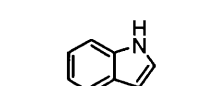
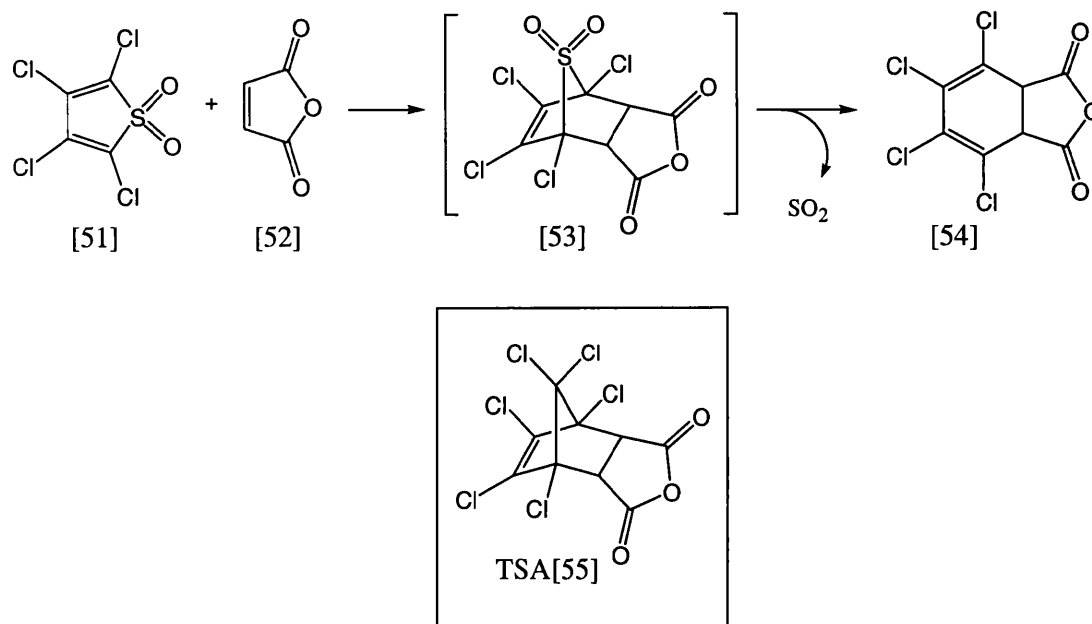
MIP catalysed reaction	TSA used as imprint molecule	Ref.
		[45]
		[46]
		[47], [48]
		[49]
		[50]
		[51]
		[52]

Table 1

An elegant example is the catalysis of the Diels Alder reaction of tetrachlorothiophene S, S dioxide [51] and maleic anhydride [52] reported by Mosbach *et al* (Scheme 12)⁵¹.



Scheme 12

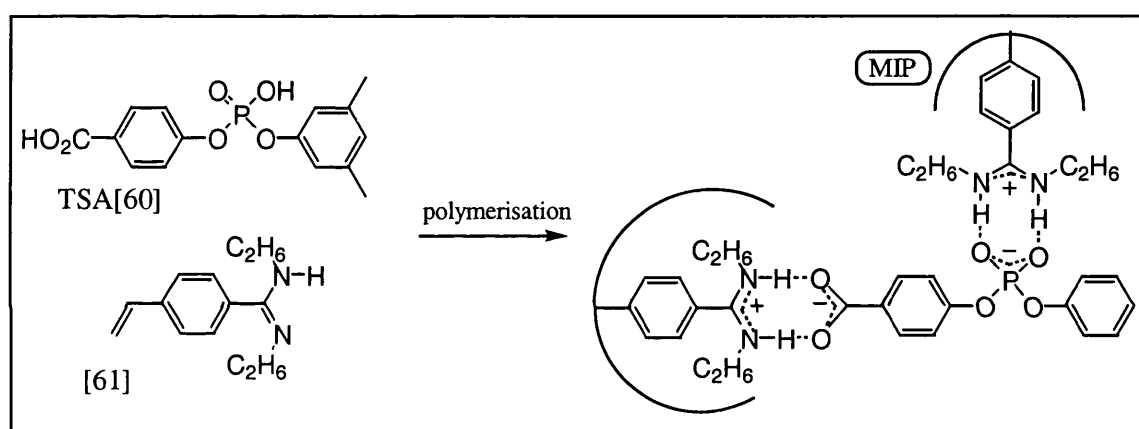
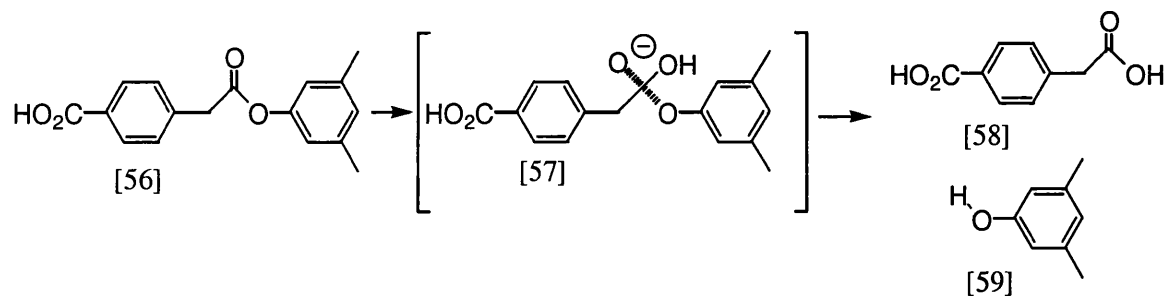
The challenge of designing an artificial enzyme to catalyse the Diels Alder reaction is that the product very often resembles the transition state and can bind to the active site inhibiting turnover. The reaction above avoids this problem since spontaneous SO₂ extrusion leads to a product sufficiently distinct from the imprinted TSA to be expelled from the active site.

Methacrylic acid (functional monomer), ethylene-glycol dimethacrylate (cross-linker) polymers imprinted with the TSA [55] selectively rebound the imprint molecule and accelerated the rate of reaction with a k_{cat}/k_{uncat} 270[#]. This rate acceleration is modest compared to the catalytic antibody equivalent³¹, but nevertheless demonstrates the feasibility of this technique.

Promise for future progress comes from the work of Wulff and co-workers⁵⁰ who recently reported a successful hydrolytic MIP. In recognition that TSA binding alone may not be enough to confer catalytic activity they designed their system to contain an appropriately positioned amidine catalytic group [61] (Scheme 13). This group mimics the active arginine residue in the catalytic antibody equivalent and was shown to bind

[#] Rate accelerations were corrected to the reaction in the presence of a non-catalytic polymer produced in the absence of the imprint molecule.

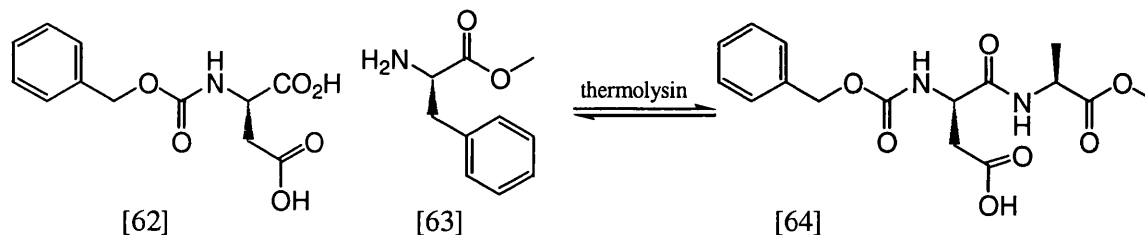
strongly to phosphonic acid monoesters such as the TSA [60]. Phosphonates such as [60] are well established mimics of the transition state of ester hydrolysis representing the tetrahedral geometry of the ester intermediate [57].



Scheme 13

The MIPs formed with [60] as imprint molecule caused a 100 fold rate acceleration of the hydrolysis of ester [56] with typical Michaelis-Menten saturation kinetics. This is by far the largest rate acceleration for ester hydrolysis achieved with the MIP technique and, by analogy with the trend in catalytic antibody technology, represents the benefits of ensuring an enzyme mimicking catalytic group is incorporated into enzyme mimic-TSA binding.

A promising novel application of the MIP technique was reported recently by Mosbach *et al*⁵³. In this example the MIP is used, not as a catalyst, but as a specific adsorbent which shifts the equilibrium of a thermodynamically unfavorable enzymatic reaction by removing the product of the reaction from solution.



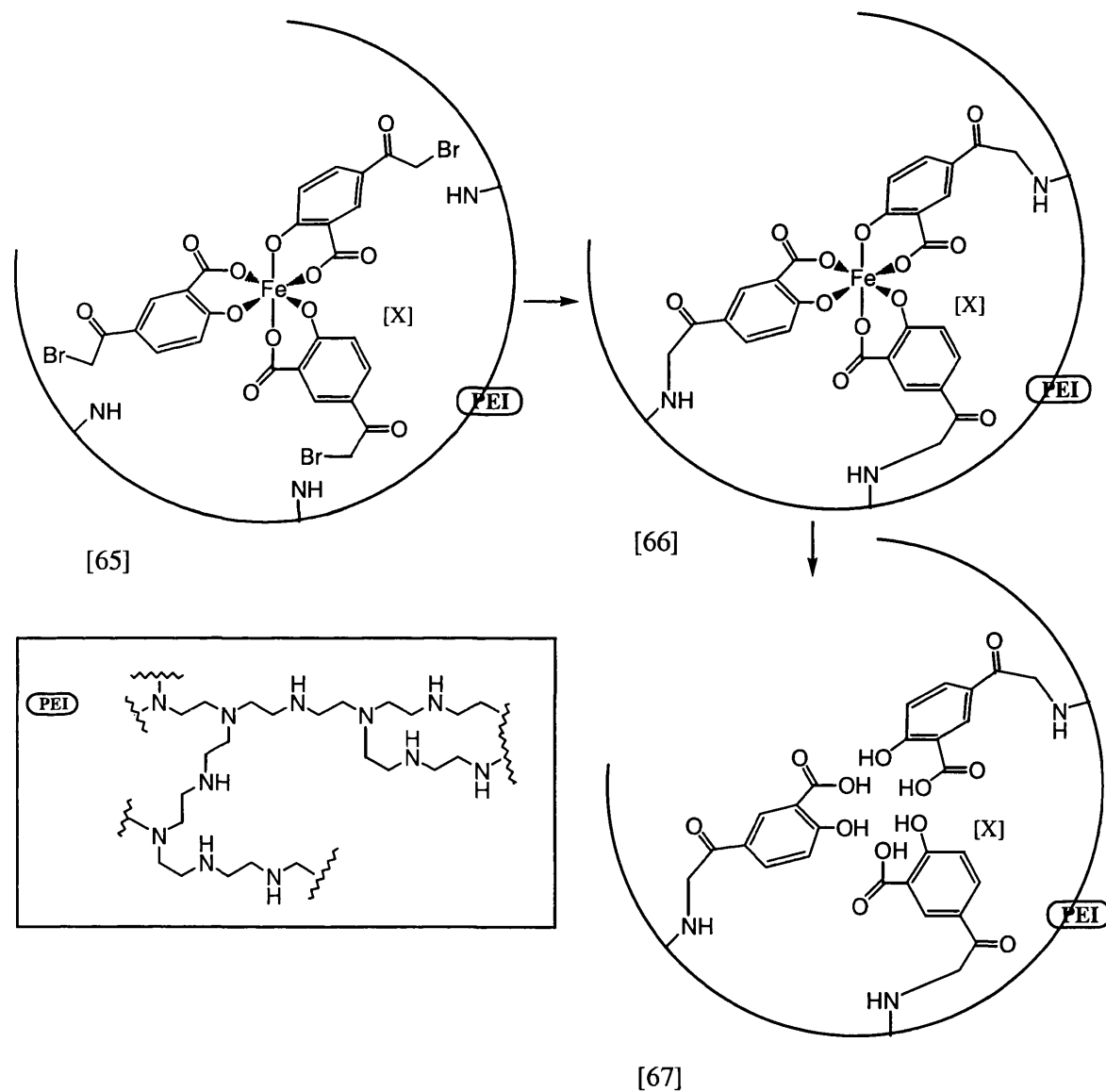
Scheme 14

The reaction chosen was the commercially interesting enzymatic conversion of Cbz-L-Asp [62] and L-Phe-OMe [63] to Cbz-Aspartame [64] (Scheme 14). An MIP was synthesised using the product of the reaction [64] as the imprint molecule. This MIP was then added to a mixture of Cbz-L-Asp [62], L-Phe-OMe [63] and the enzyme thermolysin and the course of the reaction was followed by HPLC. The presence of the imprinted polymer increased the yield of the desired product to 63% from 15% in the polymer free reaction. Furthermore, when no polymer is present the yield of Cbz-Aspartame is observed to reach a maximum (ca 20%) and then decrease with time due to non-enzymatic decomposition of L-Phe-OMe [63]⁵⁴. A problem which was avoided by the use of the MIP. This study elegantly establishes the potential of MIPs as thermodynamic traps in reversible enzymatic syntheses.

The majority of applications for MIPs are analytical. However, several other synthetic applications of MIPs which are not strictly enzyme mimics have been reported. MIPs have been used as microreactors containing reagents for selective reductions⁵⁵ and as 'protecting groups' using an external reagent⁵⁶. In both cases, catalysis is not the goal and stoichiometric quantities of MIP are required.

1.2.2 Imprinting an artificial proteinase.

Several other approaches to enzyme mimics using 'imprinting' have been reported. J. Suh *et al* attached an Fe(III) salicylate derivate complex [65] to a polyethylene imine (PEI) backbone [66] (Scheme 15)⁵⁷. Subsequent removal of the Fe (III) ion led to a polymer with three salicylate groups in close proximity [67].



Scheme 15

The polymer thus contained regions of high functionality with carboxylate groups which might be expected to mimic glutamic acid or aspartic acid side chains and three

phenolic hydroxyls as cogeners of tyrosine. The polymer [67] acted as an artificial proteinase in the cleavage of bovine serum albumin γ -globulin Gbn, and displayed substantially higher activity than a randomly functionalised PEI cogener. Both the heavy and light chains of Gbn were cleaved into peptides smaller than 5kDa at pH7 and 50°C with a half life of 1h, which is in comparison to a half life of amide bonds of ~1000 years⁵⁸ in free solution at pH7 and 25°C. Comparable data for the reaction at 50°C or for the randomly functionalised PEI standard was not available.

This approach has proved successful in a number of model systems which incorporate similar strategies⁵⁹.

1.2.3 Bioimprinting.

In a different approach, Guimin Luo *et al* reported the bioimprinting of a glutathione peroxidase (GPX) mimic⁶⁰. The natural GPX enzyme active site contains a selenocysteine catalytic group and a binding site for the cofactor glutathione (GSH). Using this information Luo *et al* 'imprinted' a denatured egg albumin protein with GSH mimic [68] and crosslinked the conformation in basic glutaraldehyde solution. The GSH derivative [68] was then removed by dialysis and the protein was treated with NaHSe to create active selenocysteine residues in the binding site. The protein was then purified and tested for activity.

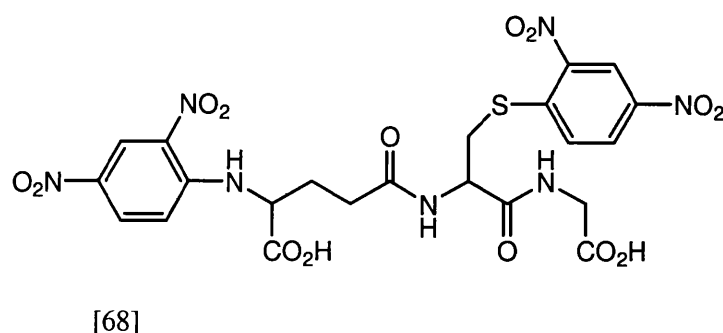
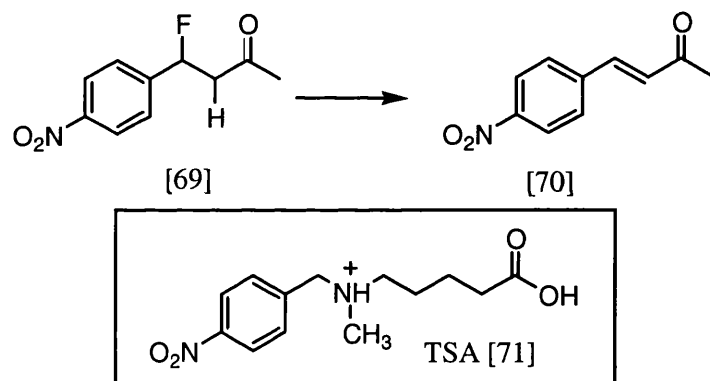


Figure 11

The imprinted protein catalysed the reduction of hydrogen peroxide to water in the presence of co-factor GSH with an 80 fold increase in activity compared to egg albumin

treated in the absence of imprint molecule [68]. Competitive inhibition with the imprint molecule was observed for the imprinted protein whilst addition of [68] had no effect on the reference treated protein, indicating that specific binding sites for GSH were involved.

In a related approach utilising a TSA rather than a co-factor mimic, the bio-imprinting of bovine serum albumin (BSA) to produce a catalyst for a dehydrofluorination reaction was reported⁶¹. The TSA [71] used was expected to interact with a complementary basic group in the protein which would be subsequently suitably placed to abstract the β proton from substrate [69] (Scheme 16). Although the rate accelerations observed were modest k_{cat} 3.3, the experiment demonstrated that it was possible to recruit enzyme activity in a non catalytic protein.



Scheme 16

The various imprinting methods above all share the advantage that the enzyme mimics produced are relatively easy and quick to assemble. In most cases synthesis is a matter of days and systems can be tested for activity immediately. However, at this stage in the development of the subject, rate accelerations which rival catalytic antibodies are rare⁵⁷.

1.3 'CATALYTIC ACTIVITY-SELECTION APPROACH'

Although some ingenious solutions to the design and synthesis of artificial enzymes have so far been described, all of the methods above have the common failing that the

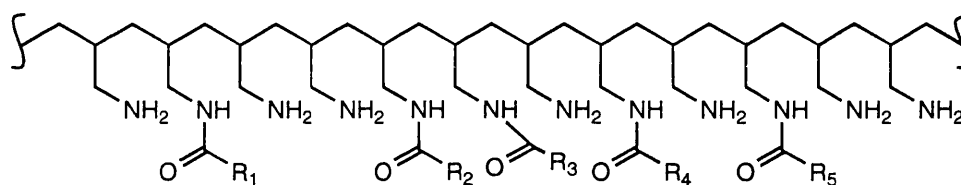
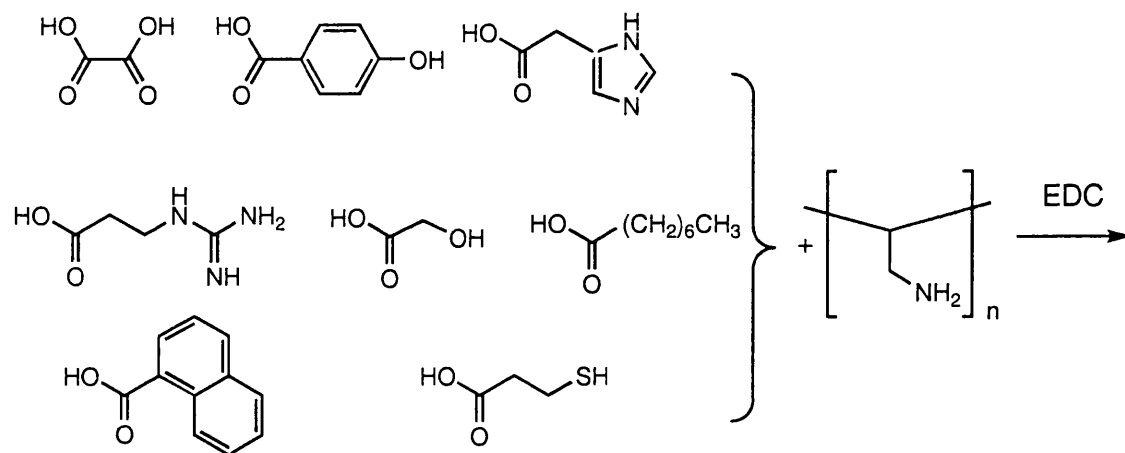
desired property of catalysis is not in the screening criteria. As a direct consequence of such an approach effective catalysts may often fail to be detected.

Combinatorial chemistry⁶² has exploded in popularity over recent years and it is now recognised that applications can extend much further than the creation of libraries for medicinal chemistry. In particular, it is now realised that combinatorial methods can be a useful tool in the discovery of effective catalysts.

1.3.0 Combinatorial polymers as enzyme mimics.

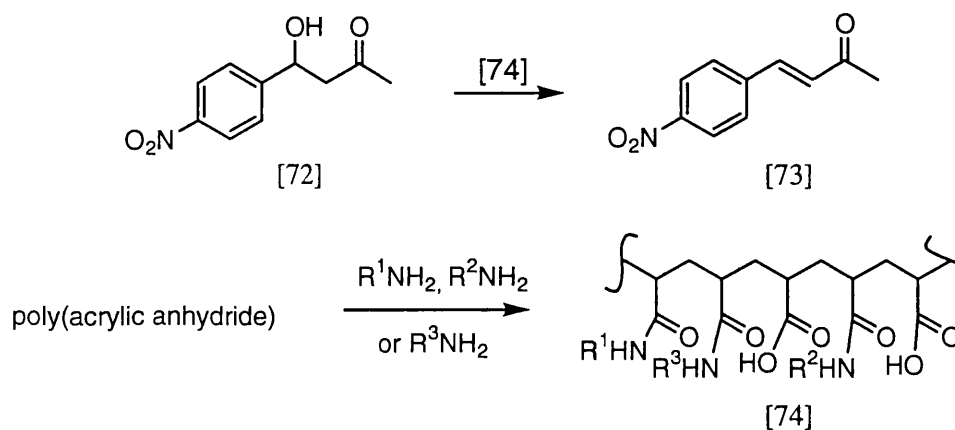
In a rather unconventional approach to artificial enzymes, Menger *et al* have developed the combinatorial derivatisation of polyallylamine^{63,64}. The basic idea was to attach various combinations of carboxylic acids to polyallylamine backbones and then screen for catalysis in the presence of a metal ion (Scheme 17).

Regions of local organisation are expected on the basis that once a particular residue has attached to the backbone it may influence subsequent neighbouring substitutions. For example, a hydrophobic residue might be expected to favour addition of another neighbouring hydrophobic residue. However, in general the composition of the polymer will be combinatorial with each individual polymer containing a range of metal ion sites. Thus, not only would each polymer made vary from the others in composition, each polymer in itself represents a combinatorial range of sites. As such it seems unlikely that 'the ensemble of countless variations' will ever be deconvoluted. Nevertheless, if the primary goal is catalysis, such a method has proved to be successful in more than one model. Both phosphatase⁶³ catalysis ($k_{\text{cat}}/k_{\text{uncat}}$ 10^3 - 10^4) and the reduction of benzylformic acid (PhCOCO_2^-) to mandelic acid (PhCH(OH)CO_2^-)⁶⁴ have been reported.



Scheme 17

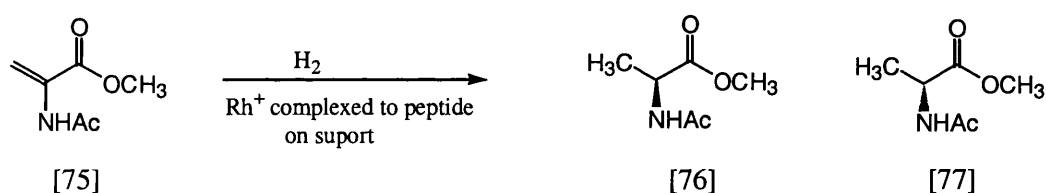
Using the same principles in the derivatisation of poly(acrylic anhydride), a combinatorial polymer capable of catalysing the biologically relevant dehydration of β -hydroxy ketone [72] with a k_{cat} 920 over the background reaction was identified⁶⁵ (Scheme 18).



Scheme 18

1.3.1. Combinatorially developed peptide catalysts.

In a more conventional application of combinatorial chemistry Gilbertson *et al* described the synthesis of a library of phosphine containing peptides^{66a,b}. A variable sequence of four to five amino acids including two phosphine derivatised amino acids was incorporated into a basic Ac-Ala-Aib-Ala-[]-Ala-Aib-Ala-NH₂ peptide. The peptides were expected to form a helical conformation presenting the two donor phosphine ligands in an appropriate orientation for metal co-ordination. Rh was complexed to the functionalised peptides whilst they were attached to a resin support and each member was screened for it's ability to catalyse the asymmetric hydrogenation of the simple enamide [75] (Scheme 19)

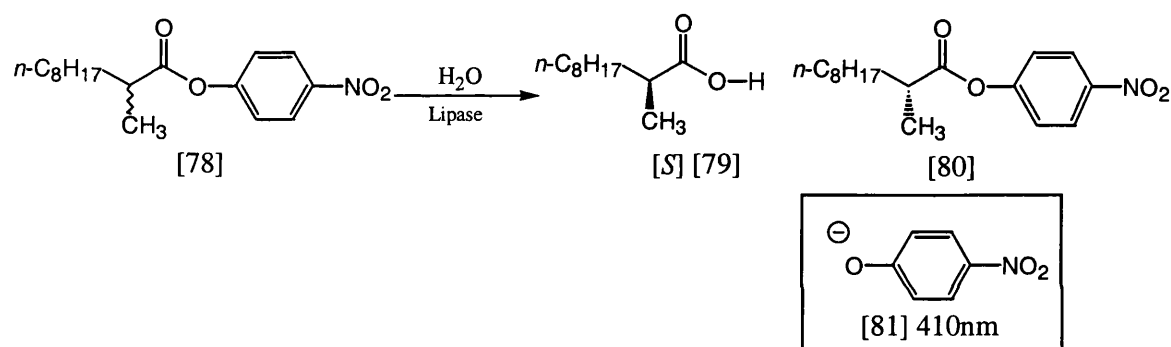


Scheme 19

Although the enantiomeric excesses observed were modest (ca 10%), some correlations between positional substitution in the peptide and stereoselectivity were observed, thus demonstrating the potential of this technique for developing catalysts. In a similar manner Hoyveda *et al* studied a library of schiff base peptides for their ability to catalyse the titanium promoted addition of CN to a variety of imines⁶⁷. Results were impressive; yields and enantiomeric excesses were in the range of 90%, but it seems unlikely that the 'representational search' strategy employed will be applicable to large artificial enzymes since the number of possible permutations of amino acids involved is prohibitively large. The discovery of effective catalysts using such a combinatorial chemistry approach has been the subject of several recent reviews all of which deal with the subject in greater depth^{68a-d} than is possible here.

1.3.2. *In vitro* evolution.

Another application of the ‘catalytic activity-selection approach’ is the *in vitro* evolution of enzymes. This method, as in catalytic antibodies, represents the cross-over between molecular biology and chemistry and several examples of artificial enzymes have been reported using this protocol⁶⁹. A recent example is the enantioselective hydrolysis of racemic *p*-nitrophenyl-2-methyldecanoate [78]. The wild type lipase from the bacterium *Pseudomonas aeruginosa* shows an enantioselectivity of only 2% for the (*S*)-configured acid [79] (Scheme 20). This poorly enantiospecific enzyme was deliberately chosen by the Reetz group for studies into the *in vitro* evolution of enzyme substrate selectivity⁷⁰.



Scheme 20

Using the error prone polymerase chain reaction (epPCR) the lipase gene was subjected to random mutagenesis under conditions such that statistically one to two base substitutions per lipase were introduced. The modified genes were then expressed in a suitable expression vector, amplified in *E.coli* and transformed into *Pseudomonas aeruginosa*. Around 1000 lipase mutants expressed by these bacteria were isolated and screened for enantioselectivity in the test reaction. In order to allow for rapid parallel screening a photometer was developed which could measure simultaneously the absorption of the *p*-nitrophenolate anion [81] at 410nm over time, in each cell of a 96 well plate. The lipase mutants were thus added to either the (*R*) or (*S*) enantiomer of starting material [78] in a 96 well plate and the level of hydrolysis for each measured. Candidates which favoured the hydrolysis of the (*S*) enantiomer of [78] to give [79] were subjected to further mutagenesis and after only four generations an artificial

enzyme which hydrolysed the racemic [78] to give an 81% ee of the (*S*) acid [79] was obtained.

In a related approach to the directed evolution of enzymes, which may also be applicable to antibody libraries, Schultz et al have reported a novel screening method for the catalytic activity selection approach^{71,72}. The basic principle is outlined in Figure 12.

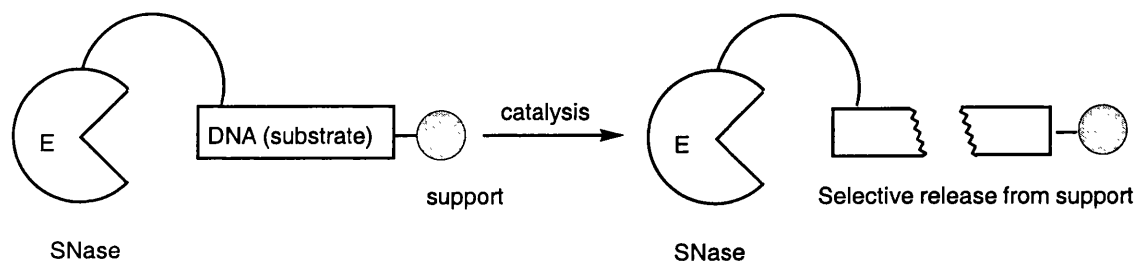


Figure 12

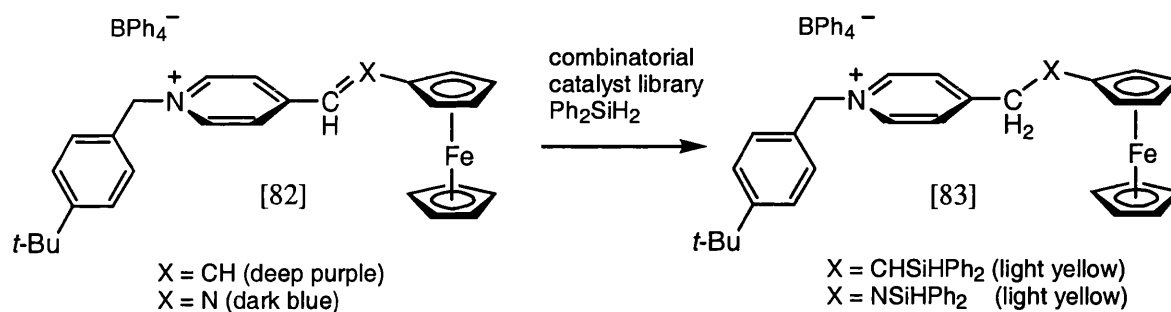
In these studies all the enzymes are expressed on solid phase bound phages where the linker used represents the substrate for a desired enzyme catalysed cleavage reaction. Catalytic activity by the enzyme results in cleavage of the phage from the solid support whilst non catalytic counterparts remain bound, thus the population eluted from the solid phase has an enhanced level of enzyme activity for the desired transformation.

In the example described, the phage expressed enzyme is attached to the solid support using a linker containing an oligonucleotide. The enzyme expressed in the model system is SNase, a Ca^{2+} dependent enzyme capable of cleaving single or double stranded DNA or RNA at A-U or A-T rich regions. It should thus be capable of cleaving the oligonucleotide linker and releasing the SNase expressing phage. The group was able to demonstrate the feasibility of the approach; the percentage of phages displaying the SNase catalytic activity was enhanced, relative to a control enzyme, in the population released from the solid support⁷¹. However, the development of such a system is a very involved process and in situations where greater quantities of catalyst are available for screening there are a range of more accessible techniques emerging.

1.3.3. Screening methods for the identification of catalysts in combinatorial mixtures.

The detection of catalytic activity in a combinatorial system is not trivial. Much of the progress described above in catalytic selection approaches has been a direct result of technological and analytical advances. Recently many ingenious solutions to the detection of catalysts in combinatorial chemistry have been developed which are highlighted in a recent review^{68a}.

A significant development in both the field of combinatorial catalyst development⁷³ and artificial enzymes, relevant to all of the examples mentioned in this section, is IR thermography⁷⁴. Whilst the desirability of screening for catalysis directly is evident, how this is achieved quickly, in a parallel combinatorial fashion, is another matter. It is obvious that the screening of a 96 well plate of artificial enzymes using HPLC is a time consuming and usually rate limiting process. In order to facilitate rate studies and analysis in selection approaches, substrates are often designed to release a UV active product or undergo a colour change upon reaction. This latter screening method is one of the simplest to monitor and has been used with success by Crabtree *et al* to detect catalytic activity in the hydrosilation of alkenes and imines (Scheme 21)⁷⁵.



Scheme 21

However, imposing such monitoring prerequisites restricts the choice of reaction for study, and it is this limitation which the advent of IR thermography, and particularly the time resolved IR thermography of Reetz *et al*⁷⁶, promises to solve. The technique uses an IR camera to monitor, in parallel, a series of test reactions run in a 96 well plate. The

camera provides a spatially addressable picture of the system and is able to identify even modest changes in temperature due to either exothermic or endothermic processes, thus the cells which contain catalytically active components are identified by the camera as 'hot (or cold) spots' respectively. It can be used to monitor a typical 96 well plate of reactions run in parallel and is broad in scope; reactions that can be monitored in this fashion range from lipase mediated acylation reactions to chiral metal mediated hydrolysis of epoxides⁷⁶.

The 'catalytic activity-selection approach' is by far the least studied area of enzyme mimics. This is reflected in the scarcity of examples using this approach. However, the improvements in combinatorial methods and the development of techniques such as IR thermography suggest that it is a growing field of research.

1.4 DYNAMIC COMBINATORIAL LIBRARIES (DCLs).

Since molecular recognition is an important aspect of enzyme action, it seems relevant to discuss some of the recent advances in the combinatorial generation of receptors. Many receptors have been generated by traditional combinatorial methods^{77a-e} but several recent examples have made use of dynamic combinatorial libraries (DCLs), sometimes referred to as virtual combinatorial libraries (VCLs). In DCLs the library members are homogeneous in solution and are allowed to equilibrate reversibly in the presence of a molecule to which binding is desired. This molecule can be either a receptor or a ligand leading to 'casting' or 'moulding' respectively (Figure 13).

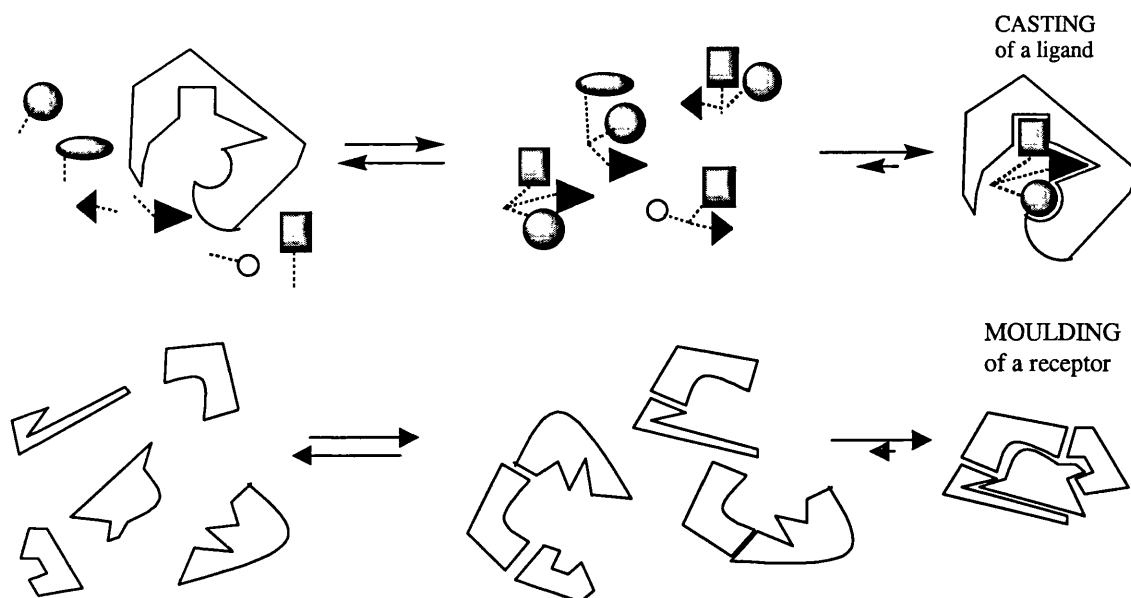


Figure 13

The freezing out of the desired receptor or ligand requires termination of the reversible association process and can be achieved by a change in temperature⁷⁸, or pH^{78,79}, or by chemical methods⁸⁰. The advantage of this technique is that of all the possible permutations of products possible in the library only the formation of those with the desired properties is thermodynamically favoured. On the down side, the choice of a suitable reversible library is not trivial. A recent in depth review of DCLs lists possible reversible reactions⁸¹, however, although much research has been carried out on DCLs including reversible libraries of hydrazones⁷⁹, alkenes^{82,88}, imines based on *o*-aryl and *o*-alkyl oximes⁷⁸, cinchona alkaloids^{83a,b}, catenanes⁸⁴, and peptides⁸⁵ only a few examples of thermodynamically driven selection have been reported⁸⁶.

Lehn *et al* employed an imine-aldehyde exchange reaction to reversibly associate a library of ligands for the receptor carbonic anhydrase II (CAII)⁸⁰. *Para*-substituted sulfonamides were known to be effective inhibitors of CAII, thus the library precursors were chosen with this in mind. After equilibration, the library was frozen chemically by the addition of NaBH₃CN. Subsequent analysis of the library members showed an increase in [84] relative to the receptor free library which is in accord with previous studies of inhibitors of CAII (Figure 14).

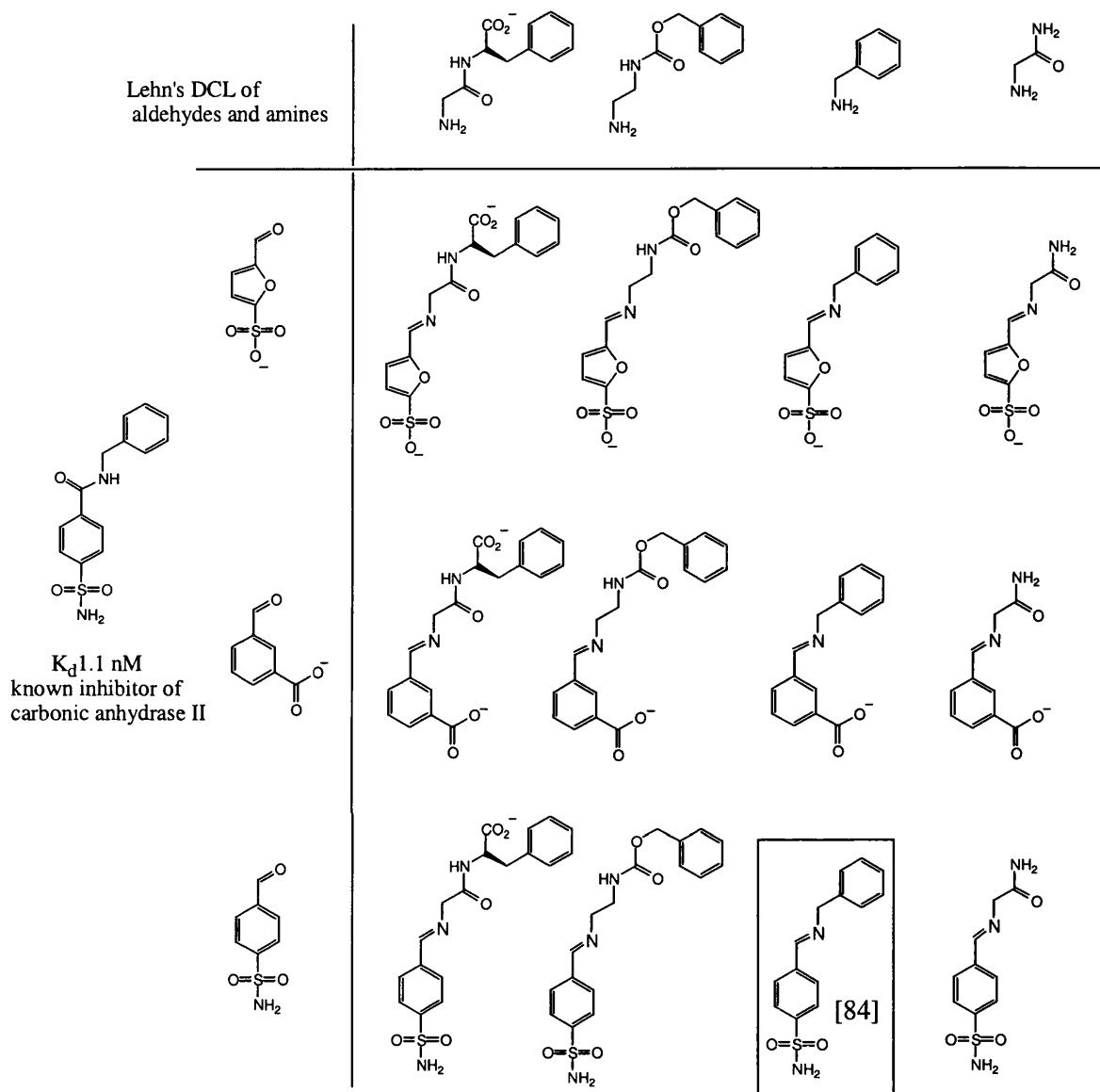


Figure 14

Using the same concept in the quest for receptors Still⁸⁷ used the thiol disulfide exchange reaction to achieve reversible assembly of a small library of receptors. The influence of a solid phase bound tri-peptide on the relative proportions of the receptors in solution was then evaluated.

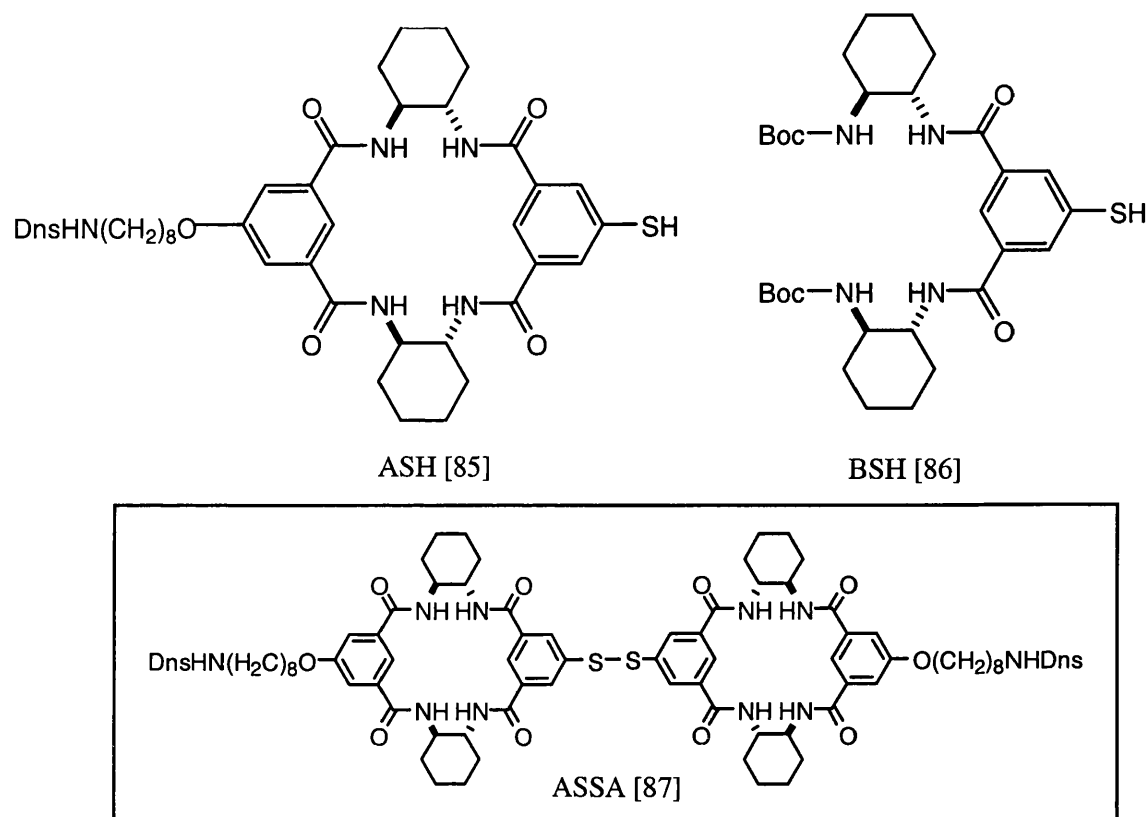


Figure 15

The receptor ASSA [87] was synthesised with a fluorescent sensor and exposed to an encoded combinatorial library of 3375 different *N*-acetyl tri-peptides on polystyrene beads. The peptide Ac(D)-Pro-(L)-Val-(D)-Val-PS was found to bind favourably with a binding constant of the order 10^4 - 10^5 .

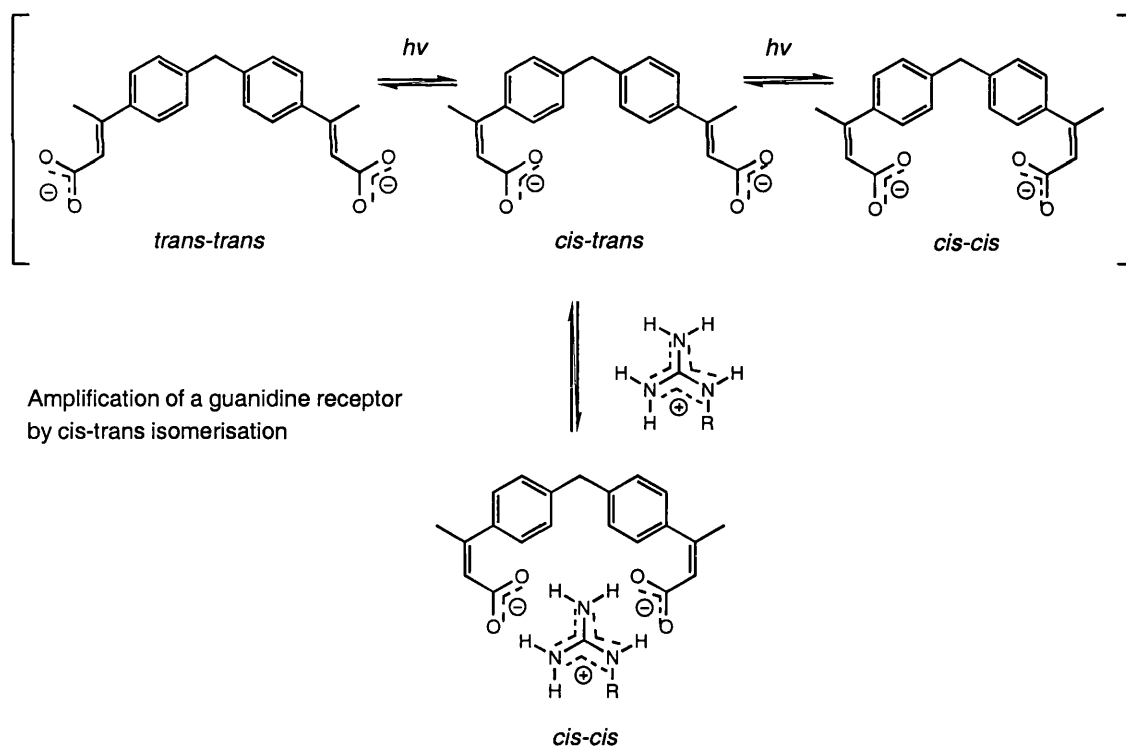
Disproportionation of A-SS-B in the presence of Ac(D)Pro(L)Val(D)Val-PS [88]

	A-SS-B	\rightleftharpoons	B-SS-B	A-SS-A
Absence of resin bound tripeptide [88]:	43%		57%	
Presence of resin bound tripeptide [88]:				
i) solution phase	13%		85%	10%
ii) resin phase	2%		0%	75%

Table 2

A mixture of ASH [85] and BSH [86] was then equilibrated in the presence and absence of the resin bound peptide (Table 2). As can be seen from the table, an equilibrium shift in favour of ASSA [87] was observed when the tripeptide [88] was present. This receptor [87] was conveniently isolated from the beads in >99% purity, allowing easy identification, a detail which will become important if this technique is applied to systems where the structure of the receptor is not known in advance.

Another receptor based library was reported by Eliseev⁸⁸ using the reversible isomerisation of *cis/trans* double bonds to isolate receptors for arginine (Scheme 22). In this case, as in most others, the DCL chosen was small and the aim of the research was more to demonstrate the potential of the technique rather than to use it as a tool for identifying useful macromolecules. The unpredicted identification of novel ligands or receptors using this method remains an experimental challenge.



Scheme 22

1.5 CONCLUSIONS

The field of artificial enzymes is a rapidly evolving subject. As the barriers between chemistry and biology become less distinct a range of new methods which combine expertise from both areas are developing. In recognition that the *de novo* design approach can be time consuming, a trend in all these techniques is the use of 'selection approaches'. The natural process of selection and amplification is after all, the way in which enzymes have evolved their sophisticated function.

The basic problem in artificial enzyme synthesis is choosing the selection event. Experimentally, selection based on binding affinity is the easiest method to use. However, many methods which have employed binding criteria, using TSA's as the ligands, have stopped short of producing the rate accelerations required to rival natural enzymes. This is perhaps predictable, since the electrostatic and geometric fidelity of a TSA to the real transition state cannot be entirely complete. To a certain extent the effect of this problem can be alleviated by introducing an element of design into the system. Using information available on the natural enzyme mechanism and catalytic groups, several researchers have improved the rate accelerations available with TSA methods by incorporating catalytic groups into TSA binding (*vide supra* catalytic antibodies and MIPs).

A problem with chemical applications of a binding-selection process can be the vast array of permutations of structures possible. This has been a problem in polymer approaches causing heterogeneity of binding sites, and can hinder combinatorial methods because identification of the desired binder may not be possible with so little material. This latter problem is not so prominent in biochemical equivalents where amplification of the selected candidate is carried out routinely. The emergence of dynamic selection approaches in combinatorial chemistry, such as DCLs may solve some of the chemical problems of isolating macromolecular receptors from complex combinatorial libraries. In this case, theory predicts that of all the possible library molecules, only those which favour binding will be produced in significant quantities. This should make deconvolution and identification a much easier process. Moreover,

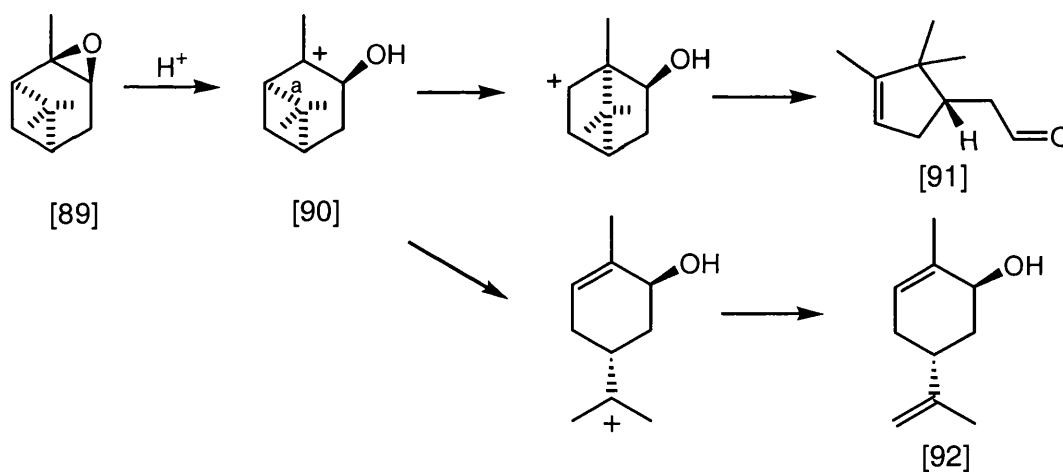
the concept of equilibrating a reversible library of compounds in the presence of a resin bound ligand (TSA), then freezing the reaction, filtering off the solution and isolating a solid phase bound receptor(s) synthesized under thermodynamic control is intellectually attractive. However, the problem with this method, and all others using a TSA strategy, remains the fact that the property required; catalytic activity, is not involved in the selection criteria.

Recent molecular biology approaches (and some combinatorial chemistry methods) have focussed on using catalytic activity as the selection criteria. This strategy has been employed with success in the field of *in vitro* evolution and has necessitated the development of experimental methods, also common to combinatorial chemistry, which allow the simultaneous screening of many reactions for catalysis. IR thermography represents an important development in this respect and will probably be influential in future research into artificial enzymes. Whilst *in vitro* evolution methods use catalytic selection directly it seems likely that catalytic antibody and chemical approaches to artificial enzymes will continue to maintain an element of TSA binding and design.

***Part 2.* RESULTS AND DISCUSSION**

Chapter 1. INSIGHTS INTO THE DESIGN AND SYNTHESIS OF ENZYMES

The aim of this project is to produce an enzyme mimic, based on the molecular imprinting approach, which is able to induce selectivity in a reaction by stabilising the transition state of the desired product. The reaction chosen for study is the acid catalysed ring opening reaction of α -pinene oxide [89]. We hope to favour formation of the commercially important *trans*-carveol [92] over campholenic aldehyde [91] which is usually the major product (Scheme 23). Interestingly, both products can be derived from the same carbocation intermediate [90] and also require participation of the same covalent σ bond (bond a, Scheme 23) in breaking the four membered ring to afford the products [91] and [92]



Scheme 23

We wish to investigate and expand upon the types of polymer systems amenable to the molecular imprinting technique with the aim of producing more ‘enzyme-like’ polymers. The molecular imprinting process⁴⁴ produces rigid macroporous polymer monoliths which are usually ground before use. These materials are very robust, however, whilst this is a desirable attribute in their main use as chiral HPLC phases, it may not be quite as advantageous in artificial enzyme applications. Enzymes are after all, highly flexible molecules and as Teague has illustrated in a recent review¹¹, they are capable of undergoing conformational change to adapt to bind particular substrates. As

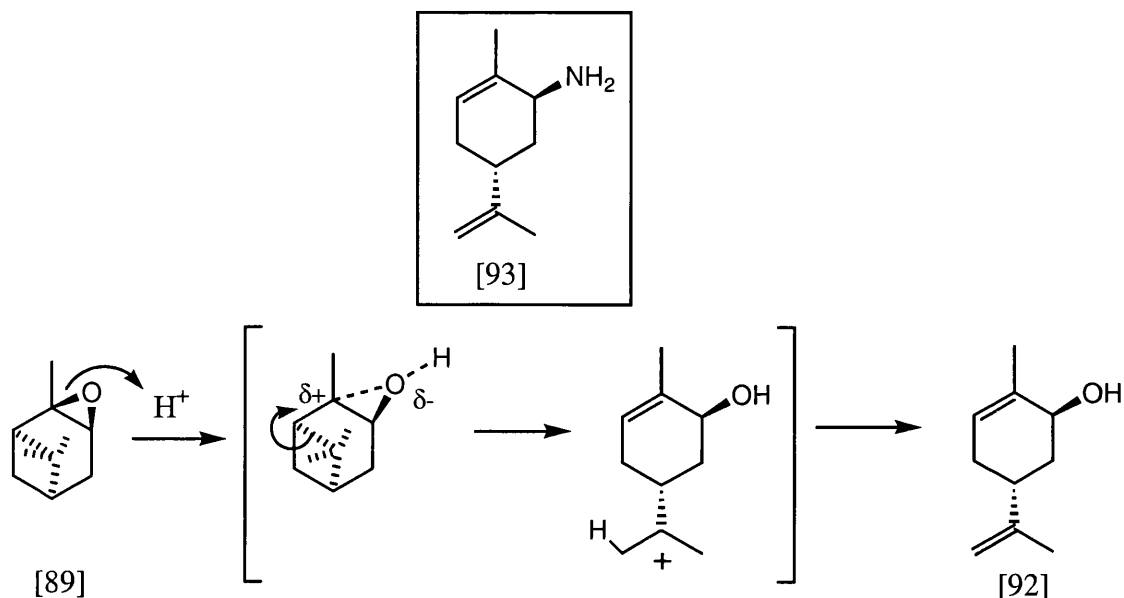
this property is likely to have a significant influence on the chemistry of enzymes it is important to take the general structural features of enzymes into consideration when designing artificial counterparts. Furthermore, most examples of MIPs reported involve the use of very hydrophobic polymers, which do not well represent the electrostatic environment in natural enzymes.

We also hope to address some of the problems associated with molecular imprinting, particularly the heterogeneity of the recognition sites, by introducing an element of design. Much has changed in the field of artificial enzymes and in molecular imprinting since this study began, and this is reflected in the work described here which is discussed, as far as is possible, in chronological fashion.

Chapter 2. POLYSTYRENE-DIVINYLBENZENE MOLECULARLY IMPRINTED POLYMERS

2.0. Choice of the polymer system and imprint molecule.

Our initial studies focussed on the use of polystyrene-divinylbenzene MIPs since the formation and use of such polymers was well characterised in the literature at that time⁸⁹. The crude transition state analogue (1*R*, 5*R*)-trans-carvyl amine [93] was chosen as the imprint molecule (Scheme 24).



Scheme 24

We reasoned that the shape of carveyl amine [93] could mimic a late transition state for the formation of *trans*-carveol [92], whilst the amino group could be used to position an acidic functional group in the complementary MIP binding site, at a suitable position to deliver a proton for catalysis of the epoxide ring opening reaction. This latter feature can be achieved by the use of an acidic ‘functional monomer’ in the polymerisation mixture which can pre-organise to form a salt with the amine [93], before incorporation into the polymer matrix, as we have seen in section 1.2.1, which summarised the molecular imprinting process.

The functional monomer must not only be acidic, but should also have similar reactivity to the styrene monomer and divinylbenzene crosslinker to allow for incorporation into the polymer during the early stages of polymerisation⁹⁰. The functional monomer chosen, 4-styrenesulfonic acid [94] and the imprint molecule [93] are expected to interact as depicted in Figure 16 below.

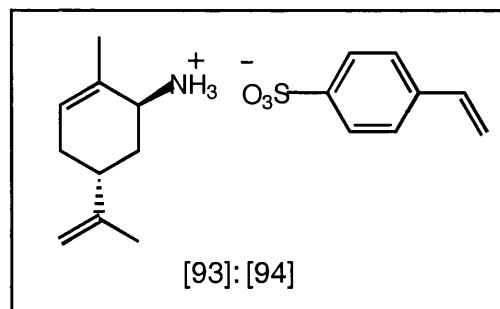
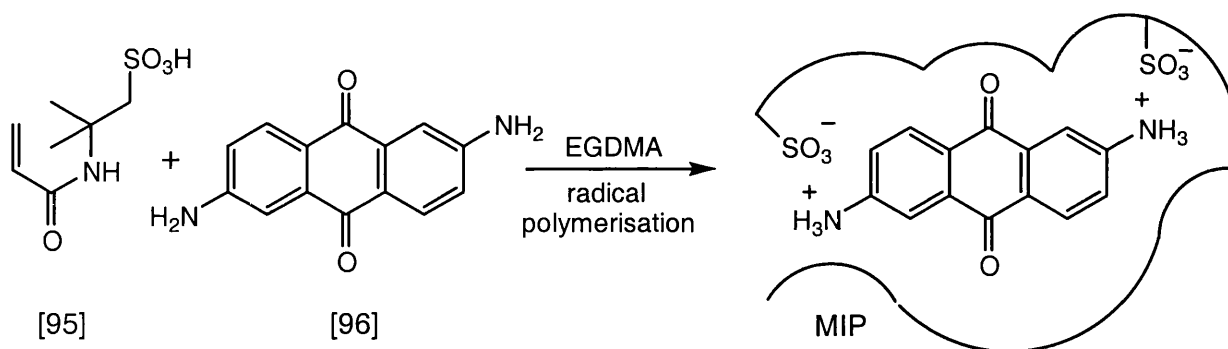


Figure 16

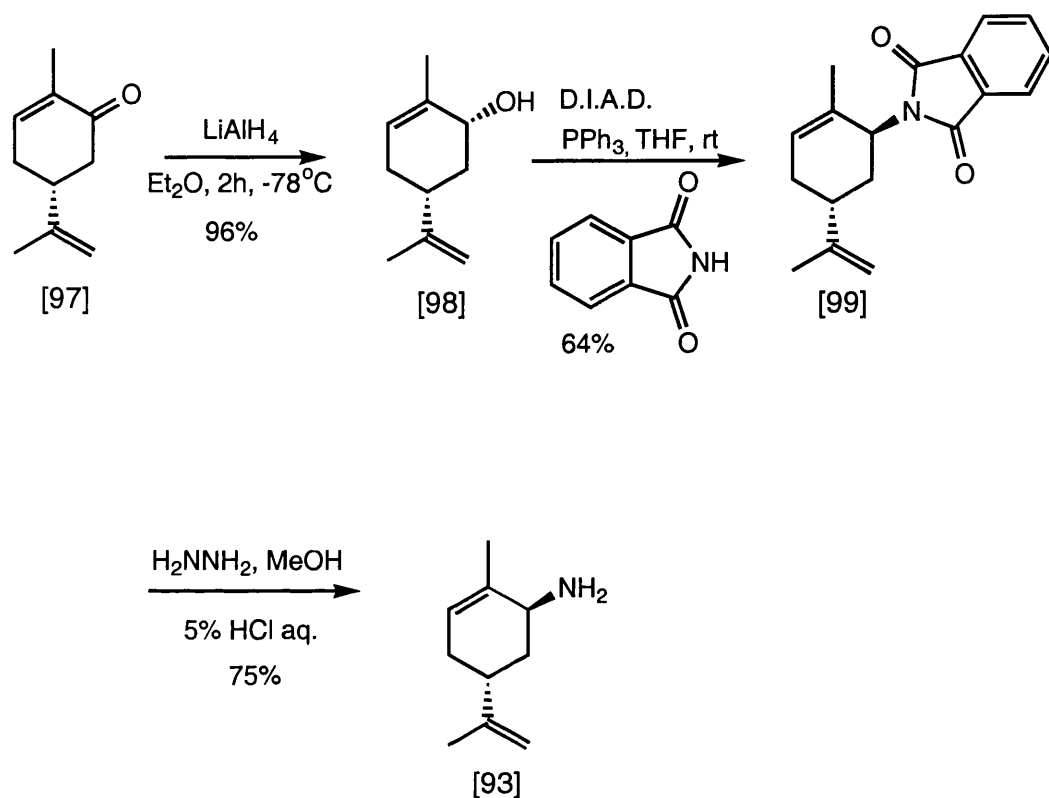
We were encouraged in this hypothesis by the fact that a similar interaction had been used successfully in ethylene glycol dimethacrylate (EGDMA) MIPs. Sherrington *et al* have successfully used 2-acrylamido-2-methylpropanesulfonic acid [95] as the functional monomer in the molecular imprinting of 2,6-diaminoanthraquinone [96]⁹¹. The monomer [95] is allowed to pre-arrange around the imprint molecule [96] before co-polymerisation with EDGMA. The template molecule is bound to the polymer matrix by salt formation with the sulfonic acid monomer and was removed by washing with DMSO and then acid (Scheme 25). Similar attempts to use methacrylic acid as the acidic functional monomer produced polymers with no selectivity for the template molecule [96]⁹¹. This was attributed to the inability of the carboxylic acid moiety of methacrylic acid to form an effective interaction with the weakly basic aromatic amino group.



Scheme 25

2.1 Synthesis of the imprint molecule.

The imprint molecule, (1*R*, 5*R*)-*trans*-carvyl amine [93] was readily prepared in a three step route from (*R*)-carvone [97] (Scheme 26).



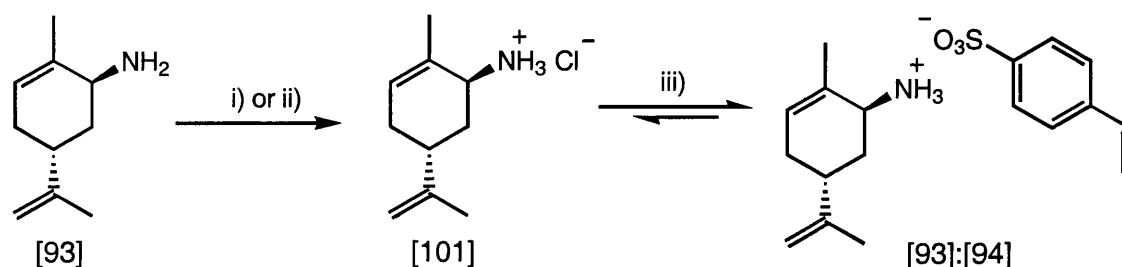
Scheme 26

The first step involves stereoselective reduction of (*R*)-carvone [97] to give (-)-*cis*-carveol [98] in 96% yield and 85% optical purity. The alcohol is then converted into the phthalimide derivative [99] in good yield using a modified Mitsunobu procedure with diisopropyl azodicarboxylate (D.I.A.D). The desired (1*R*, 5*R*)-*trans*-carvyl amine [93] is then released using a modified Inge-Manshe procedure at room temperature. In the event, the reaction was slow. However, since refluxing hydrazine hydrate conditions have been reported to cause significant allylic rearrangement to these systems⁹², the room temperature conditions were deemed to be preferable.

2.2 Synthesis of the polymers.

Due to the inherent instability of the functional monomer, 4-styrenesulfonic acid [94], it is not commercially available, but can be derived from the more stable 4-styrenesulfonic acid sodium salt [100]. We therefore decided to first form the amine hydrochloride [101] and then add this to an equimolar quantity of 4-styrenesulfonic acid sodium salt in

an organic solvent such that precipitation of sodium chloride would favour formation, and facilitate isolation, of the desired product [93]:[94] (Scheme 27).

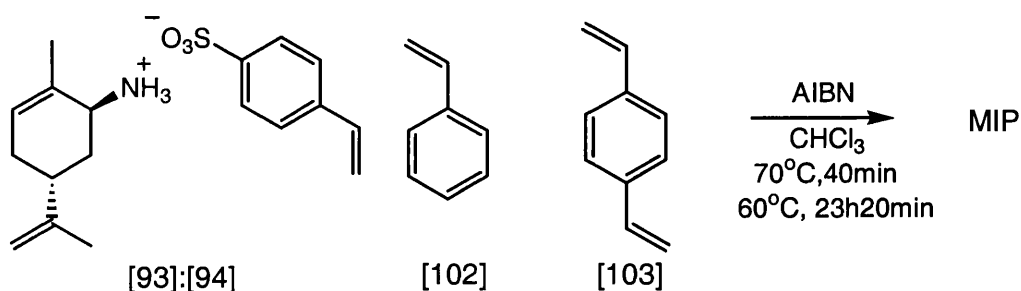


- i) MeOH:AcCl 1:20
- ii) Et₂O:HCl 1.2M
- iii) 4-styrenesulfonic acid sodium salt[100]

Scheme 27

Although several methods of salt formation were attempted, in practice formation of the desired 4-styrenesulfonic acid, (1*R*, 5*R*)-*trans*-carvyl amine salt [93]:[94] never went entirely to completion. However, as it is possible experimentally to remove any remaining 4-styrenesulfonic acid sodium salt [100] by simple precipitation in chloroform this should not pose any problem. In some cases, an excess of the imprint molecule relative to the functional monomer is expected to have a beneficial effect, since the equilibrium between the salt [93]:[94] and the free species in the polymerisation solution should be shifted towards the former⁹³. The resultant effect of this should be to reduce the number of functional monomer units that are randomly incorporated in the polymer. In our case, the presence of an excess of the hydrochloride salt [101] should not create a problem since complementary cavities formed in a styrene-divinylbenzene MIP would contain no functionality and as such, would have no influence on the overall catalytic activity of the polymer.

The crude salt [93]:[94] formed was accordingly used in the polymer forming step, since prolonged manipulation was precluded by the low stability of the product. The number of equivalents of the desired salt [93]:[94] present in the mixture was calculated using the molar ratio of the hydrochloride salt [101] to the desired salt [93]:[94] as indicated by ¹H NMR.



Scheme 28

A range of polymers of varying styrene [102] to divinylbenzene [103] ratios were synthesised with various loadings of imprint molecule complex [93]:[94] (Table 3). The relative quantities of the reagents will be reflected in the degree of crosslinking and will have important consequences on the molecular recognition properties of the MIPs produced⁹³ (*vide infra*).

Polymers synthesised with (1*R*, 5*R*)-*trans*-carvyl amine [93] as imprint molecule.

Polymer	[#] crosslinker :monomer ratio	^{\$} loading	styrene [102]/mmol	divinylbenzene [103]/mmol	[93]:[94] /mmol
[A]	6:1	1/35	2.15	12.9	0.43
[B]	3:1	1/35	1.3	3.8	0.43
[C]	2:1	1/35	5.0	10.0	0.43
[D]	2:1	1/15	2.15	4.3	0.43
[E]	3:1	1/10	1.1	3.2	0.43

Table 3

^{\$}**Loadings:** Loadings refer to the ratio of the number of moles of salt [93]:[94] to the total number of moles of polymerisable molecules. A higher loading indicates more sites per unit volume of polymer.

For example; in the case where salt [93]:[94] (1.0mmol) is polymerised with styrene (2.0mmol) and divinylbenzene (4.0mmol), the loading is 1/6.

[#]**Crosslinker monomer ratio (c:m):** The crosslinker:monomer ratio is the ratio of moles of divinylbenzene to styrene. A higher ratio indicates a higher level of crosslinking.

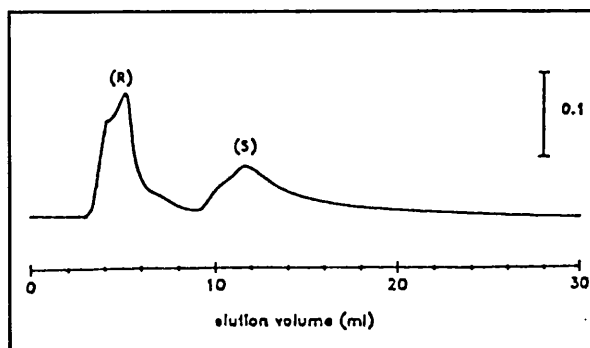
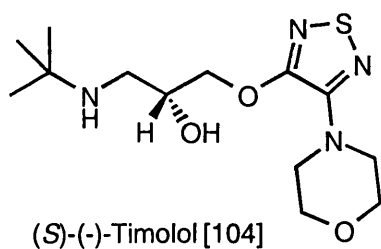
For example; in the case where salt [93]:[94] (1.0mmol) is polymerised with styrene (2.0mmol) and divinylbenzene (4.0mmol), the crosslinker:monomer ratio is 2:1.

The solvent or 'porogen' chosen was chloroform (1.7v/v of polymerisable molecules) and the radical initiator was AIBN (2mol% per polymerisable double bond).

The nature of the polymers produced perhaps needs some elaboration. Molecular imprinting involves the synthesis of 'macroporous' polymers. They are formed when a porogen* is present in the polymer mixture which causes phase separation during the polymerisation reaction. The porogen acts as a template for the permanent porous structure of the resin and at full conversion the polymer is composed of a crosslinked polymer phase and a discrete porogen or solvent phase. The porous structure of the polymer is thus highly dependent on the choice of porogen, its compatibility with the incipient polymer matrix and the level at which it is used. After removal of the porogen under vacuum, the polymer retains the porous structure even in the dry state and this can be observed experimentally by microscopy. This ability to retain the shape of the polymer is due to the highly crosslinked nature of the polymer. Thus, in our case, it is divinylbenzene which creates the highly rigid structure. The polymers synthesised in this manner are insoluble solid monoliths with high surface areas. The pore structure can be accessed by most solvents (even water⁹¹), a phenomenon which is manifested physically in the 'sponge-like' characteristics of the polymers; solvent added to the dry polymers is absorbed and can cause them to swell to twice their dry volume.

Most optimisation of MIP polymer matrices has revolved around their application in the field of chromatography^{94a,b}. An MIP is created against an enantiomer of a substrate and the polymer is then used as chiral stationary phase to separate the racemate. An early example involving the separation of (*S*)-(-)-timolol [104] is shown below⁹⁵ (Fig 17).

* 'Porogen' is the name given to the solvent used in the polymerisation mixture. It can represent any inert substance which causes phase separation during the polymerisation process and which does not participate in the polymerisation radical reaction.



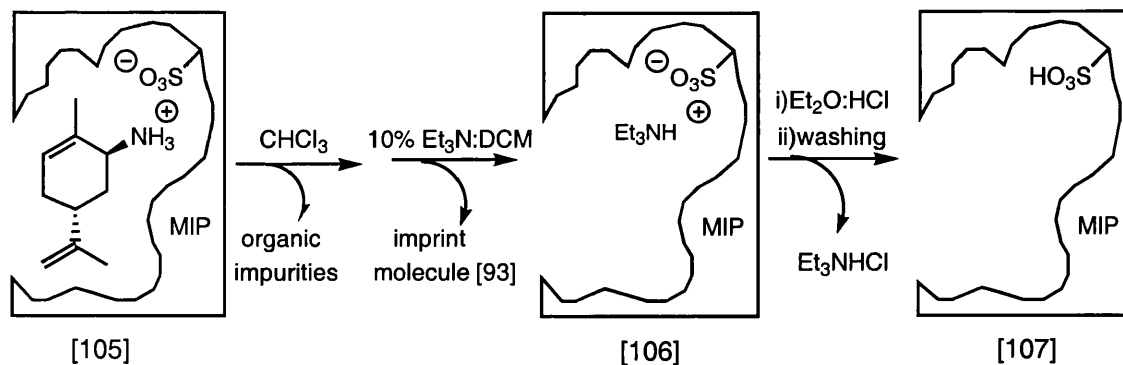
i) Chromatographic resolution of the (*S*)-enantiomer of (*rac*)-Timolol using an MIP with a methacrylic acid monomer and EGDMA crosslinker. Eluent ethanol/THF/acetic acid (50/40/10 v/v/v). Sample volume 20 μ L containing 20 μ g of *rac* [104]. Flow rate 1 mL/min, 30bar.

Figure 17

However, the criteria desired for MIPs used as HPLC chiral columns and for artificial enzyme mimics, might well be expected to be different. In the former case MIP matrices have been optimised for rigidity, robustness under pressure and binding characteristics, however, only the last of these features need necessarily be important to artificial enzyme applications. The series of polymers [A] to [E] above, was therefore synthesised to investigate the effects of crosslinking content and loading on polymer properties. Although the effect of crosslinking content on polymer rigidity is well established, the effects of loading are not so clearly understood.

2.3 Polymer Regeneration.

Before testing the polymers for catalysis it was necessary to establish that they displayed the desired molecular recognition properties. Binding studies should also give us useful information on the differences between the five polymers. In order to perform the binding studies we first needed to purify the crude polymers and remove the imprint molecule. Several methods of extracting the polymers with various solvents were investigated before settling on the process described in scheme 29.



Extraction of crude M.I.P.'s [A]*, [B]*, [C]*, [D]*, and [E]*.

Scheme 29

Firstly the polymer was ground and washed with chloroform. This removes AIBN decomposition products, any unreacted styrene or divinylbenzene and the amine hydrochloride impurity, as determined by ^1H NMR comparison with authentic samples. The (1*R*, 5*R*)-*trans*-carvyl amine [93] imprint molecule is then removed by washing with 10% triethylamine in DCM. The advantage of this over washing directly with acid is that it is possible to concentrate these fractions *in vacuo* and determine the amount of imprint molecule bound in the polymer. The MIP was then stirred in ethereal HCl to displace the bound triethylamine and generate the desired sulfonic acid in the active site. The polymer was exhaustively washed to neutral pH and dried *in vacuo* to afford the active MIPs [A]* - [E]*. Initially, we used protocols employing aqueous acid and base but these methods proved problematic due to the hydrophobicity of the polymers, as did the use of higher boiling point organic acids and bases such as pyridine and acetic acid. These latter organic reagents were difficult to remove and in the case of pyridine the high vacuum required to concentrate the fraction also led to loss of the imprint molecule [93].

2.4 Binding Studies.

With the active MIPs [A]* to [E]* in hand, it was then possible to carry out the binding studies. In most literature examples the MIP is packed into an HPLC column and used as a chiral stationary phase to evaluate the effectiveness of imprinting. During its passage down the column the imprinted molecule will be adsorbed into the cavity and then desorbed many times. Globally, since it spends more time in the pocket than a

foreign molecule such as its enantiomer, it will be eluted more slowly. However, this may not represent the best method for analysing the properties we desire. Catalytic MIPs must be able to absorb a molecule that has the choice of remaining in solution, which is a more challenging experimental requirement than retention on a column. Monitoring this process over time should provide information on the accessibility of binding sites as well as their fidelity to the imprint molecule. Since, as indicated earlier (and discussed in detail in section 3.5), the binding cavities produced using molecular imprinting are heterogeneous, a very selective binding site which is buried deep in the polymer may have less of an influence on the reaction outcome than a 'loose fitting' site on the polymer surface. We thus needed a method which would not only evaluate binding but which would also give an idea of the availability of the active sites. Using a protocol developed in our lab⁹⁶ the experimental setup depicted below was used for the binding studies (Figure 18 and Scheme 30).

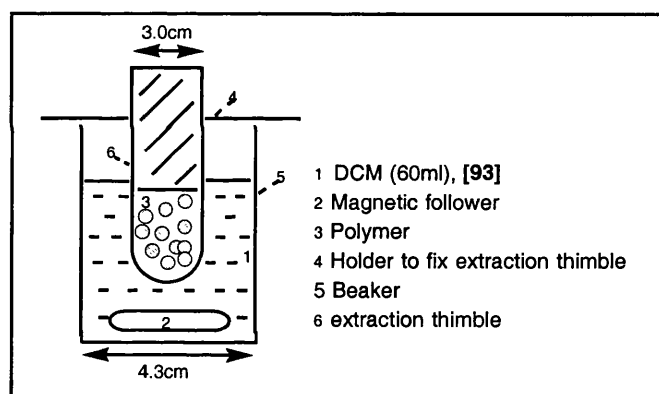
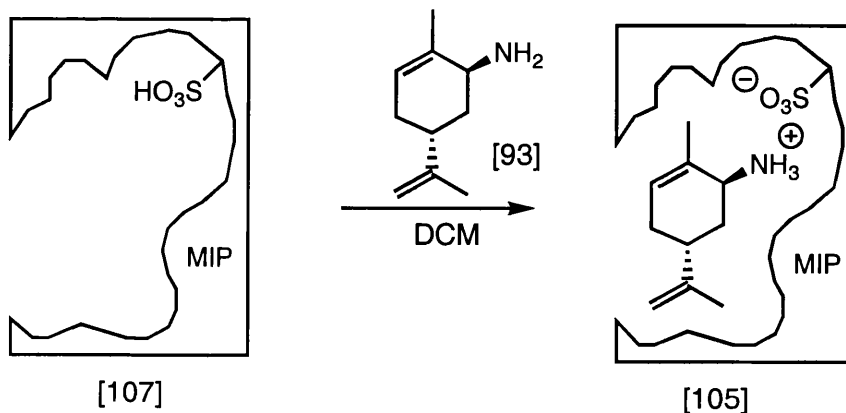


Figure 18



Binding studies on MIP's [A]*, [B]*, [C]*, [D]*. and [E]*.

Scheme 30

Using this method the rate at which the MIP absorbs the template [93] from solution can be determined. The imprint molecule [93] is stirred in solution with the MIP contained within an extraction thimble and the rate of absorbance of [93] by the polymer is monitored as a function of time.

It is important to note that a feature of this setup is that there is always a certain quantity of (1*R*, 5*R*)-*trans*-carvyl amine [93] present in the polymer due to non-specific binding. This is because the solvent absorbed by the polymer will naturally contain a certain amount of (1*R*, 5*R*)-*trans*-carvyl amine [93]. The approximation made is that the percentage of (1*R*, 5*R*)-*trans*-carvyl amine [93] present in the polymer due to 'non specific binding' is equal to the percentage of DCM absorbed by the polymer. In other words, we have assumed that the amount of (1*R*, 5*R*)-*trans*-carvyl amine [93] dissolved in the solvent absorbed by the polymer is unaffected by the polymer environment. To avoid overestimating the level of binding, the calculation of the amount of template bound in the polymer at each point in the binding study includes a correction factor to account for this phenomenon (Equation 1).

$$\text{template bound/mg} = y - x(a/b) \quad \text{Equation 1}$$

Where y = original weight of [93] (65.0mg, 0.43mmol, 1eq)

x = weight of [93] in remaining in solution

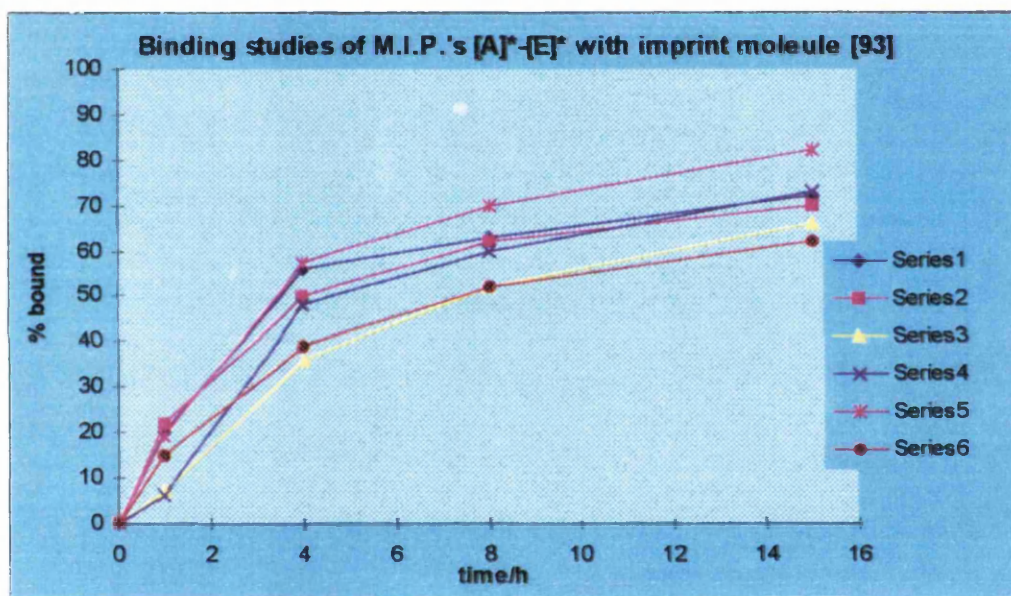
(a/b) = correction factor:

$$\frac{\text{original volume of DCM (60mL)}}{\text{original volume of DCM (60mL) - volume of DCM absorbed by polymer}}$$

The phenomenon of non specific binding can be observed experimentally: after equilibration of an MIP with the imprint molecule [93] in solution it is possible to remove a discrete amount of [93] from the MIP by washing with DCM. This represents the amount of 'non-specific binding', however, in order to remove the remaining bound

(1*R*, 5*R*)-*trans*-carvyl amine [93] ([105] Scheme 30) it is necessary to wash with acid or base.

The results of the binding studies are illustrated below (Figure 19). The MIPs [A]* to [E]* were stirred with the same quantity of (1*R*, 5*R*)-*trans*-carvyl amine [93], 0.43 mmol that was used in the initial imprinting. The percentage of this amount which binds to the polymer (the value used for the y axis), at the end of the experiment thus represents the 'yield of imprinted sites' in the polymer (Table 4).



Series 1 [A]* loading 1/35, c:m 6:1; Series 2 [B]* loading 1/35 c:m 3:1; Series 3 [C]*, loading 1/35 c:m 2:1; Series 4 loading 1/15 c:m 2:1; Series 5 loading 1/10 c:m 3:1.

The graph shows the uptake of imprint molecule (1*R*, 5*R*)-*trans*-carvyl amine [93], by MIPs [A]*-[E]*, from a stirred solution of [93] in DCM (0.43mmol [93], 60mL DCM) over time. Binding studies were carried out at 0°C

Figure 19

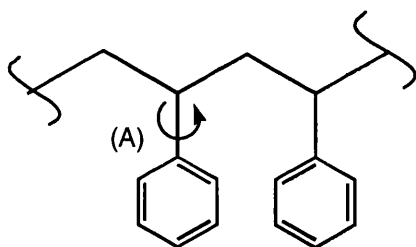
MIP	[A]*	[B]*	[C]*	[D]*	[E]*
yield of imprinted sites	72%	66%	73%	82%	62%
no of mmol of acid sites	0.31	0.28	0.31	0.35	0.27

Table 4

The results from this study demonstrates the advantage of using a method that allows the binding process to be evaluated over a period of time. Important information can be gleaned from the relative amounts bound at the beginning of the binding study as well as the final value of the 'yield of imprinted sites'. Perhaps the most striking feature is the length of time needed for the polymers to reach the equilibrium binding situation. Since most literature reports use HPLC for binding studies, a sense of how long the process takes was not previously available. A slow binding process is a distinctly undesirable feature for MIPs in catalytic applications, as the active sites need to be readily accessible. The experimental setup with the extraction thimble creating a barrier may lengthen this time artificially, but this is not expected to completely account for the above result.

The binding studies also indicate that the crosslinker: monomer ratio is the dominant factor in determining the amount of imprint molecule [93] that is eventually bound. The values at the end of 15h show that a crosslinker: monomer ratio of 2:1 produces a high 'yield of imprinted sites' with the polymers at 1/15 and 1/35 loading being first and second respectively. Similarly, the different loadings of MIPs [B]* and [E]*, both with a crosslinker: monomer ratio of 3:1, do not seem to have as great an influence as the crosslinking content: both MIPs have a low binding yield of 62-66%.

Different information can be gained from looking at the left-hand side of the graph. Details of the kinetic accessibility of the polymers can be inferred from the percentage of imprint molecule bound to the MIPs at the early stages of the binding study. Comparing MIPs [A]*, [B]* and [C]* all with the same loading (Series 1, 2 and 3 respectively) it can be seen that by using a low crosslinking content the rate at which the polymers absorb the imprint molecule (*1R, 5R-trans-carvyl* amine [93]) is decreased. This is expected since lowering the crosslinking content is expected to decrease the porosity of the MIPs making the binding sites less accessible. The polymers are very rigid and inflexible, in fact, even in the absence of crosslinking, movement of the polymer chains within the polymer is limited. In polystyrene in the solid state at room temperature individual polymer chains cannot migrate relative to each other and rotation about the bonds in the polymer backbone is very inhibited. Only rotation (A) about the phenyl side-chains occurs freely at room temperature (Figure 20). The level to which this restriction of movement is alleviated upon addition of solvent is dependent on the compatibility of the solvent to the polymer matrix and, in the case of macroporous polymers, to the degree of crosslinking.



Bond rotation in polystyrene in the solid state at room temperature.

Figure 20

The effect of lowering the crosslinking content on the rate at which the polymers absorb the imprint molecule seems to be counteracted by increasing the loading. MIPs [D]* and [E]* absorb the imprint molecule much faster than their lower 1/35 loading counterparts [C]* and [B]* respectively. However, no clear conclusion can be drawn for the effect of loading on the final yield of imprinted sites. More polymers would need to be synthesised for such a study.

In order to gain some direct experimental evidence for the differing MIP structures. Scanning electron microscope pictures were taken of MIPs [A]*, [D]* and [E]*. It can be seen from the pictures (Figure 21) that MIP [A]* has a much better defined porous structure which is attributed to the higher level of crosslinking in this MIP.

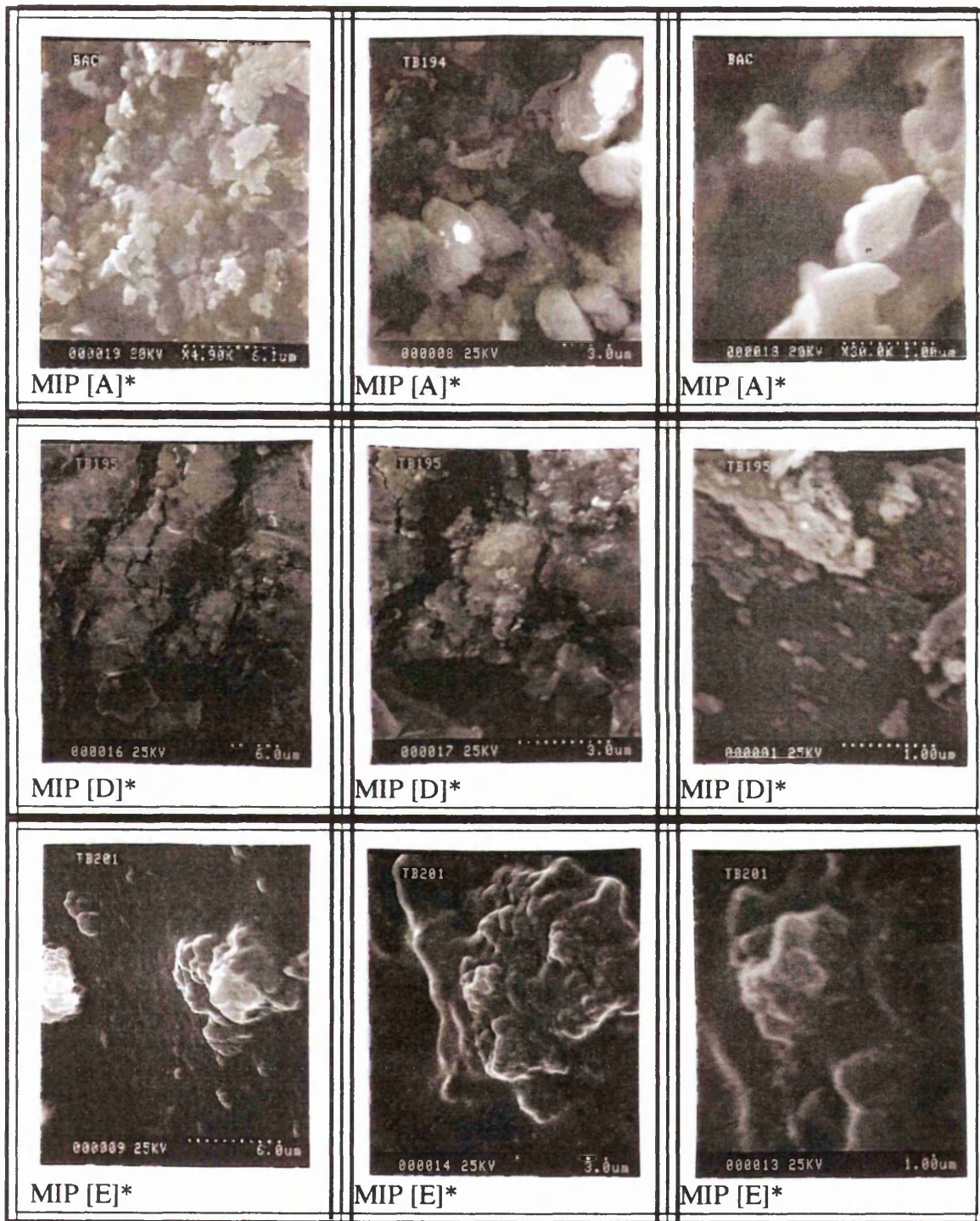
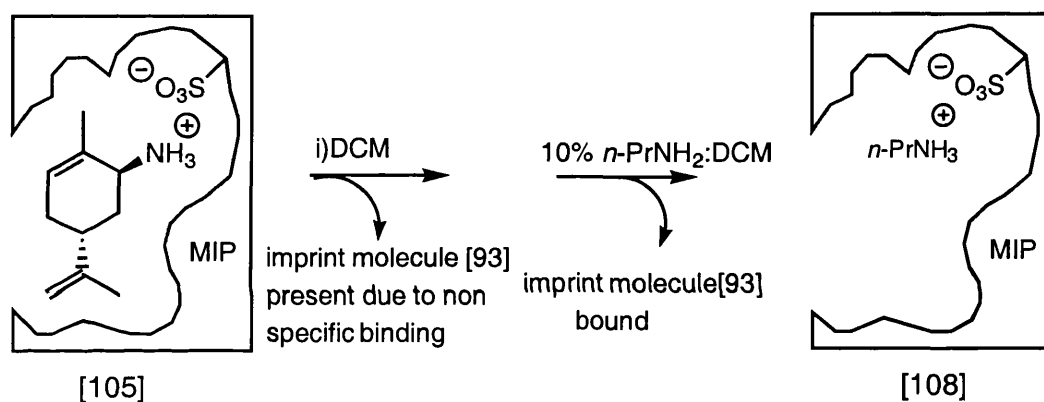


Figure 21
S.E.M Picture of MIP's [A]*, [D]* and [E]*

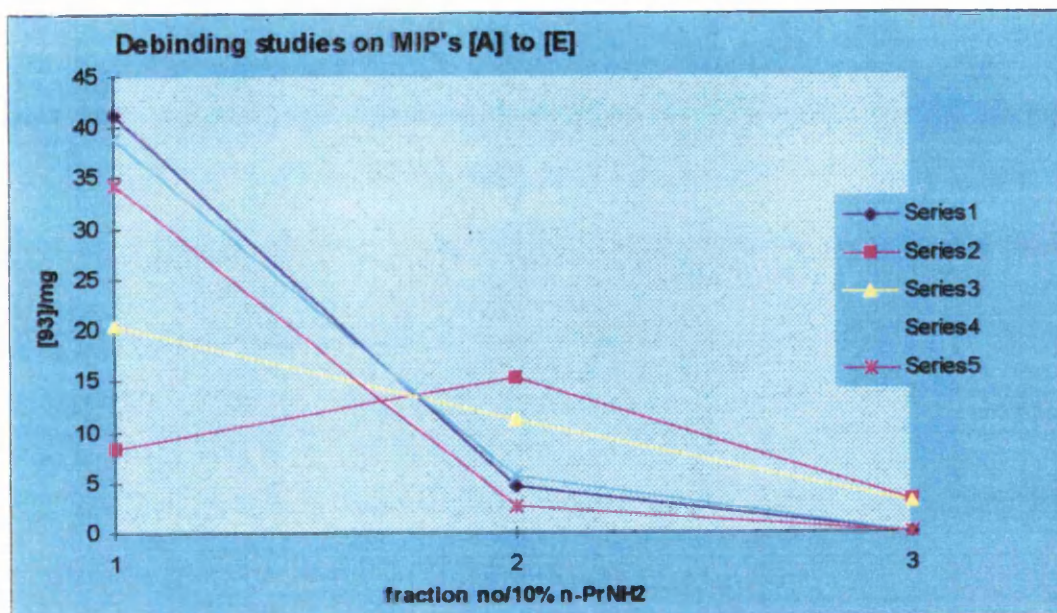
At the end of the binding studies the MIPs contain (1*R*, 5*R*)-*trans*-carvyl amine [93] in the polymer cavities (Scheme 31). Confirmation of the results obtained in the binding studies was then obtained from analysis of how easily the polymers subsequently released this imprint molecule into solution. Firstly the (1*R*, 5*R*)-*trans*-carvyl amine [93] present in the polymer due to non-specific binding was removed by washing with DCM. The bound (1*R*, 5*R*)-*trans*-carvyl amine[93] was then removed by stirring the MIP[#] with successive fractions of 10% *n*-PrNH₂:DCM. The low boiling point of *n*-propylamine means that each fraction can be concentrated *in vacuo* and analysed by ¹H NMR to give the amount of (1*R*, 5*R*)-*trans*-carvyl amine [93] released.



Debinding Experiments: MIP's were stirred with 60mL fractions of DCM(3x1h/60mL/0 °C), then 10% *n*-PrNH₂:DCM(3x2h/60mL/0°C).

Scheme 31

[#] The experimental setup used for the debinding studies was exactly the same as previously described for the binding studies figure 18.

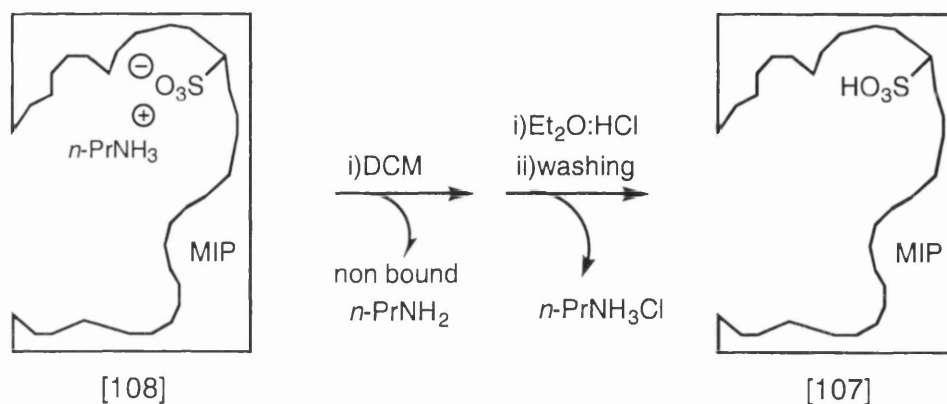


Series 1 [A]* loading 1/35, c:m 6:1; Series 2 [B]* loading 1/35 c:m 3:1; Series 3 [C]*, loading 1/35 c:m 2:1; Series 4 loading 1/15 c:m 2:1; Series 5 loading 1/10 c:m 3:1.

Figure 22

Analysis of these results reveals a correlation with the binding studies. Both MIPs [B]* (Series 2) and [C]* (Series 3) are slow to release the imprint molecule. This is in accord with the slow rate of uptake of [93] by these polymers seen in the binding studies. It is also a further indication that in MIPs [B]* and [C]* the sites are less accessible. However, the debinding studies could also be interpreted as showing that these polymers display stonger binding affinity for the imprint molecule.

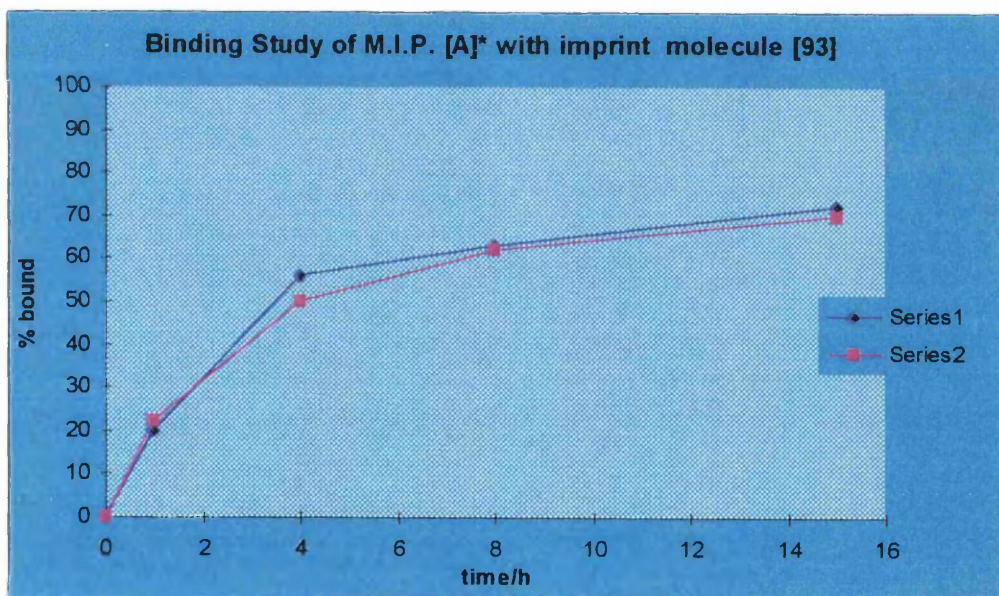
At the end of each debinding study, the MIP is expected to contain an *n*-propylammonium ion as the counter ion in the active site [108]. The polymers were thus regenerated according to the protocol described below in scheme 32.



Regeneration of M.I.P.'s [A]*, [B]*, [C]*, [D]* and [E]*: polymer s were contained within extraction thimbles and washed successively with 60mL fractions of solvent or ethereal HCl.

Scheme 32

In order to demonstrate that the regeneration was an efficient process, that the polymers were reusable, and furthermore, that the binding studies were reproducible, the binding study with polymer [A]* was repeated.

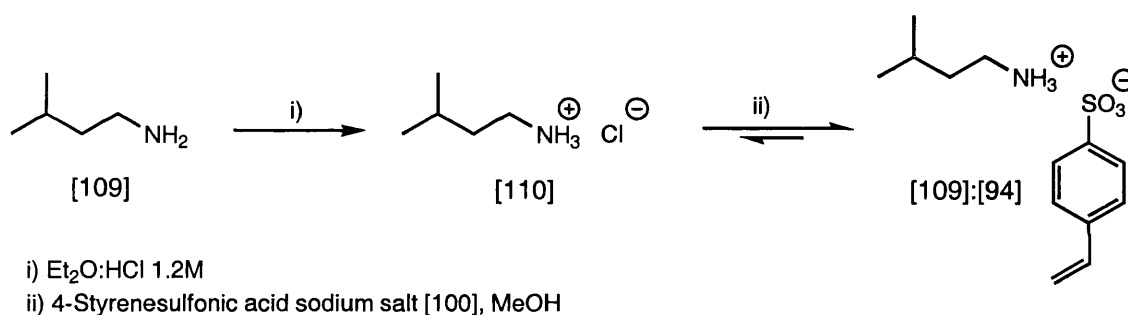


Series 1 [A]* loading 1/35, c:m 6:1; Series 2 [A]* loading 1/35, c:m 6:1 repeated

Figure 23

2.5 Synthesis of the reference polymer.

In order to study the effect of the MIPs on the outcome of the chosen reaction a blank polymer must also be made. Ideally this would be made with the functional monomer, styrene and divinylbenzene in the absence of the imprint molecule. However the instability of the functional monomer 4-styrenesulfonic acid and the insolubility of the sodium salt [100] under the polymerisation conditions meant that another approach had to be employed. Accordingly, we chose the small flexible amylamine [109] as the imprint molecule in the blank polymer as this molecule is small and should produce a very different shaped binding cavity in the MIP. The pre-organised complex was formed in exactly the same manner as for the (1*R*, 5*R*)-*trans*-carvyl amine [93] imprinted polymers (Scheme 33).



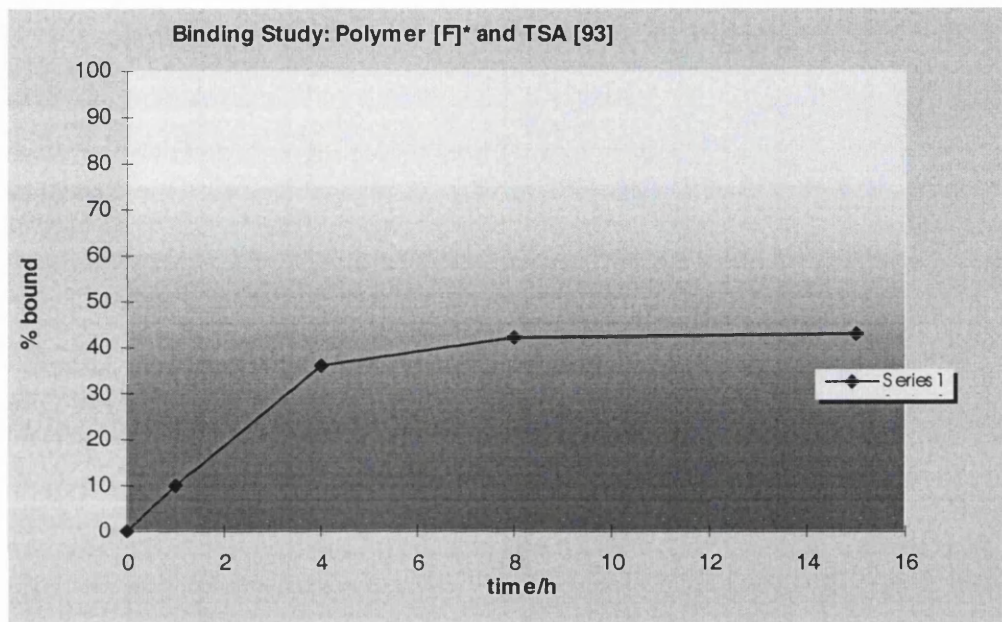
Scheme 33

The salt [109]:[94] was then polymerised with styrene and divinylbenzene as monomer and crosslinker respectively, under identical conditions to those previously described for the earlier MIPs. The loading and monomer:crosslinker ratio were chosen to be comparable with MIP [A].

Polymer	crosslinker :monomer ratio	loading	styrene [102]/mmol	divinylbenzene [103]/mmol	[109]:[94] /mmol
[F]	6:1	1/35	2.15	12.9	0.43

Table 5

The amylamine [109] was removed from the crude reference polymer and the active sulfonic acid residue was generated using an identical method to the one described previously for MIPs [A]*-[E]* to yield [F]*. The uptake of (1*R*, 5*R*)-*trans*-carvyl amine [93] by the blank polymer was then analysed using the binding study described above (Figure 24).



Series 1 [F]* reference polymer loading 1/35, c:m 6:1

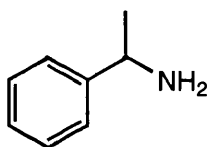
Figure 24

As expected the blank polymer absorbs much less (1*R*, 5*R*)-*trans*-carvyl amine [93] than the MIPs synthesised using [93] as the imprint molecule. The total percentage bound after 15h is 43% compared to a 71% average for MIPs [A]* to [E]*. The fact that some (1*R*, 5*R*)-*trans*-carvyl amine [93] is bound at all may be explained by salt interactions with sulfonic acid residues on the surface of the polymer, where the shape is expected to be less defined. Another explanation could be the presence of 'loose-fitting' imprinted sites which do not retain the size and shape of amylamine well enough to preclude binding of other small amines.

2.6 Competitive binding studies.

One of the best ways to determine the fidelity of the imprinted sites in MIPs [A]* to [E]* for the imprint molecule [93] is to carry out a competitive binding study. The MIP was suspended in solution containing a 1:1 mixture of the imprint molecule (1*R*, 5*R*)-*trans*-carvyl amine [93] and another ‘competitive’ amine. The solution was then stirred and after an equilibration period the ratio of the amines remaining in solution was determined. In the absence of an imprinted cavity the polymer should absorb equal amounts of both compounds.

Many factors may bias the data obtained with such a study and it was our intention to ensure that any selectivity observed could be interpreted directly as shape selectivity for the imprint molecule [93]. The ‘competitive’ amine chosen for the study was α -methyl benzyl amine [111] (Figure 25).



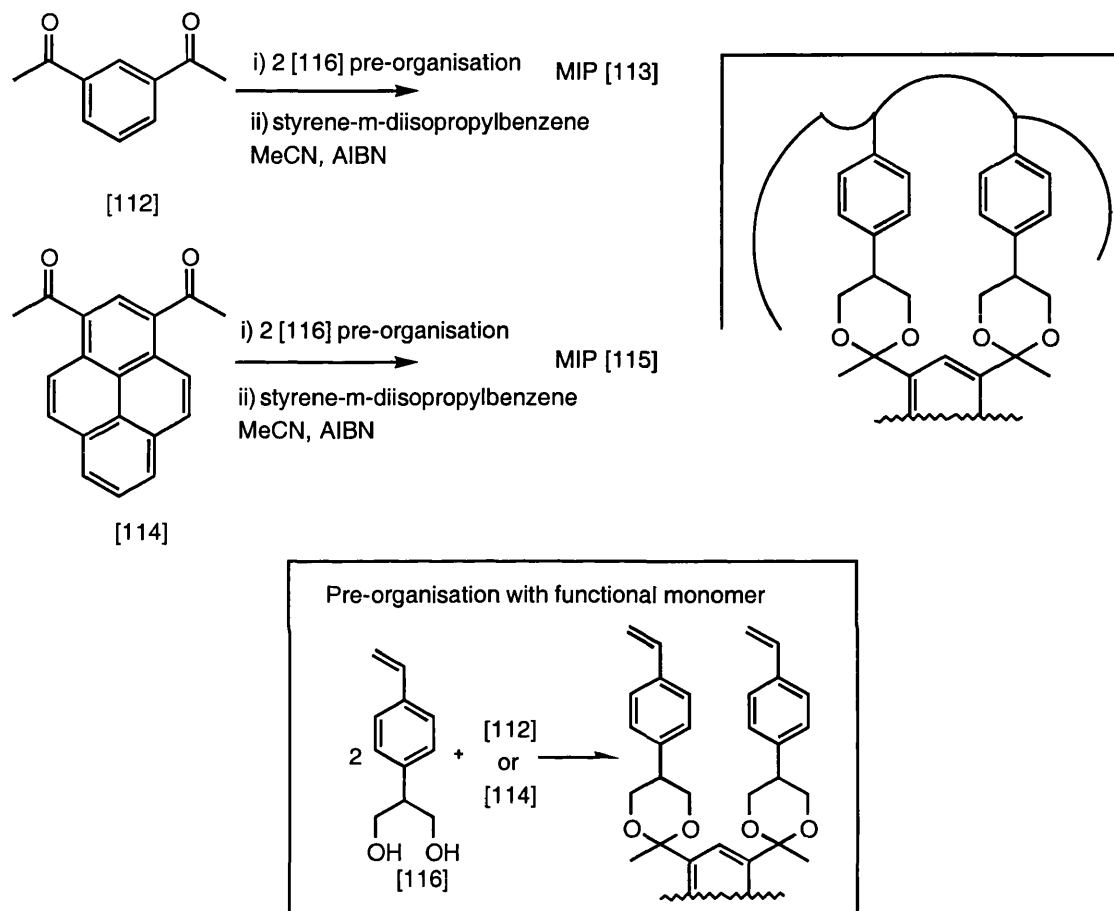
[111]

Figure 25

Several factors influenced the choice of this molecule. Firstly, the molecule is hydrophobic apart from the amino moiety. This should ensure that α -methyl benzylamine [111] is not excluded from the MIP due to incompatibility with the hydrophobic environment in the polymer. Indeed, the phenyl group might be expected to favour absorption of this molecule due to the possibility of π -stacking.

A further consideration is size. It has been shown that larger molecules will be excluded from the polymer active site on the basis of size alone⁹⁷. Shea and Sasaki created MIPs against the two imprint molecules [112] and [114]: MIP [113] and [115] respectively

(Scheme 34). In both examples the relative positioning of the two carbonyl groups is identical. As such the positioning of the functional groups should not influence the competitive rebinding of the two diketones. Any selectivity observed is predicted on the basis of shape.



Scheme 34

In a competitive rebinding study on polymer [113] employing equimolar amounts of diketones [112] and [114] the kinetic selectivity was 70:30 in favour of 1,3-diacetylbenzene [112]. Interestingly, in an identical study MIP [115] exhibited the *same* selectivity for the smaller diketone [112]. Under saturation binding conditions[#] this same MIP [115] binds equivalent amounts of [112] and [114] but still displays no overall selectivity for the larger imprint molecule [114]. The authors used these results to demonstrate the influence of shape, however, they also indicate that a larger molecule

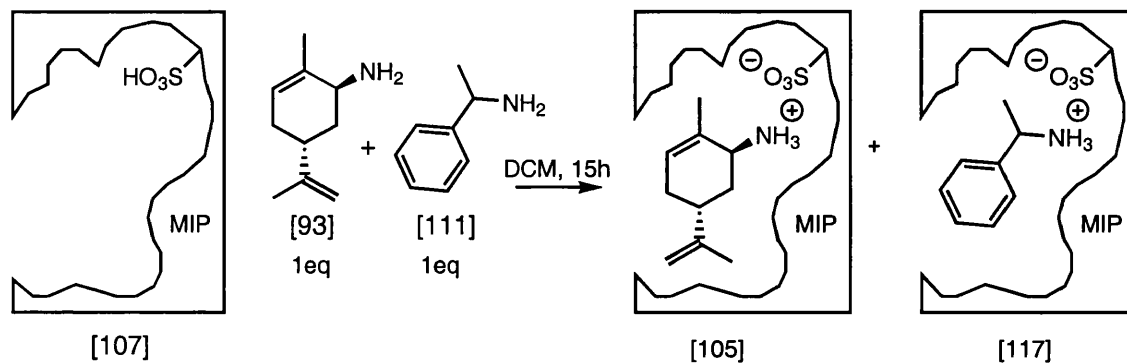
[#] The experimental details for the binding studies, or a definition of saturation and kinetic binding conditions was not available.

may be excluded from the MIP on the basis of size. In certain examples this may be a kinetic effect due to the slower rate at which the molecule is able to diffuse through the porous polymer matrix (as is probably the case in polymer [115]). However, in the case of MIPs [A]* to [F]* a larger molecule than (1*R*, 5*R*)-*trans*-carvyl amine [93] may also be excluded from the polymer binding cavity due to a size restriction. Whilst this hypothesis would lead to a favourable competitive binding result, with (1*R*, 5*R*)-*trans*-carvyl amine [93] being preferentially bound over a larger molecule, it would not provide information about the true shape of the active site. The similar size of competitive amine α -methyl benzylamine [111] was therefore an important attribute.

Finally, the boiling point of α -methyl benzylamine [111] is lower than (1*R*, 5*R*)-*trans*-carvyl amine [93]. The binding study employed involved indirect determination of the amines bound to the polymer. The ratio of the two amines [111] and [93] remaining in solution is calculated and the value is used to derive the ratio of amines bound. Any product lost during the evaporation of solvent before a ^1H NMR was obtained should therefore bias the study in the opposite sense to the desired result.

The considerations above should ensure that any selectivity observed in favour of the (1*R*, 5*R*)-*trans*-carvyl amine [93] can be interpreted as shape selectivity for the imprint molecule.

Competitive binding studies were carried out on three representative MIPs. [A]*, [D]* and the blank MIP [F]*. The setup was the same as for the binding studies (Figure 18). The regenerated MIPs were contained within an extraction thimble and a 1:1 mixture of (1*R*, 5*R*)-*trans*-carvyl amine [93] and [111] in DCM was added (Scheme 35).



Scheme 35

The value obtained for the 'yield of imprinted sites' in the binding studies was used to calculate the number of moles of sites in each polymer (Table 3 and 4). Using these values, one equivalent of each of the amines [93] and [111] was dissolved in DCM. The 1:1 ratio of the two amines was confirmed by ¹H NMR at the beginning of the experiment. The solution was then stirred with the polymer for 15h at the end of which time the solvent was removed *in vacuo* and the ratio of the amines remaining in solution was determined. This information allows indirect determination of the ratio of the amine (1*R*, 5*R*)-*trans*-carvyl amine [93] to [111] bound. The calculation required to establish the ratio of amines bound must take account of both the amount of compound remaining in solution, as well as the amount of imprint molecule bound non specifically. A detailed example of this calculation is described in Appendix 1. The results are listed below (Table 6).

MIP	[A]*	[D]*	[F]*
molar ratio [93]:[111] in solution after 15h	47:53	44:56	53:47
molar ratio [93]:[111] bound after 15h	56:44	56:44	47:53

Results of competitive binding studies in DCM (60mL) with (1*R*, 5*R*)-*trans*-carvyl amine [93] and α -methylbenzylamine [111]

Table 6

As can be seen from the table, the reference polymer [F]* leaves more (1*R*, 5*R*)-*trans*-carvyl amine [93] in solution whereas the imprinted polymers [A]* and [D]* appear to preferentially absorb the imprint molecule. The imprinting process has thus reversed the selectivity usually observed in this experiment. It is important to note that the reference polymer [F]* was not imprinted to recognise either of the molecules in the competition experiment, thus the apparent selectivity for α -methyl benzylamine [111] by MIP [F]* may well occur as a result of loss of [111] during removal of the solvent *in vacuo*. If this is the case, then the selectivity of the MIPs [A]* and [D]* for the imprint molecule is actually higher than indicated above.

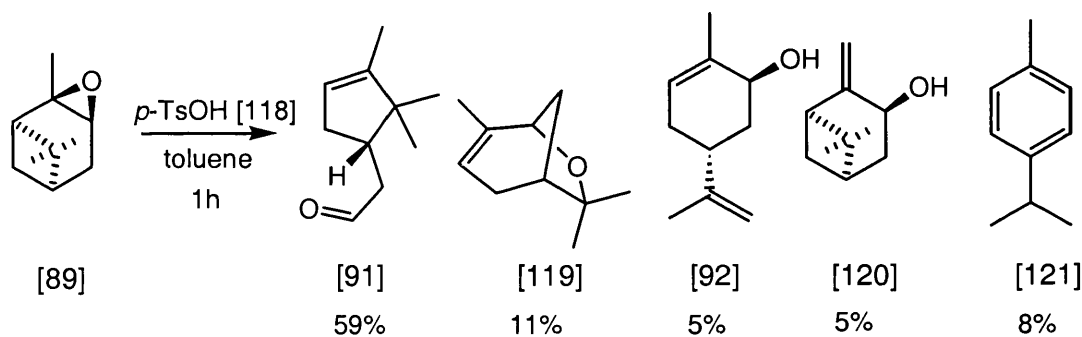
Attempts to directly determine the ratio of the amines bound in the polymer by extraction with 10% *n*-propylamine:DCM, were hampered by poor mass balances. The practical difficulty of removing the *n*-propylamine without loss of the competitive amine α -methylbenzylamine [111], led to a margin of error which was unacceptable.

Chapter 3. REACTIONS OF THE IMPRINTED POLYMERS WITH α -PINENE OXIDE [89].

The results from the binding studies indicated that the MIPs [A]* to [E]* were successfully imprinted. The next step was to study the ability of these polymers to influence the product distribution in the ring opening reaction of α -pinene oxide [89].

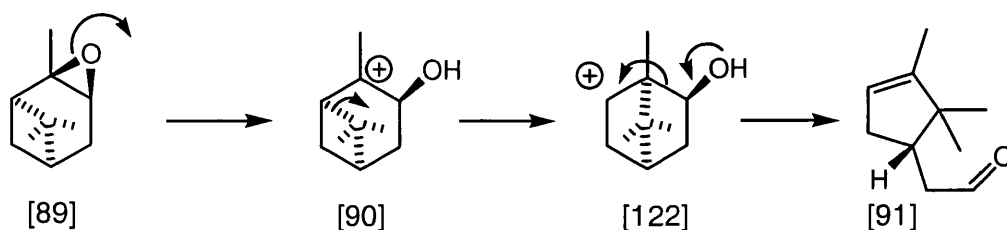
3.0. Model studies with *p*-toluenesulfonic acid [118].

The acid catalysed ring opening reaction of α -pinene oxide [89] is well characterised in the literature⁹⁸⁻¹⁰¹ and is known to produce a variety of rearrangement products under different conditions. Before using the MIPs the reaction was studied in solution to establish suitable conditions and to identify the various products. In order to mimic the reactivity of the 4-styrenesulfonic acid functional monomer in the MIP binding cavity *p*-toluenesulfonic acid [118] was chosen as the acid catalyst (Scheme 36). The reaction was carried out in toluene as this solvent should be highly compatible with the polymer matrix and thus suitable for subsequent MIP reactions.



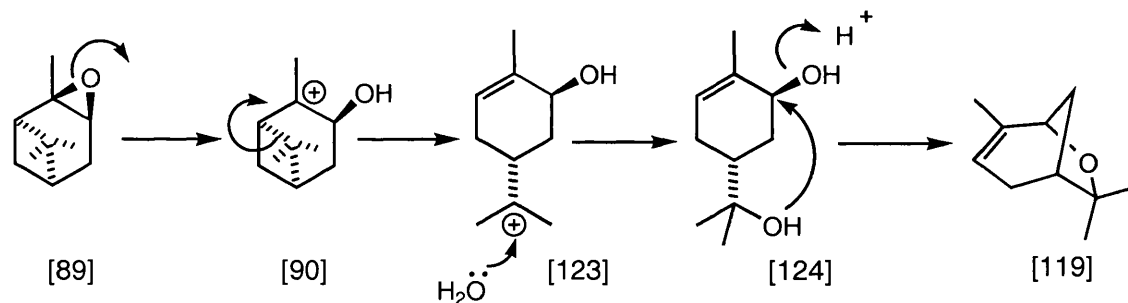
Scheme 36

The major product observed under these conditions is campholenic aldehyde [91]. This well documented product is formed by a Wagner-Meerwein shift to give [122] (Scheme 37) which then fragments to afford the product aldehyde [91]^{99,102}.



Scheme 37

The desired product *trans*-carveol [92] is formed in only 5% yield although it is likely that this yield also reflects further decomposition under the reaction conditions: acid catalysed water elimination affords dehydration products such as *p*-cymene [121] (Scheme 36). This latter dehydration process may also explain the formation of pinol [119]. The mechanism of formation of products such as *p*-cymene indicates that there is a discrete amount of water released into the reaction medium, which could trap the isopropyl cation [123] to give *trans*-sobrerol [124]. This compound can go on to react under acidic conditions to afford pinol [119] as illustrated in Scheme 38.



Scheme 38

3.1. Reactions of the MIPs with α -pinene oxide [89] in toluene.

The reactions with the MIPs [A]* to [F]* were carried out under identical conditions to the reaction with *p*-toluenesulfonic acid. Stoichiometric amounts of MIP catalyst were used in an attempt to favour any selectivity observed. The reactions were carried out on a *ca.* 20-30mg scale and thus the yields obtained are from GC analysis of the reactions using reference compounds[#].

[#] Standards for G.C. analysis of the M.I.P. catalysed reactions were identified by ¹H NMR ¹³C NMR, mass and IR comparison with literature spectra. Typical GC conditions were: flow rate 100mL/min, column head pressure 7.5psi, initial temperature 100°C, final temperature 200°C, initial time 2.0min and rate 5.0°C/min. Injections were 0.1 μ L, 0.015M.

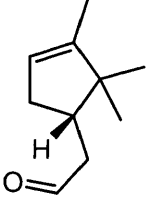
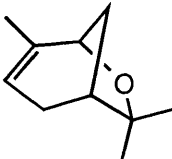
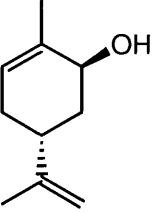
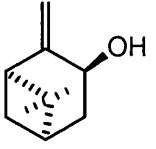
MIP/ catalyst	 [91]	 [119]	 [92]	 [120]
<i>p</i> -TsOH	59%	11%	5%	5%
1/35, 6:1 [A]*	54%	9%	16%	13%
1/35, 3:1 [B]*	60%	9%	20%	4%
1/35, 2:1 [C]*	59%	10%	20%	4.5%
1/15, 2:1 [D]*	62%	12%	11%	5%
1/10, 3:1 [E]*	61%	9%	20%	3%
1/35, 6:1 [F]*	60%	8%	22%	3%

Table 7

The speed of the reaction was a concern: the reaction was complete usually after half an hour whilst binding studies had indicated that only *ca.* 20% of sites were occupied after this time. Since the most accessible sites on the polymer are on the surface, and are also likely to be the least specific, this was a problem.

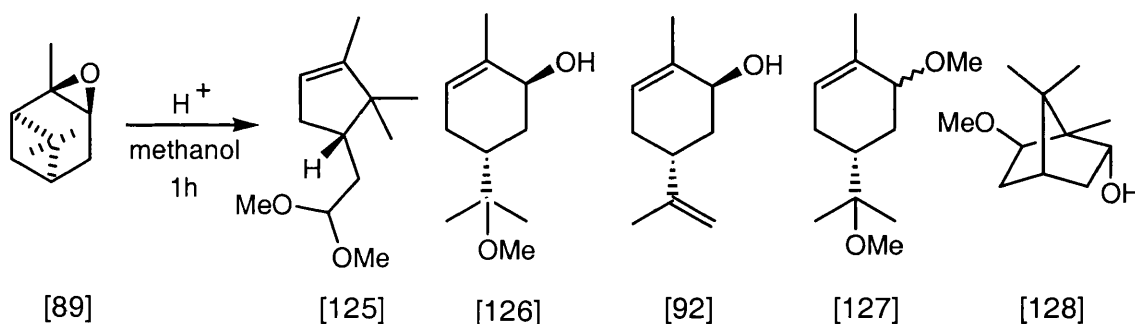
The results of the reactions in toluene indicate that, although the MIP reactions favour the formation of *trans*-carveol [92] when compared to the reaction with *p*-toluenesulfonic acid, this cannot be attributed to an imprinting effect since the reaction with the reference non imprinted MIP [F]* also gives the same result. The difference could be explained by the premise that the MIPs are less active relative to

p-TsOH, hence the product *trans*-carveol [92] is less susceptible to decomposition under the reaction conditions. This could merely be a result of the acid group being in the solid phase buried in the porous structure but it could also be explained by perturbed acidity of the sulfonic acid group in the MIP binding cavity. The hydrophobic environment is expected to decrease the acidity of the functional group, disfavoring charged species, by analogy with the catalytic antibody example in section 1.2.0. of the introduction⁴⁰.

Also it is evident that the two MIPs [A]* and [D]* exhibited a lower selectivity for the product *trans*-carveol [92] than the other MIPs, even compared to the reference MIP [F]*. The lower yield of [92] observed with MIPs [A]* and [D]* could be explained by the presence of more accessible sulfonic acid groups, resulting in faster decomposition of *trans*-carveol [92] in the reaction medium. It may be no coincidence that these two polymers had been used for the binding studies and had thus been regenerated and reused more times than MIPs [B]* [C]* and [E]* which may have affected the polymer morphology.

3.2. Reactions of the MIPs with α -pinene oxide [89] in methanol.

In order to determine the influence of the solvent or porogen on the product distribution, the reactions were also carried out in methanol (Scheme 39).



Scheme 39

In order to isolate authentic samples of the products for subsequent GC analysis, and to determine the usual product distribution, the reaction was first studied with

p-toluenesulfonic acid [118] as catalyst before comparison with the MIP catalysed reactions. The results are tabulated below in table 8.

The results are listed below for MIPs [A]* to [F]* #.

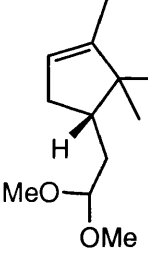
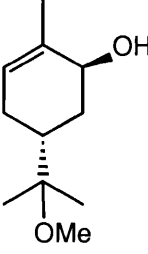
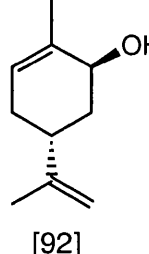
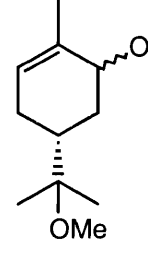
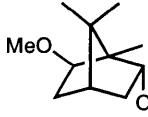
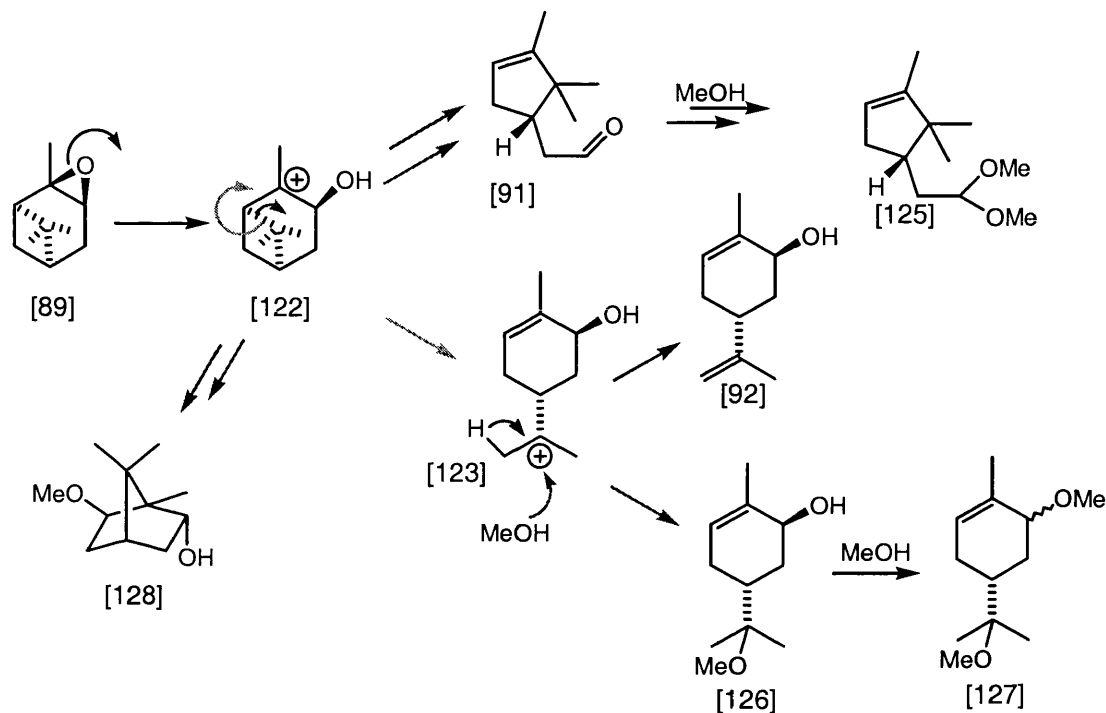
MIP	[125]	[126]	[92]	[127]	[128]
					
<i>p</i> -TsOH	23%	17%	6%	13%	10%
1/35, 6:1 [A]*	27%	41%	11%	-	11%
1/35, 3:1 [B]*	32%	36%	10%	4%	11%
1/35, 2:1 [C]*	29%	38%	12%	3%	10%
1/15, 2:1 [D]*	31%	36%	12%	-	11%
1/10, 3:1 [E]*	27%	40%	10%	2%	11%
1/35, 6:1 [F]*	26%	40%	12%	2%	10%

Table 8

Again, although the yield of trans-carveol is improved with the MIPs relative to the reaction with *p*-toluenesulfonic acid [118], the fact that the reaction with the blank MIP

Yields are based on GC analysis of MIP reactions using reference compounds. Typical GC conditions were: flow rate 100mL/min, column head pressure 7.5psi, initial temperature 100°C, final temperature 200°C, initial time 2.0min and rate 5.0°C/min. Injections were 0.1µL, 0.015M.

[F]* affords a similar product distribution indicates that this is not attributable to an imprinting effect. However, the results do indicate that the use of a more polar solvent in the reaction favours the formation of the isopropyl carbocation [123] over the product [125] or [128] derived from a Wagner-Meerwein shift to give the bicyclic cation [122] (Scheme 40).



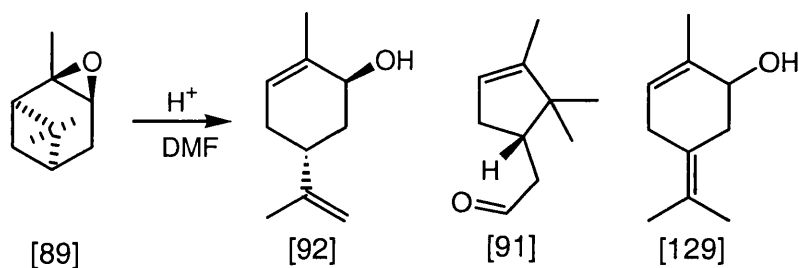
Scheme 40

The subsequent trapping of the isopropyl carbocation [123] with methanol can lead to [126] or, after further methanol addition, [127], although this latter compound is not produced in significant quantities in the MIP catalysed reactions. The alternative pathway for trapping this carbocation involves proton elimination to furnish the desired product *trans*-carveol [92].

3.2.3. Reactions of MIPs with α -pinene oxide [89] in DMF.

The results of the reaction in methanol suggest that the use of a polar solvent such as DMF, which will mimic the polar environment of methanol but which will not be able to act as a nucleophile, may favour the formation of the desired alcohol [92]. We therefore decided to study the reaction in DMF since a better understanding of the solvent effects involved should aid the development of future generation MIPs. Again,

the reaction was first studied in solution with *p*-toluenesulfonic acid [118] in order to first isolate the products, and provide a comparison with the solution phase reaction (Scheme 41).

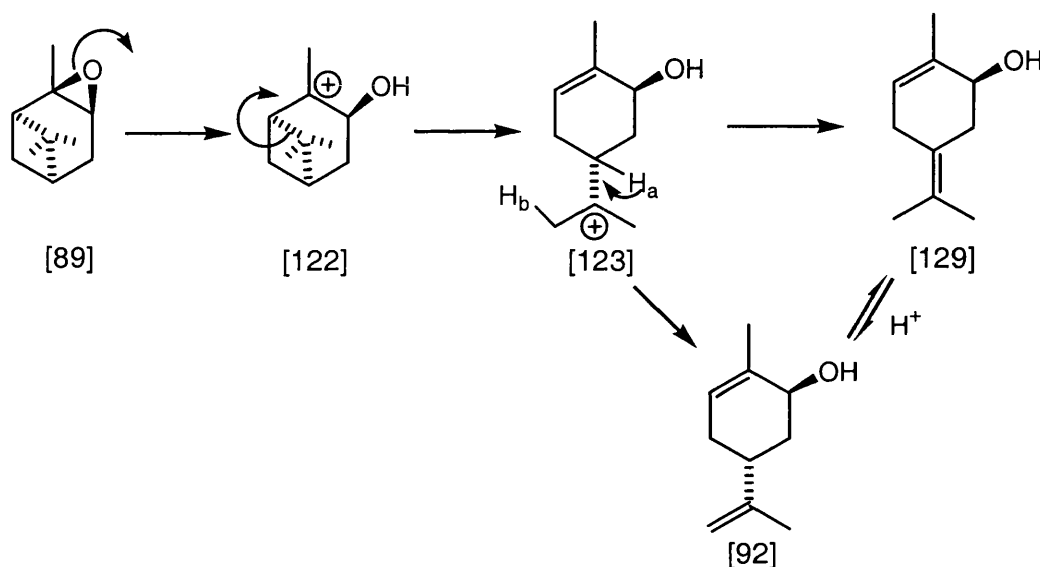


Scheme 41

M.I.P.	time/h	[91]	[92]	[129]
<i>p</i> -TsOH	1h	 21%	 42%	 24%
1/35, 6:1 [A]*	6	24%	45%	25%
1/35, 3:1 [B]*	7.5	29%	41%	24%
1/35, 2:1 [C]*	2	39%	38%	20%
1/15, 2:1 [D]*	4	31%	41%	21%
1/10, 3:1 [E]*	3	32%	39%	21%
1/35, 6:1 [F]*	6	23%	42%	23%

Table 9

The outcome of the reactions suggest that the hypothesis was correct, since the major product in each example is the desired *trans*-carveol [92]. The rather unusual product [129] is tentatively assigned on the basis of ^1H NMR ^{13}C NMR mass and IR data and can be derived from the isopropyl carbocation [123], an intermediate common to the formation of *trans*-carveol [92], by elimination of the tertiary proton H_a (Scheme 42). This product could also be derived from *trans*-carveol [92] by invoking an acid catalysed double bond migration. However, although the new double bond is more substituted in [129], the ring strain in the product may make this a thermodynamically less favoured process.



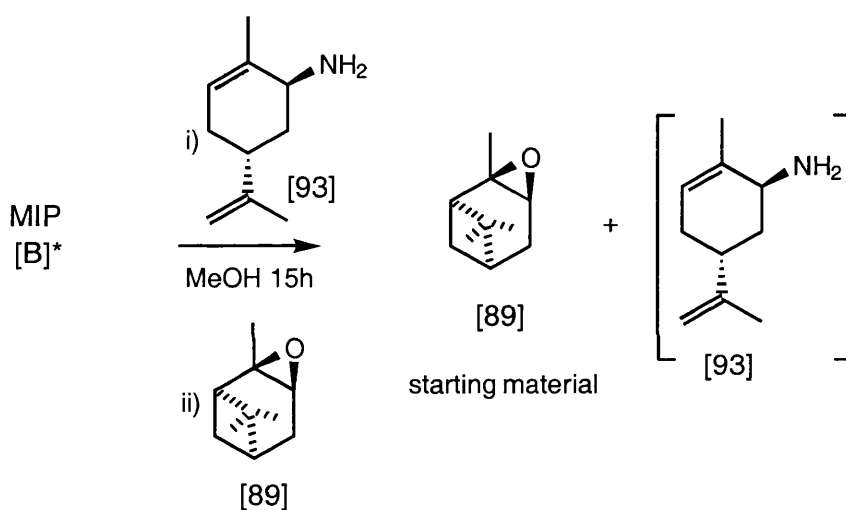
Scheme 42

3.4 Inhibition studies.

A concern was that the MIP reactions may be catalysed by the presence of HCl which was used for the polymer regeneration. Despite the fact the MIPs were washed exhaustively to $\text{pH} \sim 7$, this possibility could not be ruled out completely. Unfortunately the imprint molecule [93] used to generate the MIPs $[\text{A}]^*$ to $[\text{E}]^*$ is a base. As such, it could not be used in classical inhibition studies since this would require the addition of one equivalent of imprint molecule [93] to the MIP. For neutral inhibitor molecules, cessation or slowing of the reaction in the presence of one equivalent of an inhibitor can be attributed to the reaction being carried out in a binding site, however, in the case of (1*R*, 5*R*)-*trans*-carvyl amine [93] the imprint molecule will 'neutralise' the acid in the active site and thus any small amine would be expected to have a similar effect.

Inhibition studies will therefore give no indication of the shape of the cavity but they may indicate whether there is any HCl present, since equilibration of 1eq of imprint molecule [93] with the MIP should stop the polymer catalysed reaction thus any remaining activity will be due to HCl impurities.

The reaction of MIP [B]* with α -pinene oxide [89] in methanol was therefore carried out after equilibration of [B]* with one equivalent of (1*R*, 5*R*)-*trans*-carvyl amine [93]. The reaction was completely inhibited by the presence of the imprint molecule [93] indicating that the reaction was catalysed by polymer bound acidic groups (Scheme 43).



Scheme 43

3.5 Conclusions.

The polystyrene MIP studies provided us with an introduction into the field of catalytic molecularly imprinted polymers. However, there are many problems with the system. Perhaps the most evident is the fact that the choice of the 'pre-organised' complex [93]:[94] leads to only a single point of interaction between the imprint molecule and the MIP (Figure 25).

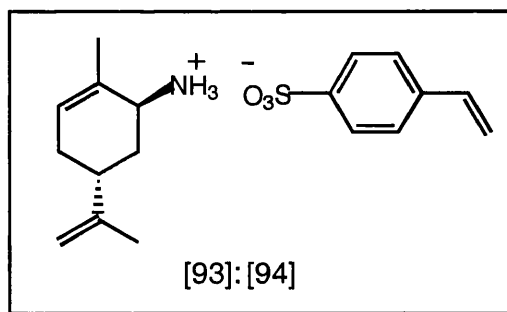


Figure 25

Although hydrophobic interactions should not be underestimated^{11,103a,b} it is unlikely that the MIP binding sites in [A]* to [E]* contain the ‘three-point’ contact required to locate a molecule in space. This ‘freedom’ for the imprint molecule to assume a variety of orientations in the growing MIP matrix during polymerisation is responsible for the heterogeneity of the polymer binding sites. Whilst this is not such a problem for MIPs required for binding applications; all the sites will still recognise the imprint molecule even if the manner of binding varies, it presents a real problem for catalytic applications.

In an attempt to understand the various mechanisms underlying MIP formation and MIP-ligand binding, Nicholls has presented a thermodynamic treatment to describe the various factors involved in recognition phenomena in molecular imprinting¹⁰⁴ (Equation 2).

$$\Delta G_{\text{bind}} = \Delta G_{\text{t+r}} + \Delta G_{\text{r}} + \Delta G_{\text{h}} + \Delta G_{\text{vib}} + \Sigma \Delta G_{\text{p}} \quad \text{Equation 2}$$

where the Gibbs free energy changes are: ΔG_{bind} , complex formation; $\Delta G_{\text{t+r}}$, translational and rotational; ΔG_{r} , restriction of rotors on complexation; ΔG_{h} , hydrophobic interactions; ΔG_{vib} , residual soft vibration modes; $\Sigma \Delta G_{\text{p}}$, the sum of interacting polar group contributions.

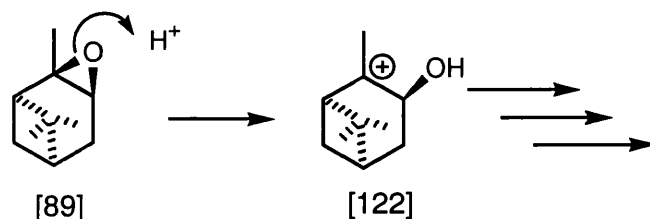
Interpretation of this equation provides an insight into the many factors which must be considered in designing an MIP:

- The term ΔG_{t+r} implies that, although more than one point of contact between the MIP and the imprint molecule is desirable, the greater the number of discrete molecular entities required for complexation of the template the lower the stability of the complex. In other words if more than one functional monomer is used to achieve multiple interactions with the imprint molecule, the less entropically favourable the pre-organised complex becomes. A result of this will be an increase in the heterogeneity of the MIP binding cavities since it is predicted that imprinted sites will be formed with all possible permutations of functional monomer-imprint molecule co-ordination, including single point contact.
- The internal rotation free energy term ΔG_r indicates that more rigid structures, ie those with fewer solution conformations will produce better-defined recognition site populations.
- The term $\Sigma \Delta G_p$, reflects the intuitive fact that the stronger the interaction between complementary functional groups in the pre-organised complex the greater the stability of the solution adducts
- The sum of the hydrophobic interactions ΔG_h , becomes more important in aqueous environments when complementary hydrophobic interactions between the MIP and the imprint molecule should favour binding.

The value of ΔG_{bind} itself represents the position of equilibrium for the formation of self-assembled functional monomer-imprint molecule complexes and determines the number and degree of receptor site heterogeneity. Fundamentally, the more stable the pre-organised complex, the greater will be the number and fidelity of the resultant MIP binding sites.

The polystyrene MIP studies have also provided important information on the reaction in question. The ring opening of α -pinene oxide is a challenging reaction to work with, not least because the rate determining step is likely to be formation of the initial carbocation [122] (Scheme 44). Since this intermediate is common to all the products

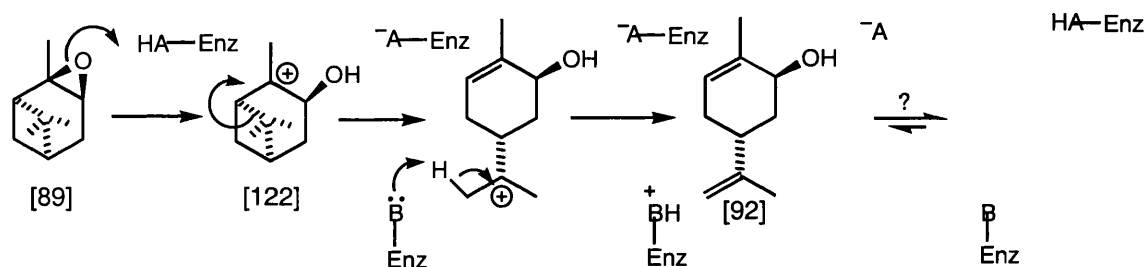
subsequently formed, inducing selectivity in the reaction presents a real challenge. However, these early results have indicated that carrying out the reaction in polar solvents such as DMF favours the desired product [92] and reverses the usually observed selectivity. This is encouraging, since our aim is to produce more polar ‘enzyme-like’ MIPs than those based on styrene and divinylbenzene which should be compatible with reactions carried out in DMF.



Scheme 44

Furthermore, even though our transition state mimic contained only a single electrostatic interaction as one point of contact we had nevertheless determined that the MIPs produced were still shape selective, as indicated by the competitive binding studies. Our greatest concern was that the proton catalysed reaction seemed to be proceeding faster than the binding of the transition state mimic. While it could be argued that α -pinene oxide is more ‘compact’ than *trans*-carvyl amine, it might also be true that after a single proton catalysed rearrangement occurring in the pocket, the perfidious proton could escape into the surrounding solvent and a percentage of products could be produced in a homogeneous reaction.

With these considerations in mind, it is notable that in naturally occurring enzyme systems a complementary base would usually also be present to assist the final proton removal, (Scheme 45) and that the ability to regain the initial resting state, with both acid and base functionality in an active site is one of an enzymes most important characteristics.



Scheme 45

Our preliminary design strategy had certainly not attempted such subtle concepts: the crude TSA [93] used for the polystyrene MIPs does not contain enough functionality for such a strategy and thus the imprint molecule will need to be improved.

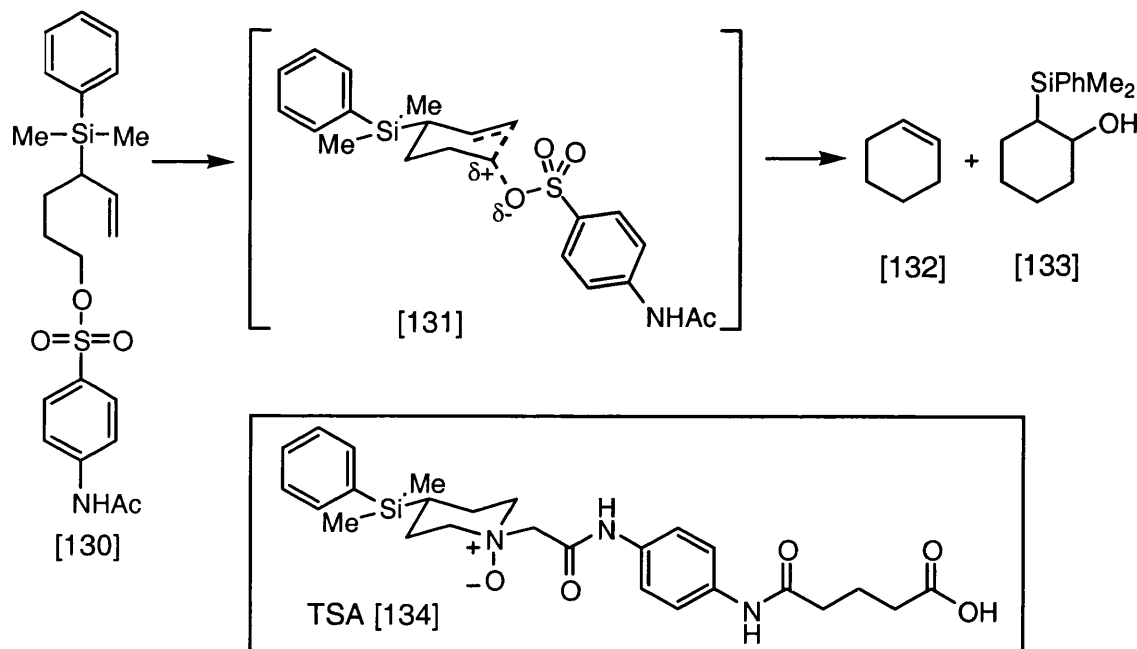
If we attempt to obtain more than one point of contact between the the imprint molecule and the MIP by using a range of functional monomers, the system becomes more susceptible to heterogeneous binding cavities, as is explained above by the term ΔG_{tr} . In order to avoid this problem we plan to incorporate a peptide as the functional monomer, this could achieve multiple point binding with the imprint molecule without increasing the molecularity of the system, thus reducing the heterogeneity of the polymer binding cavities. A further advantage of employing such a strategy is that the nature of binding between the imprint molecule and the peptide could be analysed before incorporation into an MIP. This also introduces a further element of design into the system. At present, information on the manner of binding in MIP cavities can only be inferred from binding study data.

All of these factors were considered in determining the subsequent strategy below.

Chapter 4. TRANSITION STATE ANALOGUE DEVELOPMENT

With some of these thoughts in mind, several constraints were applied to the choice of TSA for the second generation MIP studies. Firstly, if multiple binding interactions with the host MIP are required then the TSA must contain the relevant multiple functionality. Also, by analogy with our earlier studies, the TSA should mimic the shape of the late transition state, and should be chosen such that a complementary acid group can be placed in the MIP binding cavity at a position suitable for catalysis of the epoxide ring opening reaction.

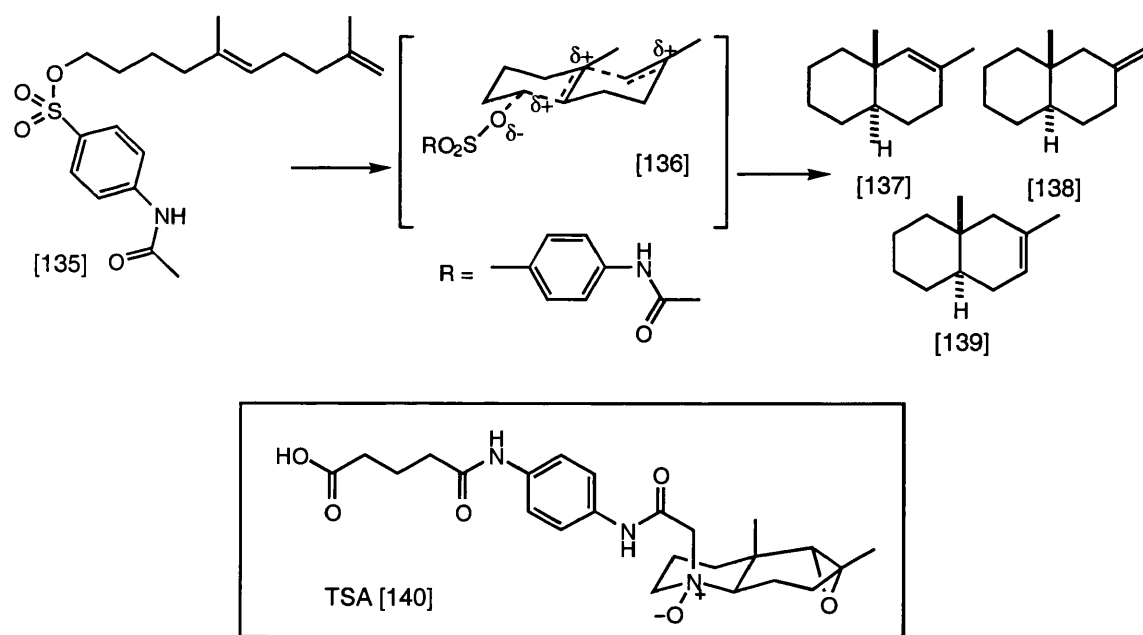
As the *de novo* design of a TSA can be a speculative process, we turned to the catalytic antibody literature for examples of successful TSAs contrived for similar transformations. Lerner and Janda have carried out a series of studies in an attempt to raise catalytic antibodies which mimic terpenoid cationic cyclases^{32-35,105}. An early example employs the cyclisation of the sulfonate ester [130] to *trans*-2-dimethylphenylsilyl cyclohexanol [133] and cyclohexene [132] as the model reaction¹⁰⁵ (Scheme 46). The TSA used as the hapten for immunisation was the amine oxide [134]. The dative *N*-oxide bond of hapten [134] was envisioned to mimic the developing cationic carbon and anionic oxygen centres, which form as the sulfonate leaving group departs [131].



Scheme 46

The catalytic antibody, generated using [134] as the hapten, catalysed the cationic cyclisation depicted above with remarkable selectivity affording 98% of the hexanol product [133] and only 2% cyclohexene. This result is particularly impressive since cationic cyclisation reactions are renowned for their lack of selectivity, usually affording a plethora of rearrangement products. The k_{cat} for the process or the usual distribution of products under the reaction conditions could not be determined since no solvolysis of the sulfonate ester [130] was observed in the absence of the antibody¹⁰⁵ (detection limit $< 0.1\mu\text{M}$).

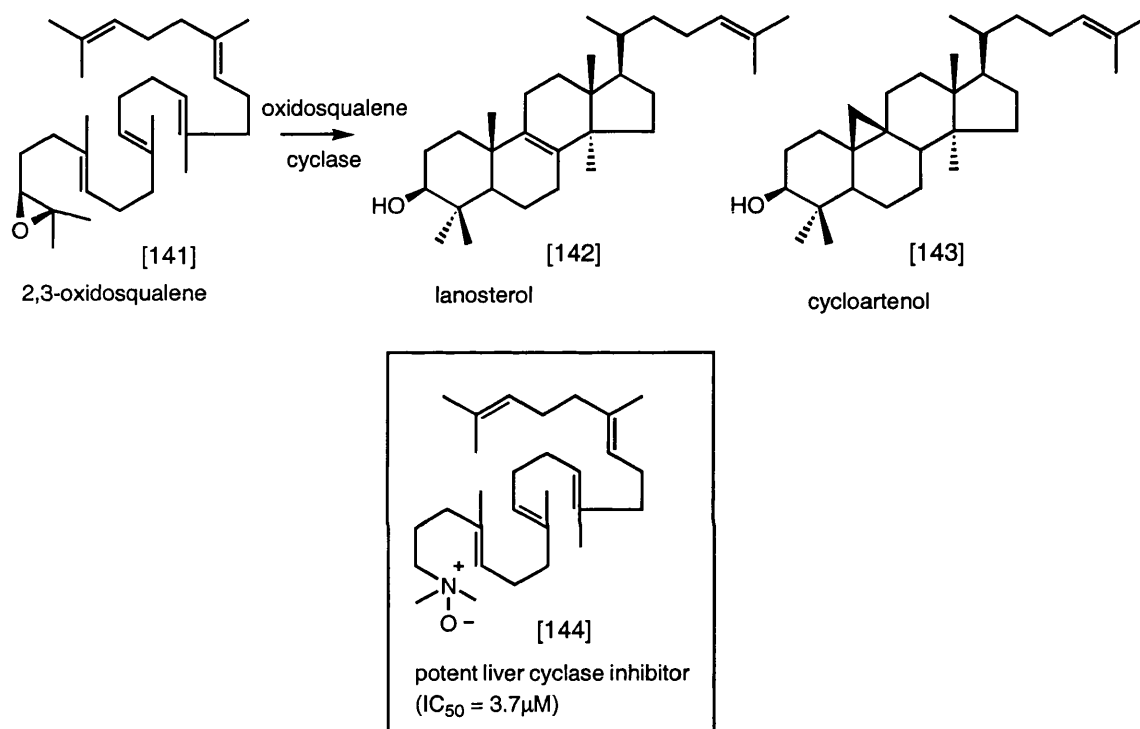
The use of amine oxide haptens to raise antibodies for cationic processes appears to be quite general. More recently Lerner and Janda have employed *N*-oxides to generate antibodies capable of catalysing an electrophilic tandem ring forming reaction that yields a bicyclic ring system at neutral pH³³ (Scheme 47). The hapten [140] and substrate [135] were chosen to mimic the first two isoprene units of 2, 3-oxidosqualene, where the epoxide oxygen has been replaced by an arylsulfonate leaving group.



Scheme 47

The challenging conversion of 2,3-oxidosqualene to lanosterol or cycloartenol is part of sterol biosynthesis and demonstrates the remarkable stereochemical control which

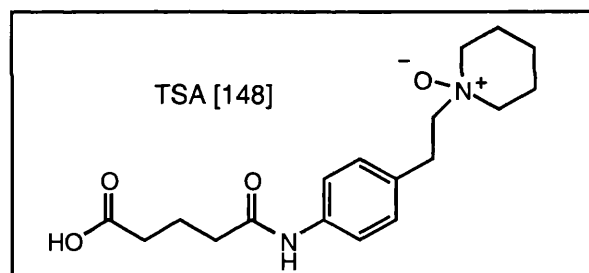
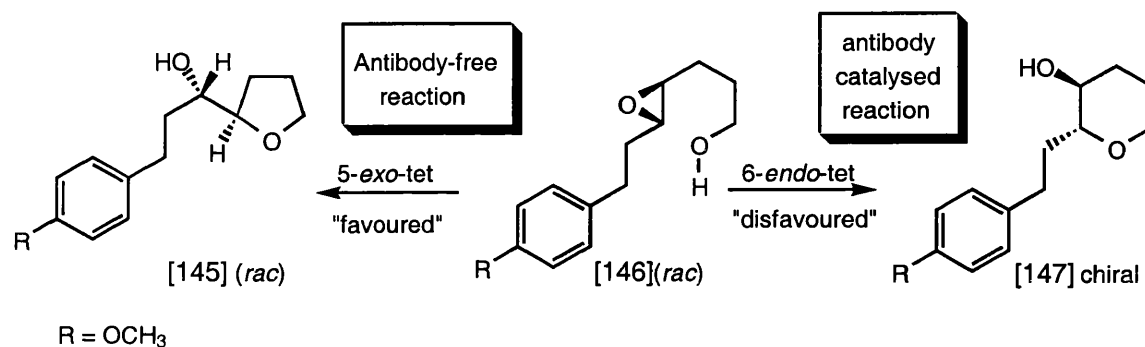
enzymes are able to exert on chemical transformations. In a single step six new stereocentres are created and four carbon carbon bonds are formed¹⁰⁶ (Scheme 48). Particularly relevant to the design of synthetic equivalents is the fact that the amine oxide [144] is known to be a potent inhibitor of the natural squalene cyclase which further reinforces the choice of [140] as a hapten in the above attempt to find a squalene cyclase mimic.



Scheme 48

The antibodies generated were shown to catalyse the formation of the three closely related decalin systems [137], [138] and [139] (Scheme 47). These bicyclic products are congeners of the A and B rings of the steroid nucleus, and account for 50% of the overall products. The influence of the catalytic antibody on the reaction outcome is highlighted by the fact that none of the products [137], [138] or [139] were observed in the antibody free system, however this detail complicated rate acceleration studies as a value for k_{uncat} was hence unavailable. Catalysis was studied indirectly; the k_{cat} for the formation of the sulfonic acid (the leaving group) was determined to be 0.021 min^{-1} .³³

The above examples both involve a sulfonate as the leaving group which initiates the cationic process. In the reaction we wish to influence, the acid catalysed ring opening reaction of α -pinene oxide [89], the initial cationic centre is created by a breaking carbon oxygen epoxide bond. With this in mind there is a pertinent literature precedent employing a catalytic antibody to effect selectivity in an epoxide ring opening transformation¹⁰⁷. In this example the incipient cation is trapped intramolecularly by an alcohol nucleophile (Scheme 49).



Scheme 49

Again the hapten [148] used is an amine oxide which mimics both the charge distribution and the lengthening carbon oxygen epoxide bond in the transition state. The TSA was chosen to mimic the transition state for the usually disfavoured 6-*endo*-tet process to afford the tetrahydropyran [147]. In the antibody free reaction this product is not observed and the expected 5-*exo*-tet tetrahydrofuran product [145] is exclusively formed according to Baldwin's rules¹⁴⁰. A successful antibody would thus reverse the usual selectivity. This was indeed the case: two of the antibodies raised against the hapten [148] were regioselective for the formation of [147]. Furthermore, one antibody was capable of kinetic resolution using only a single enantiomer of the substrate [146] to produce optically pure tetrahydropyran [147]¹⁰⁷.

The examples above encouraged us to select the *N*-oxide group as an important feature in our second generation TSA. This choice was substantiated by computational studies into the nature of the antibody catalytic groups elicited by the amine oxide hapten [148]¹⁰⁸. The predicted manner of binding in the antibody active site is depicted below [149] (Figure 25). Using this information Houk and Na investigated the optimisation of model stabilising groups around the hapten [150] and found that formic acid makes a strong hydrogen bond to the hapten oxide as reflected by the short OH distance of 1.57Å (Figure 25).

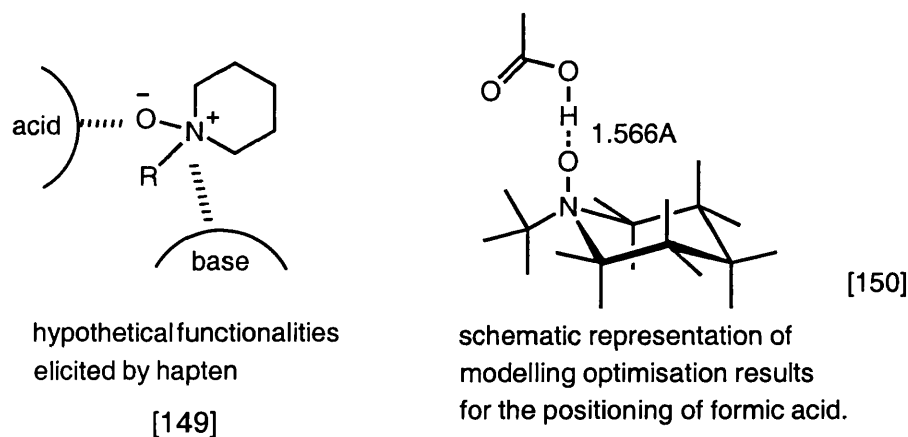
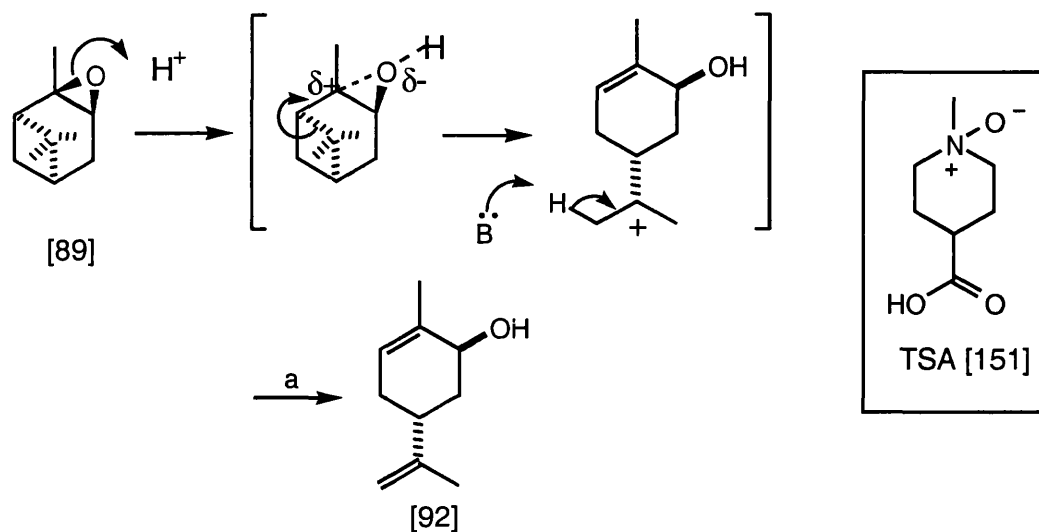


Figure 25

The complementary formic acid group (or carboxylic acid containing amino acid in the antibody site) is conveniently positioned in the binding cavity for subsequent acid catalysis of the epoxide ring opening reaction described above (Scheme 49). Since our MIP-TSA strategy must incorporate the designed positioning of the acid catalytic group in the binding site in an appropriate location for catalysis, the *N*-oxide-carboxylic acid group interaction seemed an appropriate choice.

The TSA chosen is illustrated in Figure 26 below. In order to allow for a second point of contact in the imprint molecule-functional monomer complex, we chose to incorporate further functionality into the TSA in the form of the carboxylic acid moiety at C-4. This can be used to elicit a complementary basic group in the MIP binding site which will hopefully favour the base initiated proton removal step as illustrated below (step a,

Scheme 50), to afford the desired product *trans*-carveol [92]. The third point of contact is not designed and will hopefully be produced by an interaction with the polymer matrix, which will be chosen to be more polar and functionalised than the previous polystyrene type MIPs.



Scheme 50

With the basic interactions involved in the desired pre-organised complex thus determined, it was then necessary to choose the nature of both the peptide functional monomer (proposed above in section 3.5) and the polymer matrix. The two investigations were carried out concurrently: molecular modelling was used to facilitate the choice of appropriate peptides for TSA ligation whilst studies towards improving the polymer matrix were carried out with polyacrylamides.

Chapter 5. MOLECULAR MODELLING[§]

In order to choose a suitable peptide as the 'functional monomer' we decided to use molecular modelling to provide an idea of suitable candidates. It should then be possible to study and confirm TSA-peptide binding by experimental methods, before incorporation into an MIP enzyme mimic. Primitive early models confirmed intuition

[§] Molecular modelling was carried out under the supervision and guidance of Dr Stephen Garland and Dr Mike Tennant of SmithKline Beecham.

and indicated that the optimum size of a peptide required to bind at either end of the TSA [151] incorporates three amino acids ($aa_x n = 1$, Figure 26).

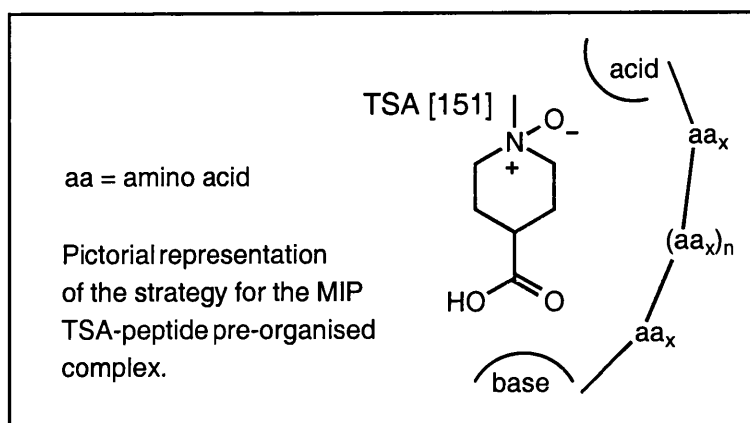
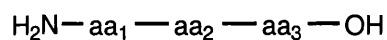


Figure 26

Since there are 20 natural and 20 unnatural[#] (ie (D) configuration) amino acids the number of available tri-peptides is represented by 40^3 , that is 64,000 possible structures to screen for binding. It was obviously impractical to carry out such a large study and so several constraints were imposed upon the system. Firstly, in order to achieve the desired functionality in the MIP binding cavity, the tri-peptide must contain an acid at one end and a base at the other (Figure 26). With these criteria in mind, it was possible to limit the candidates for the library of peptides to those containing an acidic amino acid at one end and a basic amino acid at the other end (Figure 27).

'Virtual' Synthesis of a library of tri-peptides



aa_1 = basic amino acid aa_2 = variable amino acid aa_3 = acidic amino acid

Figure 27

[#] A quirk of the computational method which we wished to use to generate a 'virtual' peptide library (to subsequently model binding with the TSA) is that both enantiomers of the amino acids are incorporated into the 'virtual' library.

Three libraries of suitable candidates for each positional amino acid aa₁, aa₂, and aa₃, were then selected. The candidates include both the natural amino acids and a range of readily available unnatural congeners, which were identified by an ACD (available chemicals directory) search using ISISbase. The variability of the two terminal amino acids was limited by the previously discussed functional group prerequisites but the nature of the central amino acid was unrestricted. The libraries used for aa₁ (10 members), aa₂ (17 members) and aa₃ (3 members) are illustrated in Appendix 2. These lists were then used to generate a virtual library of tri-peptides including all possible permutations of aa₁, aa₂, and aa₃.

In order to study the binding of the tri-peptides around the imprint molecule an electrostatic picture of the imprint molecule (TSA) [151] was first generated as is depicted in Figure 28.

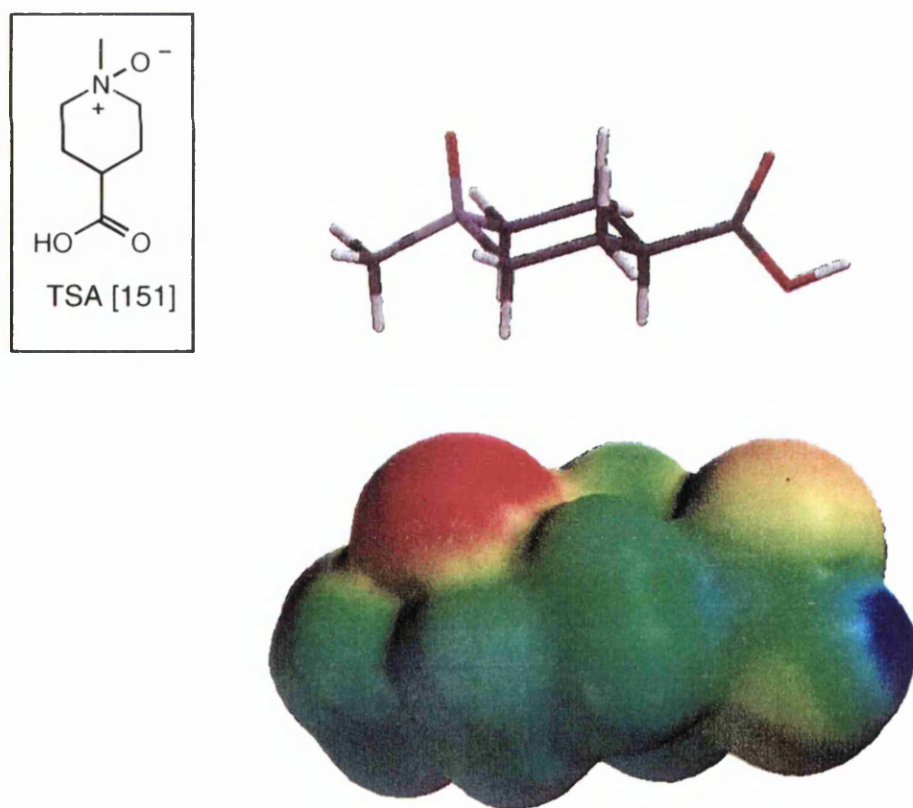


Figure 28

Out of interest we also generated an electrostatic picture of the quaternary amine [152] (Figure 29). This type of compound has been used in catalytic antibody studies to elicit cationic cyclase mimics, as an alternative to TSAs incorporating an amine oxide group.

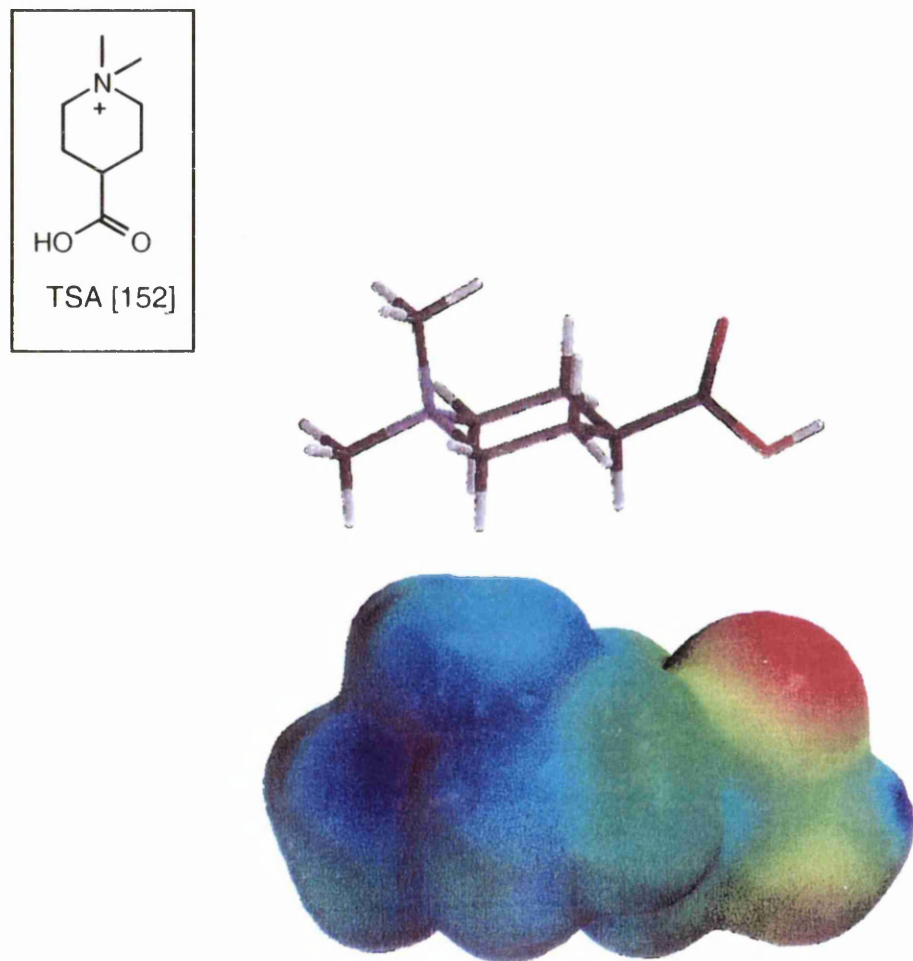


Figure 29

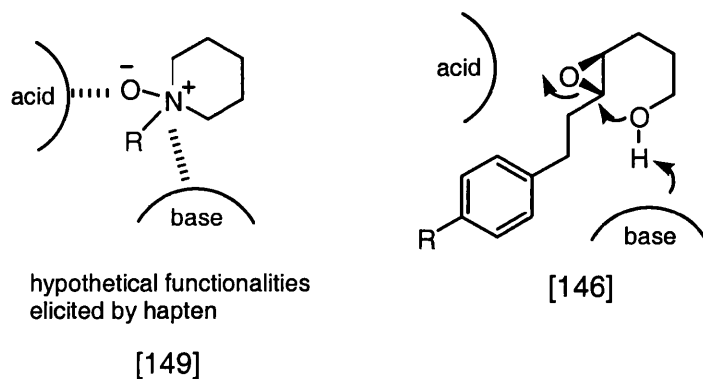
In the example described in Scheme 46 above, the product distribution observed was completely reversed when a catalytic antibody which was raised against the *N*-methyl quaternary amine equivalent of the hapten [134] was used: cyclohexene was formed in 90% yield. It has subsequently been postulated that this is due to the difference in electrostatic nature of the two haptens³². This difference is elegantly illustrated by the

electrostatic pictures of [151] and [152]. The blue regions indicate areas of positive charge, whilst the red areas indicate a negative charge. As the pictures indicate, a very different complementary electrostatic environment would be expected in the antibody binding site in response to the two different haptens. However, due to practical time constraints it was not possible to use both TSAs for imprinting therefore, only the TSA [151] was selected for further studies towards a catalytically active MIP for the ring opening reaction of α -pinene oxide [89].

In the next step of the molecular modelling studies, the peptides were docked around the TSA [151] using ICM Molsoft, which matches electrostatic, hydrogen bonding and steric interactions.

Analysis of the results identified the three tri-peptides $\text{NH}_2\text{-(D)Arg-(L)Lys-(L)Glu-OH}$ [153], $\text{NH}_2\text{-(L)Arg-(D)Lys-(L)Glu-OH}$ [154], and $\text{NH}_2\text{-(D)Arg-(D)Phe-(L)Glu-OH}$ [155] (Figure 30, 31, and 32, respectively) as suitable candidates for further study.

In each case the desired acid-base interactions with the TSA [151] were observed in the optimised structures. The relative positioning of the functional groups in peptide [154] is particularly relevant to previous catalytic antibody work with *N*-oxide haptens. In an attempt to explain the nature of catalysis in the catalytic antibody elicited for the transformation of 4,5-epoxy alcohol [146] to tetrahydropyran [147], discussed previously (Scheme 49), Lerner *et al* have proposed the *N*-oxide group may be capable of eliciting a complementary basic group to the partially positively charged nitrogen atom. (Scheme 51). It was envisaged that such a group would subsequently participate in catalysis of the reaction, by increasing the acidity of the alcohol hydrogen and aiding intramolecular nucleophilic attack on the incipient carbocation.



Scheme 51

In the peptide [154] the docking program has optimised exactly such an interaction with the amino side chain of the lysine residue. This interaction is absent however in the peptide [153]-TSA [151] optimised structure. The latter peptide was selected since, in this example, the acidic and basic groups of the peptide are on opposite faces of the molecule. This feature is desirable for the reaction we wish to study since, in the mechanism invoked, the breaking epoxide C-O bond and the ultimate isopropyl carbocation are on opposite faces of the molecule.

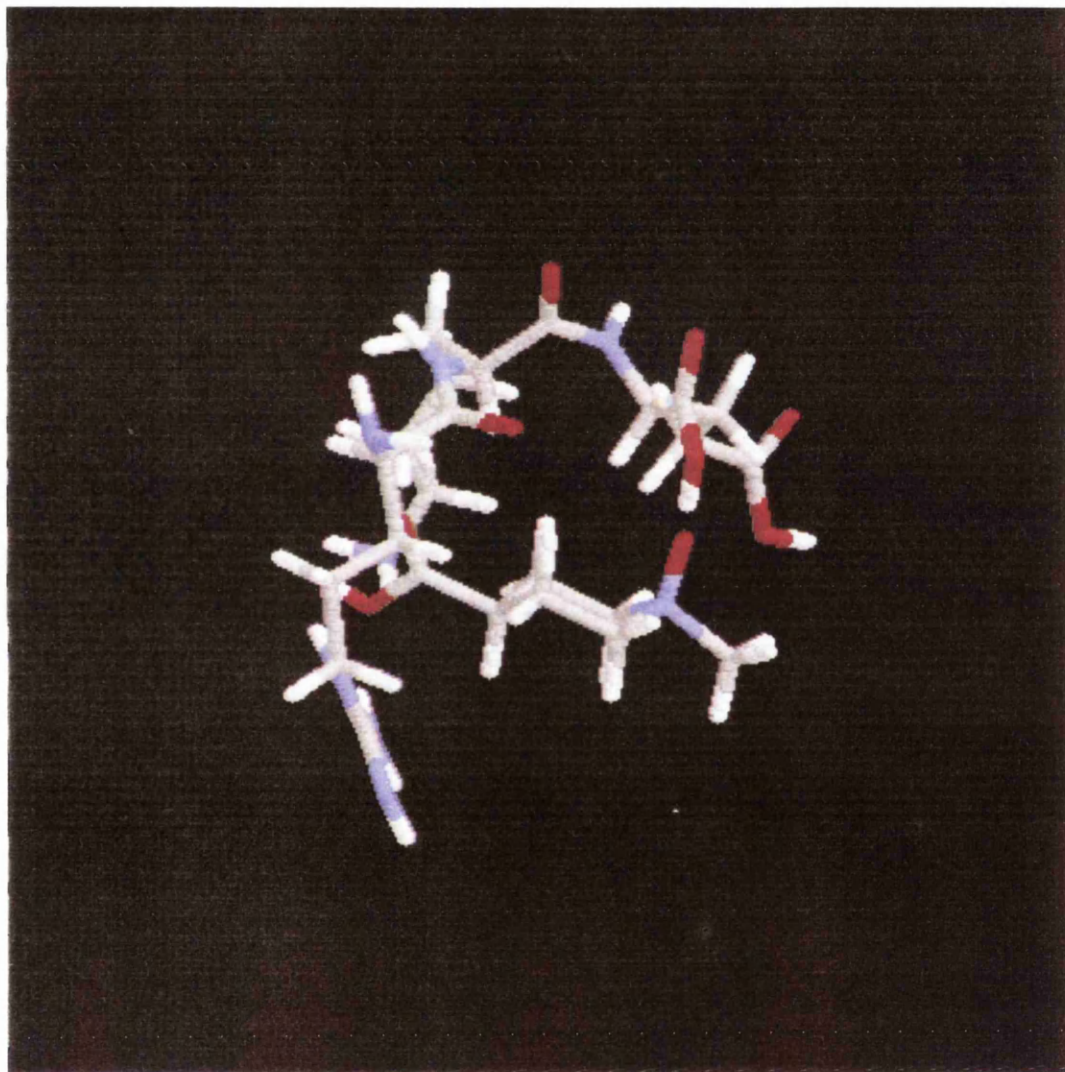


Figure 31

Peptide: NH₂-(D)Arg-(L)Lys-(L)Glu-OH [153] + TSA [151]

Energy: -1344.15 kcalmol⁻¹

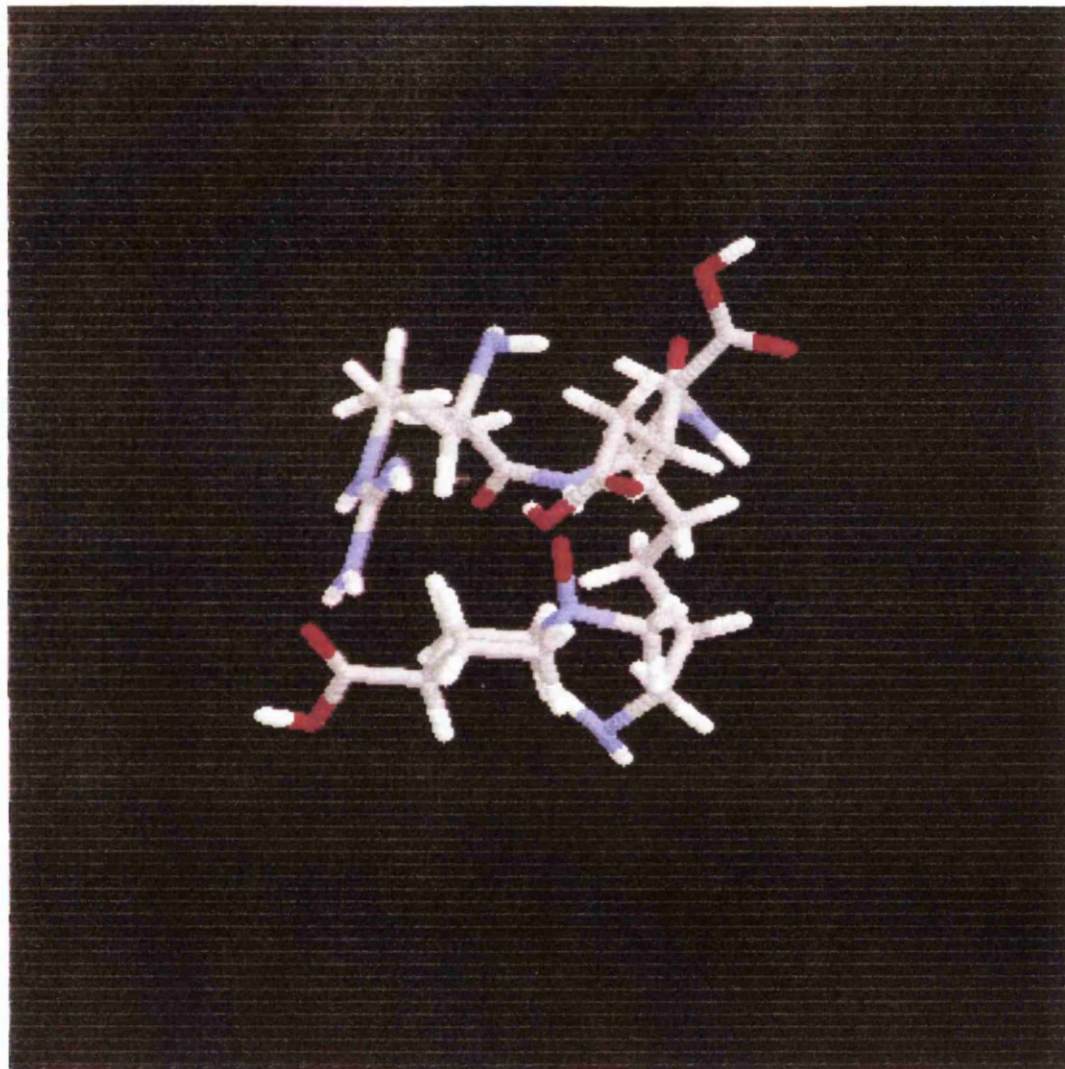


Figure 32
Peptide: NH₂-(L)Arg-(D)Lys-(L)Glu [154] + TSA [151]
Energy: -1342.65 kJmol⁻¹

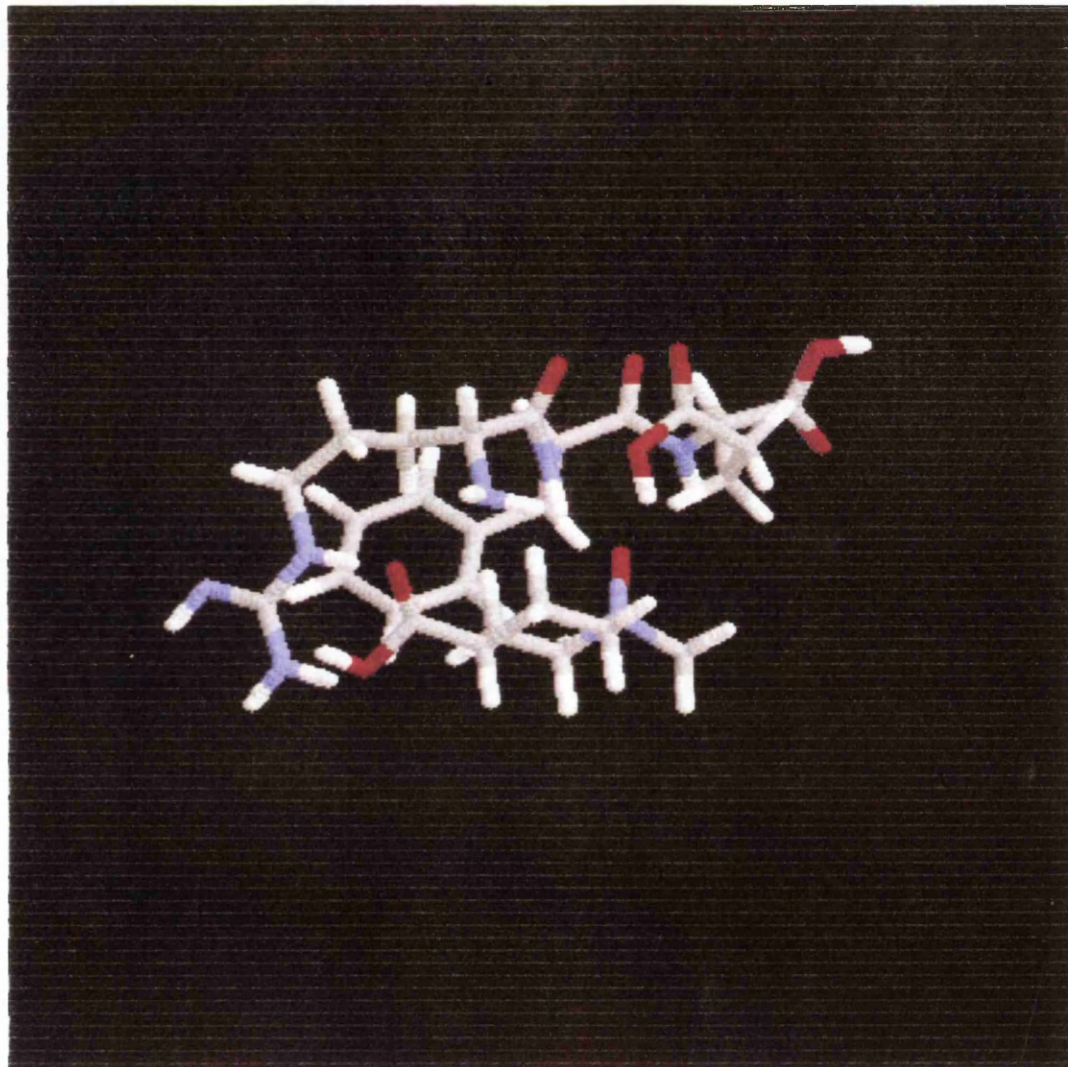
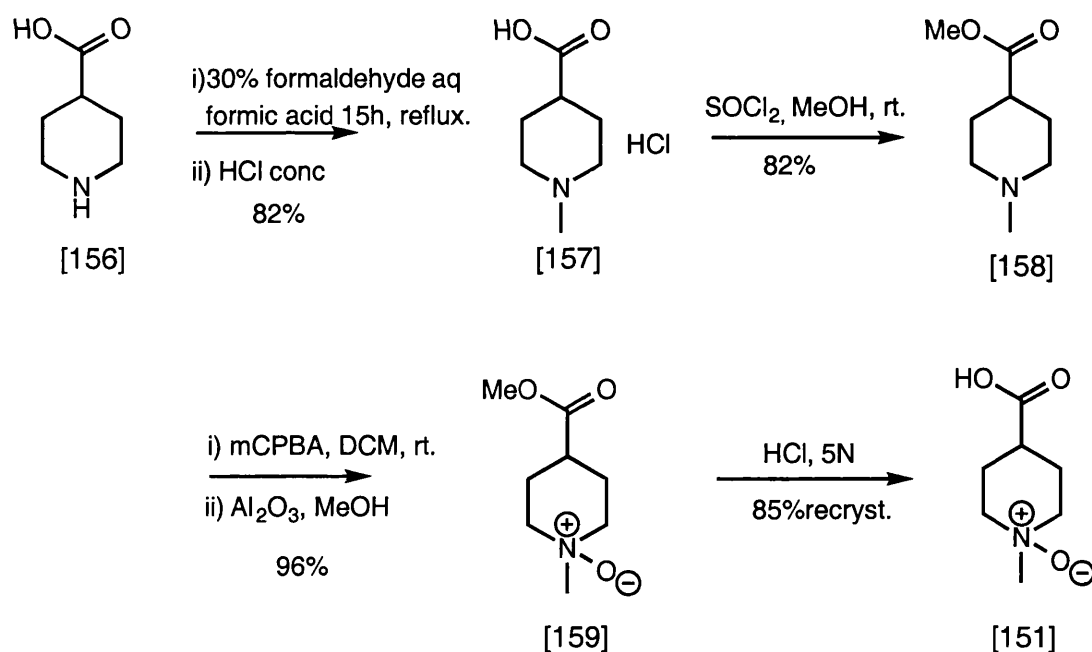


Figure 33
Peptide: NH₂-(DArg-(D)Phe-(L)Glu [155] + TSA [151]
Energy: -1326.06 kJmol⁻¹

Chapter 6. SYNTHESIS OF TSA [151] AND TRI-PEPTIDES.

6.0 Synthesis of the Imprint Molecule, (TSA) [151].

The second generation TSA [151] was synthesised in four steps using the protocol described below (Scheme 52). Protection of the carboxylic acid as the methyl ester¹⁰⁹ before the *m*-CPBA oxidation step was found to be necessary: attempted oxidation of [156] directly using *m*-CPBA or hydrogen peroxide under a range of conditions was unsuccessful¹¹⁰. The difficulty in this transformation is probably attributable to the high solubility of the product [151] in aqueous media. This leads to problems in work up and by-product purification: the *m*-chlorobenzoic acid by-product from *m*-CPBA oxidations will be particularly difficult to extract and separate from the product isonipecotic acid *N*-oxide [151]. The presence of the acidic group in the product also precludes the use of basic alumina. As a result the protection strategy outlined below was employed, since all the steps involve simple experimental and purification procedures and afford high yields of the desired substrates.



Scheme 52

The oxidation of 4 substituted *N*-alkylpiperidines is known to proceed stereoselectively to form the *trans* amine oxide with the oxygen atom occupying the axial position, as

shown below in figure 33. The diastereomeric ratio has been shown to be insensitive to the nature of the *N*- substituents and in all cases axial oxidation predominates¹¹¹. Confirmation of this stereochemistry in our TSA was obtained by ¹H NMR analysis of [151]. The chemical shift of the *N*-methyl singlet at 3.58ppm is characteristic of the *trans* amine oxide: it has been established that in compounds of this kind the axial *N*-methyl protons resonate at higher field than equatorial ones¹¹² as can be seen by comparison of the *cis* and *trans* isomers of the 4-*t*-butyl derivative [160]¹¹¹ (Figure 33).

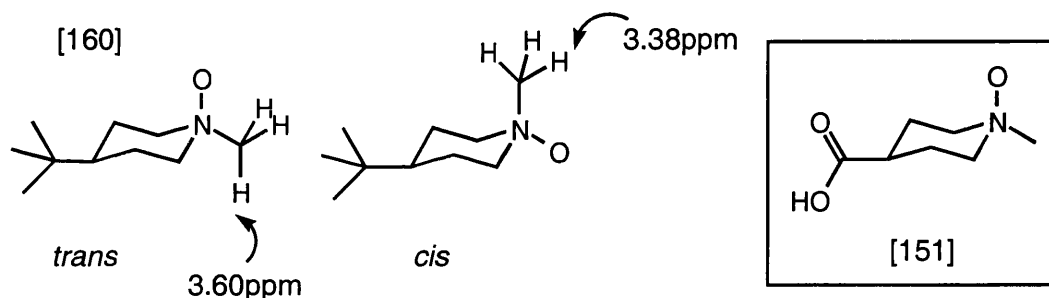
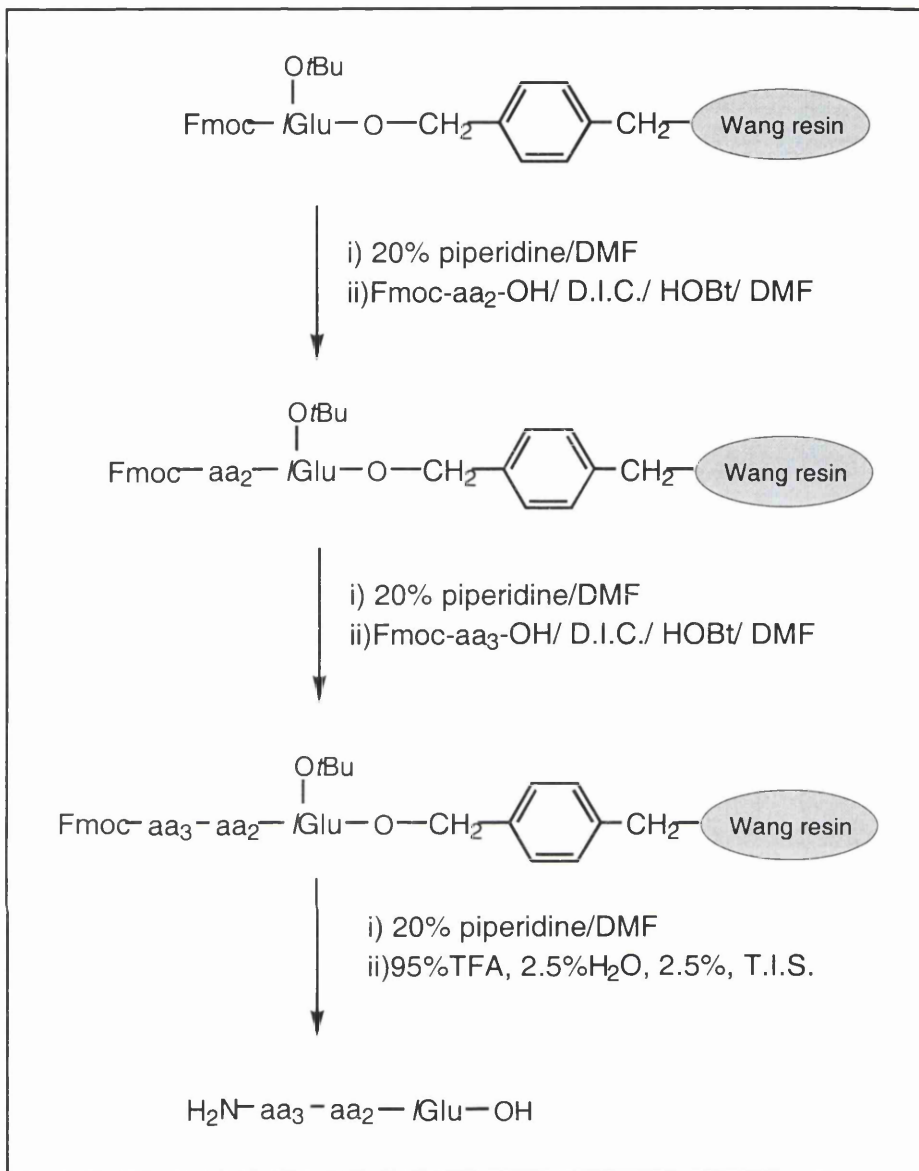


Figure 33

6.1 Synthesis of tri-peptides.

The tri-peptides NH₂-(D)Arg-(L)Lys-(L)Glu-OH [153], NH₂-(L)Arg-(D)Lys-(L)Glu-OH [154], and NH₂-(D)Arg-(D)Phe-(L)Glu-OH [155] were synthesised manually on the solid phase using standard Fmoc methodology with Boc and Pfb protecting groups for lysine and arginine respectively. Both protecting groups are TFA labile and thus deprotection and cleavage from the resin were carried out simultaneously in the final step, using 95% TFA with a triisopropylsilane scavenger. Since it was noted that all three peptides contain an (L)-glutamic acid residue at the carboxyl terminus, the strategy for all three peptides therefore incorporates the use of Wang resin with the (L)-Glu residue already bound as starting material. The general procedure used for all three peptides is outlined below in Scheme 53.

All three tri-peptides were isolated, purified by preparative HPLC where necessary, and the structures established by HRMS and NMR analysis.



For NH₂-(D)Arg-(L)Lys-(L)Glu-OH [153]: aa₂ = H₂N-(L)-Lys(Boc)OH and aa₃ = H₂N-(D)-Arg(Pfb)OH, for NH₂-(L)Arg-(D)Lys-(L)Glu-OH [154] aa₂ = H₂N-(D)-Lys(Boc)OH aa₃ = H₂N-(L)-Arg(Pfb)OH, and for NH₂-(D)Arg-(D)Phe-(L)Glu-OH [155] aa₂ = H₂N-(D)-Phe-OH aa₃ = H₂N-(D)-Arg(Pfb)OH.

Scheme 53.

With the peptides in hand, we wished to study the interaction between the TSA [151] and the peptide before incorporating them both into a molecularly imprinted polymer since, once incorporated into an MIP analysis of the binding interactions will be prohibitively complicated.

Chapter 7. NMR STUDIES.

There are a range of experimental techniques available to determine binding between a ligand and host including affinity chromatography methods, a variety of mass spectrometry techniques using MALDI-MS or ESI-MS and various NMR strategies. A review has recently been published which highlights advances and relevant applications in all of these areas¹¹³. We decided to focus on NMR methods in order to study the TSA-peptide binding since such studies could be carried out first hand in house.

7.0 Diffusion edited NMR.

Many NMR sensitive parameters change upon complex formation, including chemical shifts, relaxation rates, and diffusion rates. Perhaps the most widely used technique to observe complex formation involves studying the changes in chemical shift with varying concentrations. The signals usually involved are amide NH peaks¹¹⁴ (although they can be from other functional groups²¹) and are chosen because amide signals are downfield and usually distinct from the rest of the spectrum, therefore chemical shift changes can be clearly observed. In our case, the molecular modelling (Chapter 5) indicates that the amide NH groups are not expected to be involved in binding and, as this should make studying chemical shift changes difficult, we decided to observe changes in diffusion on complexation.

The basic principle behind diffusion NMR is that the translational diffusion of a molecule in solution is dependent on, amongst other factors, the molecular mass of the molecule. If a molecule subsequently forms a complex with a ligand or host the 'apparent' molecular mass changes, which is observable as a change (a slowing) in the rate of diffusion. The measurement of diffusion with NMR techniques relies on the pulsed-field gradient spin echo (PGSE) technique and has been known since the mid-sixties¹¹⁵.

In the last few years there have been some impressive advances in diffusion methods, most notably 'diffusion edited NMR' techniques¹¹⁶⁻¹²¹ which have been applied to the detection of ligands in combinatorial mixtures. In diffusion editing a library of ligands is

'edited' out of the NMR spectrum, in other words, to the observer a flat baseline is produced. In order to achieve this, pulsed field gradient (PFG) parameters are found which match the rate of diffusion of the ligands such that no signals are observed on the NMR timescale. If a host is then added to the library, the apparent molecular mass of any ligands that are suitable guests will change, and this is reflected in a change in diffusion rate. The parameters which edited out the ligands are no longer suitable for the binding ligands and thus an edited spectrum is observed which contains only signals from the host and the successful ligands. As such the experiment represents combinatorial chemistry in an NMR tube, with an in-built deconvolution method.

Such a method would be particularly useful for studies into TSA-peptide binding, since, not only could the desired peptides [153], [154] and [155] be studied, but also a range of random peptides could be screened.

Since diffusion edited NMR is a relatively new technique we decided to first establish suitable PFG conditions on a test system. The system we chose was based on the work of Shapiro *et al*¹¹⁷ and incorporates a range of ligands: DL-isocitric lactone [161], (*S*)-(+)-*o*-acetylmandelic acid [162] methyl isobutyrate [163] *t*-butylpropionate [164] and the host quinine [165] (Figure 34).

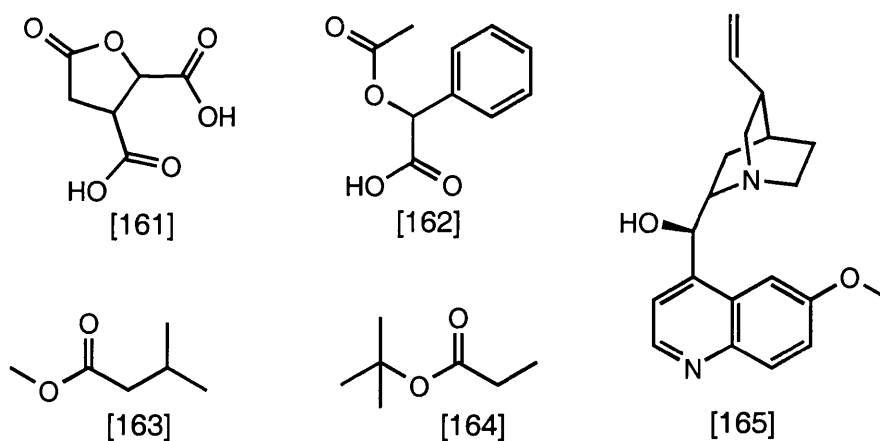


Figure 34

A series of studies in chloroform established the parameters required for diffusion editing, and the results are illustrated in figure 35.

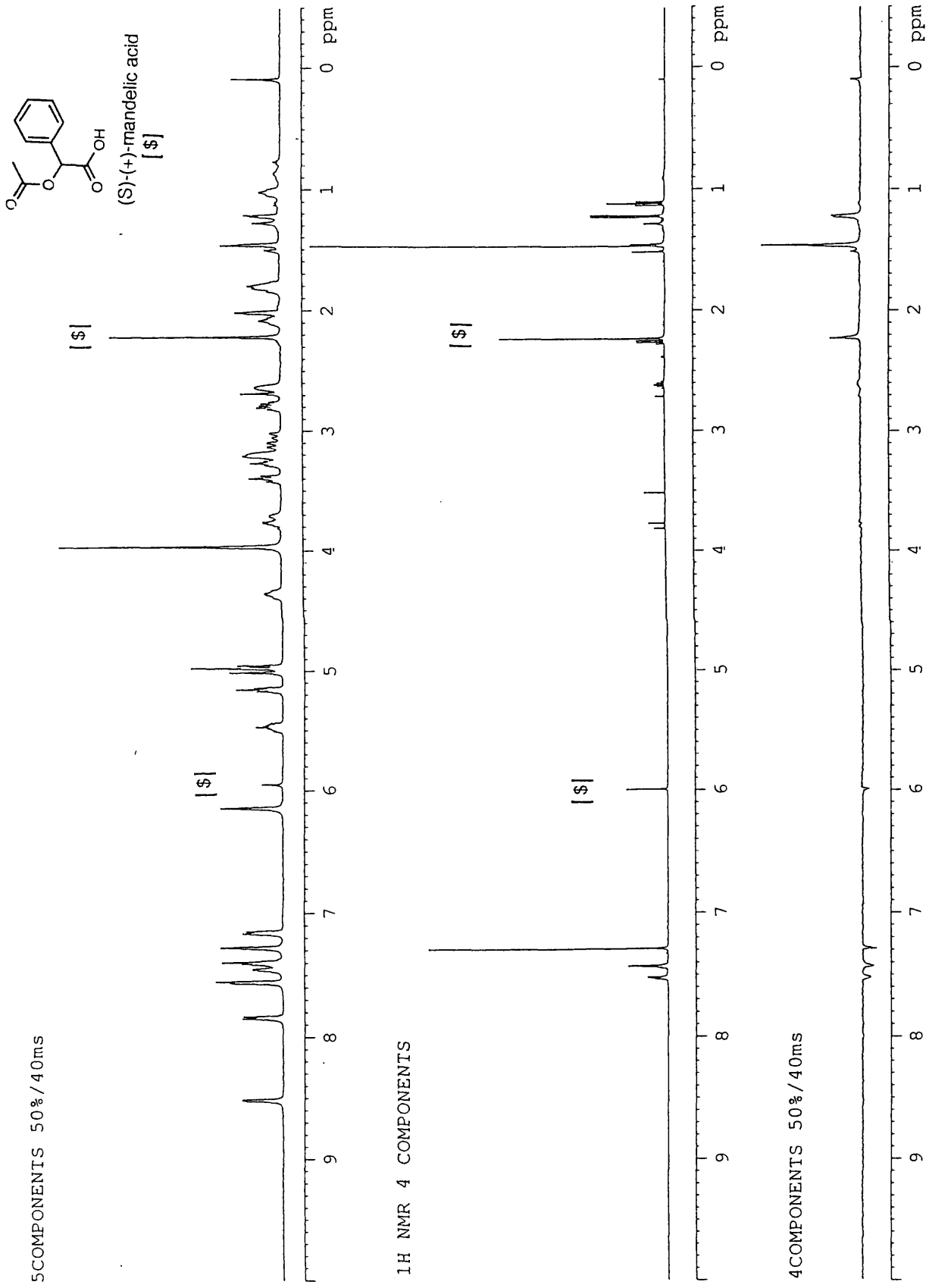


Figure 35

The host quinine is known to bind to the carboxylic acids DL-isocitric lactone [161] and (*S*)-(+)-*o*-acetylmandelic acid [162]¹²². This was confirmed by this experiment as the signals due to both of these compounds were observed in the presence of the host under the PFG conditions found for ligand suppression[#]. In contrast the two non-binding molecules [163] and [164] were not observed under the PFG conditions, either in the presence or absence of the quinine host [165]. This can be clearly seen by comparing the *t*-butyl peak at 1.46ppm and the quartet at 2.25ppm, both due to the non-binding substrate [164], which are completely suppressed under the PFG conditions in both the presence and absence of the host. In comparison, the singlet at 2.2ppm assigned to the CH₃ of (*S*)-(+)-*o*-acetylmandelic acid [162] is enhanced relative to the other ligand peaks in the PFG experiment with the quinine host. This result corroborates the observed experimental results of Shapiro *et al* in a very similar system¹²² and was particularly encouraging since the molecular weight changes involved were so small. This is important. The molecular weight difference between the TSA [151] and the TSA-peptide complex with [153], [154] or [155] is in the order of 200, thus it was a concern that the window for discovering the correct parameters for diffusion editing the ligand without affecting the host was too small.

The above result encouraged us to attempt a diffusion edited NMR experiment on the three tripeptide-TSA systems. Before such an approach could be attempted several factors had to be considered:

- The peptides are not yet derivatised as functional monomers and are insoluble in deuterated chloroform. Although a deuterated polar non-protic solvent would optimise the interactions involved, and would thus be preferable for such studies, the expense is prohibitive. Another solvent, such as deuterated water must be used for the NMR binding studies.
- Water is expected to disrupt and weaken the TSA-peptide hydrogen bonding and electrostatic interactions, by increasing solvation of the functional groups. This

[#] In the case of DL-isocitric lactone [161] the solubility was so low in the absence of quinine that it was barely observable in the ¹H NMR spectrum without the host [165].

effect was noted previously in work by Shapiro *et al* into the diffusion edited NMR of a library of ligands for vancomycin¹²⁰. In this study problems were also attributed to the small size differences between the ligands and vancomycin which became especially significant in cases where the binding affinity for the ligands was relatively weak.

- Finally, the small difference in molecular weight between the host and the ligand means that, in initial studies, it may be preferable to edit out the TSA rather than the peptides and study a single TSA-peptide complex to optimise the apparent molecular weight change.

In order to carry out the NMR experiment it was first necessary to determine the correct pD for the studies. Amine oxides behave as weak bases forming stable salts with acids¹²³. The pK_a values of the conjugate acids are normally in the range of 5, however, little physical data is available for aliphatic amine oxides. To study binding in solution it was thus necessary to first determine the pD range at which the *N*-oxide group was protonated and the carboxylic acid binding group in the peptide was deprotonated. In order to study the protonation behaviour of the TSA imprint molecule [151], a range of ¹H NMRs at different pDs were obtained (Figure 36).

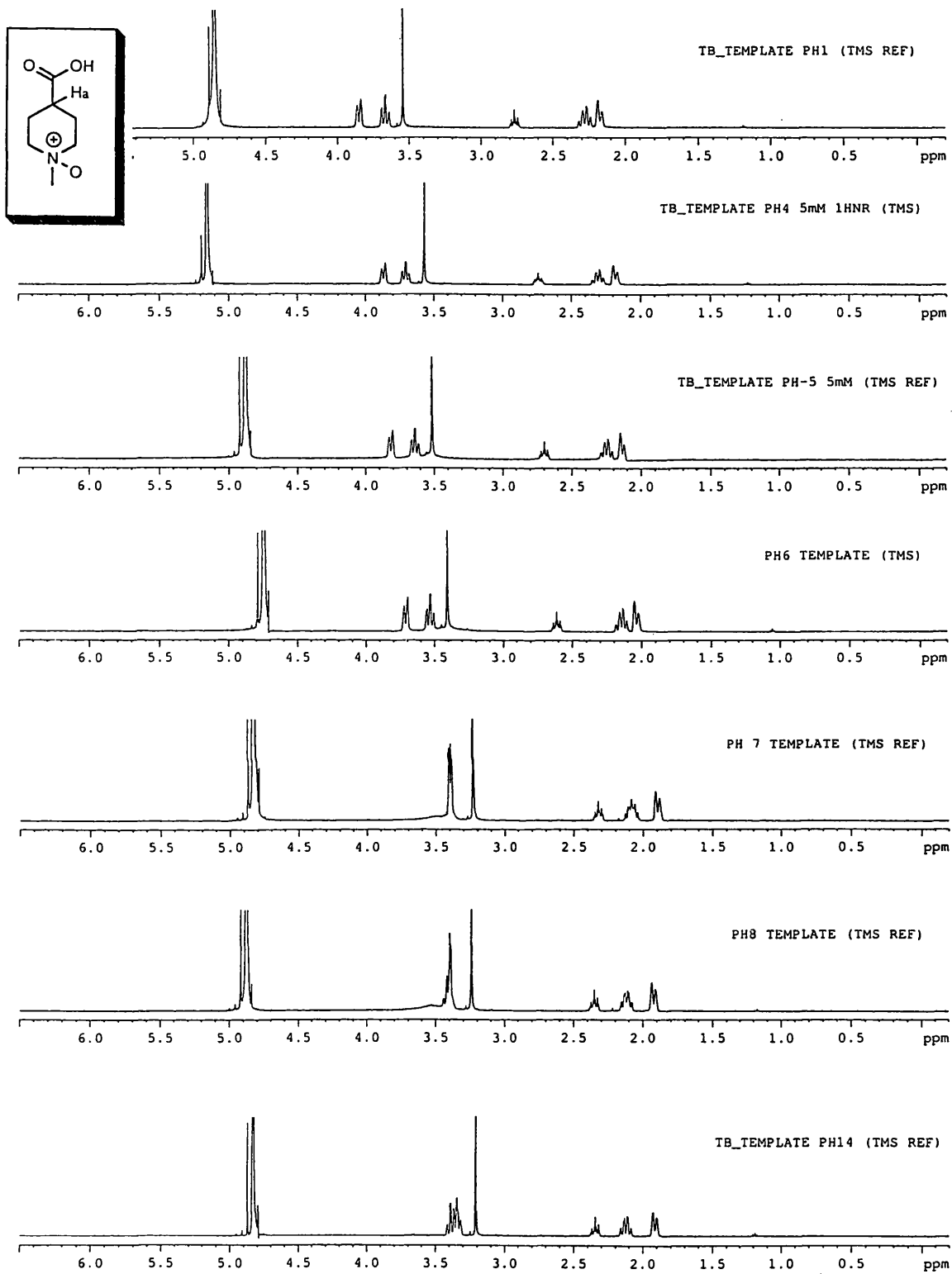


Figure 36

As can be seen from figure 36 the protonation of the *N*-oxide group occurs between pD 7 and 6. Protonation is accompanied by a drastic change in chemical shift, however, analysis of the J coupling constants of the peak attributed to H_a (Figure 37) indicates that this is not due to a conformational change. In the absence of water the presence of an intramolecular hydrogen bond such as in [166] might be possible (Figure 37). However, the coupling constants for the triple triplet at 2.40-2.70ppm do not change, indicating that the dihedral angles are unaffected and the change in chemical shift is not due to a conformational variation.

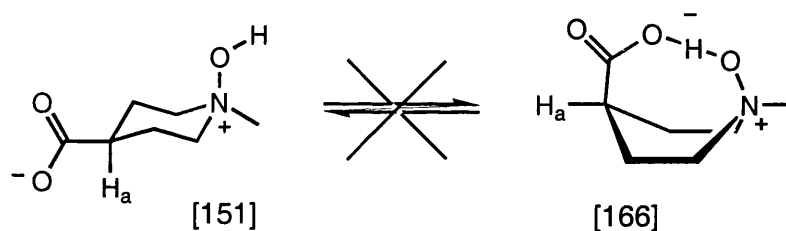


Figure 37

The pD studies indicated that NMR studies at pD 5 should allow for optimal binding, since at this pD the protonation state required for the desired complementary TSA [151]-peptide interactions illustrated by the modelling (Figures 30,31,and 32; p104, 105 and 106) should be favourable.

Initial attempts at diffusion edited NMR experiments were disappointing. An exhaustive range of PFG parameters were tried but no suitable conditions could be found. In order to carry out the experiment, PFG parameters must be discovered which suppress signals due to the TSA, but which do not suppress a separate sample of the peptide. In all cases conditions which led to suppression of the TSA also suppressed the peptide sample. This may demonstrate the molecular weight difference limitation of the diffusion edited experiments in water.

7.1 Diffusion Measurements.

In order to investigate TSA-peptide binding we therefore turned to a more linear strategy. The diffusion constant for the TSA [151] was determined in the presence and

absence of the individual tri-peptide ligands. As discussed previously, a slowing in the rate of diffusion is an indication that binding is involved. The rate of diffusion of a molecule can be related to the NMR parameters according to the following equation^{124,125} (Equation 2).

$$\text{Ln}I = \text{Ln} I_0 - \gamma^2 \delta^2 g^2 D (\Delta - \delta/3 - \tau/2) \quad \text{Equation 2}$$

Where I = intensity of the resonance in the 1D spectrum “integral intensity”

γ = gyromagnetic ratio

δ = 2 x duration of the gradient pulse

g = amplitude of the gradient pulse

τ = gradient recovery time

Δ = diffusion delay

D = Diffusion coefficient

$\text{Ln}I_0$ = Natural log of the integral intensity at $g=0$, which is constant for a given concentration.

Simplistically, if all other parameters are kept constant, the diffusion constant can be calculated from the variation in Ln integral intensity with gradient strength or amplitude squared g^2 , ie:

$$\text{Ln}I \propto -CDg^2 \quad \text{Equation 3}$$

Where C is a constant.

Using this equation a series of experiments were carried out to determine the diffusion constant of the TSA in the presence and absence of the tri-peptides. In each case a series of NMR's at different gradient strengths were obtained and a plot of LnI against gradient strength squared was drawn for each clearly resolved peak. The numerical results are tabulated below. In each case the diffusion coefficient was calculated using

all resolved peaks due to that compound. The maximum gradient strength of 0.51T was determined according to standard procedures¹²⁵.

pD	sample	CD/TSA [151]	CD/PEP [153]	CD/PEP [154]	CD/PEP [155]	Diffusion coefficient TSA [151] m ² /s, 10 ⁻¹⁰	Diffusion coefficient PEP [153] m ² /s, 10 ⁻¹⁰	Diffusion coefficient PEP [154] m ² /s, 10 ⁻¹⁰	Diffusion coefficient PEP [155] m ² /s, 10 ⁻¹⁰
5	TSA [151]	7.96 ± 0.3	--	--	--	9.33 ± 0.4	--	--	--
5	TSA [151] + PEP[153]	7.78 ± 0.4	4.64 ± 0.01	--	--	9.12 ± 0.5	5.44 ± 0.01	--	--
5	TSA [151] + PEP[154]	7.62 ± 0.1	--	4.64 ± 0.01	--	8.93 ± 0.1	--	5.44 ± 0.01	--
5	TSA [151] + PEP[155]	7.56 ± 0.2	--	--	4.66 ± 0.01	8.83 ± 0.2	--	--	5.46 ± 0.01
5	PEP [153]	--	4.64 ± 0.01	--	--	--	5.44 ± 0.01	--	--
5	PEP [154]	--	--	4.64 ± 0.01	--	--	--	5.44 ± 0.01	--
5	PEP [155]	--	--	--	4.76 ± 0.1	--	--	--	5.25 ± 0.1

PFG ¹H NMR diffusion measurements. C = 8.53 x 10⁹ T⁻² s. D = diffusion coefficient. Values for CD represent the average slope of LnI against gradient strength squared: g² (Appendix 3) over all resolved peaks for each compound. PFG range from 3-66% log increment (100% = 0.51T), δ = 4ms, τ = 50 μs, Δ = 0.03s.

Table 10

The results show that in all cases the rate of diffusion of the TSA [151] decreased in the presence of the peptide. It would be remarkable if this consistency were due to coincidence, however, the margin of error in these values is within the realms of the change we wish to observe. To alleviate this problem it is possible to exclude the 'unreliable' peaks, which for example, lie on the shoulder or close to the peptide peaks and afford a large error value for CD. The *N*-methyl resonance, a singlet at 3.5ppm, from the TSA [151] is particularly clear from the rest of the spectrum and can be easily integrated affording a low error. Using this peak for the plot of LnI against gradient strength squared, the following values were obtained (Table 11).

sample	CD/ TSA [151]	Diffusion coefficient for TSA [151] m ² /s
TSA [151]	8.31 ± 0.02	(9.74 ± 0.02) × 10 ⁻¹⁰
TSA [151] + PEP [153]	7.82 ± 0.02	(9.17 ± 0.02) × 10 ⁻¹⁰
TSA [151] + PEP [154]	7.57 ± 0.02	(8.71 ± 0.02) × 10 ⁻¹⁰
TSA [151] + PEP [155]	7.43 ± 0.02	(8.87 ± 0.02) × 10 ⁻¹⁰

PFG 1H NMR diffusion measurements. $C = 8.53 \times 10^9 T^{-2} s$. D = diffusion coefficient. Values for CD represent slope of LnI against gradient strength squared: g^2 (Appendix 3). PFG range from 3-66% log increment (100% = 0.51T), $\delta = 4ms$, $\tau = 50 \mu s$, $\Delta = 0.03s$,

Table 11

The results indicate that there is an association between the peptides and the TSA [151], as in all cases the diffusion rate of the TSA [151] slowed in the presence of the peptide. Using both methods of calculating the diffusion coefficient the peptide [153] appears to have the least influence on the TSA [151] whilst the peptide [155] has the most influence. This is unlikely to be attributable to a difference in diffusion rates of the free peptides since they are all very similar and peptide [155] actually has a faster rate of diffusion in D₂O solution than [153] or [154].

The study above does not give much of an indication about the manner of binding involved. In order to gain more information, the diffusion coefficient for the TSA [151] in the presence of the 'best' peptide [155] was determined at pD 7. At this pD the

contribution from the *N*-oxide - carboxylic acid interaction should be negligible since both groups will, in theory, be deprotonated. This can provide important information, since the actual diffusion coefficient observed is an apparent diffusion rate corresponding to the ‘apparent’ molecular weight change on complexation and is described by equation 4 below.

$D = x_{\text{free}}D_{\text{free}} + x_{\text{bound}}D_{\text{bound}}$	Equation 4
---	------------

Where *D* is the observed diffusion co-efficient of TSA [151] in the presence of the peptide, *D*_{free} and *D*_{bound} represent the diffusion co-efficients for the free and bound TSA [151] and *x*_{free} and *x*_{bound} are the fractions of the TSA [151] in each of these states. Thus, the ‘apparent’ diffusion co-efficient is actually the sum of the contributions of the free and bound species and therefore a slower value in the presence of the same peptide is an indication that a greater percentage of the ligand is bound at that pD value.

The results are illustrated below (Table 12).

pD	sample	CD/ TSA [151]	Diffusion coefficient TSA [151] m ² /s
7	TSA [151]	7.25 ± 0.02	(8.50 ± 0.02) x 10 ⁻¹⁰
7	TSA [151] + PEP[155]	7.01 ± 0.02	(8.22 ± 0.02) x 10 ⁻¹⁰

PFG 1H NMR diffusion measurements. *C* = 8.53 x 10⁹ T⁻²s. *D* = diffusion coefficient. Values for CD represent the average slope of Ln*I* against gradient strength squared: *g*² (Appendix 3) for the multiplet at 3.35-3.4ppm.. PFG range from 3-66% log increment (100% = 0.51T), δ = 4ms, τ = 50 μs, Δ = 0.03s,

Table 12

This result indicates qualitatively that the amine oxide - carboxylic acid interaction is involved in binding, since the slowing in diffusion rate for the TSA [151] in the presence of the peptide [155] at pD 7 is to a lesser extent than at pD 5 (Table 11). This suggests that this interaction, which is possible at the latter pD, contributes towards

binding at pD 5. However, although this result indicates that both TSA [151] functional groups are involved in binding, the nature of the experiment is such that the *de facto* existence of synergistic binding cannot be assumed.

7.2 Conclusions.

The ^1H NMR studies thus indicate that the peptides [154] and [155] are suitable candidates for further study. Although they are by no means definitive, the results from the NMR binding studies suggest that the interactions illustrated in Figure 38 are feasible. It is hoped that the possibilities for multiple interactions with the imprint molecule which they provide should allow for better, well defined, binding site populations when they are used as functional monomers in imprinting.

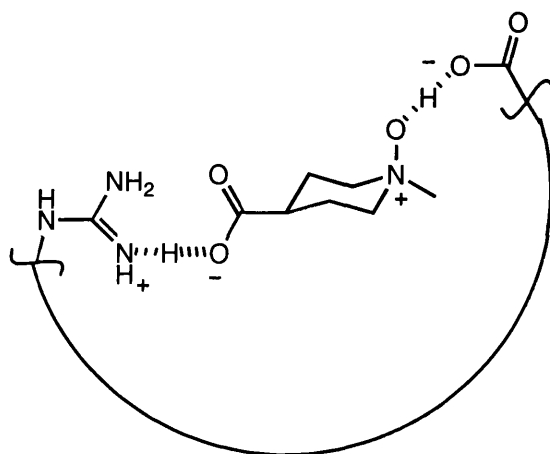
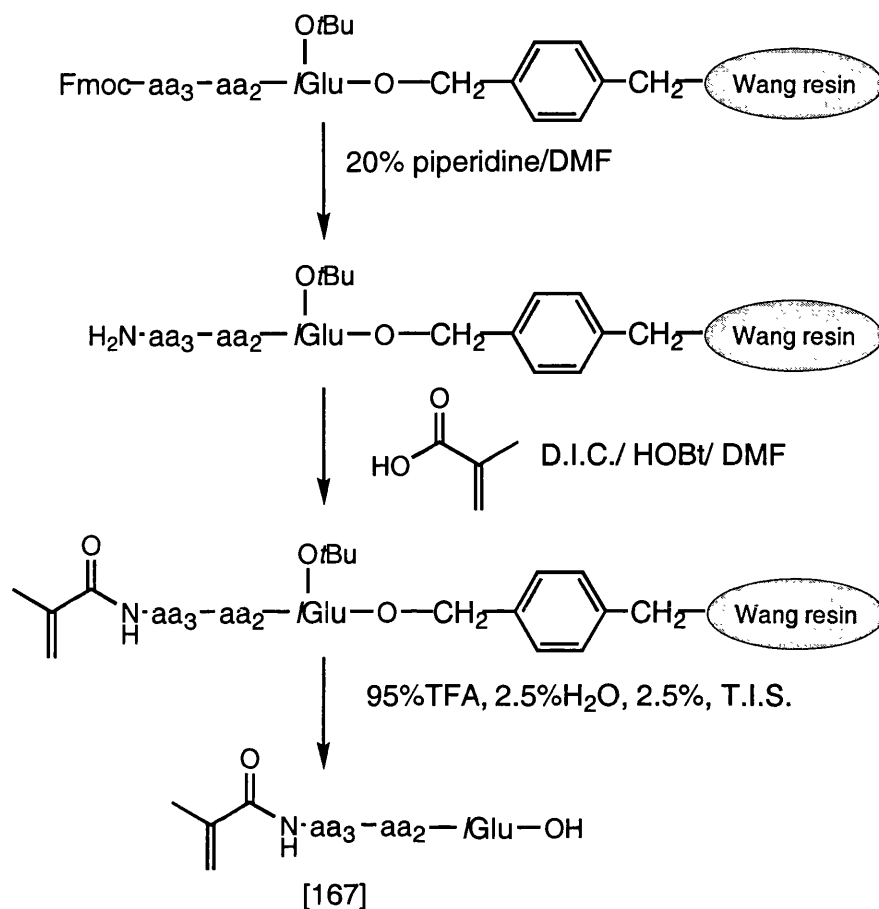


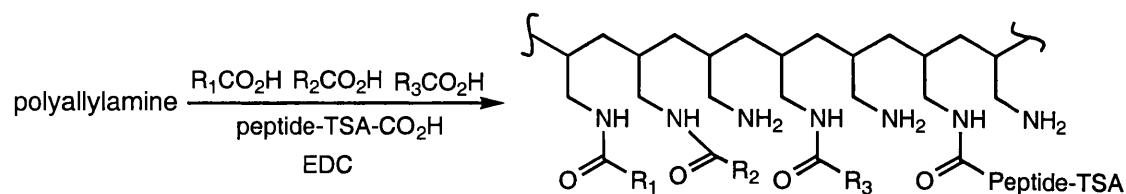
Figure 38

The incorporation of the tri-peptides [154] and [155] into an artificial enzyme mimic can be achieved in a number of ways. Firstly, as a continuation of the previous radical polymerisation approaches, the peptides could be incorporated into a polyacrylamide by functionalisation of the terminal amino residue with an acrylate group before cleavage from the resin (Scheme 54). This peptide functional monomer [167] could then be used in a classical molecular imprinting approach with an acrylamide monomer and crosslinker to produce an MIP with highly functionalised and pre-designed binding cavities.



Scheme 54

Alternatively, during the course of the present study, much literature has emerged on a variety of novel combinatorial approaches to artificial enzymes and receptors, as discussed in the introduction (Part 1), which may be relevant to the study in hand. Menger *et al* have shown that the random derivatisation of polyallylamine^{63,64} with a range of carboxylic acids can produce active artificial enzymes. We therefore envisaged that by incorporating the peptides [154] and [155] in the presence of the TSA [151], into this process, it would be possible to ‘imprint’ the polyallylamine produced, thus increasing the possibility of discovering a catalyst for the chosen transformation (Scheme 55).



Scheme 55

Furthermore, if the reaction used to create the linkage between the peptide and the polyallylamine were reversible then hopefully the interaction between the peptide and the TSA [151] would be favoured. This is reminiscent of the thermodynamic control seen in the synthesis of receptors from DCLs in the introductory chapter (part 1).

Although all of these methods were feasible, the first method was the simplest to investigate, and thus, due to time restrictions, the use of polyacrylamides as MIP matrices was chosen for further investigation. The aim was to first optimise and investigate the nature of the polymer matrix in these systems before incorporation of the more complex peptide functional monomers.

Chapter 8. POLYACRYLAMIDE MOLECULARLY IMPRINTED POLYMERS.

Since enzymes are highly polar macromolecules and are based on a polyamide backbone it seemed logical to investigate the potential of polyacrylamide MIPs as enzyme mimics. Several studies into the use of polyacrylamides as MIPs have been reported¹²⁷. However, although successful imprinted polyacrylamides have been synthesised^{128,129}, to our knowledge these have never been used for catalysis. Polyacrylamide MIPs embody a much less developed field of research than EGDMA and divinylbenzene based MIPs, thus it was germane to first investigate appropriate systems for successful imprinting before incorporation of complicated functional monomer-TSA [151] systems.

8.0 TSA selection and synthesis.

The TSA [168] chosen for the polyacrylamide studies is illustrated below (Figure 39). This molecule resembles the previously described TSA [151]. The TSA [168] was chosen with a primary amide group at C-4 instead of a carboxylic acid group, as the former moiety will hopefully be able to form an interaction with a complementary amide group in the polymer backbone.

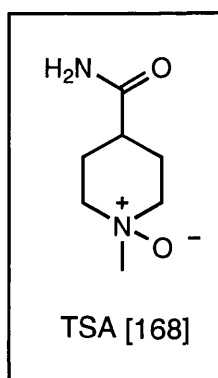
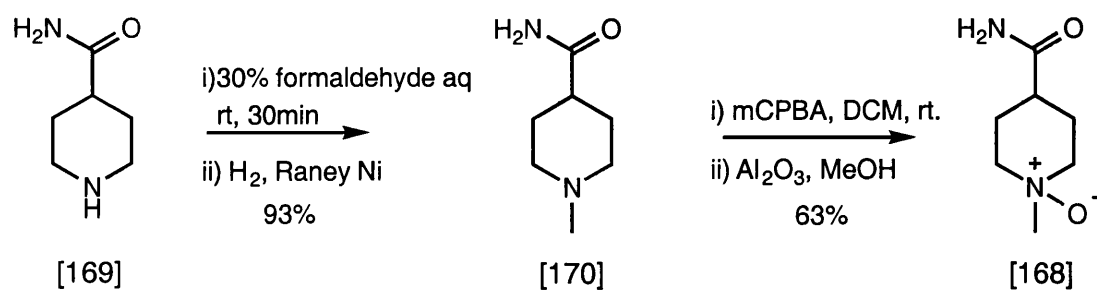


Figure 39

A further factor influencing the choice of TSA [168] was the short length of the synthesis involved. TSA [168] was synthesised in two steps in 59% overall yield (Scheme 56).



Scheme 56

8.1 Synthesis and selection of functional monomer, crosslinker and monomer.

Previous studies with polystyrene-divinylbenzene MIPs indicated that the sulfonic acid group may be too strong an acid to catalyse the ring opening of α -pinene oxide [89] with a rate suitable for catalysis studies. This information, coupled with the known interaction of the *N*-oxide group with carboxylic acids, led us to choose a carboxylic acid as the functional monomer.

With this in mind we selected the functional monomer [171] which is readily available from glycine and methacryloyl chloride (Figure 40). Previous work in the group had identified [174] as a suitable crosslinker and [172] as a suitable monomer respectively⁹⁶. The alternative crosslinker *N,N'*-ethylene bisacrylamide [173] was also considered. Any reagents which were not commercially available could be readily synthesised from the appropriate amine with methacryloyl chloride.

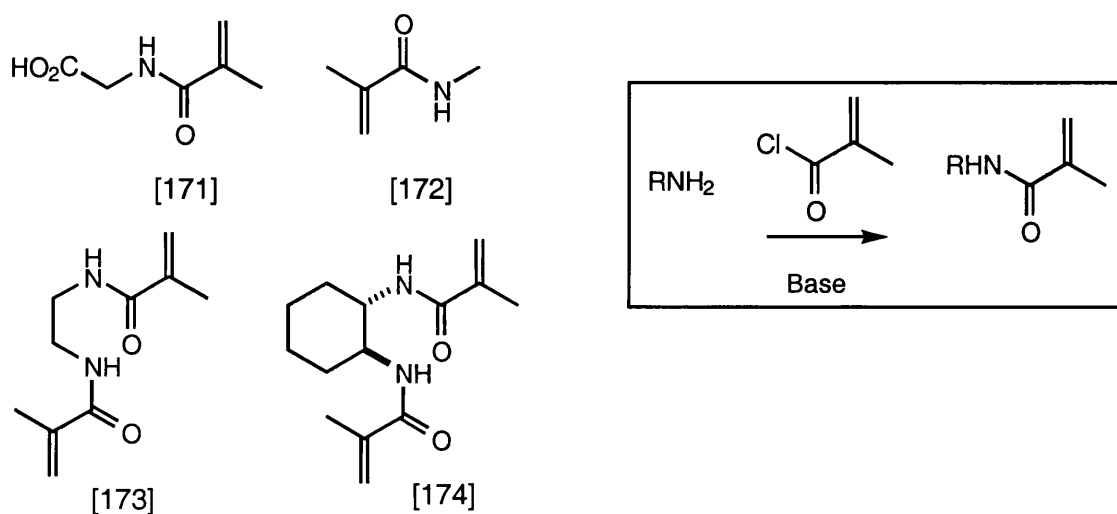
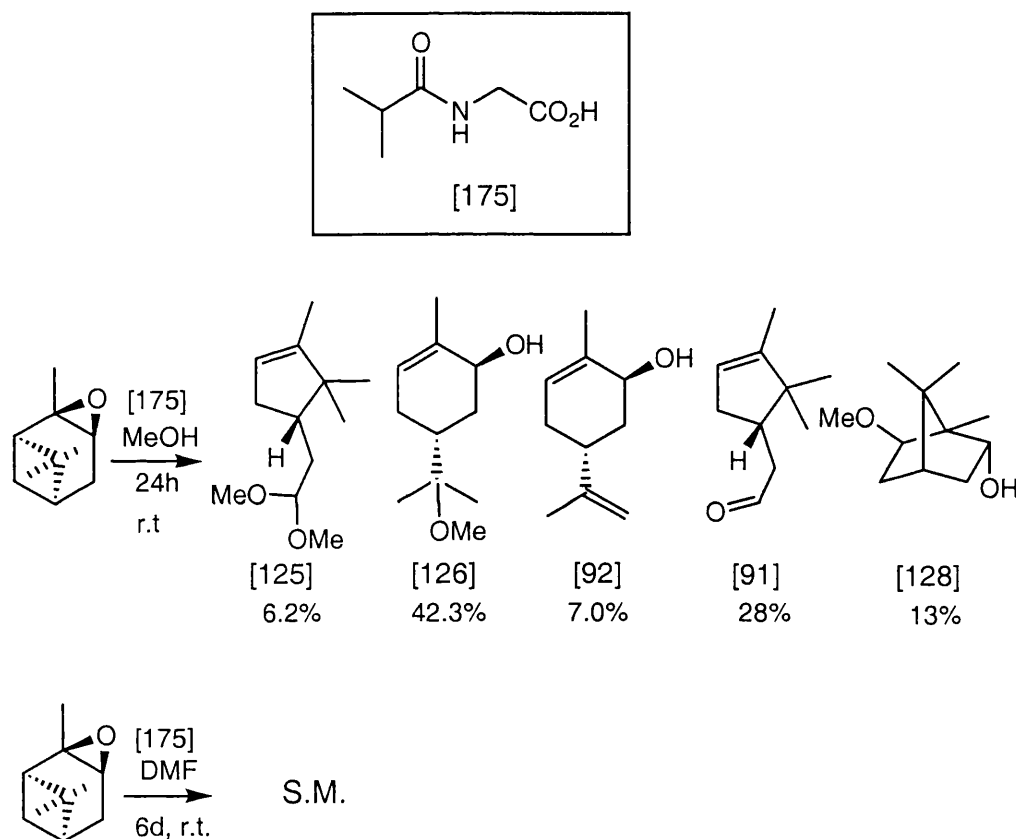


Figure 40

8.2. Studies on a model catalytic system.

In order to test the feasibility of using the carboxylic acid group as a catalyst in the ring-opening reaction of α -pinene oxide the functional monomer mimic [175] (Scheme 57) was synthesised. This molecule resembles the carboxylic acid group which will be incorporated into the MIP binding site, and was used as a model compound to test the reactivity of the carboxylic acid group towards the ring opening of α -pinene oxide (Scheme 57).



Scheme 57

As can be seen from the results, the acid [175] catalyses the ring opening of α -pinene oxide [89] in the presence of the nucleophilic solvent, methanol, but has no effect on the starting material in DMF. These results were encouraging since any rate acceleration due to the polymer MIPs should be observable with such a rate of reaction. The contrasting behaviour of the carboxylic acid and the sulfonic acid studies earlier is also noteworthy.

8.3 The pre-organised complex.

A problem with the new TSA-MIP system is that both the imprint molecule [168] and the functional monomer [171] are insoluble in non-polar solvents. The polymerisations were therefore carried out in methanol and, as this may be expected to disrupt the non-hydrophobic binding interactions, the presence of the pre-organised complex in this medium was investigated.

A ^1H NMR in deuterated methanol of the TSA [168] in the presence and absence of the functional monomer [171] indicates that the desired pre-organised complex is formed (Figure 41): the spectrum of the TSA [168] alone is typical of the non-protonated amine oxide (*vide supra*), however, the spectrum in the presence of the functional monomer is drastically different. This latter spectrum is typical of the protonated TSA, a fact which was confirmed by a ^1H NMR of the TSA in acidic deuterated water (Figure 41). Since the carboxylate anion is expected to be associated with the counterion the result suggests the formation of the desired pre-organised complex.

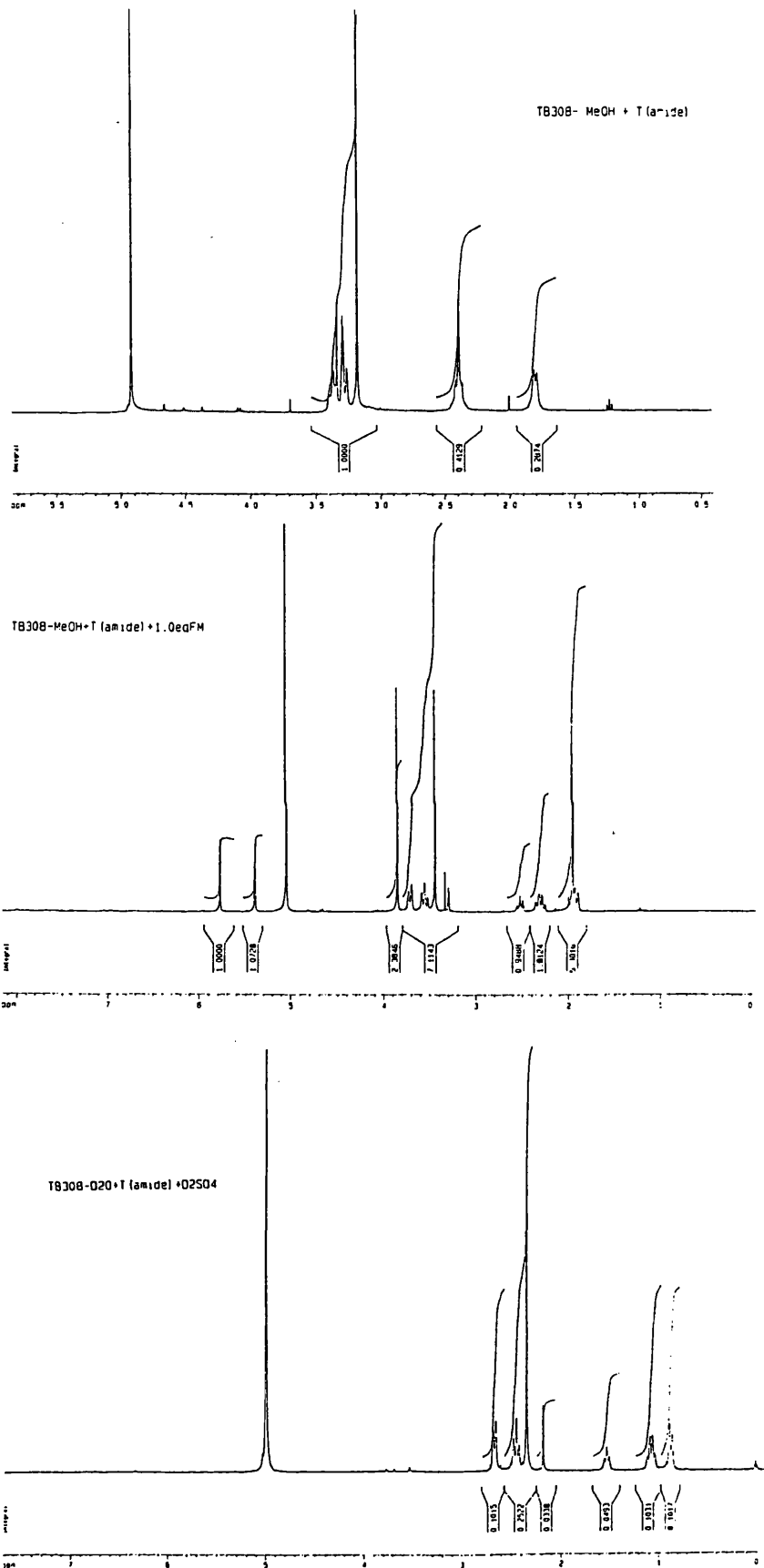
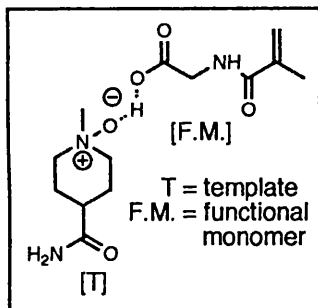
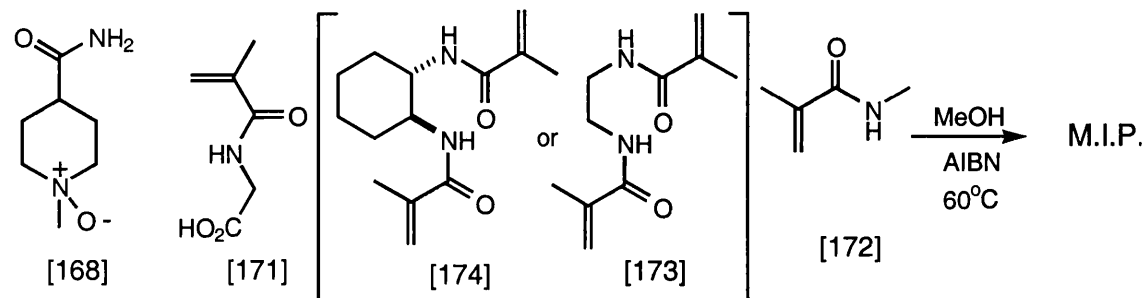


Figure 41

8.4 Synthesis of Polyacrylamide MIPs.



Scheme 58

A range of polymers of varying *N*-methyl methacrylamide[172] to (+/-)-*N*, *N*-dimethacryloyl-*trans*-(1, 2)-diaminocyclohexane [174] or *N,N'*-ethylene bisacrylamide [173] ratios were synthesised, with various loadings of imprint molecule [168] and functional monomer [171] (Table 13). By analogy with the polystyrene-divinylbenzene MIPs, the relative quantities of the reagents have important consequences on the molecular recognition properties of the MIPs produced (*vide supra*). In order to compare the polyacrylamide polymers with the previous styrene based MIPs one MIP was synthesised with TSA (*1R, 5R*)-*trans*-carvyl amine [93] as imprint molecule.

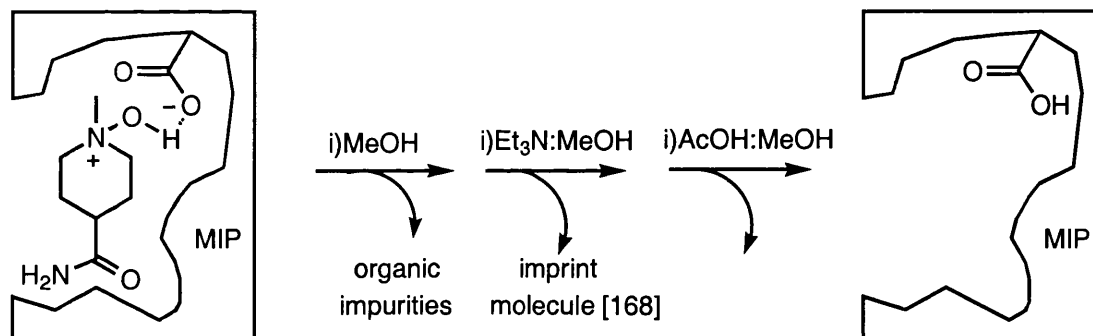
MIP	loading	crosslinker: monomer ratio	monomer [172] mmol	cross- linker [174]/ mmol	cross- linker [173]/ mmol	functional monomer [171] mmol	TSA [168] mmol	TSA [93] mmol
[G]	1/10	2:1	1.6	3.2	--	0.48	0.48	--
[H]	1/10	6:1	0.7	4.1	--	0.48	0.48	--
[I]	1/7	6:1	1.3	7.6	--	1.3	1.3	--
[J]	1/35	6:1	1.6	9.5	--	0.36	0.36	--
[K]	1/7	6:1	0.63	--	3.8	0.63	0.63	--
[L]	1/35	6:1	1.6	9.5	--	0.36	--	0.36

Table 13

The definitions of loading and crosslinker:monomer ratio are the same as for the previous MIPs [A] to [F]. The porogen was methanol (2.5v/v of polymerisable molecules) and the radical initiator was AIBN (2mol% per polymerisable double bond).

8.5 Polymer regeneration and binding studies.

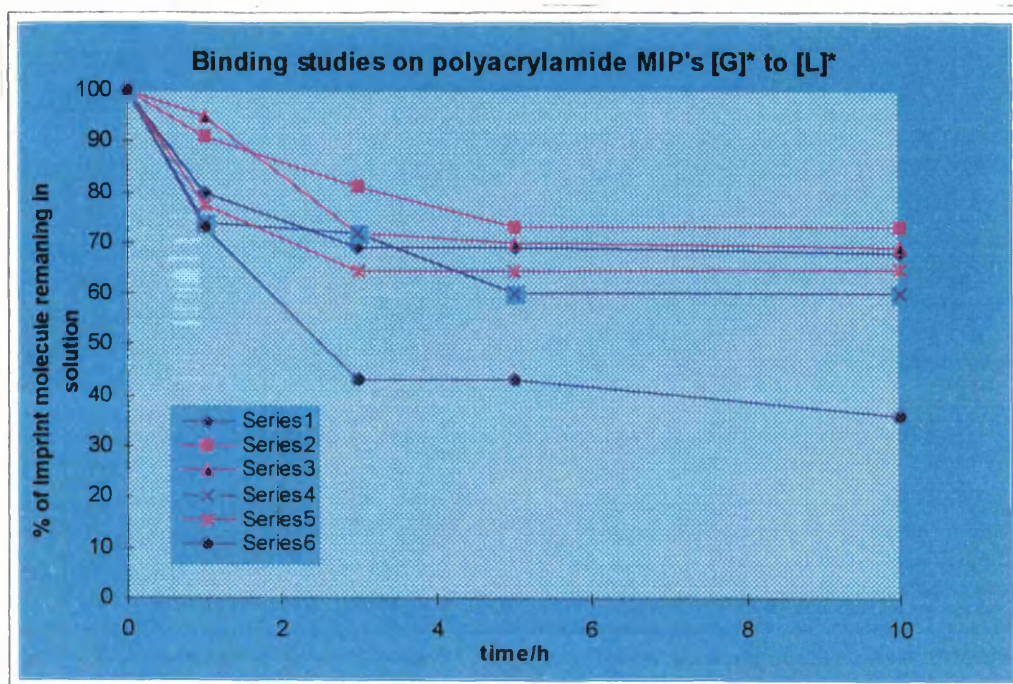
Binding studies are an effective method for comparing the imprinting of the MIPs [G] to [L] however, the imprint molecule must first be removed and the carboxylic acid group regenerated. This was achieved using the base-acid wash protocol described in Scheme 59. The subsequent regenerated MIPs are denoted by a * notation.



Scheme 59

The binding studies were carried out using the same setup as for the polystyrene-divinylbenzene MIPs discussed previously. The solvent used was methanol and the uptake of the imprint molecule [168] or [93] from solution was monitored as a function of time.

In the case of the polyacrylamide MIPs it was discovered that the approximation used previously to calculate the non-specific binding fraction was inappropriate since the calculation described in Equation 1 (Section 2.4) led to negative values for the percentage of imprint molecule bound. The binding studies were thus represented indirectly: the amount of imprint molecule remaining in solution was plotted as a function of time (Figure 42).



Binding studies were carried out with *N*-methyl isonipecotamide *N*-oxide [168] unless otherwise stated Series 1; MIP [G]*, loading 1/10, m:c 2:1: Series 2; MIP [H]*, loading 1/10, m:c 6:1: Series 3; MIP [I]*, loading 1/7, m:c 6:1: Series 4; MIP [J]*, loading 1/35, m:c 6:1: Series 5; MIP [K]*, loading 1/7, m:c 6:1 (crosslinker [173]) : Series 6; MIP [L]*, loading 1/35, m:c 6:1 (imprint molecule (1*R*, 5*R*)-*trans*-carvyl amine [93]).

Figure 42

The immediately obvious result from these binding studies is that the imprinting of the (1*R*, 5*R*)-*trans*-carvyl amine imprint molecule [93] in MIP [L]* is much more efficient than for the TSA [168] imprinted equivalent [J]*. This may be expected from the difference in basicity of the two functional groups involved in the interaction with the acidic functional monomer. However, the values for the TSA [168] imprinted MIPs are disappointing. Despite this fact several tentative conclusions can be made from a comparison of the TSA [168] imprinted polyacrylamides:

- A comparison of MIPs [I]* and [K]* (Series 3 and 5 respectively), which are synthesised under identical conditions except for the fact that [I] uses (+/-)-*N*, *N*-dimethacryloyl-*trans*-(1, 2)-diaminocyclohexane [174], whilst [K] uses *N,N*-ethylene bisacrylamide [173] as crosslinker, indicates that the latter crosslinker is marginally preferable for successful imprinting.

-
- For reasons that are unclear, both MIPs which are synthesised with a 1/10 loading produce a slow rate of uptake at the beginning of the binding experiment.
 - Comparison of the relative positions of each of the MIPs at the end of the study indicate that a low loading is preferable for good binding characteristics: both MIPs with a 1/35 loading absorb a greater amount of the imprint molecule. A cautionary note is however necessary, these results may be skewed slightly because the 1/35 polymers are also greater in volume and thus absorb more solvent. As no correction is made to account for non-specific binding this could be evidenced by an apparently higher yield of imprinted sites.

8.6 Reactions of the polyacrylamide MIPs.

Although the binding studies indicated that the polyacrylamide MIPs were not as effectively imprinted as the previous polystyrene MIPs, the influence of MIP [G]* on the product distribution of the ring opening reaction of α -pinene oxide [89] was investigated. Since, in our model studies with [175], the rate of the reaction had been shown to be much much slower with a carboxylic acid rather than a sulfonic acid catalyst, it was hoped that catalysis may still be observable. The reactions were carried out in both methanol and DMF, however, no catalysis of the reaction, or influence on product distribution was observable in either case.

8.7 Conclusions.

It is evident that there is still room for improvement in the synthesis of our polyacrylamide MIPs. There are several influential variables which are immediately obvious. Firstly, successful imprinting should be favoured by carrying out the polymerisations at lower temperature since this should disrupt the weak non covalent interactions in the pre-organised complex less, and could be an avenue for further research. Moreover, the choice of polyacrylamide monomer and crosslinker could doubtlessly be improved. These studies have shown that the nature of the crosslinker can have a significant influence on the imprinting process; changing from (+/-)-*N,N*-dimethacryloyl-*trans*-(1, 2)-diaminocyclohexane [174] to *N,N'*-ethylene bisacrylamide

[173] produced an MIP which absorbed a greater amount of the imprint molecule [168] in the subsequent binding study.

The investigation of polyacrylamides as catalytic MIPs represents a subject in its infancy. However, these early studies have shown that polyacrylamides are suitable polymer matrices for molecular imprinting and it is hoped that, by incorporation of complex functional monomers such as the tri-peptides [154] and [155], it will be possible to improve the efficiency of the imprinting process as well as including designed catalytic groups in the binding cavity. Due to time restrictions, further investigation involving the incorporation of the two tri-peptides [154] and [155] as functional monomers, was not possible in this work. However, it is expected that the use of functional monomers that are known to bind to the TSA will allow for more defined binding cavity, and will better mimic the environment in a natural enzyme active site.

Chapter 9. CONCLUSIONS AND PERSPECTIVES FOR FUTURE RESEARCH.

We have described the development of a novel approach to the synthesis of artificial enzymes, which combines the classical molecular imprinting methodology, with a new method for creating the desired functionality in the binding site.

Our early studies with the polystyrene-divinylbenzene MIPs served us well in understanding many of the subtleties which influence the character and heterogeneity of the polymer binding cavities. Despite the fact that our crude transition state mimic [93] contained only a single electrostatic interaction as a point of contact with the polymer we were nevertheless able to determine that the MIPs produced were still shape selective, as was demonstrated by the competitive binding studies. Furthermore, analysis of the MIP reactions furnished important information on the product distribution of the acid catalysed ring-opening reaction of α -pinene oxide [89]. Preliminary results suggested that formation of the desired product *trans*-carveol [92] was favoured when a polar aprotic solvent such as DMF was employed. Reflection on this information, and on the polypeptide nature of natural enzymes, encouraged us to investigate the use of polyacrylamides as MIPs.

We also chose to refine the interactions involved in the binding of the imprint molecule to the MIP binding cavity. Although the polystyrene-divinylbenzene MIPs had a designed acid group in the MIP binding site, we felt that this was not enough functionality to achieve the subtleties in catalysis which we wished to investigate.

With these considerations in mind we developed our second generation transition state analogue [151], which contained appropriate functionality to generate an electrostatic interaction with both an acid and a base in a suitable host. In order to address the issues of both the heterogeneity of the MIP binding sites, and the problem of analysing the MIP cavities once they have been formed, we proposed a novel strategy for forming the MIPs using a tripeptide as the functional monomer. This not only allowed us to study

the interactions involved in binding, prior to incorporation into an MIP, it also enabled us to introduce an element of design into the system, since we could to a certain extent, select the multiple interactions between the polymer and the imprint molecule. We therefore employed molecular modelling to chose a series of three peptides which displayed the desired acid-base interactions with the transition state analogue. Subsequent NMR studies confirmed that the peptides [154] and [155] selected by the molecular modelling, were involved in binding, and were feasible functional monomer candidates. Simultaneous studies into the synthesis of polyacrylamide MIPs suggested that they would be suitable polymer matrices[#] for catalytic MIPs.

The field of artificial enzymes is a rapidly evolving subject. Within this genre molecular imprinting embodies a subject in its infancy, which is reflected in the work described here. As a result there are many possible avenues for further research, as discussed in section 7.2.

The derivatisation of the peptide as a classical acrylamide functional monomer and use in a radical polymerisation is perhaps the most obvious choice, however, as the literature review in part 1 has indicated, there are several other possibilities. One option may be to move away from the classical MIP systems and take inspiration from the developing combinatorial approaches to artificial enzymes. Menger's randomly derivatised polyallylamines were highly successful in achieving catalysis and although the use of a TSA during the generation of such 'combinatorial polymers' has been postulated, no such example has yet been reported to our knowledge. In a related approach, using a very basic derivatisation of a polymer backbone PEI, Suh *et al* have achieved proteinase activity at pH 7 (Section 1.2.3). It would thus be highly interesting to investigate incorporating the molecular imprinting approach, and our TSA-peptide system in particular, into a novel system based on a pre-formed polymer such as PEI or polyallylamine. Crosslinking or subsequent random derivatisation of the polymer could be investigated with the aim of stabilising the structure and realising a third point of

[#] Since the writing of this thesis, a recent publication which describes the use of polyacrylamide MIP as a catalyst for an aminolysis reaction has been published: Idziak, I.; Gravel, D.; Zhu, X. X., *Tetrahedron Lett.*, **1999**, *40*, 9167.

contact respectively. Indeed, as both the groups of Suh and Menger have demonstrated, crosslinking may not be so important to MIPs used for enzyme mimic applications.

The advent of the molecular imprinting technique encouraged many to attempt the synthesis of artificial enzymes using this novel methodology. However, as this study has illustrated, the complexities involved in biomimetic catalysis are difficult to incorporate into classical molecular imprinting in a fashion which allows for subsequent control or analysis of the catalytic system. The heterogeneity of the binding sites produced is a persistent problem, and since the radical polymerisation procedure is inherently under kinetic control, it is difficult to foresee a solution to this problem. This is reflected in the work here which has moved away from the classical MIP strategies and has established the foundations for research into a different method for producing catalytic polymers, which will hopefully overcome some of the difficulties attributed to employing a radical polymerisation process.

Part 3. EXPERIMENTAL

Chapter 1. GENERAL EXPERIMENTAL

¹H NMR Spectra were recorded at 500MHz on a Bruker Avance 500, at 400MHz on a Varian VXR-400 or a Bruker AMX-400 or at 300MHz on a Bruker AMX-300. ¹³C NMR spectra were recorded at 125.8MHz, 100.6 MHz or 75.4MHz on the instruments above. ¹³C Assignments are supported by DEPT editing. Residual protic solvent was taken as the internal standard excepting spectra obtained in D₂O or 90% H₂O/D₂O where either T.S.P. as an external standard, or 1,4-dioxane as an internal standard was used. Pulsed Field Gradient (P.F.G.) experiments were carried out on a Bruker Avance 500 with a Bruker GAB-type gradient accessory. The abbreviations used to indicate multiplicity are s=singlet, d=doublet, t=triplet, q=quartet, dd=double doublet, dt=double triplet, dd=double, m=multiplet, sept=septet, br=broad. Infrared spectra were recorded as thin films on KBr plates or as KBr discs on a Perkin-Elmer FT-IR 1605 instrument. The abbreviations used to denote peak intensity are w=weak, m=medium, s=strong, b=broad. Mass spectra were recorded under either electron impact, atmospheric pressure chemical ionisation, or fast atom bombardment conditions at the School of Pharmacy, University of London ULRS service. Melting points were taken with a Reichert hot stage or an Electrothermal 9100 instrument and are uncorrected. Boiling points for Kugelrohr distillations refer to uncorrected air temperatures. Pressure was recorded on a standard Gallenkamp manometer. Microanalyses were performed in the University College London Chemistry Department. Optical Rotations were taken with a 'POLAAR 2000' instrument. S.E.M. profiles were performed on a Hitachi S570.

Petroleum ether (b.p. 40-60°C) was distilled prior to use. DMF was dried with MgSO₄(s) and distilled over Linde type 4A molecular sieves under reduced pressure. All other solvents used were distilled under nitrogen immediately prior to use. Diethyl ether and tetrahydrofuran were both distilled from sodium-benzophenone. Dichloromethane and chloroform were distilled from either phosphorus pentoxide or calcium hydride. Toluene was distilled over sodium and methanol was distilled from magnesium turnings. Triethylamine and isopropylamine was distilled over calcium hydride.

Styrene (inhibitor 10-15ppm *p-t*-butylcatechol) and 80% divinylbenzene tech. (mixture of *cis* and *trans* isomers, inhibitor 1000ppm *p-t*-butylcatechol) were supplied by Aldrich and were distilled from hydroquinone at low pressure prior to use. *N*-methylmethacrylamide was also distilled over hydroquinone at low pressure and stored under nitrogen at -5°C. A.I.B.N. was recrystallised from DCM. All amine reagents were distilled before use.

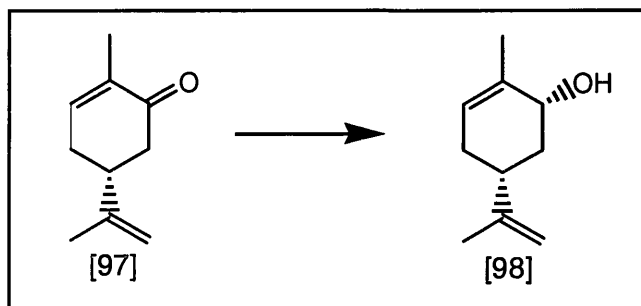
Analytical thin layer chromatography was performed on pre-coated glass-backed plates (Merck Keisekgel F₂₅₄) and visualised with ultraviolet light (254nm), basic potassium permanganate, acidic ammonium molybdate (IV), or acidic anisaldehyde solution. Flash chromatography was performed using BDH silica gel (40-60µm). Preparative HPLC was carried out on a Gilson 231 XL Sample Injector with an FC204 fraction collector, 118 UV/VIS Detector, 306 Pump, 806 Manometric Module, 811 Dynamic Mixer and a 250 x 22mm Pep 100A C18 8U Column from Alltech. A 300 x 4.6mm Waters Spherisorb™ 55 OPS2 Column was used for analytical HPLC. Solvents were HPLC grade and degassed prior to use. Gas Chromatography was performed on a Hewlett-Packard 5890A machine (flame ionisation detector) with a 25m x 0.50mm BPX5 column using hydrogen as the carrier gas.

All glassware was oven dried and cooled under a flow of nitrogen. All reactions requiring dry solvents were carried out under an atmosphere of nitrogen.

Chapter 2. SYNTHESIS AND ANALYSIS OF POLYSTYRENE-DIVINYLBENZENE MIPs

2.1 SYNTHESIS OF THE IMPRINT MOLECULE

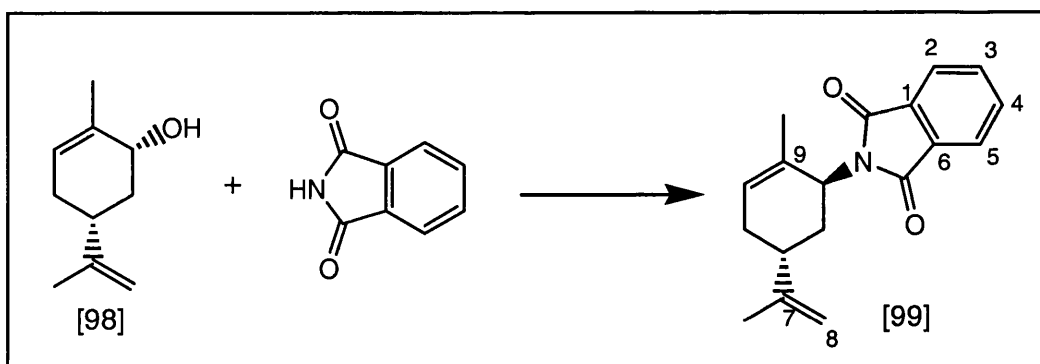
2.1.1. Synthesis of (1*S*, 5*R*)-*cis*-carveol [98]¹³⁰



A suspension of lithium aluminium hydride (1.33g, 35mmol) in diethyl ether (70mL) was stirred at -78°C . (*R*)-(-)-Carvone (5.20g, 5.4mL, 35mmol, 1eq) was added dropwise as a solution in diethyl ether (5mL) over 20min. The reaction was stirred at -78°C for 2h, then quenched by the addition of wet diethyl ether. The resulting mixture was poured onto a slurry of ice (~20g) and 10% H_2SO_4 aq. (30mL) and the aqueous and organic layers were separated. The aqueous layer was further extracted with diethyl ether (3x70mL). The combined organic extracts were dried over $\text{MgSO}_4(\text{s})$ and concentrated *in vacuo* to afford (1*S*, 5*R*)-*cis*-carveol [98] as a colourless liquid (5.12g, 33.7mmol, 96%).

$^1\text{H NMR}$ (CDCl_3 , 400MHz) $\delta_{\text{H}}/\text{ppm}$: 5.45 (1H, m, $\text{CCH}=\text{CMe}$), 4.69 (2H, s, $=\text{CH}_2$), 4.15 (1H, m(br), CHOH), 2.56 (1H, s(br), OH), 2.22-1.75 (5H, m), 1.72 (3H, s, $\text{CR}=\text{CRCH}_3$), 1.70 (3H, s, $\text{CH}_2=\text{CRCH}_3$), 1.46 (1H, m). $^{13}\text{C NMR}$ (CDCl_3 , 100MHz) $\delta_{\text{C}}/\text{ppm}$: 148.9 ($\text{R}_2\text{C}=\text{CH}_2$), 136.2 ($\text{RCH}=\text{CCH}_3\text{R}$), 123.8 ($\text{RCH}=\text{CCH}_3\text{R}$), 109.1 ($\text{CR}_2=\text{CH}_2$), 70.8 (R_2CHOH), 40.5 (CR_3CH), 37.9 (CH_2), 31.0 (CH_2), 20.6 (CH_3), 19.0 (CH_3). **IR** (neat): $\nu_{\text{max}}/\text{cm}^{-1}$: 3321 (b, OH), 3083 (m), 2916 (s), 2855 (s), 1645 (s), 1451 (s), 1375 (s), 1287 (m), 1082 (m), 1038 (s), 998 (m), 974 (w). **LRMS** (EIMS) m/z : 153 (8%, $[\text{M}+\text{H}]^+$), 135 (100%, -OH), 120 (24%), 110 (64%, $-\text{C}_3\text{H}_6^+$), 95 (30%), 84 (87%), 69 (32%), 55 (37%)

2.1.2 Synthesis of (1*R*, 5*R*)-*trans*-carvyl phthalimide [99]¹³¹

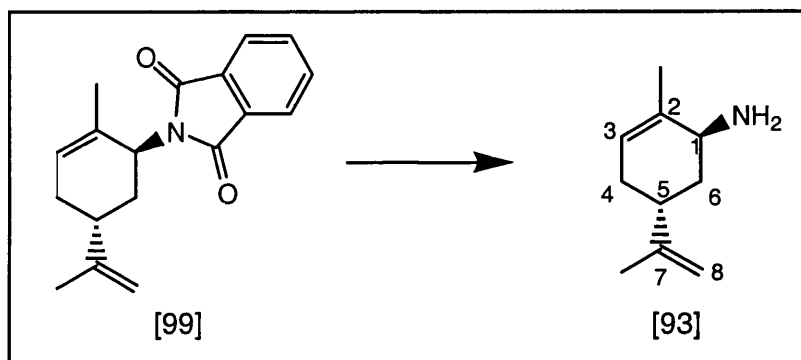


A solution of (1*S*, 5*R*)-*cis*-carveol [98] (0.50g, 3.3mmol, 1eq), phthalimide (0.63g, 4.3mmol, 1.3eq), and triphenylphosphine (1.13g, 4.3mmol, 1.3eq) in dry THF (12mL) was stirred in the dark at room temperature. A solution of diisopropyl azodicarboxylate (D.I.A.D.) (0.87g, 0.85mL, 4.3mmol, 1.3eq) was added dropwise over 10min. The reaction was left stirring at room temperature for 4h after which time distilled water (40mL) was added. The reaction mixture was extracted with a mixture of petrol (40mL) and ether (40mL), and the solvents were concentrated *in vacuo* until triphenylphosphine oxide began to precipitate out. The solid was filtered off and the remaining solution was concentrated *in vacuo*. The crude product was purified by flash column chromatography (SiO₂, 5% EtOAc:petrol 40-60°C, increasing to 50% EtOAc; **R_f** 0.4 (SiO₂, 20% EtOAc:petrol 40-60°C)) to give the pure (1*R*, 5*R*)-*trans*-carvyl phthalimide [99] as a colourless glutinous oil (0.598g, 2.1mmol, 64%).

$[\alpha]_D^{25}$: -165.5° (CHCl₃, c=0.2). ¹H NMR (CDCl₃, 300MHz) δ_H/ppm: 7.82 and 7.71 (4H, AA'BB',m, ArH), 5.77 (1H, m, =CHR), 4.76 (1H, s, =CH₂), 4.72 (1H, s, =CH₂), 4.71 (1H, m(br), CHN), 2.67 (1H, m, R₃CH), 2.39 (1H, dm, J17.5Hz), 2.09 (1H, dt, J13.5Hz, 4.0Hz), 2.03-1.89 (2H, m), 1.74 (3H, s, CH₃), 1.58 (3H, s, CH₃). ¹³C NMR (CDCl₃, 75MHz) δ_C/ppm: 168.5 (C=O), 148.1 (6-C, 1-C), 133.9 (ArCH), 131.8 (quaternary C), 128.9 (quaternary C), 126.2 (=CHR), 123.1 (ArCH), 109.3 (=CH₂), 49.1 (CHN), 36.9 (CHR₃), 33.2 (CH₂), 30.2 (CH₂), 21.3 (CH₃), 20.5 (CH₃). IR (neat): ν_{max}/cm⁻¹: 3466 (w), 3082 (w), 2987 (s), 2916 (s), 1770 (s, C=O), 1713 (s, C=O), 1644 (m, C=C), 1612 (m, C=C), 1467 (m), 1441 (m), 1388 (s), 1353 (s), 1325 (s), 1241 (m), 1111 (m), 1042

(m), 890 (m), 794 (w), 721 (w). LRMS (FAB) m/z : 282 (53%, $[M+H]^+$), 238 (15%), 154 (15%), 148 (100%, phthalimide), 133 (50%), 119 (38%).

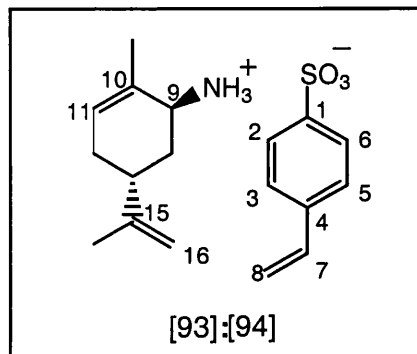
2.1.3. Synthesis of (1*R*, 5*R*)-*trans*-carvyl amine [93]¹³¹



(1*R*, 5*R*)-*trans*-Carvyl phthalimide [99] (6.46g, 23.0mmol, 1eq) was dissolved in methanolic hydrazine hydrate (0.3M, 138mL) and stirred at room temperature for 48h. 5% HCl aq. (52mL) was added and the reaction stirred for 24h over which time a white precipitate was observed. Distilled water (200mL) was added and the precipitate removed by suction filtration. The acidic aqueous solution was washed with diethyl ether (3x200mL) and then adjusted to pH ~10 with KOH(s). The basic solution was extracted with diethyl ether (3x200mL), dried over MgSO₄(s) and concentrated *in vacuo* to afford the crude amine [93] (2.91g) which was purified by Kugelrohr distillation to give pure (1*R*, 5*R*)-*trans*-carvyl amine [93] as a colourless liquid (2.56g, 17mmol, 74%).

b.p.: 95-98°C/0.75mBar. $[\alpha]_D^{25}$: -182.4 (CH₂Cl₂, c=1). ¹H NMR (CDCl₃, 400MHz) δ_H /ppm: 5.40 (1H, m, =CHR), 4.68 (1H, s, =CH₂), 4.67 (1H, s, =CH₂), 3.15 (1H, s(br), CHN), 2.23-1.57 (5H, m, ring H), 1.72 (3H, s, CH₃), 1.69 (3H, s, CH₃), 1.29 (2H, s(br), NH₂). ¹³C NMR (CDCl₃, 100MHz) δ_C /ppm : 149.5 (7-C), 136.2 (2-C), 122.8 (3-C), 108.7 (=CH₂), 49.8 (CHN), 37.5, 35.1, 31.0, 21.2 (CH₃), 20.9 (CH₃). **IR** (neat): ν_{max}/cm^{-1} : 3293 (w), 3217 (w), 3074 (w), 2959 (m), 2914 (s), 1648 (m), 1441 (s), 1375 (m), 1150 (w), 1046 (w), 942 (w), 883 (s), 806 (m). LRMS (FAB) m/z : 152 (100%, $[M+H]^+$), 135 (63%, M-NH₂), 119 (15%), 107 (65%).

2.1.4. Synthesis of 4-styrenesulfonic acid, (1R, 5R)-trans-carvyl amine salt [93]:[94]



Method 1:

A solution of acetyl chloride:MeOH (1:20 v/v, 6.0mL) was made up under nitrogen at 0°C and added dropwise with stirring to (1R, 5R)-trans-carvyl amine [93] (500mg, 3.3mmol, 1eq) at 0°C. After 20min the solution was concentrated *in vacuo* to afford the amine hydrochloride. This was immediately dissolved in methanol (25mL) and added to a solution of 4-styrenesulfonic acid, sodium salt (680mg, 3.3mmol, 1eq) in methanol (125mL). The solution was stirred for 4h, then concentrated *in vacuo* to give an off white solid. Chloroform (30mL) was added and any remaining solid was removed by suction filtration. The filtrate was concentrated *in vacuo* to afford a yellow solid (1.05g) containing a mixture of (1R, 5R)-trans-carvyl amine hydrochloride [101] and 4-styrenesulfonic acid, (1R, 5R)-trans-carvyl amine salt [93]:[94]. The ratio ([93]:[94]):[101], 1.4:1 was determined by ¹H NMR.

¹H NMR (CDCl₃, 300MHz) δ_H/ppm: 8.11 (3H, s(br) NH₃), 7.69 (2H, AA'BB',d, J_{12.5}Hz, ArH 2-H, 6-H), 7.40 (2H, AA'BB', d, J_{12.5}Hz, ArH, 5-H, 3-H), 6.69 (1H, dd, J_{17.5}Hz, 11.0Hz, 7-H), 5.72 (1H, d, J_{trans}17.5Hz, 8-H), 5.63 (1H, m, 11-H), 5.30 (1H, d, J_{cis}11.0Hz, 8-H), 4.68 (1H, s, 16-H), 4.64 (1H, s, 16-H), 3.60 (1H, m(br), CHN), 2.49 (1H, m(br), ring H), 2.10 (2H, m, ring H), 1.79 (3H, s, CH₃), 1.63 (3H, s, CH₃). ¹³C NMR (CDCl₃, 100MHz) δ_C/ppm: 147.8 (15-C), 143.2 (quaternary C), 139.5 (quaternary C), 135.9 (7-C), 129.3 (11-C), 128.4 (quaternary C), 126.2 (ArCH), 126.0 (ArCH), 115.5 (8-C), 109.5 (16-C), 50.1 (CHN), 34.3 (13-CH), 31.7 (CH₂), 30.3 (CH₂-), 20.9 (CH₃). LRMS (FAB) m/z: 336 (5%, M_{salt}+H); (CI negative) m/z : 182.8 (100%, M_{acid}-H) ; (CI positive) m/z: 151.9 (68%, M_{amine}+H).

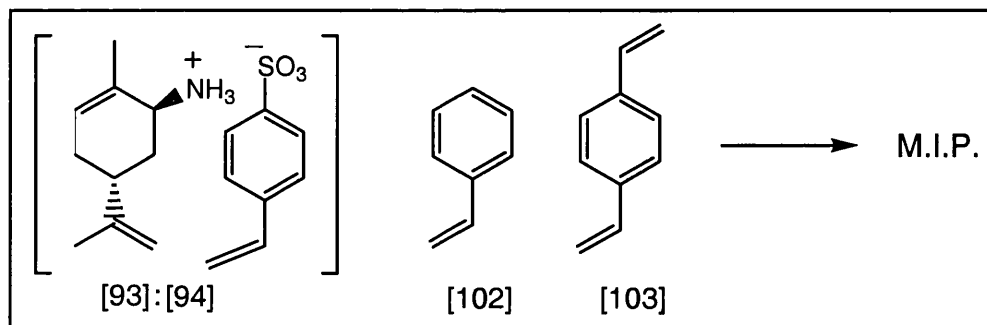
Method 2:

A solution of ethereal HCl (1.2M, 10mL) was added dropwise with stirring at 0°C to (1*R*, 5*R*)-*trans*-carvyl amine [93] (500mg, 3.3mmol, 1eq) at 0°C. After 20min the solution was concentrated *in vacuo* to afford the amine hydrochloride. This was immediately dissolved in methanol (25mL), and added to a solution of 4-styrenesulfonic acid, sodium salt (680mg, 3.3mmol, 1eq) in methanol (60mL). The solution was stirred for 4h and then concentrated *in vacuo* to give an off white solid. Chloroform (30mL) was added and any remaining solid was removed by suction filtration. The filtrate was concentrated *in vacuo* to afford a yellow solid (0.956g) containing a mixture of (1*R*, 5*R*)-*trans*-carvyl amine hydrochloride [101] and 4-styrenesulfonic acid, (1*R*, 5*R*)-*trans*-carvyl amine salt [93]:[94]. The ratio ([93]:[94]): [101], 1.5:1 was determined by ¹H NMR.

Spectra as above.

2.2. SYNTHESIS OF POLYSTYRENE-DIVINYLBENZENE MIPs

2.2.1. General Procedure for the synthesis of polystyrenes.



Styrene, divinylbenzene, 4-styrenesulfonic acid, (1*R*, 5*R*)-*trans*-carvyl amine salt [93]:[94], and AIBN (2mol% per polymerisable double bonds) were dissolved in chloroform (1.7 v/v of polymerisable molecules) in a Schlenk flask of diameter 3.0cm. Three freeze thaw cycles were carried out and the polymerisation mixture was placed in a preheated bath at 70°C and heated under nitrogen with stirring (300 rpm) for 40min.

The bath was cooled to 60°C and the polymerisation mixture was incubated for a further 23h 20min. The Schlenk flask was cooled to room temperature and placed under high vacuum to remove the solvent directly. The resultant polymer monolith was ground manually with a mortar and pestle.

Loadings: Loadings refer to the ratio of the number of moles of salt [93]:[94] to the total number of moles of polymerisable molecules. A higher loading indicates more sites per unit volume of polymer.

For example; in the case where salt [93]:[94] (1.0mmol) is polymerised with styrene (2.0mmol) and divinylbenzene (4.0mmol), the loading is 1/6.

Crosslinker monomer ratio: The crosslinker:monomer ratio is the ratio of moles of divinylbenzene to styrene. A higher ratio indicates a higher level of crosslinking.

For example; in the case where salt [93]:[94] (1.0mmol) is polymerised with styrene (2.0mmol) and divinylbenzene (4.0mmol), the crosslinker: monomer ratio is 2:1.

2.2.2. Synthesis of Polystyrene [A]. Loading:1/35, Crosslinker-monomer ratio 6:1.

4-Styrenesulfonic acid, (1*R*, 5*R*)-*trans*-carvyl amine salt [93]:[94] (200mg, 0.43mmol[#]), styrene (224mg, 246μL, 2.15mmol), divinylbenzene (1.68g, 1.84mL, 12.9mmol), AIBN (92mg, 0.6mmol) and chloroform (3.55mL) were polymerised according to the general procedure.

2.2.3. Synthesis of Polystyrene [B]. Loading:1/35, Crosslinker-monomer ratio 3:1.

4-Styrenesulfonic acid, (1*R*, 5*R*)-*trans*-carvyl amine salt [93]:[94] (200mg, 0.43mmol), styrene (329mg, 430μL, 1.3mmol), divinylbenzene (1.47g, 1.61mL, 3.8mmol), AIBN (86.5mg, 0.53mmol) and chloroform (3.47mL) were polymerised according to the general procedure.

[#] The number of moles of salt [93]:[94] was calculated using the molar ratio of the 4-styrenesulfonic acid, (1*R*, 5*R*)-*trans*-carvyl amine salt [93]:[94] to (1*R*, 5*R*)-*trans*-carvyl amine hydrochloride [101], as determined by ¹H NMR. This method was used throughout.

2.2.4. Synthesis of Polystyrene [C]. Loading:1/35, Crosslinker-monomer ratio 2:1.

4-Styrenesulfonic acid, (1*R*, 5*R*)-*trans*-carvyl amine salt [93]:[94] (200mg, 0.43mmol), styrene (523mg, 575 μ L, 5.0mmol), divinylbenzene (1.31g, 1.43mL, 10.0mmol), AIBN (82mg, 0.5mmol) and chloroform (3.41mL) were polymerised according to the general procedure.

2.2.5 Synthesis of Polystyrene [D]. Loading:1/15, Crosslinker-monomer ratio 2:1.

4-Styrenesulfonic acid, (1*R*, 5*R*)-*trans*-carvyl amine salt [93]:[94] (200mg, 0.43mmol), styrene (224mg, 246 μ L, 2.15mmol), divinylbenzene (560mg, 612 μ L, 4.3mmol), AIBN (35mg, 0.22mmol) and chloroform (1.46mL) were polymerised according to the general procedure.

2.2.6 Synthesis of Polystyrene [E]. Loading:1/10, Crosslinker-monomer ratio 3:1.

4-Styrenesulfonic acid, (1*R*, 5*R*)-*trans*-carvyl amine salt [93]:[94] (184mg, 0.43mmol), styrene (115mg, 126 μ L, 1.1mmol), divinylbenzene (417mg, 456 μ L, 3.2mmol), AIBN (24.6mg, 0.15mmol) and chloroform (1.0mL) were polymerised according to the general procedure.

2.2.7 Optimised procedure for the washing and generation of acid sites in the crude polystyrenes [A], [B], [C], [D], and [E].

The ground crude polymer was placed in a sintered glass funnel and washed with chloroform (5x10mL). The solvent was removed *in vacuo* and the residue analysed by ¹H NMR, which identified AIBN decomposition products and trace amounts of unreacted reagents as determined by comparison with reference spectra. The polymer was washed with 10% Et₃N:DCM (5x10mL) to remove the bound (1*R*, 5*R*)-*trans*-carvyl amine [93], as determined by ¹H NMR analysis of the filtrate, then DCM (10mL). The polymer was stirred in HCl:diethyl ether (20mL) for 3h at 0°C, filtered, then washed

with diethyl ether (2x20mL), DCM (2x20mL), water (2x20mL), methanol (2x20mL or until pH 7), and DCM (5x10mL). The polymer was then dried *in vacuo* to give the active polymer [A]*, [B]*, [C]*, [D]* or [E]*.

Polymer [A]* 1/35 6:1 **Elemental analysis:** Found C 88.16, H 7.85, N 0.18, S 0.70.

Polymer [B]* 1/35 3:1 **Elemental analysis:** Found C 86.92, H 7.74, N 0.32, S 0.85

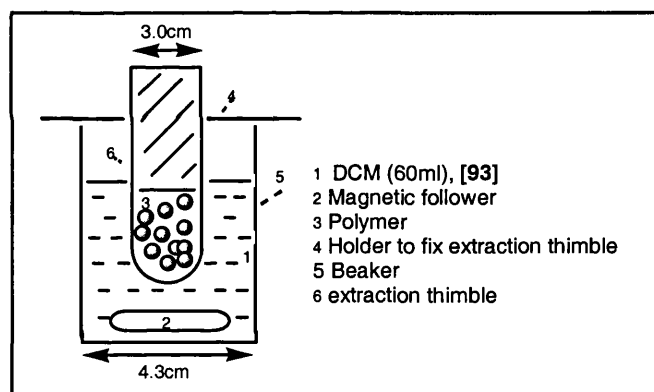
Polymer [C]* 1/35 2:1 **Elemental analysis:** Found C 88.02, H 8.01, N 0.27, S 0.82.

Polymer [D]* 1/15 2:1 **Elemental analysis:** Found C 86.04, H 7.76, N 0.24, S 0.93.

Polymer [E]* 1/10 3:1 **Elemental analysis:** Found C 85.04, H 7.72, N 0.38, S 0.92.

2.3 BINDING STUDIES OF POLYSTYRENE-DIVINYLBENZENE MIPs

2.3.1 General Method for Binding Studies



The dried polymer [A]*, [B]*, [C]*, [D]* or [E]* was placed in a sealed soxhlet extraction thimble and suspended in a beaker containing a known quantity of DCM (60mL). The solution was stirred for 20min at 0°C, the level of the solvent was marked and the thimble removed. The amount of solvent absorbed by the polymer was measured using the difference between the volume of DCM remaining and the original volume of DCM (60mL). (1R, 5R)-*trans*-Carvyl amine [93] (65mg, 0.43mmol, 1eq) was then added to the beaker, the extraction thimble was suspended as previously and DCM was added up to the mark* (*vide supra*). The solution was stirred and at specific intervals the

* An important distinction between adding DCM (60mL) and adding the solvent up to the mark is necessary here. The polymers absorb significant quantities of solvent which they retain for a considerable

thimble was removed, the solvent removed *in vacuo* and the quantity of (1*R*, 5*R*)-*trans*-carvyl amine [93] remaining in solution was determined. After each measurement the (1*R*, 5*R*)-*trans*-carvyl amine [93] was redissolved in DCM to the previously marked level.

2.3.2. General Method for determining the percentage of imprint molecule: (1*R*, 5*R*)-*trans*-carvyl amine [93] bound in the polymer.

In the binding studies carried out according to the general method above there is always a certain quantity of (1*R*, 5*R*)-*trans*-carvyl amine [93] present in the polymer due to non-specific binding (ie the solvent absorbed by the polymer will naturally contain a certain amount of (1*R*, 5*R*)-*trans*-carvyl amine [93]). The approximation we have made is that the percentage of (1*R*, 5*R*)-*trans*-carvyl amine [93] bound due to 'non specific binding' is equal to the percentage of DCM absorbed by the polymer. To avoid overestimating the level of binding, the calculation of the amount of template bound in the polymer at each point in the binding study includes a correction factor to account for this phenomenon (Equation 1).

$$\text{template bound/mg} = y - x(a/b) \quad \text{.....Equation 1}$$

Where y = original weight of [93] (65.0mg, 0.43mmol, 1eq)

x = weight of [93] in remaining in solution

(a/b) = correction factor:

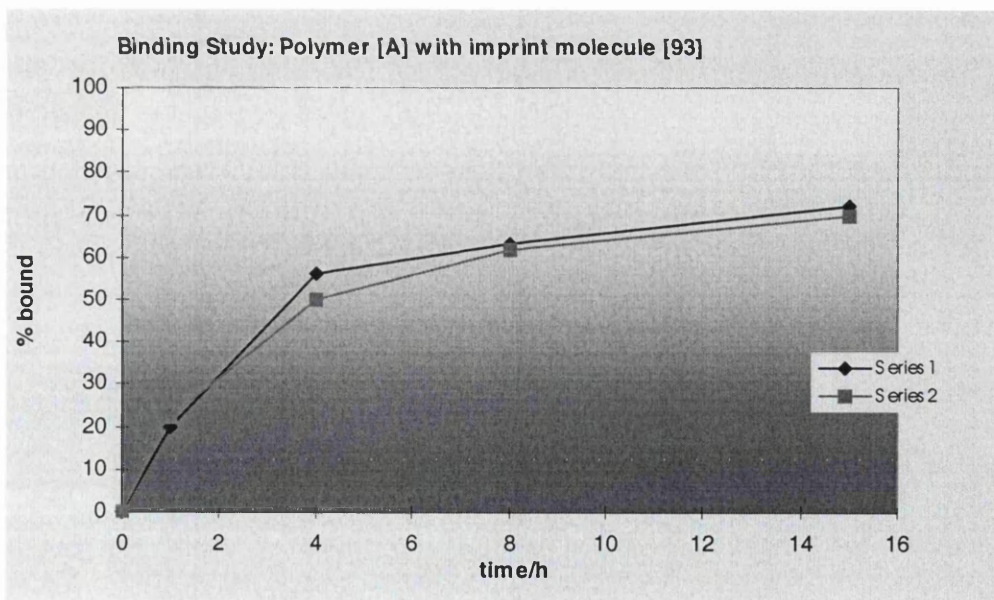
$$\frac{\text{original volume of DCM (60mL)}}{\text{original volume of DCM (60mL) - volume of DCM absorbed by polymer}}$$

time. If one adds another (60mL) of solvent then there will be more solvent present due to preabsorbed DCM in the polymer. In order to avoid lengthy drying procedures in between steps the marked level is used. This is the level at which the total of the DCM absorbed in the polymer and in the rest of the beaker is equal to 60mL.

2.3.3. Binding Study of Polystyrene [A]*, Loading:1/35, crosslinker:monomer 6:1#.

The amount of DCM (12.0mL) absorbed by the polymer was determined according to the general method (2.3.1). The binding study was carried out according to the general method and repeated to test for reproducibility

time/h	[93] in solution/mg	[93] bound (%) Series 1	[93] in solution/mg (repeat)	[93] bound (%) (repeat) Series 2
0	65.0	0	65.0	0
1	41.8	20	40.7	34
4	23.1	56	26.1	50
8	19.3	63	19.6	62
15	14.3	72	15.4	70



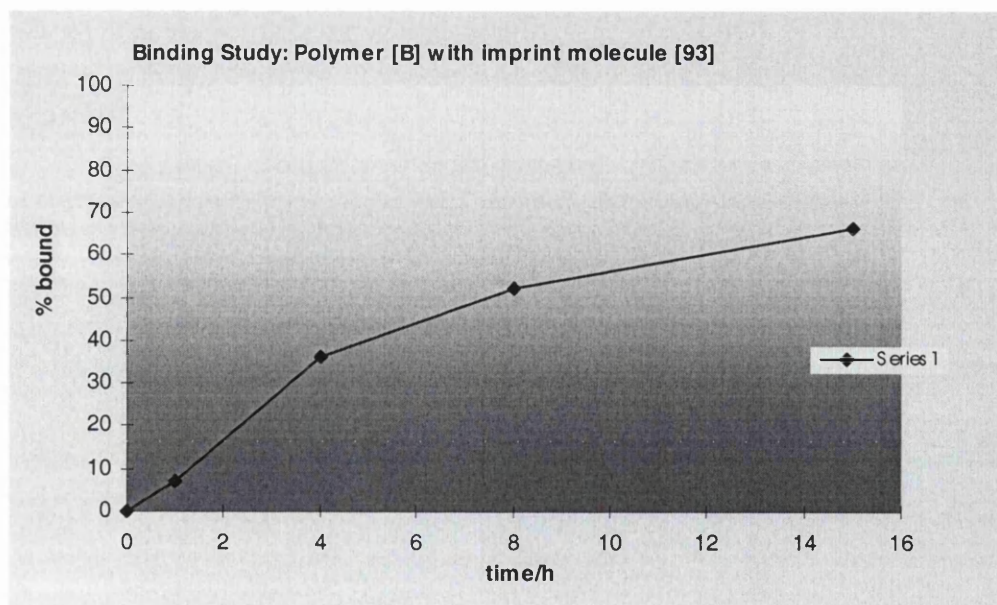
For 71% bound, the polymer [A] has 0.31mmol of available acid binding sites.

* Polystyrene binding studies were carried out by Dr Y. Six.

2.3.4 Binding Study of Polystyrene [B]*, Loading 1/35, crosslinker:monomer 3:1.

The amount of DCM (14.0mL) absorbed by the polymer was determined according to the general method (2.3.1). The binding study was carried out according to the general method.

time/h	[93] in solution/mg	[93] bound (%) Series 1
0	65.0	0
1	46.4	7
4	31.9	36
8	23.7	52
15	16.9	66

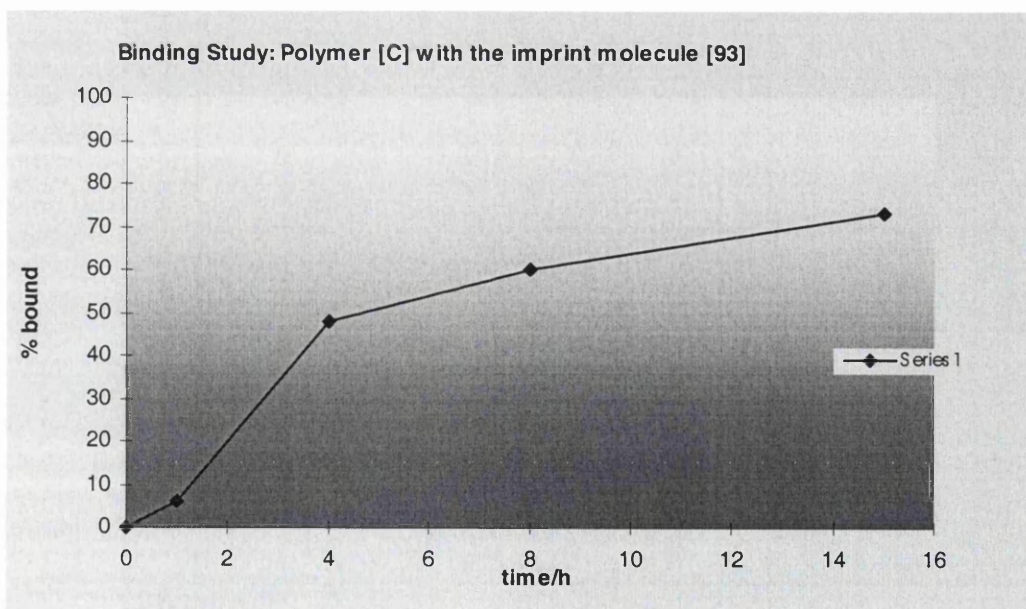


For 66% bound, the polymer [B] has 0.28mmol of available acid binding sites.

2.3.5. Binding Study of Polystyrene [C]*, Loading:1/35, crosslinker:monomer 2:1.

The amount of DCM (13.0mL) absorbed by the polymer was determined according to the general method (2.3.1). The binding study was carried out according to the general method.

time/h	[93] in solution/mg	[93] bound (%) Series 1
0	65.0	0
1	48.0	6
4	26.7	48
8	20.5	60
15	13.9	73

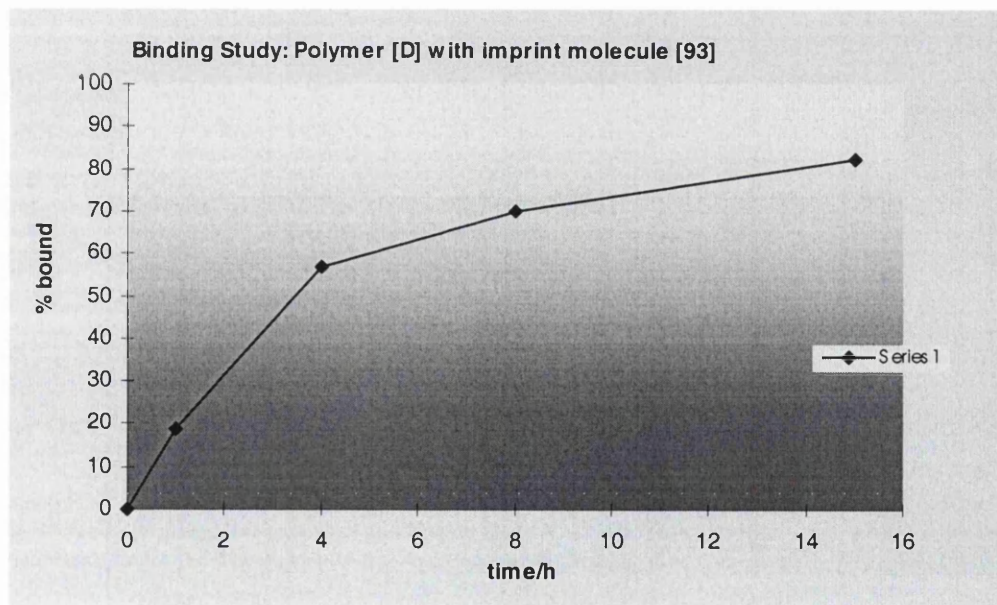


For 73% bound, the polymer [C] has 0.31mmol of available acid binding sites.

2.3.6 Binding Study of Polystyrene [D]*, Loading:1/15, crosslinker:monomer 2:1.

The amount of DCM (8.0mL) absorbed by the polymer was determined according to the general method (2.3.1). The binding study was carried out according to the general method.

time/h	[93] in solution/mg	[93] bound (%) Series 1
0	65.0	0
1	44.6	19
4	23.5	57
8	16.4	70
15	10.0	82

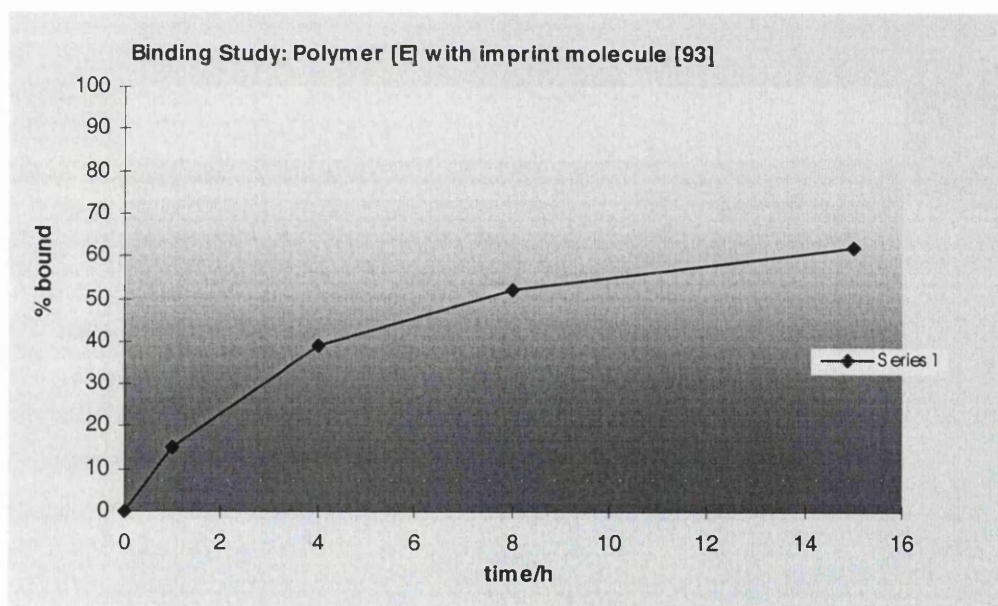


For 82% bound, the polymer [D] has 0.35mmol of available acid binding sites.

2.3.7 Binding Study of Polystyrene [E]*, Loading:1/10, crosslinker:monomer 3:1.

The amount of DCM (7.5mL) absorbed by the polymer was determined according to the general method (2.3.1). The binding study was carried out according to the general method.

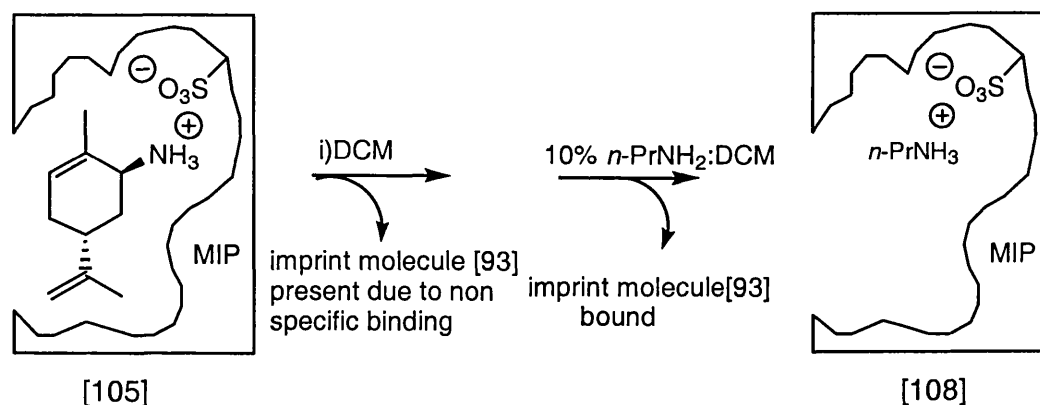
time/h	[93] in solution/mg	[93] bound (%) Series 1
0	65.0	0
1	48.1	15
4	34.6	39
8	27.3	52
15	21.5	62



For 62% bound, the polymer [E] has 0.27mmol of available acid binding sites.

2.3.8 General method for the debinding studies of polystyrene-divinylbenzene

MIP s [A]*, [B]*, [C]*, [D]*, and [E]*.



Debinding Experiments: MIP's were stirred with 60mL fractions of DCM(3x1h/60mL/0°C), then 10% *n*-PrNH₂:DCM(3x2h/60mL/0°C).

The apparatus used was the same as for the binding studies 2.3.1. The beaker was filled with up to the mark with DCM (*vide supra* 2.3.1). The solution was stirred at 0°C for 1h then reduced *in vacuo* and the residue analysed by ¹H NMR. This was carried out three times[#]. The beaker was then filled with 10% *n*-PrNH₂:DCM (60mL), stirred at 0°C for 2h, then reduced *in vacuo* and the residue analysed by ¹H NMR. This was carried out three times. The amount of (1*R*, 5*R*)-*trans*-carvyl amine [93] in each fraction was calculated from the weight and the molar ratio of [93]: *n*-PrNH₃(CO₃)₂: *n*-PrNH₂ as observed by ¹H NMR. In each case the mass balance of (1*R*, 5*R*)-*trans*-carvyl amine [93] over the entire binding-debinding experiment was in the region of 90%.

In each case the ratios were determined by comparing the integration of the following peaks:

¹H NMR (CDCl₃, 300MHz) δ_H/ppm: (1*R*, 5*R*)-*trans*-carvyl amine [93] 5.40 (1H, m, =CHR) and/or 4.67 (2H, 2s, =CH₂); *n*-PrNH₃(CO₃)₂ 0.79 (3H, t, J7.5Hz, CH₃); *n*-PrNH₂ 0.68, (3H, t, J7.5Hz, CH₃).

2.3.9 Debinding of Polystyrene [A]. Loading:1/35, Crosslinker-monomer ratio 6:1.

The debinding study was carried out according to the general method.

solvent (60mL)	time/h	total weight/mg	molar ratio [93]: <i>n</i> -PrNH ₃ (CO ₃) ₂ : <i>n</i> -PrNH ₂	weight of [93]/mg
DCM	1	1.9	1:0:0	1.9
DCM	1	1.9	1:0:0	1.9
DCM	1	2.2	1:0:0	2.2
DCM: <i>n</i> -PrNH ₂ 10%	2	41.2	1:0:0	41.2
DCM: <i>n</i> -PrNH ₂ 10%	2	28.2	15:56:29	4.5
DCM: <i>n</i> -PrNH ₂ 10%	2	28.9	no [93]	0

2.3.10. Debinding of Polystyrene [B]. Loading:1/35, Crosslinker-monomer ratio

3:1.

The debinding study was carried out according to the general method.

solvent (60mL)	time/h	total weight/mg	molar ratio [93]: <i>n</i> -PrNH ₃ (CO ₃) ₂ : <i>n</i> -PrNH ₂	weight of [93]/mg
DCM	1	1.2	1:0:0	1.2
DCM	1	2.4	1:0:0	2.4
DCM	1	1.6	1:0:0	1.6
DCM: <i>n</i> -PrNH ₂ 10%	2	19.9	37:33:30	8.4
DCM: <i>n</i> -PrNH ₂ 10%	2	31.1	42:26:32	15.3
DCM: <i>n</i> -PrNH ₂ 10%	2	19.1	14:50:36	3.1

This process removes any (1*R*, 5*R*)-*trans*-carvyl amine [93] present in the polymer due to non specific

3.2.11. Debinding of Polystyrene [C]. Loading:1/35, Crosslinker-monomer ratio

2:1.

The debinding study was carried out according to the general method

solvent (60mL)	time/h	total weight/mg	molar ratio [93]: $n\text{-PrNH}_3(\text{CO}_3)_2$: $n\text{-PrNH}_2$	weight of [93]/mg
DCM	1	3.0	1:0:0	3.0
DCM	1	2.1	1:0:0	2.1
DCM	1	0.0	1:0:0	0.0
DCM: $n\text{-PrNH}_2$ 10%	2	29.9	66:14:20	20.4
DCM: $n\text{-PrNH}_2$ 10%	2	23.2	40:24:36	11.2
DCM: $n\text{-PrNH}_2$ 10%	2	18.3	13:40:47	3.0

2.3.12 Debinding of Polystyrene [D]. Loading:1/15, Crosslinker:monomer ratio 2:1.

The debinding study was carried out according to the general method

solvent (60mL)	time/h	total weight/mg	molar ratio [93]: $n\text{-PrNH}_3(\text{CO}_3)_2$: $n\text{-PrNH}_2$	weight of [93]/mg
DCM	1	0.7	1:0:0	0.7
DCM	1	0.1	1:0:0	0.1
DCM	1	1.9	1:0:0	1.9
DCM: $n\text{-PrNH}_2$ 10%	2	38.8	1:0:0	38.8
DCM: $n\text{-PrNH}_2$ 10%	2	34.6	14:51:35	5.5
DCM: $n\text{-PrNH}_2$ 10%	2	24.5	no [93]	0.0

2.3.13. Debinding of Polystyrene [E] Loading:1/10, Crosslinker-monomer ratio 3:1.

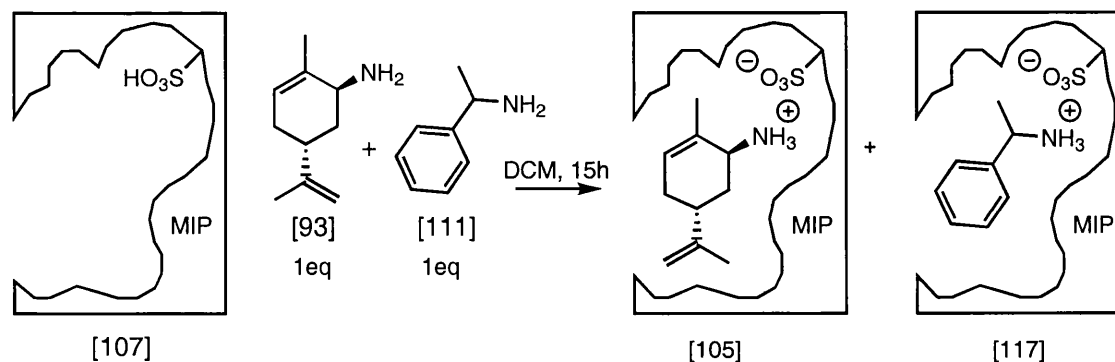
The debinding study was carried out according to the general method

solvent (60mL)	time/h	total weight/mg	molar ratio [93]: <i>n</i> -PrNH ₃ (CO ₃) ₂ : <i>n</i> -PrNH ₂	weight of [93]/mg
DCM	1	3.1	1:0:0	3.1
DCM	1	1.0	1:0:0	1.0
DCM	1	0.9	1:0:0	0.9
DCM: <i>n</i> -PrNH ₂ 10%	2	34.2	1:0:0	34.2
DCM: <i>n</i> -PrNH ₂ 10%	2	13.1	20:68:13	2.5
DCM: <i>n</i> -PrNH ₂ 10%	2	16.5	no [93]	0

2.3.14. General method for polymer regeneration.

The apparatus used was the same as for the binding studies 2.3.1. The polymer was washed with DCM (2x60mL/1h/0°C) to remove any excess *n*-PrNH₂ and then stirred with HCl :diethyl ether (60mL/1h/0°C) to regenerate the acid sites. The polymer was washed with ether (3x60mL), methanol (nx60mL until pH neutral) and DCM (2x60mL).

2.3.15 General method for competitive binding studies.



The apparatus used was the same as for the binding studies 2.3.1. The amount of solvent absorbed by the polymer was determined as previously (2.3.1). (1*R*, 5*R*)-*trans*-carvylamine [93] (1eq of the calculated number of binding sites in the polymer (see 2.3.1))

and α -methyl benzylamine [111] (1eq) were added to the beaker and the 1:1 ratio was confirmed by ^1H NMR. DCM (60mL) was added up to the mark (*vide supra* 2.3.1) and the solution was stirred at 0°C for 15h. The solution was then concentrated *in vacuo* and the ratio [93]:[111] of the amines not bound by the polymer was determined by ^1H NMR. To debind the amines, the polymer was stirred with 10% *n*-PrNH₂:DCM (60mL/2hx3). The 10% *n*-PrNH₂:DCM fractions were combined, concentrated *in vacuo* and the ratio [93]:[111] of substrates bound by the polymer was determined by ^1H NMR.

In each case the ratio's were determined by comparing the integration of the following peaks:

^1H NMR (CDCl₃, 300MHz) δ_{H} /ppm: α -methyl benzylamine [111] 4.27 (1H, q, J6.5Hz, CH₃CHN). (1*R*, 5*R*)-*trans*-carvyl amine [93] 5.40 (1H, m, =CH $\underline{\text{R}}$) and/or 4.67 (2H, 2s, =CH $\underline{\text{H}}$ ₂).

2.3.16. Competitive binding study of polymer [A] Loading 1/35, crosslinker-monomer 6:1.

The polymer was regenerated according to the general method (2.3.1). The amount of DCM (10.5mL) absorbed by the polymer was determined. (1*R*, 5*R*)-*trans*-carvyl amine [93] (46.2mg, 0.31mmol, 1eq) and α -methyl benzylamine [111] (37.0mg, 0.31mmol, 1eq) were used in the competitive binding study (2.3.15). The ratio of the amines left in solution (1*R*, 5*R*)-*trans*-carvyl amine [93]: α -methyl benzylamine [111] was 47:53. The ratio of the amines extracted from the polymer was (1*R*, 5*R*)-carvyl amine [93]: α -methyl benzylamine [111] 61:39.

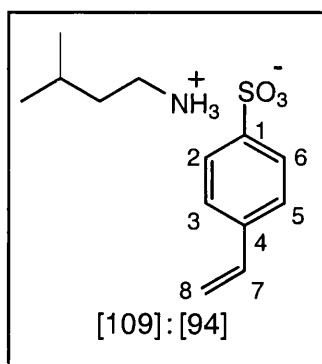
2.3.17 Competitive binding study of polymer [D] Loading 1/15, crosslinker-monomer 2:1.

The polymer was regenerated according to the general method (2.3.1). The amount of DCM (8.0mL) absorbed by the polymer was determined. (1*R*, 5*R*)-*trans*-carvyl amine [93] (53.3mg, 0.35mmol, 1eq) and α -methyl benzylamine [111] (42.7mg, 0.35mmol, 1eq) were used in the competitive binding study (2.3.15). The ratio of the amines left in solution (1*R*, 5*R*)-*trans*-carvyl amine [93]: α -methyl benzylamine [111] was 57:43. The

ratio of the amines extracted from the polymer was (1*R*, 5*R*)-*trans*-carvyl amine [93]: α -methyl benzylamine [111] 59:41.

2.4 SYNTHESIS OF BLANK POLYSTYRENE [F]

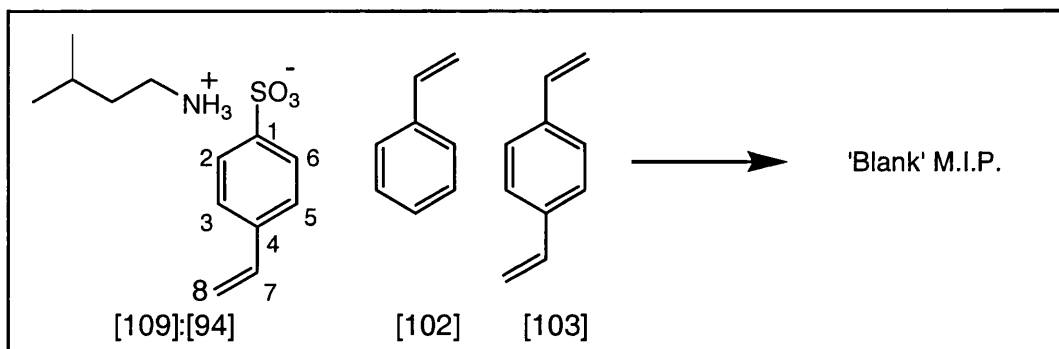
2.4.1 Synthesis of 4-styrenesulfonic acid, isoamylamine salt [109]:[94]



HCl:Diethyl ether (5mL) was added dropwise to a stirred solution of isoamylamine (435.9mg, 50mmol, 1eq) in diethyl ether (15mL) to produce a white precipitate. The solvent was removed *in vacuo* and the residue taken up in MeOH (60mL) and stirred at room temperature. 4-Styrenesulfonic acid, sodium salt (1.02g, 60mmol, 1.2eq) was added and the solution stirred for 18h. The solvent was removed *in vacuo*, the residue taken up in chloroform (70mL), filtered, and concentrated *in vacuo* to afford a yellow solid (776mg) containing a mixture of 4-styrenesulfonic acid, isoamylamine salt [109]:[94] and isoamylamine hydrochloride [110]. The ratio ([109]:[94]):[110] 1.3:1 was determined by ^1H NMR.

^1H NMR (CDCl_3 , 300MHz) δ_{H} /ppm: 7.77 (2H, AA'BB', d, $J_{12.5\text{Hz}}$ ArH, 2-H, 6-H), 7.71 (3H, s(br), NH₃), 7.38 (2H, AA'BB', d, $J_{12.5\text{Hz}}$ ArH, 3-H, 5-H), 6.66 (1H, dd, $J_{17.5\text{Hz}}$, $J_{11.0\text{Hz}}$, 7-H), 5.74 (1H, d, $J_{\text{trans } 17.5\text{Hz}}$, 8-H), 5.28 (1H, d, $J_{\text{cis } 11.0\text{Hz}}$, 8-H), 2.84 (1H, m, R₃CH), 1.49 (4H, m(br), CH₂), 0.75 (6H, d, $J_{3.5\text{Hz}}$, C(CH₃)₂). ^{13}C NMR (CDCl_3 , 75MHz) δ_{C} /ppm: 143.0 (quaternary C), 139.7 (quaternary C), 135.7 (7-C), 126.1 (ArCH), 115.8 (=CH₂), 38.4 (NCH₂), 35.9 (NCH₂CH₂), 25.5 (CH), 22.0 ((CH₃)₂). LRMS (CI negative) m/z : 183 (100%, $M_{\text{acid-H}}$) ; (CI positive) m/z : 88 (68%, $M_{\text{amine+H}}$).

2.4.2 Synthesis of Blank polystyrene [F].



Styrene (224mg, 246 μ L, 2.1mmol), divinylbenzene (1.68g, 1.84mL, 12.9mmol), 4-styrenesulfonic acid, isoamylamine salt [109]:[94] (158mg, 0.43mmol) and AIBN. (92mg, 0.6mmol, 2mol% per polymerisable double bond) were dissolved in chloroform (3.55mL, 1.7 v/v of polymerisable molecules) in a Schlenk flask of diameter 3.0cm. Three freeze thaw cycles were carried out and the polymerisation mixture was placed in a preheated bath at 70°C and heated under nitrogen with stirring (300 rpm) for 40 min. The bath was cooled to 60°C and the polymerisation mixture was incubated for a further 23h 20min The flask was cooled to room temperature and the solvent removed under vacuum. The resultant polymer monolith was ground.

2.4.3 Washing and generation of acid sites in the crude blank polystyrene [F].

The ground crude polymer was placed in a sintered glass funnel and washed with chloroform (5x10mL). The solvent was removed *in vacuo* and the residue analysed by ^1H NMR which identified AIBN. decomposition products and trace amounts of unreacted reagents as determined by comparison with reference spectra. The polymer was washed with 10% Et₃N:DCM (5x10mL) to remove the bound isoamylamine, then DCM (10mL). The polymer was stirred in HCl:diethyl ether (20mL) for 3h at 0°C, filtered, then washed with diethyl ether (2x20mL), DCM (2x20mL), water (2x20mL), methanol (2x20mL or until pH 7), and DCM (5x10mL). The polymer was then dried *in vacuo* to give the active polymer [F]*.

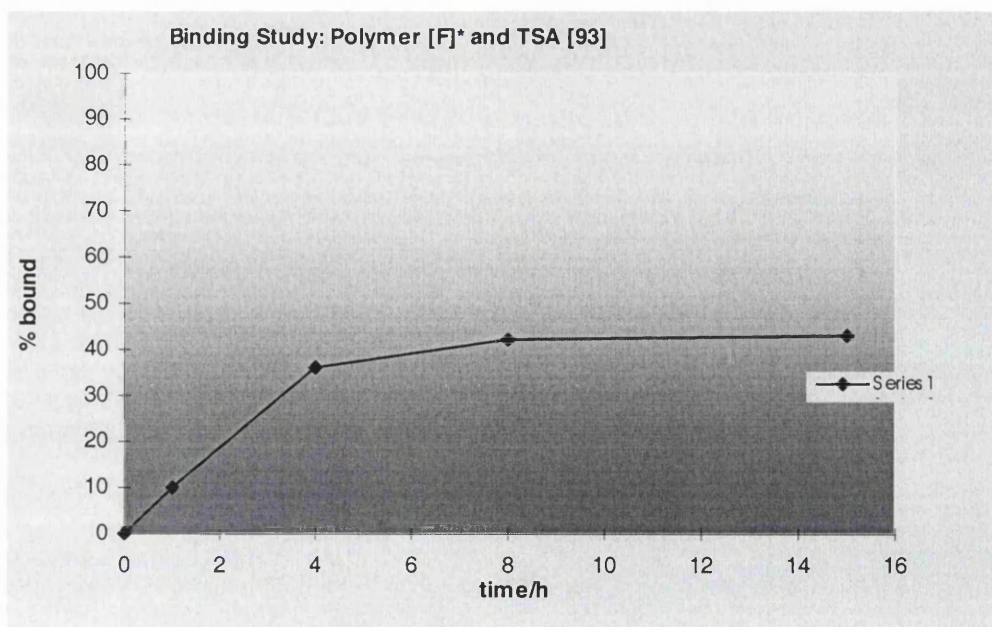
Polymer [F]* 1/35 6:1 **Elemental analysis:** Found **C** 88.25, **H** 7.82, **N** 0.24, **S** 0.75.

2.4.4. Binding Study of Blank Polystyrene [F]*. Loading:1/35, crosslinker: monomer 6:1.

The binding study was carried out in the same manner as for the imprinted polystyrenes discussed previously. For the general procedure see section 2.3.1.

The amount of DCM (14.0mL) absorbed by the polymer was determined.

time/h	[93] in solution/mg	[93] bound (%) Series 1
0	65.0	0
1	42.0	10
4	22.2	36
8	17.6	42
15	16.6	43



For 43% bound, the polymer [F] has 0.13mmol of available acid binding sites.

2.4.5. Debinding of Blank Polystyrene [F]. Loading:1/35, Crosslinker-monomer ratio 6:1.

The debinding study was carried out according to the general method described for the imprinted polystyrenes in section 2.3.8.

solvent (60mL)	time/h	total weight/mg	molar ratio [93]: <i>n</i> -PrNH ₃ (CO ₃) ₂ : <i>n</i> -PrNH ₂	weight of [93]/mg
DCM	1	7.6	1:0:0	7.6
DCM	1	3.1	1:0:0	3.1
DCM	1	1.8	1:0:0	1.8
DCM: <i>n</i> -PrNH ₂ 10%	2	40.5	61:33:6	24.0
DCM: <i>n</i> -PrNH ₂ 10%	2	21.8	18:79:15	3.3
DCM: <i>n</i> -PrNH ₂ 10%	2	42.0	no [93]	0

2.5.5. Blank Polystyrene [F], polymer regeneration.

The apparatus used was the same as for the binding studies 2.3.1. The polymer was washed with DCM (2x60mL/1h/0°C) to remove any excess *n*-PrNH₂ and then stirred with HCl:diethyl ether (60mL/1h/0°C) to regenerate the acid sites. The polymer was washed by stirring with ether (3x60mL), methanol (nx60mL until pH neutral) and DCM (2x60mL).

2.5.6. Competitive binding study of blank polymer [F]. Loading 1/35, crosslinker-monomer 6:1.

The amount of DCM (10.5mL) absorbed by the polymer was determined (2.3.1).

The apparatus used was the same as for the binding studies 2.3.1. (1*R*, 5*R*)-*trans*-Carvyl amine [93] (1eq of the calculated number of binding sites in the polymer) and α -methyl benzylamine [111] (1eq) were added to the beaker and the 1:1 ratio was confirmed by ¹H NMR. DCM (60mL) was added up to the mark (*vide supra* 2.3.1) and the solution was stirred at 0°C for 15h. The solution was then concentrated *in vacuo* and the ratio [93]:[111] of the amines not bound by the polymer was determined by ¹H NMR to be

(1*R*, 5*R*)-*trans*-carvyl amine [93]: α -methyl benzylamine [111] 47:53. To debind the amines, the polymer was stirred with 10% *n*-PrNH₂:DCM (60mL/2hx3). The 10% *n*-PrNH₂:DCM fractions were combined, concentrated *in vacuo* and the ratio of substrates extracted from the polymer was determined by ¹H NMR to be (1*R*, 5*R*)-*trans*-carvyl amine [93]: α -methyl benzylamine [111] 56:44.

In each case the ratio's were determined by comparing the integration of the following peaks:

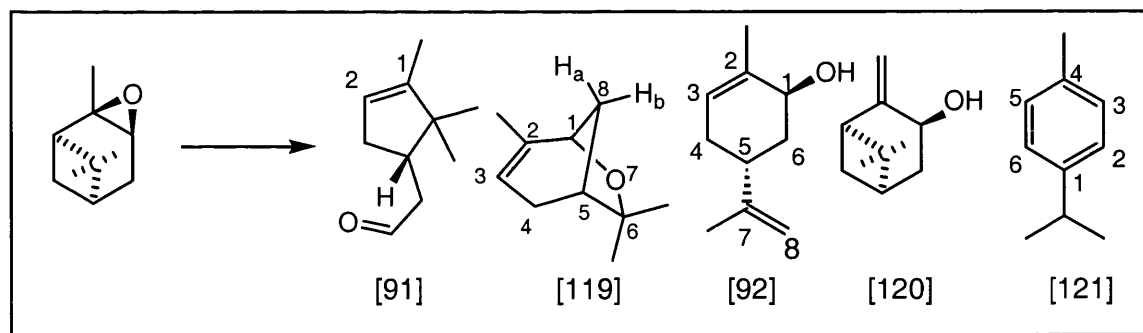
¹H NMR (CDCl₃, 300MHz) δ_H /ppm: α -methyl benzylamine [111] 4.27 (1H, q, J6.5Hz, CH₃CHN). (1*R*, 5*R*)-*trans*-carvyl amine [93] 5.40 (1H, m, =CHR) and/or 4.67 (2H, 2s, =CH₂).

Chapter 3. REACTIONS OF POLYSTYRENE-DIVINYLBENZENE POLYMERS

3.1 SOLUTION REACTIONS OF *p*-TOLUENESULFONIC ACID MONOHYDRATE WITH α -PINENE OXIDE [89].

The reactions listed below are described using the same reaction scale as for the polymer catalysed reactions. All reactions were also carried out on a larger scale and worked up according to standard procedures. Products were isolated by flash column chromatography (SiO₂, 5% EtOAc: petrol 30-40° with a solvent gradient) and characterised (*vide supra*). These products were used as standards for G.C. analysis of the M.I.P. catalysed reactions. Typical conditions were: flow rate 100mL/min, column head pressure 7.5psi, initial temperature 100°C, final temperature 200°C, initial time 2.0min and rate 5.0°C/min. Injections were 0.1 μ L, 0.015M.

3.1.1. Reaction of α -pinene oxide [89] with *p*-toluenesulfonic acid monohydrate in toluene.



α -Pinene oxide [89] (24 μ L, 0.15mmol, 1eq) was added to a stirred solution of *p*-toluenesulfonic acid (28.5mg, 0.15mmol, 1eq) in toluene (10.0mL) and the reaction stirred at room temperature for 1h. G.C. analysis of the reaction after 1h identified: campholenic aldehyde [91] (59%), Pinol [119] (11%), pinocarveol [120] (5%), *trans*-carveol [92] (5%).

Large scale: α -Pinene oxide (2.4mL, 15mmol, 1eq) was added to a stirred solution of *p*-toluenesulfonic acid (2.85g, 15mmol, 1eq) in toluene (100mL) and the reaction stirred at room temperature for 1h. Water (50mL) and DCM (4x20mL) were added and the aqueous and organic layers were separated. The organic layer was washed with Na₂CO₃ aq. (30mL), dried over MgSO₄(s) and concentrated *in vacuo*. The crude reaction mixture was purified by column chromatography (SiO₂, 5% EtOAc:petrol 40-60°C increasing to 30% EtOAc) to afford *p*-cymene [121] (15mg, 0.1mmol, 1%) campholenic aldehyde [91] (687mg, 4.5mmol, 30%), Pinol [119] (110mg, 0.7mmol, 5%), pinocarveol [120] (83mg, 0.5mmol, 5%) and *trans*-carveol [92] (289mg, 1.9mmol, 13%) all as colourless oils.

***p*-Cymene [121]¹³²:** Rf 0.8 (SiO₂, 20% EtOAc:petrol 40-60°C). ¹H NMR (CDCl₃, 300MHz) δ_{H} /ppm: 7.15 (4H, s, ArH), 2.90 (1H, sept, J7.0Hz, CH(CH₃)₂), 2.35 (3H, s, ArCH₃), 1.26 (6H, d, J7.0Hz, CH(CH₃)₂). ¹³C NMR (CDCl₃, 75MHz) δ_{C} /ppm: 145.9 (1-C), 135.2 (4-C), 129.0 (3-C), 126.3 (2-C), 33.7 (R₃CH), 24.1 (CH₃), 21.0 (CH₃). IR (neat): ν_{max} /cm⁻¹: 3376 (w), 2959 (s), 2924 (s), 1514 (m), 1461 (m), 1379 (w), 1216 (m), 1193 (m), 1134 (w), 1050 (w), 815 (s). LRMS (EIMS) m/z: 134 (20%, [M⁺]), 119 (100%, -CH₃), 91 (17%), 77 (6%), 65 (8%), 38 (10%).

Campholenic aldehyde [91]¹³³: Rf 0.7 (SiO₂, 20% EtOAc:petrol 40-60°C). ¹H NMR (CDCl₃, 400MHz) δ_{H} /ppm: 9.80 (1H, t, J2.5Hz, CHO), 5.29 (1H, m, CH=C), 2.55-2.25 (4H, m, ring H, CH₂), 1.89 (1H, m), 1.61 (3H, d(br), J2.5Hz, =CCH₃), 1.00 (3H, s, CH₃), 0.79 (3H, s, CH₃). ¹³C NMR (CDCl₃, 100MHz) δ_{C} /ppm: 201.8 (CHO), 147.8 (2-C), 121.5 (1-C), 46.8 (C(CH₃)₂), 45.0 (CH₂CHO), 44.3 (R₃CH), 35.4 (CH₂), 25.5 (CH₃), 19.9 (CH₃), 12.5 (=CCH₃). IR (neat): ν_{max} /cm⁻¹: 3038 (w), 2957 (s), 2716 (w, CHO), 1726 (s, C=O), 1463 (m), 1437 (w), 1384 (w), 1362 (m), 1016 (w), 794 (m). LRMS (EIMS) m/z: 152 (5%, [M⁺]), 108 (85%, -C₂H₄O), 93 (45%), 82 (100%), 67 (30%), 57 (35%).

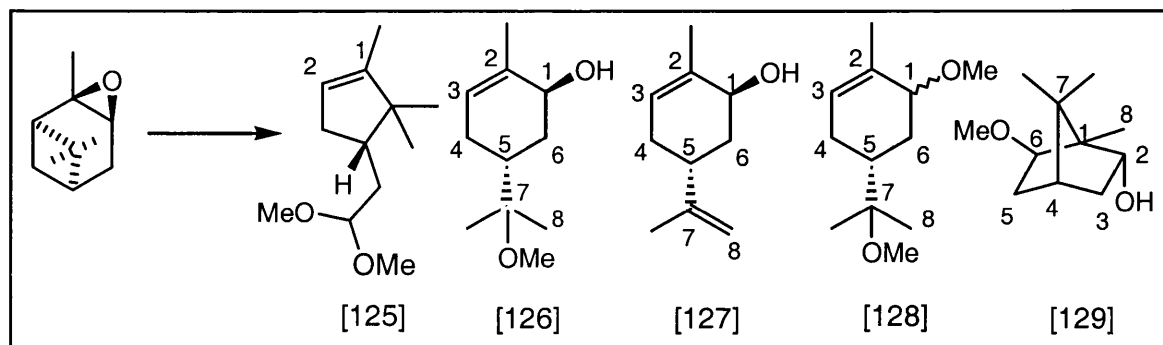
Pinol [119]¹³⁴: Rf 0.7 (SiO₂, 20% EtOAc:petrol 40-60°C). ¹H NMR (CDCl₃, 500MHz) δ_{H} /ppm: 5.16 (1H, m, =CHR), 3.95 (1H, d, J5.0Hz, 1-CHOH), 2.22-2.19 (2H, m, 4-

CH₂), 2.18 (1H, dd, J10.5Hz, 5.0Hz, 8-**H_a**), 2.10 (1H, m, 5-**CH**), 1.80 (1H, d, J10.5Hz, 8-**H_b**), 1.67 (3H, m, =C**CH₃**), 1.28 (3H, s, **CH₃**), 1.16 (3H, s, **CH₃**). ¹³C NMR (CDCl₃, 75MHz) δ_C/ppm: 139.5 (2-C), 120.2 (3-C), 82.7 (6-C), 76.6 (1-C), 41.8 (5-C), 34.5 (8-C), 30.4 (CH₃), 30.3 (4-CH₂), 25.4 (CH₃), 21.4 (CH₃). IR (neat): ν_{max}/cm⁻¹: 2968 (s), 2874 (m), 2840 (m), 1441 (m), 1358 (m), 1297 (w), 1209 (m), 1114 (m), 1033 (m), 1006 (s). LRMS (CI) m/z: 153 (16%, [M+H]⁺), 135 (100%, -OH), 107 (68%), 93 (53%).

Pinocarveol [120]¹⁰²: Rf 0.3 (SiO₂, 20% EtOAc:petrol 40-60°C). ¹H NMR (CDCl₃, 400MHz) δ_H/ppm: 4.97 (1H, s, =**CH₂**), 4.80 (1H, s, =**CH₂**), 4.40 (1H, d, J7.5Hz, **CHOH**), 2.49 (1H, t, J5.5Hz, ring **H**), 2.36 (1H, m, ring **H**), 2.22 (1H, d, J14.5Hz, 7.5Hz, ring **H**), 1.97 (1H, m, ring **H**), 1.82 (1H, dd, J14.5Hz, 4.0Hz, ring **H**), 1.69 (1H, d, J10Hz, ring **H**), 1.25 (3H, s, **CH₃**), 0.62 (3H, s, **CH₃**). ¹³C NMR (CDCl₃, 75MHz) δ_C/ppm: 156.3 (R₂**C=CH₂**), 111.8 (=CH₂), 67.2 (**CHOH**), 51.0 (**CH**), 40.8 (quaternary **C**), 40.2 (**CH**), 34.9 (**CH₂**), 28.6 (**CH₂**), 26.3 (**CH₃**), 21.5 (**CH₃**). IR (neat): ν_{max}/cm⁻¹: 3383 (s, b, OH), 3071 (w), 2974 (s), 2921 (s), 2869 (s), 1646 (m, C=C), 1452 (m), 1384 (s), 1387 (m), 1340 (w), 1296 (m), 1145 (m), 1106 (w), 1086 (w), 1022 (m), 1002 (m), 895 (m). LRMS (CI) m/z: 153 (3%, [M+H]⁺), 135 (100%, -OH), 107 (30%, 93 (27%), 79 (10%).

trans-Carveol [92]¹³⁵: Rf 0.3 (SiO₂, 20% EtOAc:petrol 40-60°C). ¹H NMR (CDCl₃, 400MHz) δ_H/ppm: 5.59 (1H, dm, J5.5Hz, =**CHR**), 4.11 (1H, s, =**CH₂**), 4.09 (1H, s, =**CH₂**), 4.02 (1H, s(br), **CHOH**), 2.32 (1H, m), 2.14 (1H, dm, J13.5Hz), 2.03-1.55 (4H, m, ring **H**, **OH**), 1.80 (3H, s, **CH₃**), 1.75 (3H, s, **CH₃**). ¹³C NMR (CDCl₃, 100MHz) δ_C/ppm: 149.2 (R₂**C=CH₂**), 134.3 (2-**C**), 125.4 (3-**C**), 109.0 (8-**C**), 68.6 (**CHOH**), 36.7, 35.2, 31.0, 20.9 (**CH₃**). IR (neat): ν_{max}/cm⁻¹: 3333 (s, OH), 3082 (w), 2966 (s), 2916 (s), 1645 (m, C=C), 1438 (s), 1375 (m), 1264 (m), 1156 (m), 1164 (m), 1054 (s), 1032 (s), 962 (s), 944 (m), 887 (s). LRMS (EIMS) m/z: 152 (20%, [M⁺]), 109 (100%, -C₃H₇⁺), 84 (90%), 69 (30%), 54 (50%), 38 (60%).

3.1.2. Reaction of α -pinene oxide [89] with *p*-toluenesulfonic acid monohydrate in Methanol.



α -Pinene oxide (24 μ L, 0.15mmol, 1eq) was added to a stirred solution of *p*-toluenesulfonic acid (28.5mg, 0.15mmol, 1eq) in methanol (10.0mL) and the reaction stirred at room temperature for 1h. G.C. analysis of the reaction after 1h identified: *p*-cymene [121] (5%), 1,1-dimethoxy-2-[(2,2,3)-trimethyl-3-cyclopenten-1-yl] ethane [125] (23%), *trans*-2-methyl-5-(1-methoxy, 1-methylethyl)-2-cyclohexenmethyl ether [128] (13%), 1,7,7-trimethyl-6-*exo*-methoxy bicyclo[2.2.1] heptan-2-*endo*-ol [129] (10%), *trans*-2-methyl 5(1-methoxy, 1-methylethyl)-2-cyclohexen-1-ol [127] (17%) as colourless oils.

Large scale: α -Pinene oxide (200mg, 207 μ L, 1.3mmol, 1eq) was added to a stirred solution of *p*-toluenesulfonic acid (250mg, 1.3mmol, 1eq) in methanol (10mL) and the reaction stirred at room temperature for 1h. The reaction was quenched with Na₂CO₃ aq. (20mL) and extracted with diethyl ether (3x50mL). The combined extracts were washed with water, dried over MgSO₄(s) and concentrated *in vacuo*. The reaction mixture was purified by column chromatography (SiO₂, 5% EtOAc:petrol 40-60°C increasing to 30% EtOAc) to afford 1,1-dimethoxy-2-[(2,2,3)-trimethyl-3-cyclopenten-1-yl] ethane [125] (18mg, 0.09mmol, 7%), *trans*-2-methyl-5-(1-methoxy, 1-methylethyl)-2-cyclohexenmethyl ether [126] (21mg, 0.11mmol, 8%), *trans*-carveol [92] (9mg, 0.06mmol, 6%), 1,7,7-trimethyl-6-*exo*-methoxy bicyclo[2.2.1] heptan-2-*endo*-ol [128] (12mg, 0.06mmol, 5%), *trans*-2-methyl 5(1-methoxy, 1-methylethyl)-2-cyclohexen-1-ol [127] (22mg, 0.12mmol, 9%).

1,1-dimethoxy-2-[(2,2,3)-trimethyl-3-cyclopenten-1-yl] ethane [125]: Rf 0.5 (SiO₂, 20% EtOAc:petrol 40-60°C). m.p. (petrol 30-40°C/EtOAc): 76-78°C. ¹H NMR (CDCl₃, 400MHz) δ_H/ppm: 5.23 (1H, m, =CH_R), 4.43 (1H, dd, J7.5Hz, 4.0Hz, CHC(OMe)₂), 3.34 (3H, s, OCH₃), 3.31 (3H, s, OCH₃), 2.31 (1H, m), 1.90-1.76 (3H, m, ring H, CH₂CH(OMe)₂), 1.61 (3H, d, J1.5Hz, =CCH₃), 1.54 (1H, m), 0.99 (3H, s, CH₃), 0.76 (3H, s, CH₃). ¹³C NMR (CDCl₃, 100MHz) δ_C/ppm: 148.5 (3-C), 121.7 (4-C), 104.0 (C(OMe)₂), 53.0 (OCH₃), 52.0 (OCH₃), 46.8 (R₂C(CH₃)₂), 45.9 (1-C), 35.5 (CH₂), 32.8 (CH₂), 25.6 (CH₃), 19.7 (CH₃), 12.7 (CH₃). IR (neat): ν_{max}/cm⁻¹: 3036 (w), 2953 (s), 2830 (m), 1464 (m), 1382 (m), 1361 (m), 1193 (w), 1138 (m), 1124 (s), 1059 (s), 1016 (m), 965 (m), 937 (w), 795 (m). LRMS (FABS) m/z: 198 (25%, [M]⁺), 133 (100, [M-2MeOH]⁺).

trans-2-methyl-5-(1-methoxy, 1-methylethyl)-2-cyclohexenmethyl ether [127]: Rf 0.4 (SiO₂, 20% EtOAc:petrol 40-60°C). ¹H NMR (CDCl₃, 400MHz) δ_H/ppm: 5.59 (1H, m, =CHR), 3.50 (1H, m, CHOCH₃), 3.40 (3H, s, OCH₃), 3.19 (3H, s, OCH₃), 2.11 (1H, dd, J15.5Hz, 2.0Hz), 1.98 (2H, m), 1.76 (3H, d, J1.5Hz, CH=CCH₃), 1.76-1.69 (2H, m), 1.12 (3H, s, CH₃), 1.11 (3H, s, CH₃). ¹³C NMR (CDCl₃, 100MHz) δ_C/ppm: 133.2 (2-C), 125.8 (3-C), 79.7 (CHOMe), 76.1 (COMe), 57.1 (OCH₃), 48.6 (OCH₃), 34.7 (R₃CH), 27.2 (CH₂), 26.8 (CH₂), 22.7 (CH₃), 22.5 (CH₃), 21.0 (CH₃). IR (neat): ν_{max}/cm⁻¹: 2972 (s), 2921 (s), 2834 (s), 1455 (m), 1381 (m), 1384 (m), 1333 (w), 1250 (m), 1189 (m), 1157 (m), 1140 (m), 1078 (s), 914 (m), 807 (w).

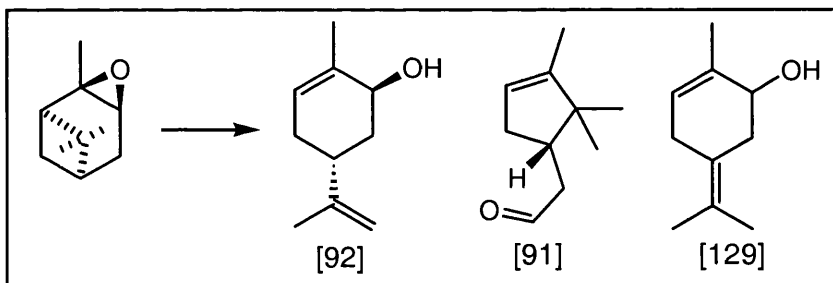
trans-carveol [92]: spectra as above

1,7,7-trimethyl-6-exo-methoxy bicyclo[2.2.1] heptan-2-endo-ol [128]: Rf 0.3 (SiO₂, 20% EtOAc:petrol 40-60°C). ¹H NMR (CDCl₃, 500MHz) δ_H/ppm: 4.79 (1H, d, J10.5Hz, OH), 4.02 (1H, m, 2-CH_{endo}OH), 3.79 (1H, dt, J9.5Hz, 3.0Hz, 6-CH_{exo}OMe), 3.32 (3H, s, OCH₃), 2.38 (1H, m, 3-CH_{endo}), 2.27 (1H, m, 5-CH_{endo}), 1.73 (1H, t, J5.0Hz, 4-CH), 1.32 (1H, dd, J13.0Hz, 3.5 Hz, 5-CH_{exo}), 1.20 (1H, dd, J13.5Hz, 4.0Hz, 3-CH_{exo}), 1.03 (3H, s, 8-CH₃), 0.80 (3H, s, C(CH₃)₂), 0.81 (3H, s, C(CH₃)₂). ¹³C NMR (CDCl₃, 75MHz) δ_C/ppm: 89.9 (CHOH), 79.0 (CHOMe), 58.2 (OCH₃), 50.1

(quaternary **C**), 48.8 (quaternary **C**), 43.2 (4-**CH**), 39.8 (**CH**₂), 36.0 (**CH**₂), 20.0 (**CH**₃), 19.7 (**CH**₃), 12.1 (**CH**₃). **IR** (neat): $\nu_{\max}/\text{cm}^{-1}$: 3483 (s, OH), 2986 (m), 2952 (s), 2877 (m), 1450 (m), 1369 (m), 1298 (w), 1190 (m), 1230 (s), 1190 (m), 1130 (s), 1086 (s), 1062 (m), 1004 (w), 970 (w), 899 (w).

trans-2-methyl 5(1-methoxy, 1-methylethyl)-2-cyclohexen-1-ol [92]: **Rf** 0.1 (SiO₂, 20% EtOAc:petrol 40-60°C). ¹H NMR (CDCl₃, 400MHz) $\delta_{\text{H}}/\text{ppm}$: 5.57 (1H, dm, J5.0Hz, =**CHR**), 4.01 (1H, m, **CHOH**), 3.19 (3H, s, **OCH**₃), 2.04-1.89 (3H, m), 1.78 (3H, s, =**CCH**₃), 1.74 (1H, s(br), **OH**), 1.38 (1H, td, J13.0Hz, 4.0Hz), 1.1 (6H, s, **C(CH**₃)₂). ¹³C NMR (CDCl₃, 100MHz) $\delta_{\text{C}}/\text{ppm}$: 134.3 (2-**C**), 125.4 (3-**C**), 76.2 (**COCH**₃), 68.5 (**CHOH**), 48.7 (**OCH**₃), 35.3 (5-**CH**), 32.7 (**CH**₂), 27.0 (**CH**₂), 22.4 (**CH**₃), 22.1 (**CH**₃), 20.9 (**CH**₃). **IR** (neat): $\nu_{\max}/\text{cm}^{-1}$: 3394 (s, b, OH), 2970 (s), 2919 (s), 1456 (m), 1380 (m), 1364 (m), 1252 (w), 1158 (m), 1140 (m), 1075 (s), 1035 (m), 961 (w), 805 (w).

3.1.3. Reaction of α -pinene oxide [89] with *p*-toluenesulfonic acid monohydrate in DMF.



α -Pinene oxide (24 μ L, 0.15mmol, 1eq) was added to a stirred solution of *p*-toluenesulfonic acid (28.5mg, 0.15mmol, 1eq) in DMF (10.0mL) and the reaction stirred at room temperature for 1h. G.C. analysis of the reaction after 1h identified: campholenic aldehyde [91] (21%), *trans*-carveol [92] (42%) and 5-isopropylidene-2-methyl-cyclohex-2-enol [129] (24%).

Large scale: α -Pinene oxide (1.2mL, 7.5mmol, 1eq) was added to a stirred solution of *p*-toluenesulfonic acid (1.42g, 7.5mmol, 1eq) in DMF (50mL) and the reaction stirred at

room temperature for 1h. DCM (60mL) was added and the organic phase was washed with CuSO₄ aq. (2x20mL), water (3x20mL), dried over MgSO₄(s) and concentrated *in vacuo*. The crude reaction mixture was purified by column chromatography (SiO₂, 5% EtOAc:petrol 40-60°C increasing to 30% EtOAc) to afford campholenic aldehyde [91] (209mg, 1.4mmol, 18%), 5-isopropylidene-2-methyl-cyclohex-2-enol [129] (126mg, 11%) and *trans*-carveol [92] (347mg, 2.3mmol, 30%).

Campholenic aldehyde [91]: Spectra as above

***trans*-Carveol [92]:** Spectra as above

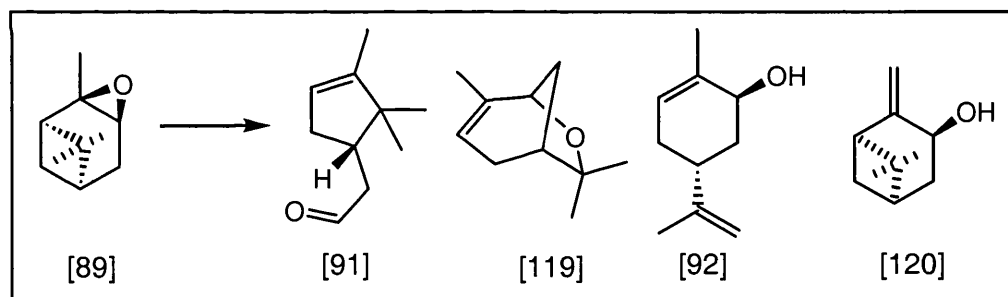
5-Isopropylidene-2-methyl-cyclohex-2-enol [129]: Rf 0.4 (SiO₂, 20% EtOAc:petrol 40-60°C). ¹H NMR (CDCl₃, 500MHz) δ_H/ppm: 5.47 (1H, m, =CHR), 3.97 (1H, m, CHOH), 2.85 (1H, d(br), J20Hz, ring H), 2.65 (1H, dd, J 13.5Hz, 4.0Hz, ring H), 2.31 (1H, dm, 24Hz, ring H), 1.77 (3H, m, =CCH₃), 1.71 (3H, s, CH₃), 1.66 (3H, s, CH₃), 1.44 (1H, s(br), OH). ¹³C NMR (CDCl₃, 100MHz) δ_C/ppm: 135.9 (quaternary C), 125.8 (quaternary C), 124.3 (=CHR), 123.1 (quaternary C), 70.4 (CHOH), 35.9 (CH₂), 29.8 (CH₂), 20.4 (CH₃), 20.2 (CH₃), 19.9 (CH₃). IR (neat): ν_{max}/cm⁻¹: 3257 (s, OH), 3160 (m), 2966 (m), 2935 (m), 2884 (m), 1607 (w), 1436 (w), 1366 (w), 1320 (w), 1058 (w), 1014 (s), 912 (w), 803 (w). LRMS (FABS) m/z: 152 (45%, [M]⁺), 149, (100%), 133, (80%), 107, (80%).

3.2 REACTIONS OF POLYSTYRENE-DIVINYLBENZENE MIPs WITH α -PINENE OXIDE [89].

3.2.1. General method for polymer regeneration.

Polymers were regenerated after the binding studies. The apparatus used was the same as for the binding studies 5.1.3. The polymer was washed with DCM (2x60mL/1h/0°C) to remove any excess *n*-PrNH₂ and then stirred with HCl:diethyl ether (60mL/1h/0°C) to regenerate the acid sites. The polymer was washed with ether (3x60mL), methanol (nx60mL until pH neutral) and DCM (2x60mL).

3.2.2. General Procedure for the reaction of α -pinene oxide [89] with polystyrene-divinylbenzene MIPs in toluene.

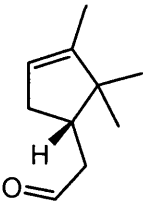
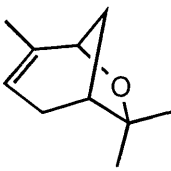
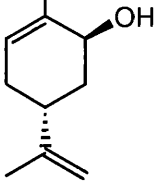
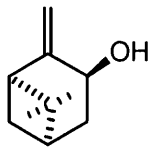


For each MIP the number of moles of available acid binding sites (calculated in the binding studies 2.3.1) was used to determine the number of equivalents employed.

α -Pinene oxide [89] was added to a stirred suspension of the polystyrene-divinylbenzene MIP (1eq) in toluene (0.015M to [89]) at room temperature. An example of the reaction scale is α -pinene oxide [89] (22.9mg, 24 μ L, 0.15mmol, 1eq), MIP 1/35, 6:1 [A] (913mg, 0.15mmol, 1eq), and toluene (10.0mL). The reaction was stirred for 1h

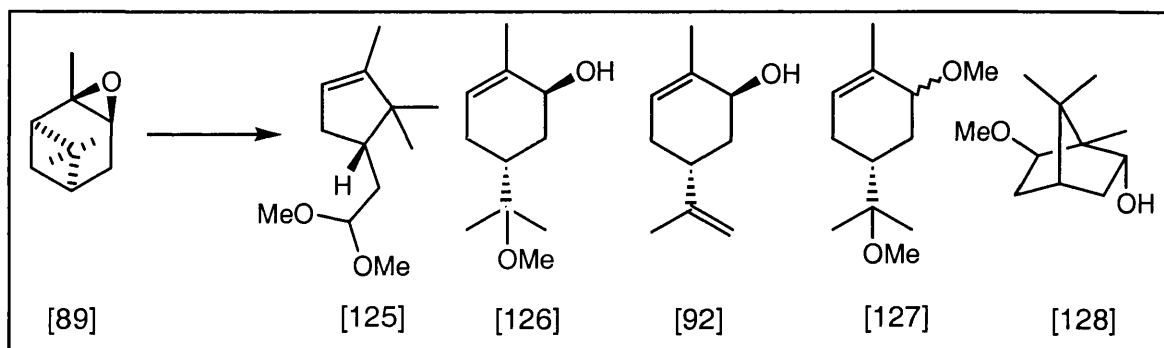
and analysed by G.C[#]. The polymer was then filtered off, washed with DCM (3x10mL) and the filtrate concentrated *in vacuo* and analysed by ¹H and ¹³C NMR.

The results are tabulated below[#]:

MIP/ catalyst	 [91]	 [119]	 [92]	 [120]
1/35, 6:1 [A]*	54%	9%	16%	13%
1/35, 3:1 [B]*	60%	9%	20%	4%
1/35, 2:1 [C]*	59%	10%	20%	4.5%
1/15, 2:1 [D]*	62%	12%	11%	5%
1/10, 3:1 [E]*	61%	9%	20%	3%
1/35, 6:1 [F]*	60%	8%	22%	3%

[#] Yields are quoted from G.C.analysis of the crude reaction mixture 1μL, 0.015M, using our standard conditions (3.2.2). Authentic samples of each product were used as standards.

3.2.3. General Procedure for the reaction of α -pinene oxide [89] with polystyrene-divinylbenzene MIPs in methanol.



For each MIP the number of moles of available acid binding sites (calculated in the binding studies 2.3.1) was used to determine the number of equivalents employed.

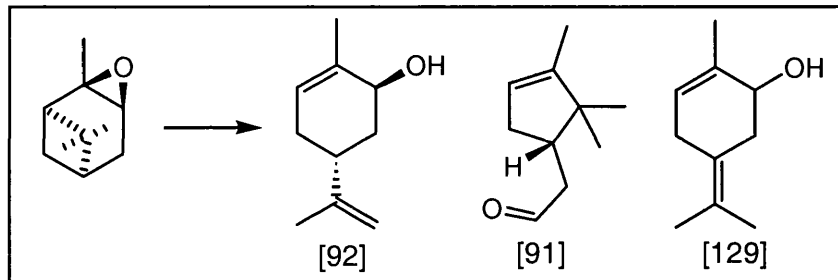
α -Pinene oxide [89] was added to a stirred suspension of the polystyrene-divinylbenzene MIP (1eq) in methanol (0.015M to [89]) at room temperature. An example of the reaction scale is α -pinene oxide [89] (22.9mg, 24 μ L, 0.15mmol, 1eq), MIP 1/35, 6:1 [A] (913mg, 0.15mmol, 1eq), and methanol (10.0mL). The reaction was stirred for 1h and analysed by G.C[#]. The polymer was then filtered off, washed with DCM (3x10mL) and the filtrate concentrated *in vacuo* and analysed by ¹H and ¹³C NMR.

[#] Yields are quoted from G.C.analysis of the crude reaction mixture 1 μ L, 0.015M, using our standard conditions (3.2.2). Authentic samples of each product were used as standards.

The results are tabulated below[#] :

MIP	[125]	[126]	[92]	[127]	[128]
1/35, 6:1 [A]*	27%	41%	11%	-	11%
1/35, 3:1 [B]*	32%	36%	10%	4%	11%
1/35, 2:1 [C]*	29%	38%	12%	3%	10%
1/15, 2:1 [D]*	31%	36%	12%	-	11%
1/10, 3:1 [E]*	27%	40%	10%	2%	11%
1/35, 6:1 [F]*	26%	40%	12%	2%	10%

3.2.4. General Procedure for the reaction of α -pinene oxide [89] with polystyrene-divinylbenzene MIPs in DMF.

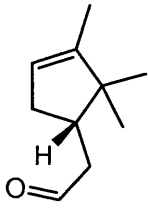
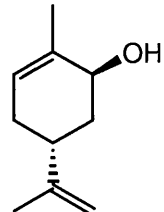
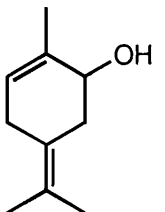


For each MIP the number of moles of available acid binding sites (calculated in the binding studies 2.3.1) was used to determine the number of equivalents employed.

α -Pinene oxide [89] was added to a stirred suspension of the polystyrene-divinylbenzene MIP (1eq) in DMF (0.015M to [89]) at room temperature. An example of the reaction scale is α -pinene oxide [89] (22.9mg, 24 μ L, 0.15mmol, 1eq), MIP 1/35, 6:1 [A] (913mg, 0.15mmol, 1eq), and DMF (10.0mL). The reaction was stirred until consumption of all the starting material was observed by G.C.(3-7.5h). The polymer was then filtered off, and washed with DCM (3x10mL). The organic layer was washed with distilled water (5x10mL), dried over $MgSO_4(s)$, concentrated *in vacuo* and analysed by 1H and ^{13}C NMR.

Yields are quoted from G.C.analysis of the crude reaction mixture 1 μ L, 0.015M, using our standard conditions (3.2.2). Authentic samples of each product were used as standards.

The results are tabulated below[#] :

M.I.P.	time/h	 [91]	 [92]	 [93]
1/35, 6:1 [A]*	6	24%	45%	25%
1/35, 3:1 [B]*	7.5	29%	41%	24%
1/35, 2:1 [C]*	2	39%	38%	20%
1/15, 2:1 [D]*	4	31%	41%	21%
1/10, 3:1 [E]*	3	32%	39%	21%
1/35, 6:1 [F]*	6	23%	42%	23%

[#] Yields are quoted from G.C.analysis of the crude reaction mixture 1 μ L, 0.015M, using our standard conditions (3.2.2). Authentic samples of each product were used as standards.

Chapter 4. MOLECULAR MODELLING

'Virtual' Synthesis of a library of tri-peptides



aa₁ = basic amino acid
aa₂ = variable amino acid
aa₃ = acidic amino acid

Three libraries of suitable candidates for each positional amino acid aa₁, aa₂, and aa₃, were selected. The candidates selected include both the natural amino acids and a range of readily available unnatural congeners which were identified by an ACD (available chemicals directory) search using ISISbase. The variability of the two terminal amino acids was limited by side chain functionality: aa₁ = basic side chain, aa₃ = acid side chain, but the nature of the central amino acid was unrestricted. The libraries used for aa₁ (10 members), aa₂ (17 members) and aa₃ (3 members) are illustrated in Appendix 2.

The aa₁, aa₂, and aa₃, library members were converted into SMILES notation and all the possible permutations of tri-peptides were virtually synthesised using DAYLIGHT* and then CHIRALIFY to distinguish the stereochemistry and generate all possible enantiomers. CONCORD distance geometry was then used to convert the SMILES structures into 3D to give the desired 'virtual library' of tri-peptides.

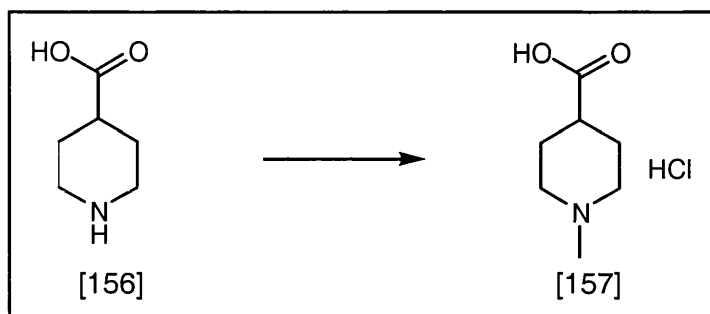
In order to study the binding of the tri-peptides around the imprint molecule an electrostatic picture of the imprint molecule (TSA) [151] was generated using spartan geometry optimisation (ρ PMS (semiempirical), electro ρ 6-31G*). The peptides were then docked around this TSA using ICM Molsoft docking program matching electrostatic, hydrogen bonding and steric interactions. Analysis of the results identified the three tri-peptides NH₂-(D)Arg-(L)Lys-(L)Glu-OH [153], NH₂-(L)Arg-(D)Lys-(L)Glu-OH [154], and NH₂-(D)Arg-(D)Phe-(L)Glu-OH [155] (Fig 31, 32, and 33 respectively, illustrated in Results and Discussion) as suitable candidates.

* DAYLIGHT is a program written by Dr Stephen Garland, SKB.

Chapter 5. SYNTHESIS OF TRANSITION STATE ANALOGUE

[151].

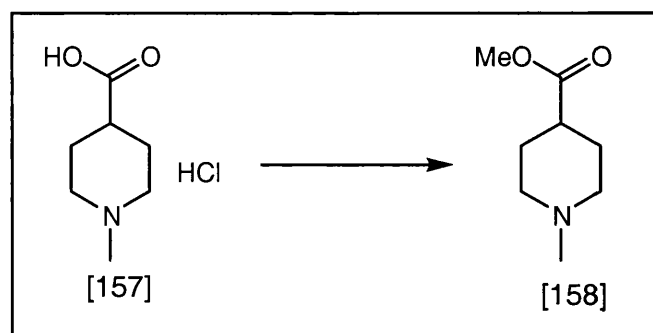
5.1 Synthesis of *N*-methyl isonipecotic acid hydrochloride [157].



Formaldehyde solution (37%, 6.8mL) was added to a stirred solution of isonipecotic acid [156] (5.0g, 39mmol, 1eq) in formic acid (10.5mL). The solution was heated to reflux for 24h and then reduced *in vacuo* to afford a colourless syrup. Conc HCl (1mL) was added followed by acetone (40mL) and the resulting suspension was reduced *in vacuo* to give a white solid. Recrystallisation from acetone/MeOH gave white crystals of *N*-methyl isonipecotic acid hydrochloride [157] (5.68g, 32mmol, 82%).

m.p. (acetone/MeOH): 228-229°C. ¹H NMR (D₂O, 300MHz) δ_H/ppm: 3.41 (2H, d(br), J12.5Hz, NCH_{eq}), 2.88 (2H, t(br), J13.0Hz, NCH_{ax}), 2.70 (3H, s, NCH₃), 2.54 (1H, tt, J12.5Hz, 4.0Hz, CHCO₂H), 2.09 (2H, d(br), J14.5Hz, 3-H_{eq}, 5-H_{eq}), 1.69 (2H, qd, J12.5Hz, 4.0Hz 3-H_{ax}, 5-H_{ax}). ¹³C NMR (D₂O, 75MHz) δ_C/ppm: 178.3 (C=O), 54.4 (NCH₂), 44.0 (NCH₃), 38.6 (CHCO₂H), 26.4 (3-, 5-CH₂). **IR** (neat): ν_{max}/cm⁻¹ : 3429 (b, w, OH), 2948 (s), 2727 (s), 1717 (s, C=O), 1465 (w), 1401 (w), 1366 (w), 1203 (s), 1180 (s), 1160 (m), 1042 (w), 923 (w), 833 (w). **LRMS** (EIMS) m/z : 142 (100%, [M_{HCl}-H⁺]), 128 (15%, -CH₃), 98 (40%, -CO₂), 69 (90%), 54 (35%). **Elemental analysis:** Calc C 46.81, H 8.31, N 7.74, Found C 46.81, H 8.76, N 7.80.

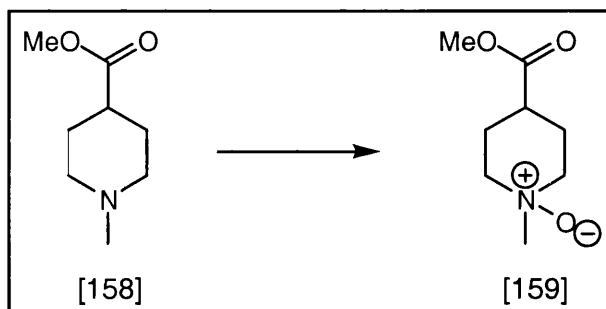
5.2 Synthesis of Methyl *N*-methylisonipecotate [158].



To a stirred solution of *N*-methylisonipecotic acid hydrochloride [157] (5.50g, 31mmol, 1eq) in methanol (50mL) at -10°C was added thionyl chloride (5.46g, 3.4mL, 46mmol, 1.5eq), dropwise over 10min. The reaction was allowed to come to room temperature and stirred for 18h. Saturated NaCO_3 aq. was added portionwise to pH~9 and the mixture extracted with DCM (3x100mL). The combined extracts were dried over $\text{Na}_2\text{SO}_4(\text{s})$ and concentrated *in vacuo* to afford methyl *N*-methylisonipecotate [158] as a colourless liquid (4.52g, 29mmol, 94%).

$^1\text{H NMR}$ (CDCl_3 , 300MHz) $\delta_{\text{H}}/\text{ppm}$: 3.57 (3H, s, CH_3) 2.69 (2H, d(br), J11.0Hz, NCH_{eq}) 2.15 (4H, s+m, NCH_3 , CHCO_2H), 1.80-1.76 (4H, m, NCH_{ax} , $\text{R}_2\text{CH}_{\text{eq}}$), 1.70-1.63 (2H, m, $\text{R}_2\text{CH}_{\text{ax}}$). $^{13}\text{C NMR}$ (CDCl_3 , 75MHz) $\delta_{\text{C}}/\text{ppm}$: 175.2 ($\text{C}=\text{O}$), 54.8 (NCH_2), 51.3 (OCH_3), 46.2 (NCH_3), 40.2 (CHCO_2), 23.1 (CH_2R_2) **IR** (neat): $\nu_{\text{max}}/\text{cm}^{-1}$: 3346 (w), 3351 (w), 3224 (w), 2945 (s), 2783 (w), 2678 (s), 1736 (s, $\text{C}=\text{O}$), 1440 (s), 1377 (s), 1318 (s), 1276 (s), 1180 (s), 1047 (s), 1013 (s), 900 (m), 853 (m), 770 (s), 734 (s). **LRMS** (FAB+) m/z : 158 (100%, $[\text{M}+\text{H}]^+$), 136 (22%), 109 (26%). **HRMS**: Calc for $\text{C}_8\text{H}_{16}\text{NO}_2$ $[\text{M}+\text{H}]^+$; 158.1175, Measured: 158.1181.

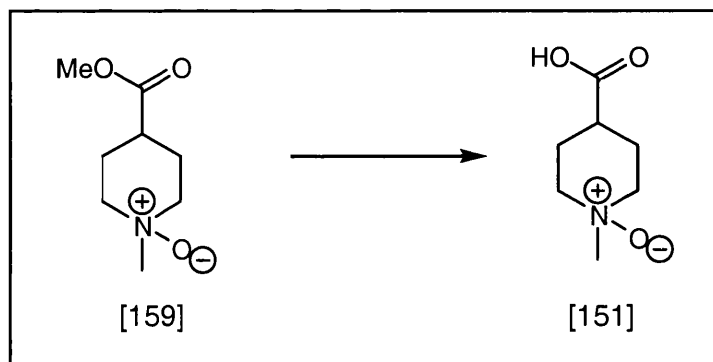
5.3 Methyl *N*-methylisonipecotate *N*-oxide [159]



Methyl *N*-methylisonipecotate [158] (11.81g, 75mmol, 1eq) in DCM (150mL) was stirred at 0°C. A solution of mCPBA (>57%, 193mg, >1.1mmol, >1eq). in DCM (200mL) was added dropwise via a cannula over 15 min and the reaction allowed to come to room temperature. The reaction was stirred for 2h at room temperature and then passed over a pad of basic alumina eluting with DCM (100mL) then methanol (150mL). The methanol fraction was concentrated *in vacuo* to afford methyl *N*-methylisonipecotate *N*-oxide [159] as an off white solid (11.74g, 67mmol, 89%).

m.p. (i-PrOH/EtOAc): 115-117°C. $^1\text{H NMR}$ (D_2O , 300MHz) δ_{H} /ppm: 3.53 (3H, s, OCH_3), 3.28-3.10 (4H, m, NCH_2), 3.01 (3H, s, NCH_3), 2.45 (1H, tt, $J_{12.0\text{Hz}}$, 4.0Hz, CHCO_2), 1.99 (2H, qd, $J_{12.0\text{Hz}}$, 4.5Hz, $\text{R}_2\text{CH}_{\text{ax}}$), 1.82 (2H, m, $\text{R}_2\text{CH}_{\text{eq}}$). $^{13}\text{C NMR}$ (D_2O , 75MHz) δ_{C} /ppm: 177.4 ($\text{C}=\text{O}$), 65.6 (NCH_2), 60.3 (OCH_3), 53.5 (NCH_3), 38.7 (CHCO_2), 23.6 (R_2CH_2). **IR** (neat): $\nu_{\text{max}}/\text{cm}^{-1}$: 3389 (b, s, **N-OH?**), 2948 (s), 1725 (s, $\text{C}=\text{O}$), 1666 (m), 1449 (m), 1378 (w), 1334 (w), 1288 (m), 1211 (m), 1057 (w), 1011 (m), 962 (w). **LRMS** (FAB+) m/z : 347 (30%, $[\text{2M}+\text{H}]^+$), 174 (100%, $[\text{M}+\text{H}]^+$), 156 (15%, $\text{M}-\text{O}$), 142 (8%). **HRMS**: Calc for $\text{C}_8\text{H}_{16}\text{NO}_3$ $[\text{M}+\text{H}]^+$; 174.1130 Measured 174.1127.

5.4. Isonipecotic acid *N*-oxide [151].

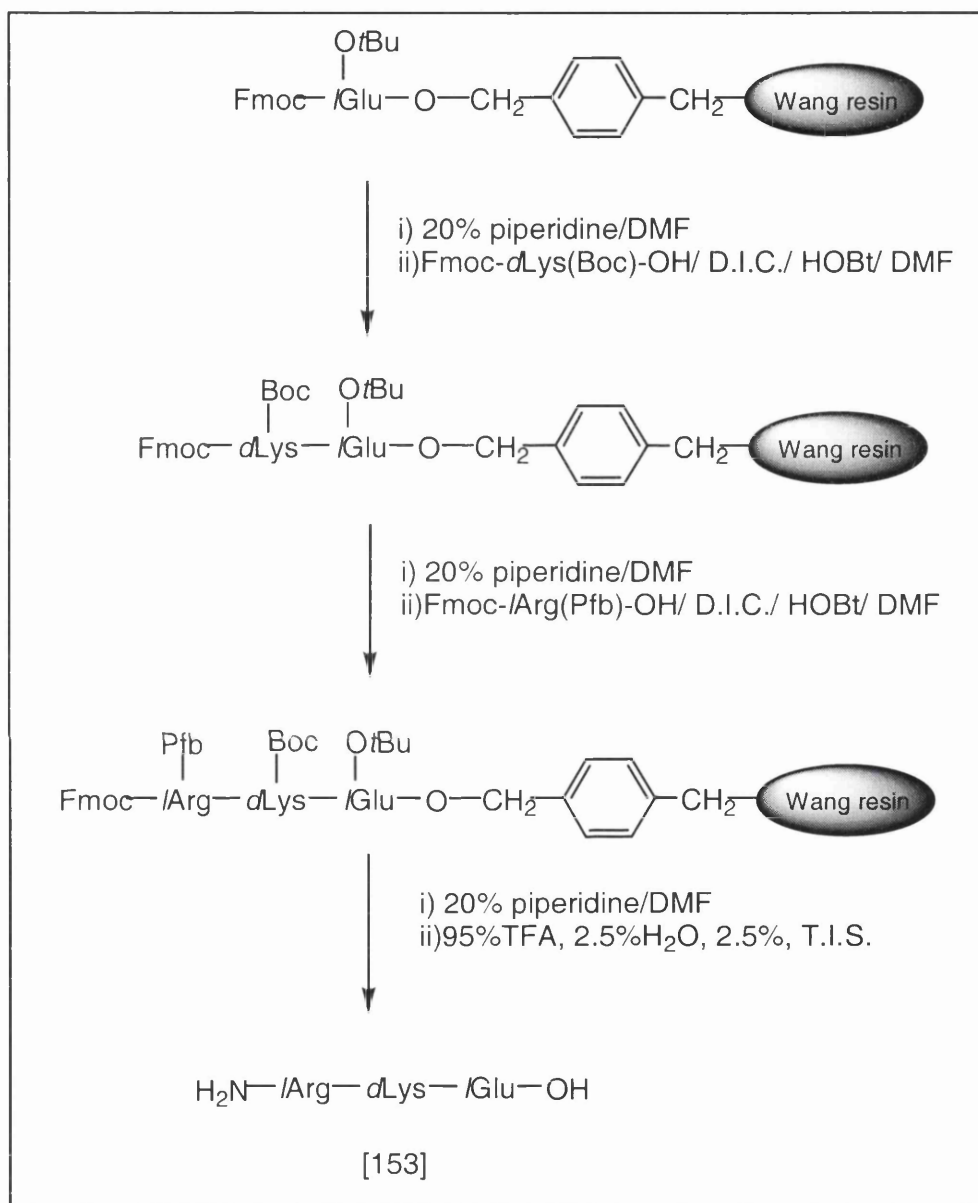


Methyl *N*-methylisonipecotate *N*-oxide [159] (115mg, 0.7mmol, 1eq) was dissolved in HCl aq. (5M, 10mL) and stirred at room temperature for 18h. The solution was freeze dried. Distilled water (4x10mL) was added and the product was freeze dried four times. The white solid was recrystallised from i-PrOH/EtOAc to give white needles of Isonipecotic acid *N*-oxide [151] (106mg, 0.7mmol, quantitative).

m.p. (i-PrOH/EtOAc): dcmp 162-168°C $^1\text{H NMR}$ (CD_3OD , 300MHz) $\delta_{\text{H}}/\text{ppm}$: 3.82-3.67 (4H, m, 6-, 2- CH_2N), 3.58 (3H, s, NCH_3), 2.73-2.63 (1H, m, 4-CH), 2.28-2.11 (4H, m, 3-, 5- CH_2). $^{13}\text{C NMR}$ (CD_3OD , 75MHz) $\delta_{\text{C}}/\text{ppm}$: 176.0 (C=O), 65.4 (6-, 2- CH_2N), 58.1 (NCH_3), 38.2 (4-CH), 24.0 (3-, 5- CH_2). **IR** (KBr): $\nu_{\text{max}}/\text{cm}^{-1}$: 3429 (w), 3031 (w), 2880 (m), 1736 (s, C=O), 1651 (m), 1518 (m), 1448 (m), 1263 (w), 1195 (m), 1140 (s), 1106 (m), 1037 (w), 914 (m), 715 (m). **LRMS** (FAB+) m/z : 319 (29%, $[\text{2M}+\text{H}]^+$), 160 (100%, $[\text{M}+\text{H}]^+$), 136 (10%), 107 (5%). **HRMS**: Calc for $\text{C}_8\text{H}_{16}\text{NO}_2$ $[\text{M}-\text{H}]$; 160.0974 Measured 160.0978.

Chapter 6. SYNTHESIS OF TRI-PEPTIDES.

Experimental set-up: All three tri-peptides were synthesised manually using Fmoc resin methodology. The resin and reaction solution were suspended in a vessel with a sintered frit as a base under a positive pressure of nitrogen from below. After each manipulation in the synthesis the reaction solution was filtered off under vacuum and then the positive pressure of nitrogen reapplied.

6.1. Synthesis of H₂N-(L)Arg-(D)Lys-(L)Glu-OH [153]

Fmoc removal: Fmoc-(L)Glu(OtBu)-Wang Resin (0.51mmolg⁻¹, 1.47g, 0.75mmol) was swelled with DMF (3x30mL). The resin was bubbled with 20% piperidine/DMF (30mL) for 3min, drained, a further 20% piperidine/DMF (30mL) was bubbled for 20min and the reaction solution then removed. The resin was washed with DMF (5x30mL).

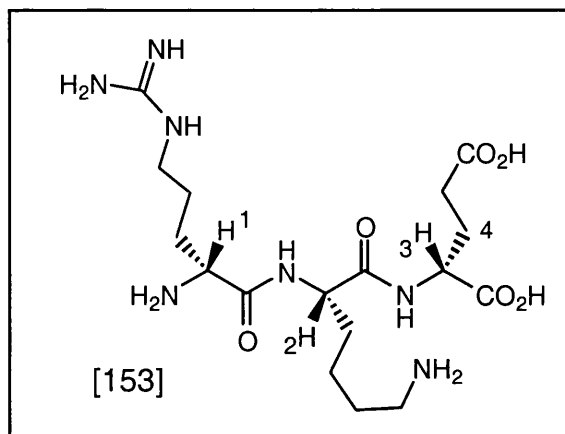
First coupling: Fmoc-(D)Lys(Boc)OH (0.878g, 1.9mmol, 2.5eq) as a solution in DMF (20mL) was added followed by HOBt/DMF (0.5M, 3.7mL, 1.9mmol, 2.5eq), and DIC/DMF (0.5M, 3.7mL, 1.9mmol, 2.5eq). The reaction was bubbled at room temperature for 2h after which time the Kaiser test^{137,136} indicated complete reaction of the resin bound free amine. The resin was then washed with DMF (3x30mL).

Fmoc removal: The resin was bubbled with 20% piperidine/DMF (30mL) for 3min, drained, a further 20% piperidine/DMF (30mL) was bubbled for 20min and the reaction solution then removed. The resin was washed with DMF (5x30mL). The Kaiser test indicated the presence of free resin bound amine groups.

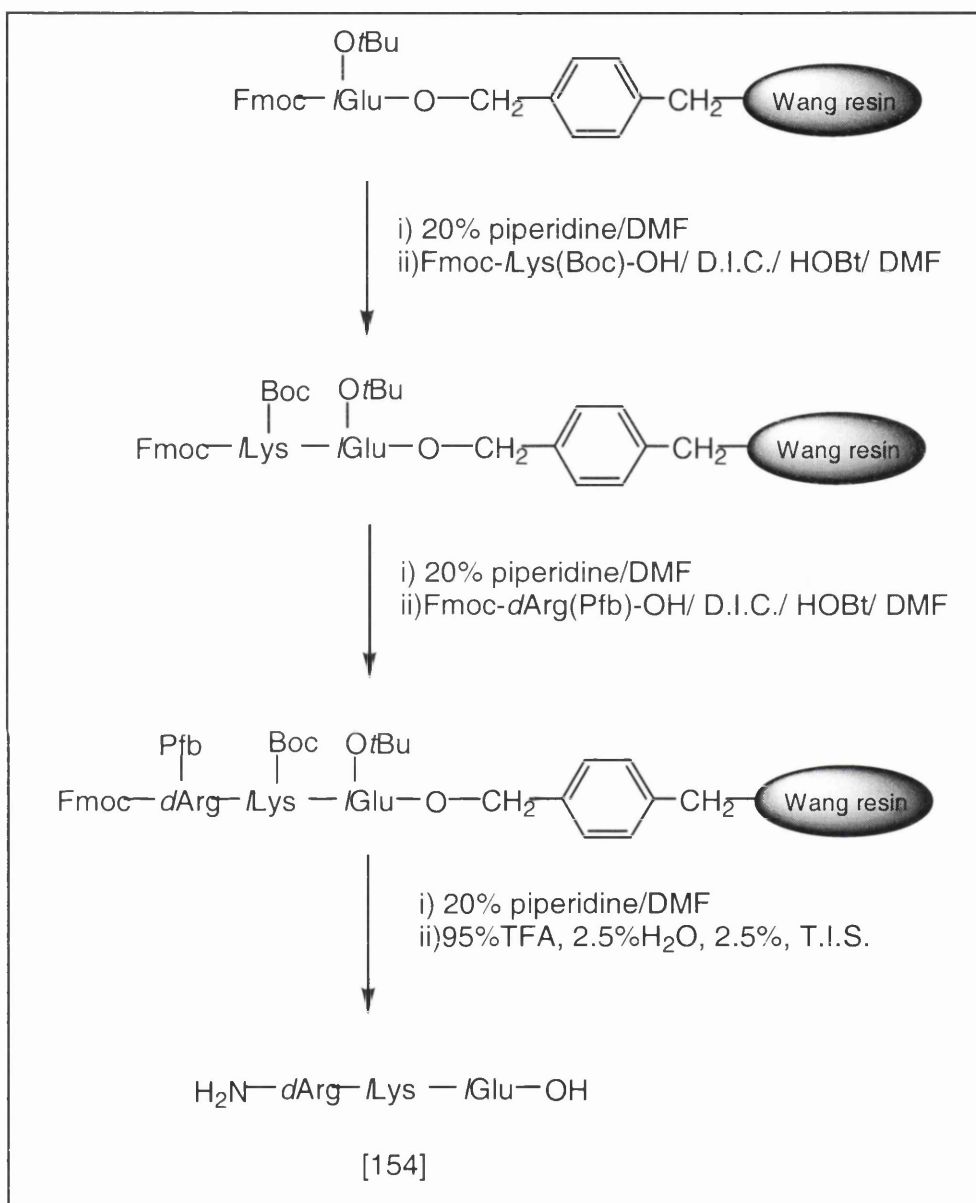
Second coupling: Fmoc-(L)Arg(Pfb)OH (0.878g, 1.9mmol, 2.5eq) as a solution in DMF (20mL) was added followed by HOBt/DMF (0.5M, 3.7mL, 1.9mmol, 2.5eq), and DIC/DMF (0.5M, 3.7mL, 1.9mmol, 2.5eq). The reaction was bubbled at room temperature for 17h after which time the Kaiser test indicated complete reaction of the resin bound free amine. The resin was then washed with DMF (5x30mL).

Fmoc removal: The resin was bubbled with 20% piperidine/DMF (30mL) for 3min, drained, a further 20% piperidine/DMF (30mL) was bubbled for 20min and the reaction solution then removed. The resin was washed with DMF (5x30mL). The Kaiser test indicated the presence of free resin bound amine groups.

Cleavage from the resin and protecting group removal: The resin was transferred to a round bottomed flask at 0°C and a solution of 95% TFA, 2.5% H₂O, 2.5% T.I.S. (30mL) was added. The suspension was stirred for 2.25h during which time the reaction was allowed to come to room temperature. The resin was filtered off and the filtrate concentrated *in vacuo* and azeotroped with toluene. The resultant semi-solid was triturated with diethyl ether (3x20mL) to afford a near white solid. This was taken up in water (100mL) and freeze dried to afford the TFA salt of H₂N-(L)Arg-(D)Lys-(L)Glu-OH [153] as a very pale yellow flocculent solid (402.3mg, 0.52mmol, 69%). Preparative HPLC (elution of CH₃CN/H₂O (0.1%TFA), solvent gradient 1-50%CH₃CN over 11min, flow rate 8mL/min).was used to purify samples for analysis.



^1H NMR (90% $\text{H}_2\text{O}/\text{D}_2\text{O}$, 500MHz) $\delta_{\text{H}}/\text{ppm}$: 8.82 (1H, d, J 7.0Hz, CONH), 8.48 (1H, d, J 7.5Hz, CONH), 7.50 (1H, s(br), NH), 7.27 (1H, t, J 5.0Hz, NH-C(=NH)NH_2), 6.69 (1H, s(br), NH), 4.41-4.32 (2H, m, 2- H , 3- H), 4.05 (1H, t, J 6.5Hz, 1- H), 3.21 (2H, q, J 6.5Hz, $\text{CH}_2\text{NHC(=NH)}$), 3.08-2.96 (2H, m, CH_2N), 2.46 (2H, t, J 7.0Hz, $\text{CH}_2\text{CO}_2\text{H}$), 2.22-2.15 (1 H , m, 4- CH), 2.03-1.58 (9H, m, CH_2), 1.47-1.31 (2H, m, CH_2). **^{13}C NMR** (90% $\text{H}_2\text{O}/\text{D}_2\text{O}$, 100MHz) $\delta_{\text{C}}/\text{ppm}$: 177.8 (CO_2H), 175.6 (CO_2H), 173.9 (CONH), 170.2 (CONH), 157.3 (C=N), 54.4 (CHN), 53.5 (CHN), 53.0 (CHN), 40.8 (CH_2N), 39.6 (CH_2N), 31.0 (CH_2), 30.7 (CH_2), 28.5 (CH_2), 27.0 (CH_2), 26.1 (CH_2), 24.2 (CH_2), 22.6 (CH_2). **LRMS** (FAB) m/z : 454 (5%, $[\text{M}+\text{Na}]^+$), 432 (100%, $[\text{M}+\text{H}]^+$), 386 (6%, $[\text{M}-\text{CO}_2]$), 174 (4%, ArgOH). **HRMS**: $[\text{M}+\text{H}]^+$ Calc 432.2571, Measured: 432.2578.

6.2 Synthesis of H₂N-(D)Arg-(L)Lys-(L)Glu-OH [154]

Fmoc removal: Fmoc-(L)Glu(OtBu)-Wang Resin (0.51mmolg⁻¹, 1.47g, 0.75mmol) was swelled with DMF (3x30mL). The resin was bubbled with 20% piperidine/DMF (30mL) for 3min, drained, a further 20% piperidine/DMF (30mL) was bubbled for 20min and the reaction solution then removed. The resin was washed with DMF (5x30mL).

First coupling: Fmoc-(L)Lys(Boc)OH (0.878g, 1.9mmol, 2.5eq) as a solution in DMF (20mL) was added followed by HOBt/DMF (0.5M, 3.7mL, 1.9mmol, 2.5eq), and DIC/DMF (0.5M, 3.7mL, 1.9mmol, 2.5eq). The reaction was bubbled at room temperature for 2h after which time the Kaiser test indicated complete reaction of the resin bound free amine. The resin was then washed with DMF (3x30mL).

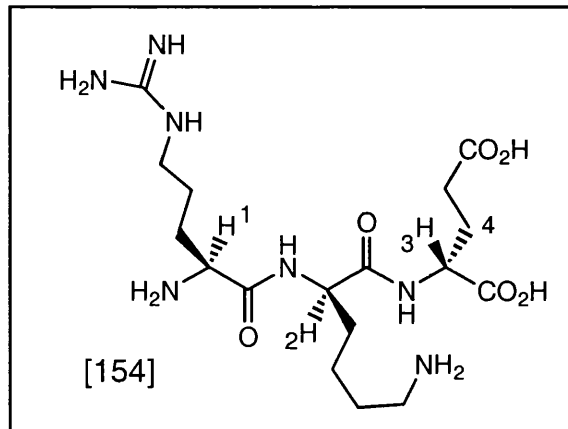
Fmoc removal: The resin was bubbled with 20% piperidine/DMF (30mL) for 3min, drained, a further 20% piperidine/DMF (30mL) was bubbled for 20min and the reaction solution then removed. The resin was washed with DMF (5x30mL). The Kaiser test indicated the presence of free resin bound amine groups.

Second coupling: Fmoc-(D)Arg(Pfb)OH (0.878g, 1.9mmol, 2.5eq) as a solution in DMF (20mL) was added followed by HOBt/DMF (0.5M, 3.7mL, 1.9mmol, 2.5eq), and DIC/DMF (0.5M, 3.7mL, 1.9mmol, 2.5eq). The reaction was bubbled at room temperature for 17h after which time the Kaiser test indicated complete reaction of the resin bound free amine. The resin was then washed with DMF (5x30mL).

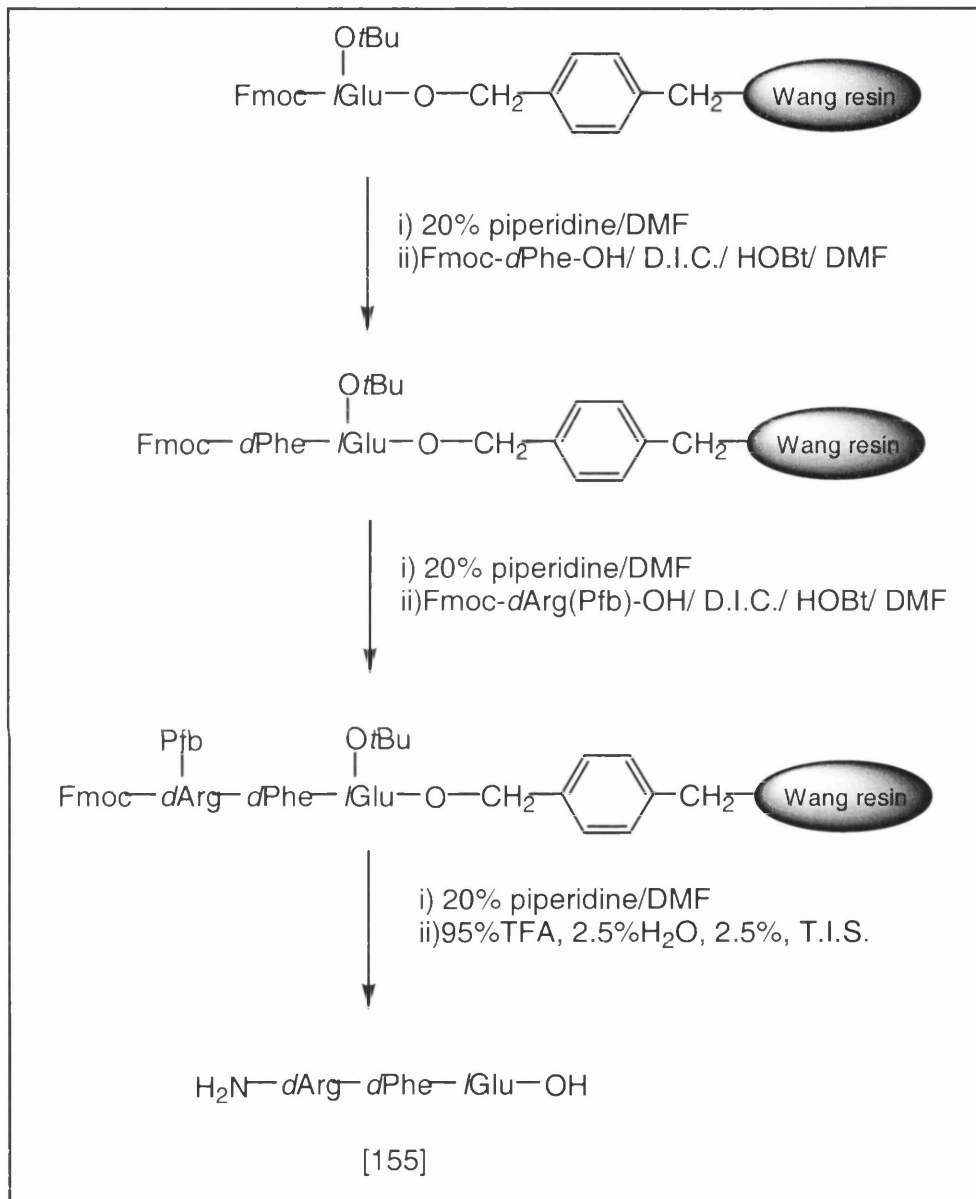
Fmoc removal: The resin was bubbled with 20% piperidine/DMF (30mL) for 3min, drained, a further 20% piperidine/DMF (30mL) was bubbled for 20min and the reaction solution then removed. The resin was washed with DMF (5x30mL). The Kaiser test indicated the presence of free resin bound amine groups.

Cleavage from the resin and protecting group removal: The resin was transferred to a round bottomed flask at 0°C and a solution of 95% TFA, 2.5% H₂O, 2.5% T.I.S. (30mL) was added. The suspension was stirred for 2.5h over which time the reaction was allowed to come to room temperature. The resin was filtered off and the filtrate concentrated *in vacuo* and azeotroped with toluene. The resultant semi-solid was triturated with diethyl ether (3x20mL) to afford a near white solid. This was taken up in water (100mL) and freeze dried to afford the TFA salt of H₂N-(D)Arg-(L)Lys-(L)Glu-OH [154] as a very pale yellow flocculent solid (414.2mg, 0.54mmol, 71%). Preparative HPLC (elution of CH₃CN/H₂O (0.1%TFA), solvent

gradient 1-50%CH₃CN over 11min, flow rate 8mL/min).was used to purify samples for analysis.



¹H NMR (90% H₂O/D₂O, 500MHz) δ_{H} /ppm: 8.78 (1H, d, J6.5Hz, CONH), 8.34 (1H, d, J7.5Hz, CONH), 7.43 (1H, s(br), NH), 7.19 (1H, t, J5.5Hz, NH-C(=NH)NH₂), 6.85 (1H, s(br), NH), 4.29-4.19 (2H, m, 2-H, 3-H), 3.93 (1H, t, J6.5Hz, 1-H), 3.12 (2H, q, J6.0Hz, CH₂NHC(=NH)), 2.88 (2H, m, CH₂N), 2.35 (2H, td, J7.5Hz, J2.0Hz, CH₂CO₂H), 2.09 (1H, m, 4-CH₂), 1.89-1.51 (9H, m, CH₂), 1.33 (2H, m, CH₂). **¹³C NMR** (90% H₂O/D₂O, 100MHz) δ_{C} /ppm: 177.6 (CO₂H), 175.9 (CO₂H), 173.4 (CONH), 169.7 (CONH), 157.0 (C=N), 55.5 (CHN), 54.1 (CHN), 53.1 (CHN), 40.5 (CH₂N), 39.4 (CH₂N), 30.7 (CH₂), 30.4 (CH₂), 28.2 (CH₂), 26.6 (CH₂), 26.2 (CH₂), 23.9 (CH₂), 22.2 (CH₂). **LRMS** (FAB) m/z: 454 (5%, [M+Na]⁺), 432 (100%, [M+H]⁺), 386 (6%, [M-CO₂]), 174 (4%, ArgOH). **HRMS**: [M+H]⁺ Calc 432.2571, Measured: 432.2578.

6.1. Synthesis of H₂N-(D)Arg-(D)Phe-(L)Glu-OH [155]

Fmoc removal: Fmoc-(L)Glu(OtBu)-Wang Resin (0.51mmolg⁻¹, 1.47g, 0.75mmol) was swelled with DMF (3x30mL). The resin was bubbled with 20% piperidine/DMF (30mL) for 3min, drained, a further 20% piperidine/DMF (30mL) was bubbled for 20min and the reaction solution then removed. The resin was washed with DMF (5x30mL).

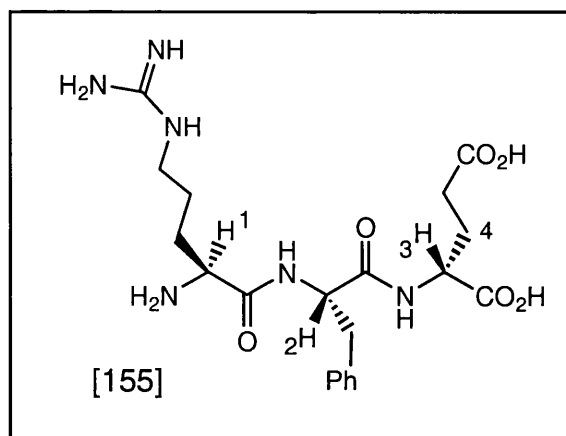
First coupling: Fmoc-(D)Phe-OH (0.726g, 1.9mmol, 2.5eq) as a solution in DMF (20mL) was added followed by HOBt/DMF (0.5M, 3.7mL, 1.9mmol, 2.5eq), and DIC/DMF (0.5M, 3.7mL, 1.9mmol, 2.5eq). The reaction was bubbled at room temperature for 2h after which time the Kaiser test indicated complete reaction of the resin bound free amine. The resin was then washed with DMF (3x30mL).

Fmoc removal: The resin was bubbled with 20% piperidine/DMF (30mL) for 3min, drained, a further 20% piperidine/DMF (30mL) was bubbled for 20min and the reaction solution then removed. The resin was washed with DMF (5x30mL). The Kaiser test indicated the presence of free resin bound amine groups.

Second coupling: Fmoc-(D)Arg(Pfb)OH (0.878g, 1.9mmol, 2.5eq) as a solution in DMF (20mL) was added followed by HOBt/DMF (0.5M, 3.7mL, 1.9mmol, 2.5eq), and DIC/DMF (0.5M, 3.7mL, 1.9mmol, 2.5eq). The reaction was bubbled at room temperature for 17h after which time the Kaiser test indicated complete reaction of the resin bound free amine. The resin was then washed with DMF (5x30mL).

Fmoc removal: The resin was bubbled with 20% piperidine/DMF (30mL) for 3min, drained, a further 20% piperidine/DMF (30mL) was bubbled for 20min and the reaction solution then removed. The resin was washed with DMF (5x30mL). The Kaiser test indicated the presence of free resin bound amine groups.

Cleavage from the resin and protecting group removal: The resin was transferred to a round bottomed flask at 0°C and a solution of 95% TFA, 2.5% H₂O, 2.5% T.I.S. (30mL) was added. The suspension was stirred for 2.75h during which time the reaction was allowed to come to room temperature. The resin was filtered off and the filtrate concentrated *in vacuo* and azeotroped with toluene. The resultant semi-solid was triturated with diethyl ether (3x20mL) to afford a near white solid. This was taken up in water (100mL) and freeze dried to afford the TFA salt of H₂N-(D)Arg-(D)Phe-(L)Glu-OH [155] as a white flocculent solid (428.5mg, 0.63mmol, 84%). Analytical HPLC (elution of CH₃CN/H₂O (0.1%TFA), solvent gradient 1-90% CH₃CN over 30min, flow rate 1mL/min) indicated a single compound.



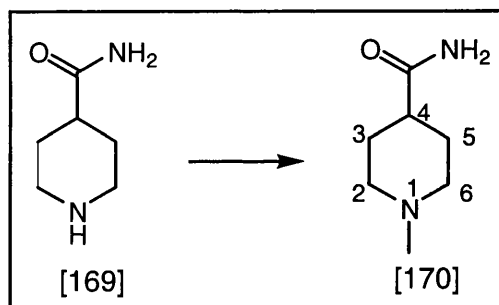
^1H NMR (90% $\text{H}_2\text{O}/\text{D}_2\text{O}$, 500MHz) $\delta_{\text{H}}/\text{ppm}$: 8.74 (1H, d, J 7.0Hz, CONH), 8.21 (1H, d, J 7.5Hz, CONH), 7.24-6.97 (5H, m, ArH), 6.81 (1H, t, J 7.5Hz, $\text{NHC}(=\text{NH})\text{NH}_2$), 6.52 (1H, s(br), NH), 4.54 (1H, dt, J 10.0Hz, 6.8Hz, 2-H), 4.10-4.08 (1H, m, 1-H), 3.89 (1H, t, J 6.0Hz, 3-H), 3.02 (2H, q, J 6.5Hz, $\text{CH}_2\text{NH-C}=\text{NH}$), 3.01 (1H, dd, J 13.5Hz, 6.8Hz, CH_2Ph), 2.85 (1H, dd, J 13.5Hz, 10.0Hz, CH_2Ph), 1.81-0.88 (8H, m, CH_2). ^{13}C NMR (90% $\text{H}_2\text{O}/\text{D}_2\text{O}$, 75MHz) $\delta_{\text{C}}/\text{ppm}$: 180.0 (CO_2H), 178.0 (CO_2H), 175.2 (CONH), 172.0 (CONH), 159.8 ($\text{C}=\text{N}$), 138.6 (ArC), 132.1 (ArC), 131.8 (ArC), 130.4 (ArC_{ipso}), 58.2 (CHN), 55.6 (CHN), 55.1 (CHN), 43.4 (CH_2Ph), 40.1 (CH_2N), 32.4 (CH_2), 31.0 (CH_2), 28.6 (CH_2), 26.2 (CH_2). LRMS (FAB) m/z : 473 (15%, $[\text{M}+\text{Na}]^+$), 451 (100%, $[\text{M}+\text{H}]^+$), 405 (10%, $[\text{M}-\text{CO}_2]$), 347 (15%), 276 (17%, $[\text{M}-\text{Arg}]$). HRMS: $[\text{M}+\text{H}]^+$: Calc 451.2305, Measured 451.2299.

Chapter 7. SYNTHESIS AND ANALYSIS OF POLYACRYLAMIDE

MIPs

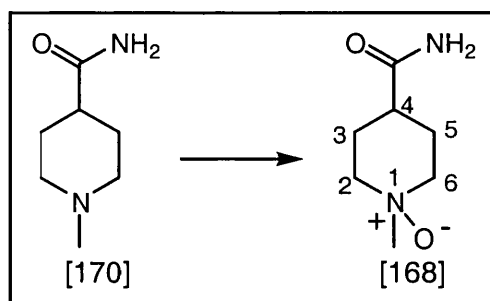
7.1 SYNTHESIS OF IMPRINT MOLECULE [168].

7.1.1 Synthesis of *N*-methyl isonipecotamide [170]¹³⁸.



35-37% w/v Formaldehyde solution (6.4mL, 56mmol, 1.2eq) was added dropwise at room temperature to a stirred solution of isonipecotamide [169] (6.0g, 47mmol, 1eq) in methanol (30mL). The reaction was stirred at room temperature for 3h. RaneyTM Nickel was added as a 50% slurry in water (3 portions ca 0.5mL each), the flask was flushed with hydrogen and then left under a hydrogen balloon with stirring for 18h. The reaction mixture was filtered over florasilTM, washed with methanol (3x50mL) and concentrated *in vacuo* to give the crude product (6.18g) as a white solid. Recrystallisation from EtOH/Et₂O afforded white crystals of *N*-methyl isonipecotamide [170] (5.11g, 36mmol, 64%).

m.p.: (EtOH/Et₂O) dcmp 190-194°C. **¹H NMR** (CD₃OD, 400MHz) δ_H/ppm: 2.90 (2H, d(br), J12.0Hz, NCH_{eq}), 2.25 (3H, s, NCH₃), 2.20 (1H, tt, J11.5Hz, 3.0Hz, R₃CH), 2.04 (2H, td, J12.0Hz, 3.0Hz, NCH_{ax}), 1.83-1.67 (4H, m, 5-, 3-CH₂). **¹³C NMR** (CD₃OD, 75MHz) δ_C/ppm: 180.5 (C=O), 64.1 (NCH₂), 46.3 (NCH₃), 42.8 (R₃CH), 29.6 (5-, 3-CH₂). **IR** (neat): ν_{max}/cm⁻¹: 3348 (s, NH), 3195 (m), 2939 (m), 2779 (m), 1664 (s, amide I), 1621 (s, amide II), 1428 (m), 1376 (m), 1229 (w), 1276 (m), 767 (w). **LRMS** (CI) m/z: 143 (65%, [M+H]⁺), 126 (100%, -CH₄). **HRMS:** [M+H]⁺, Calc 143.1184, Measured 143.1179.

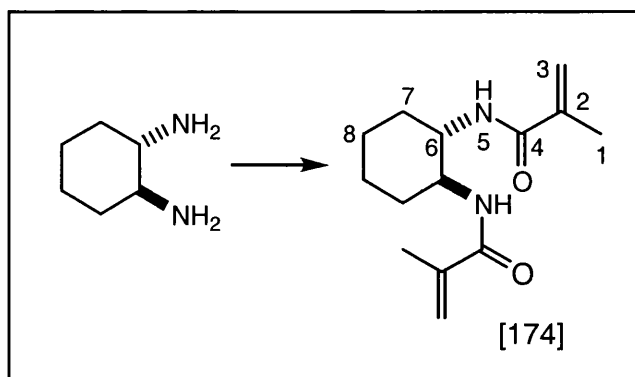
7.1.2. Synthesis of *N*-methyl isonipecotamide *N*-oxide [168].

A solution of mCPBA (>70%, 8.29g) in DCM:MeOH 4:1 (50mL) was added to a stirred solution of *N*-methyl isonipecotamide [170] (4.0g, 28mmol, 1eq) at 0°C. The reaction was allowed to come to room temperature and stirred for 18h over which time a white ppt. was observed. The reaction mixture was reduced *in vacuo*, the residue was taken up in methanol (20mL), passed over basic alumina and eluted with methanol (100mL). The filtrate was concentrated *in vacuo* and recrystallised from *i*-PrOH/EtOAc to afford *N*-methyl isonipecotamide *N*-oxide [168] (2.65g, 17mmol, 60%).

m.p.: (*i*-PrOH/EtOAc) dcmp 184-186°C. **¹H NMR** (D₂O, 500MHz) δ_H/ppm: 3.28-3.18 (4H, m, NCH₂) 3.06 (3H, s, NCH₃), 2.37 (1H, tt, J12.0Hz, 4.0Hz, R₃CH), 2.06 (2H, qd, J14.5Hz, 4.5Hz, 5-, 3-CH_{ax}), 1.75 (2H, d(br), J14.0Hz, 5-3-CH₂). **¹³C NMR** (CD₃OD, 75MHz) δ_C/ppm: 178.9 (C=O), 66.2 (NCH₂), 60.8 (NCH₂), 40.7 (R₃CH), 24.8 (R₂CH₂). **IR** (neat): ν_{max}/cm⁻¹: 3068 (m), 1681 (s, amide I), 1554 (s), 1449 (s), 1412 (s), 1382 (m), 1247 (m), 985 (m), 720 (m). **LRMS** (FAB) m/z: 181 (21%, [M+Na]⁺), 159 (100%, [M+H]⁺), 141 (51%, -O), 127 (10%) **HRMS:** [M+H]⁺, Calc 159.1134, Measured 159.1130.

7.2 SYNTHESIS OF CROSSLINKERS AND MONOMERS.

7.2.1. Synthesis of (+/-)-*N,N*-dimethacryloyl-*trans*-(1, 2)-diaminocyclohexane [174].

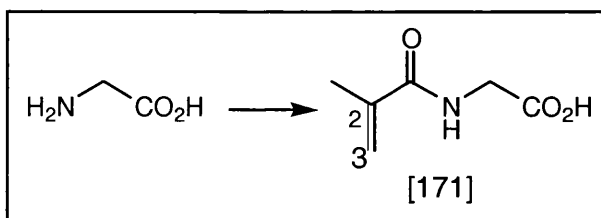


Preparation of methacryloyl chloride: A solution of distilled thionyl chloride (27.4mL, 0.38mol, 2.5eq), methacrylic acid (31.8mL, 0.38mol, 2.5eq) in chloroform (250mL) was refluxed for 14h, then cooled to room temperature.

Acylation of 1, 2-diaminocyclohexane: A solution of 1, 2-diaminocyclohexane (18.0mL, 0.15mol, 1eq) and NaOH (36.0g, 0.90mol, 6eq) in water (100mL) was stirred at 0°C. The solution of methacryloyl chloride prepared above was added dropwise via a cannula over 1h maintaining the temperature at 0°C. The reaction was allowed to come to room temperature and stirred for a further hour. The aqueous and organic layers were separated. The organic layer was washed with 1M HCl aq. (100mL), dried over MgSO₄(s) and concentrated *in vacuo* to afford the crude product (35.1g) as an off white solid. Recrystallisation from DCM yielded white needles of (+/-)-*N,N*-dimethacryloyl-*trans*-(1, 2)-diaminocyclohexane [174] (27.0g, 0.11mol, 72%).

m.p.: (DCM) 207-208°C. ¹H NMR (CDCl₃, 400MHz) δ_H/ppm: 6.70 (2H, s(br), NH), 5.64 (2H, s(br), 3-H), 5.23 (2H, s, 3-H), 3.67 (2H, s(br), NCH), 1.98 (2H, m, 10-, 7-H), 1.86 (6H, s, CH₃), 1.84 (2H, m, 10-, 7-H), 1.25 (4H, m, CH₂). ¹³C NMR (CDCl₃, 75MHz) δ_C/ppm: 168.9 (C=O), 139.5 (2-C), 119.8 (3-C), 53.8 (NCH), 31.9 (CH₂), 24.6 (CH₂), 18.4 (CH₃). **IR** (neat): ν_{max}/cm⁻¹: 3324 (s, NH), 2934 (s), 2858 (m), 1654 (s, amide I), 1617 (s, C=C), 1538 (s, amide II), 1455 (m), 1373 (w), 1327 (w), 1220 (w), 1103 (w), 922 (m). **LRMS** (FAB) m/z: 273 (7%, [M+Na]⁺), 251 (100%, [M+H]⁺), 166 (50%), 133 (40%).

7.2.2. Synthesis of *N*-methacryloyl glycine [171].

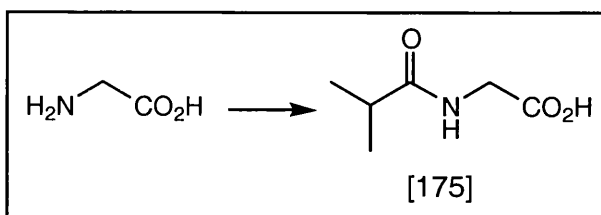


Preparation of methacryloyl chloride: A solution of distilled thionyl chloride (1.0mL, 13.5 mmol, 1eq) and methacrylic acid (1.1mL, 13.5mmol, mol, 1eq) in chloroform (25mL) was refluxed for 14h, then cooled to 0°C.

Acylation of glycine: A solution of glycine (1.0g, 13.5mmol, 1eq) in 5M NaOH aq. (18mL, 4eq) was stirred at 0°C. The solution of methacryloyl chloride prepared above was added dropwise with stirring over 5min. The reaction was allowed to come to room temperature and stirred for 30min. The aqueous and organic layers were separated and the aqueous layer was washed with diethyl ether (3x25mL). The aqueous layer was acidified to pH~2 with 5M HCl aq. and extracted with diethyl ether (3x25mL). These extracts were dried over MgSO₄(s) and concentrated *in vacuo* to afford *N*-methacryloyl glycine [171] as a white solid (1.16g, 8.1mmol, 60%).

m.p.(DCM/ether): 108-109°C. **¹H NMR** (D₂O, 300MHz) δ_H/ppm: 5.80 (1H, s, =CH₂), 5.52 (1H, s, =CH₂), 4.04 (2H, s, CH₂), 1.96 (3H, s, CH₃). **¹³C NMR** (D₂O, 75MHz) δ_C/ppm: 173.4 (C=O acid), 171.9 (C=O), 138.2 (2-C), 122.0 (3-C), 41.2 (CH₂), 17.5 (CH₃). **IR** (KBr): ν_{max}/cm⁻¹: 3361 (s, NH), 2937 (s, b), 2714 (s), 2601 (s), 2519 (s), 1757 (s, C=O acid), 1659 (s, amide I), 1587 (s, amide II), 1444(s), 1407 (s), 1331 (s), 1199 (s), 1027 (m), 894 (s). **LRMS** (FAB) m/z: 166 (20%, [M+Na]⁺), 144 (100%, [M+H]⁺), 126 (10%), 116 (5%), 109 (10%).

7.2.3 Synthesis of *N*-(2-methyl)-propanoyl glycine [175]¹³⁹.

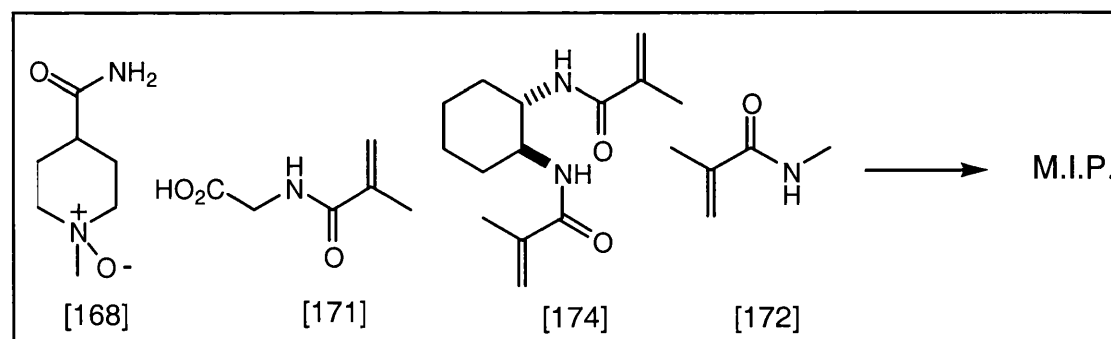


To a stirred suspension of glycine (1.0g, 13.3mmol, 1eq) and $K_2CO_3(s)$ (30g) in diethyl ether was added isobutyryl chloride (15.0g, 14.7mL, 14.7mmol, 1.1eq). The reaction was heated at reflux for 24h then cooled to room temperature and concentrated *in vacuo*. The solid was dissolved in 2M HCl aq. (to pH~2) and then continuously extracted with diethyl ether for 24h. The diethyl ether extract was cooled to room temperature and the white needles which formed were filtered off to afford *N*-(2-methyl)-propanoyl glycine [175] (386mg, 2.7mmol, 20%).

m.p.: (Diethyl ether) 107°C (lit 103-104°C). 1H NMR ($CDCl_3$, 300MHz) δ_H/ppm : 6.14 (1H, s(br), \underline{NH}), 4.07 (2H, d, $J_{5.0Hz}$, $\underline{CH_2}$), 2.45 (1H, m, $J_{7.0Hz}$, $(CH_3)_2\underline{CH}$), 1.17 (6H, d, J_{7Hz} , $\underline{CH_3}$). ^{13}C NMR (D_2O , 75MHz) δ_C/ppm : 182.7 ($\underline{CO_2H}$), 174.7 ($\underline{CONH_2}$), 42.1 ($\underline{CH_2}$), 35.8 (\underline{CH}), 19.5 ($\underline{CH_3}$). **IR** (film): ν_{max}/cm^{-1} : 3358 (s, NH), 2940 (m), 1740 (s, C=OOH), 1650 (s, amide I), 1586 (s, C=C), 1544 (s, amide II), 1441 (w), 1403 (m), 1332 (w), 1198 (s), 1026 (w), 895 (w). **LRMS** (FAB) m/z : 168 (25%, $[M+Na]^+$), 146 (100%, $[M+H]^+$), 137 (15%), 128 (7%), 107 (7%). **HRMS**: $[M+H]^+$, Calc 146.0817, Measured 146.0823.

7.3 SYNTHESIS OF THE POLYACRYLAMIDE MIPs.

7.3.1 General Procedure for the synthesis of polyacrylamides with (+/-)-*N*, *N*-dimethacryloyl-*trans*-(1, 2)-diaminocyclohexane [174] as crosslinker.



N-methyl methacrylamide, (+/-)-*N*, *N*-dimethacryloyl-*trans*-(1, 2)-diaminocyclohexane [174], *N*-methacryloyl glycine [171], *N*-methyl isonipecotamide *N*-oxide [168] and

AIBN (2mol% per polymerisable double bond) in methanol (2.5 v/v of polymerisable molecules) were placed in a schlenk flask of diameter 3.0cm. Two freeze thaw cycles were carried out and the polymerisation mixture was placed in a preheated bath and incubated at 60°C for 24h. The flask was cooled to room temperature and the solvent removed under vacuum. The resultant polymer monolith was ground.

7.3.2 Synthesis of Polyacrylamide [G]. Loading: 1/10, Crosslinker-monomer ratio 2:1.

N-methyl methacrylamide [172] (157mg, 160µL, 1.6mmol), (+/-)-*N*, *N*-dimethacryloyl-*trans*-(1, 2)-diaminocyclohexane [174] (791mg, 3.2mmol), *N*-methacryloyl glycine [171] (68mg, 0.48mmol), *N*-methyl isonipecotamide *N*-oxide [168] (75mg, 0.48mmol) and AIBN (26mg) in methanol (2.38ml) were polymerised according to the general procedure.

7.3.3. Synthesis of Polyacrylamide [H]. Loading: 1/10, Crosslinker-monomer ratio 6:1.

N-methyl methacrylamide [172] (67mg, 70µL, 0.7mmol), (+/-)-*N*, *N*-dimethacryloyl-*trans*-(1, 2)-diaminocyclohexane [174] (1.02g, 4.1mmol), *N*-methacryloyl glycine [171] (68mg, 0.48mmol), *N*-methyl isonipecotamide *N*-oxide [168] (75mg, 0.48mmol) and AIBN (30mg) in methanol (2.73mL) were polymerised according to the general procedure.

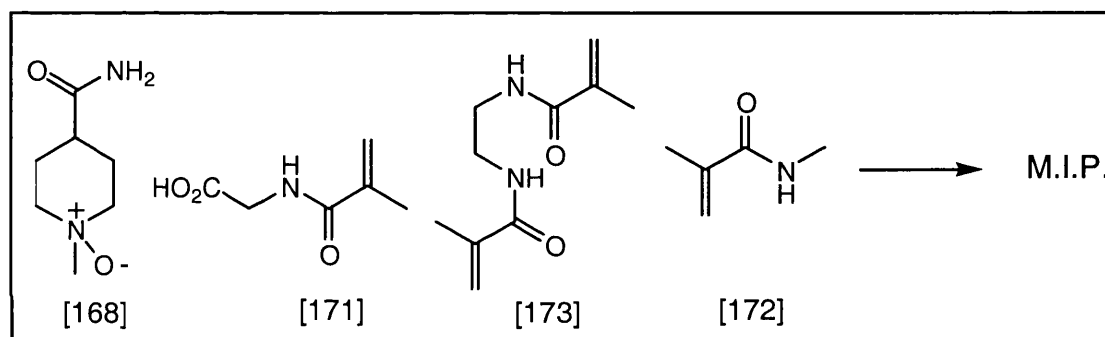
7.3.4 Synthesis of Polyacrylamide [I]. Loading: 1/7, Crosslinker-monomer ratio 6:1.

N-methyl methacrylamide [172] (125mg, 129µL, 1.3mmol), (+/-)-*N*, *N*-dimethacryloyl-*trans*-(1, 2)-diaminocyclohexane [174] (1.90g, 7.6mmol), *N*-methacryloyl glycine [171] (181mg, 1.3mmol), *N*-methyl isonipecotamide *N*-oxide [168] (200mg, 1.3mmol) and AIBN (54mg) in methanol (5.0mL) were polymerised according to the general procedure.

7.3.5. Synthesis of Polyacrylamide [J]. Loading: 1/35, Crosslinker-monomer ratio 6:1.

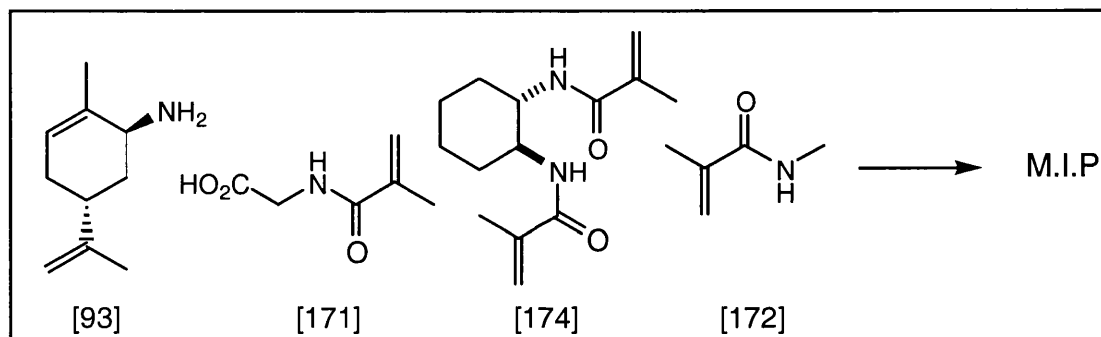
N-methyl methacrylamide [172] (157mg, 162 μ L, 1.6mmol), (+/-)-*N,N*-dimethacryloyl-*trans*-(1, 2)-diaminocyclohexane [174] (2.37g, 9.5mmol), *N*-methacryloyl glycine [171] (45mg, 0.36mmol), *N*-methyl isonipecotamide *N*-oxide [168] (50mg, 0.36mmol) and AIBN (67.5mg) in methanol (6.3mL) were polymerised according to the general procedure.

7.3.6 Synthesis of Polyacrylamide [K] using *N,N'*-ethylene bisacrylamide [173] as crosslinker. Loading: 1/7, Crosslinker-monomer ratio 6:1.



N-methyl methacrylamide [172] (63mg, 64 μ L, 0.63mmol) *N,N'*-ethylene bisacrylamide [173] (639mg, 3.8mmol), *N*-methacryloyl glycine [171] (90.5mg, 0.63mmol), *N*-methyl isonipecotamide *N*-oxide [168] (100mg, 0.63mmol) and AIBN (27mg, 2mol% per polymerisable double bond) in methanol (3.35mL, 2.5 v/v of polymerisable molecules) were placed in a schlenk flask of diameter 3.0cm. Two freeze thaw cycles were carried out and the polymerisation mixture was placed in a preheated bath and incubated at 60°C for 24h. The flask was cooled to room temperature and the solvent removed under vacuum. The resultant polymer monolith was ground.

7.3.7 Synthesis of Polyacrylamide [L] using (1*R*, 5*R*)-*trans*-carvyl amine [93] as imprint molecule. Loading: 1/35, Crosslinker-monomer ratio 6:1.



N-methyl methacrylamide (157mg, 162 μ L, 1.6mmol), (+/-)-*N,N*-dimethacryloyl-*trans*-(1,2)-diaminocyclohexane [174] (2.37g, 9.5mmol), *N*-methacryloyl glycine [171] (45mg, 0.36mmol), *N*-methyl isonipecotamide *N*-oxide [168] (48mg, 0.36mmol) and AIBN (67.5mg, 2mol% per polymerisable double bonds) in methanol (6.3mL, 2.5 v/v of polymerisable molecules) were placed in a schlenk flask of diameter 3.0cm. Two freeze thaw cycles were carried out and the polymerisation mixture was placed in a preheated bath and incubated at 60°C for 24h. The flask was cooled to room temperature and the solvent removed under vacuum. The resultant polymer monolith was ground.

7.3.8. Optimised procedure for the washing and generation of acid sites in the crude polyacrylamides [G], [H], [I], [J], [L], and [M].

The ground crude polymer was placed in a sintered glass funnel and washed with chloroform (5x10mL) and methanol (5x10mL). The solvent was removed *in vacuo* and the residue analysed by ¹H NMR which identified AIBN decomposition products, trace amounts of unreacted reagents as determined by comparison with reference spectra, and *N*-methyl isonipecotamide *N*-oxide [168]. The polymer was washed with 10% Et₃N:MeOH (5x10mL), methanol (20mL) and then 10% AcOH:MeOH (5x10mL). The polymer was cleaned with methanol (4x50mL, or until pH 7). The polymer was then dried *in vacuo* to give the active polymer [G]*, [H]*, [I]*, [J]*, [K]* or [L]*.

Polymer [G]* 1/10 2:1 **Elemental analysis:** Found C 55.42, H 9.15, N 9.75.

Polymer [H]* 1/10 6:1 **Elemental analysis:** Found C 59.02, H 8.50, N 10.10.

Polymer [I]* 1/7 6:1 **Elemental analysis:** Found C 55.68, H 9.31, N 9.52.

Polymer [J]* 1/7 6:1 **Elemental analysis:** Found C 46.30, H 8.20, N 12.77.

Polymer [K]* 1/35 6:1 **Elemental analysis:** Found C 55.77, H 9.04, N 9.44.

Polymer [L]* 1/35 6:1 **Elemental analysis:** Found.C 55.44, H 9.07, N 9.18.

7.4 BINDING STUDIES ON THE POLYACRYLAMIDE MIPs

7.4.1 General Method for Binding Studies.

The apparatus used is described in 2.3.1.

The dried polymer [G]*, [H]*, [I]*, [J]*, [K]* or [L]* was placed in a sealed extraction thimble and suspended in a beaker containing a known quantity of methanol (60mL). The solution was stirred for 20min at 0°C, the level of the solvent was marked, and the thimble removed. The amount of solvent absorbed by the polymer was measured using the difference between the volume of methanol remaining and the original volume of methanol (60mL). *N*-methyl isonipecotamide *N*-oxide [168] (1eq) was then added to the beaker, the extraction thimble was suspended as before and methanol was added up to the mark* (*vide supra*). The solution was stirred and at specific intervals the thimble was removed, the solvent removed *in vacuo* and the quantity of *N*-methyl isonipecotamide *N*-oxide [168] remaining in solution was determined. After each measurement the *N*-methyl isonipecotamide *N*-oxide [168] was redissolved in methanol to the previously marked level.

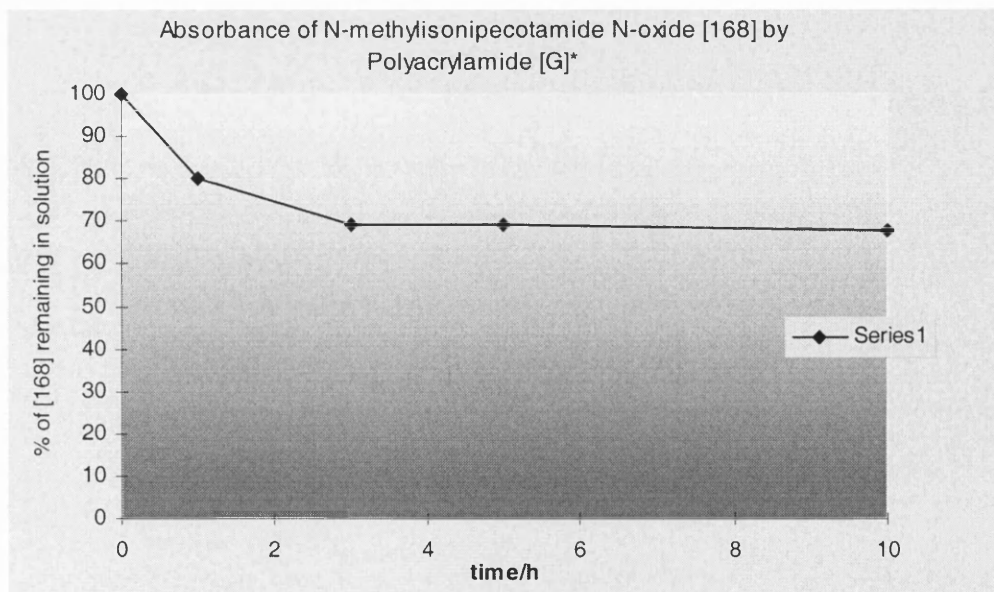
In the case of the polyacrylamide [L] which used (1*R*, 5*R*)-*trans*-carvyl amine [93] as the imprint molecule, the above procedure is the same except (1*R*, 5*R*)-*trans*-carvyl amine [93] is substituted for *N*-methyl isonipecotamide *N*-oxide [168] throughout.

* An important distinction between adding MeOH (60ml) and adding the solvent up to the mark is necessary here. The polymers absorb significant quantities of solvent which they retain for a considerable time. If one adds another (60ml) of solvent then there will be more solvent present due to preabsorbed MeOH in the polymer. In order to avoid lengthy drying procedures in between steps the marked level is used. This is the level at which the total of the MeOH absorbed in the polymer and in the rest of the beaker is equal to 60ml.

7.4.2 Binding study of Polyacrylamide [G]. Loading: 1/10, Crosslinker-monomer ratio 2:1.

The amount of methanol (5.6mL) absorbed by the polymer was determined according to the general method. *N*-methyl isonipecotamide *N*-oxide [168] (75mg, 0.48mmol, 1eq) was used in the binding study.

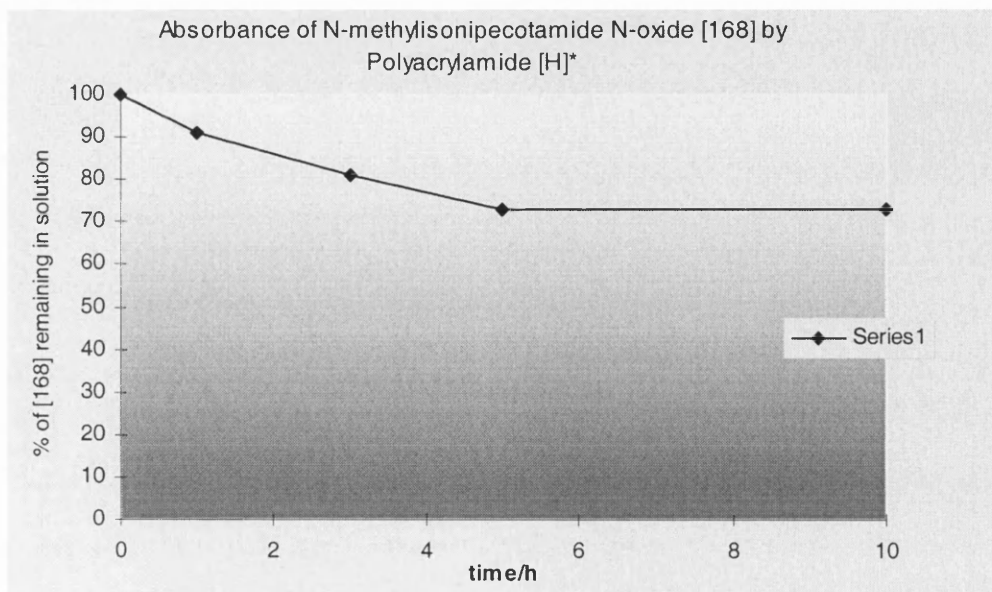
time/h	weight of [168] in solution /mg	% weight of [168] in solution Series 1
0	75	100
1	60	80
3	52	69
5	52	69
10	51	68



7.4.3 Binding Study of Polyacrylamide [H]. Loading: 1/10, Crosslinker-monomer ratio 6:1.

The amount of methanol (8.5mL) absorbed by the polymer was determined according to the general method. *N*-methyl isonipecotamide *N*-oxide [168] (75mg, 0.48mmol, 1eq) was used in the binding study.

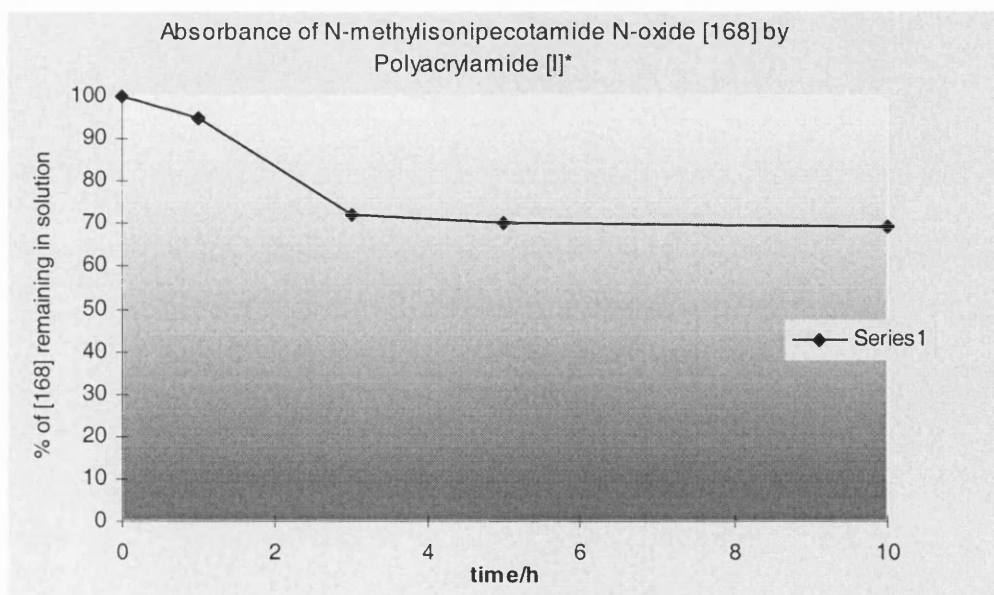
time/h	weight of [168] in solution /mg	% weight of [168] in solution Series 1
0	75	100
1	68	91
3	61	81
5	55	73
10	55	73



7.4.5 Binding Study of Polyacrylamide [I]. Loading: 1/7, Crosslinker-monomer ratio 6:1.

The amount of methanol (11.5mL) absorbed by the polymer was determined according to the general method. *N*-methyl isonipecotamide *N*-oxide [168] (200mg, 1.3mmol, 1eq) was used in the binding study.

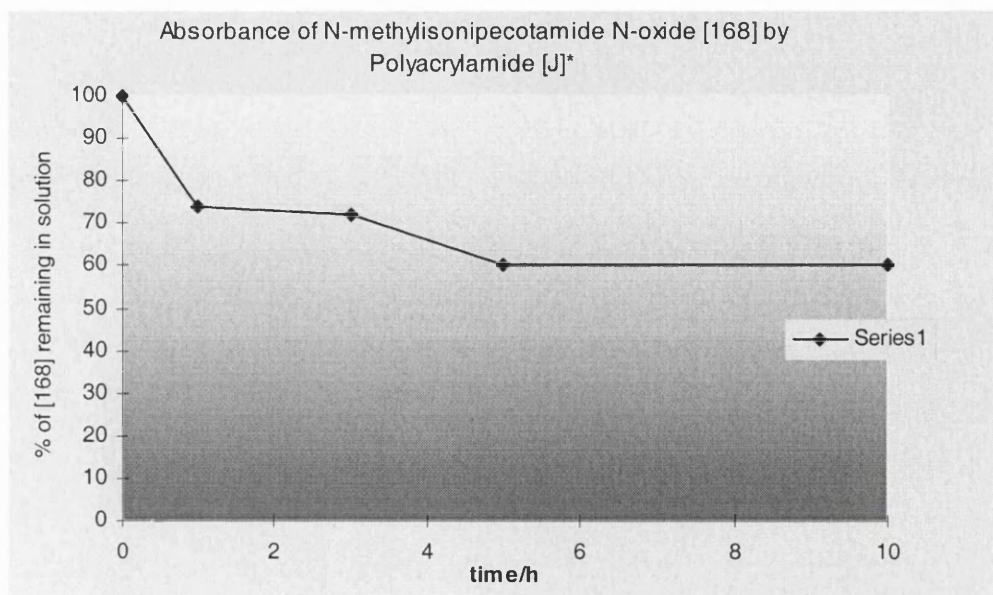
time/h	weight of [168] in solution /mg	% weight of [168] in solution Series 1
0	200	100
1	189	95
3	144	72
5	139	70
10	138	69



7.4.6 Binding Study of Polyacrylamide [J]. Loading: 1/35, Crosslinker-monomer ratio 6:1.

The amount of methanol (17.0mL) absorbed by the polymer was determined according to the general method. *N*-methyl isonipecotamide *N*-oxide [168] (50mg, 0.36mmol, 1eq) was used in the binding study.

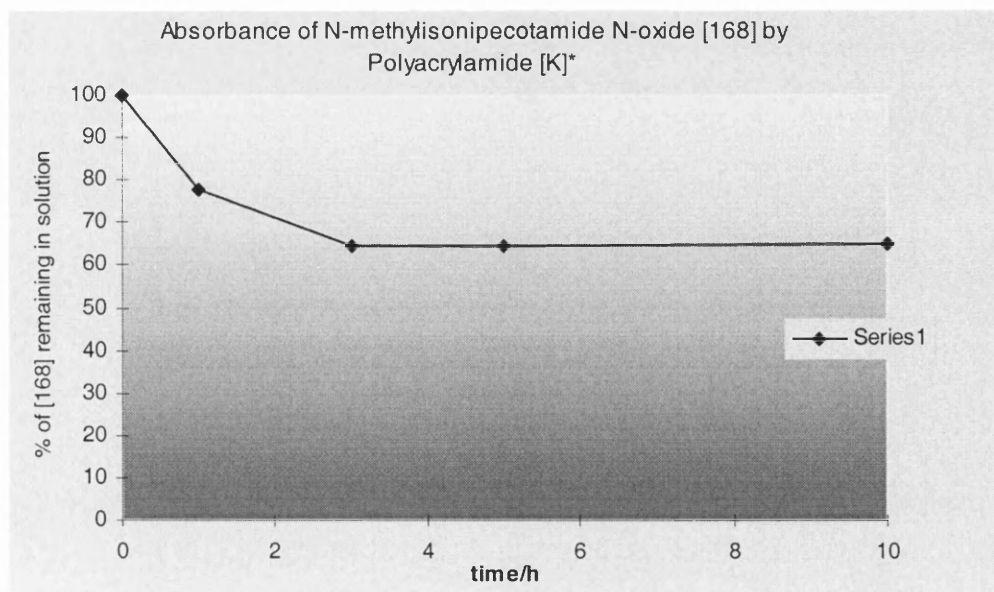
time/h	weight of [168] in solution /mg	% weight of [168] in solution Series 1
0	50.0	100
1	37.2	74
3	36.0	72
5	30.0	60
10	30.0	60



7.4.7. Binding Study of Polyacrylamide [K] using N,N'-ethylene bisacrylamide as crosslinker. Loading: 1/7, Crosslinker-monomer ratio 6:1.

The amount of methanol (10.0mL) absorbed by the polymer was determined according to the general method. *N*-methyl isonipecotamide *N*-oxide [168] (100mg, 0.63mmol, 1eq) was used in the binding study.

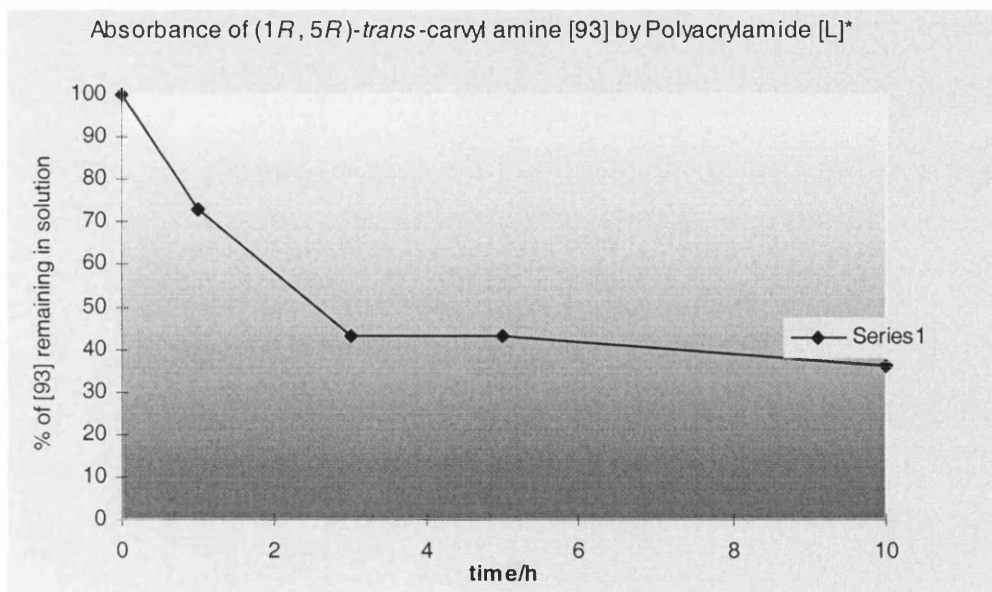
time/h	weight of [168] in solution /mg	% weight of [168] in solution Series 1
0	100	100
1	77.5	77.5
3	64.5	64.5
5	64.5	64.5
10	65.0	65.0



7.4.8. Binding Study of Polyacrylamide [L] using (1*R*, 5*R*)-*trans*-carvyl amine [93] as imprint molecule. Loading: 1/35, Crosslinker-monomer ratio 6:1.

The amount of methanol (15.0mL) absorbed by the polymer was determined according to the general method. (1*R*, 5*R*)-*trans*-carvyl amine [93] (65mg, 0.43mmol, 1eq) was used in the binding study.

time/h	weight of [168] in solution /mg	% weight of [168] in solution Series 1
0	65.0	100
1	47.4	73
3	28.0	43
5	28.0	43
10	23.4	36



7.4.9. General method for polyacrylamide regeneration.

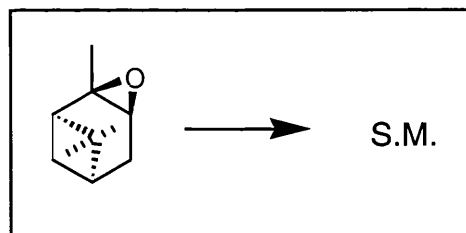
The apparatus used was the same as for the binding studies 5.1.3. The polymer was washed with methanol (2x60mL/1h/0°C) to and then stirred with 10% HOAc:methanol (60mL/1h/0°C) to regenerate the acid sites. The polymer was washed with methanol (nx60mL until pH neutral) and dried under vacuum.

Chapter 8. REACTIONS OF POLYACRYLAMIDE POLYMERS

8.1 SOLUTION REACTIONS OF *N*-(2-methyl)-propanoyl glycine [175] WITH α -PINENE OXIDE [89].

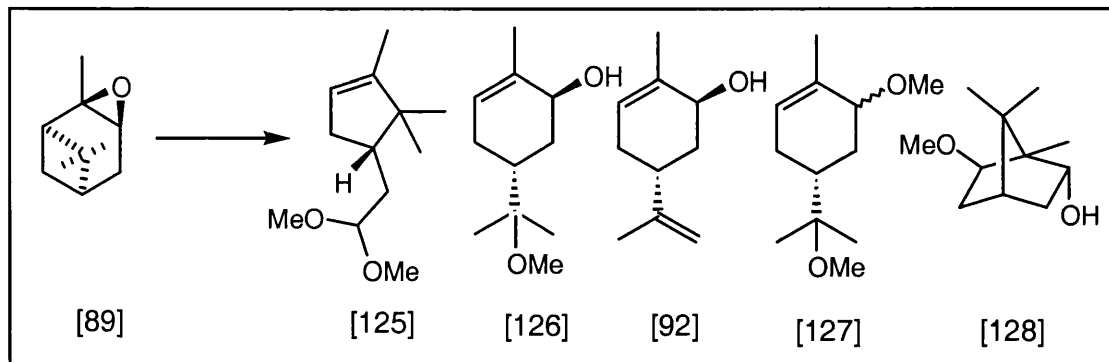
Products were identified by comparison with authentic samples used as standards for G.C. analysis of the M.I.P. catalysed reactions. Typical conditions were: flow rate 100mL/min, column head pressure 7.5psi, initial temperature 100°C, final temperature 200°C, initial time 2.0min and rate 5.0°C/min. Injections were 0.1 μ L.

8.1.1 Reaction of α -pinene oxide [89] with *N*-(2-methyl)-propanoyl glycine [175] in DMF.



α -Pinene oxide (316 μ L, 2.0mmol, 1eq) was added to a stirred solution of *N*-(2-methyl)-propanoyl glycine [175] (29.0mg, 0.2mmol, 0.1eq) in DMF (8.5mL) and the reaction stirred at room temperature for 6days after which time over 80% starting material remained. The reaction was repeated at 80°C for 6days and in the presence of MgCl (0.1eq) or ZnCl (0.1eq) and in all cases only starting material α -pinene oxide was recovered.

8.1.2 Reaction of α -pinene oxide [89] with *N*-(2-methyl)-propanoyl glycine [175] in Methanol.



α -Pinene oxide (316 μ L, 2.0mmol, 1eq) was added to a stirred solution of *N*-(2-methyl)-propanoyl glycine [175] (29.0mg, 0.2mmol, 0.1eq) in methanol (8.5mL) and the reaction stirred at room temperature for 24h to afford campholenic aldehyde [91] (28%), 1,1-dimethoxy-2-[(2,2,3)-trimethyl-3-cyclopenten-1-yl] ethane [128] (6.2%), *trans*-carveol [92] (7.0%), 1,7,7-trimethyl-6-*exo*-methoxy bicyclo[2.2.1] heptan-2-*endo*-ol [128] (13%), and *trans*-2-methyl 5(1-methoxy, 1-methylethyl)-2-cyclohexen-1-ol [126] (42.3%).

Spectra as previous.

8.2. REACTIONS OF POLYACRYLAMIDE MIP [G].

8.2.1 Reaction of polyacrylamide [G] 2:1, 1/10. with α -pinene oxide [89] in DMF.

α -pinene oxide (95 μ L, 0.6mmol, 1eq) was added to a stirred suspension of polyacrylamide [G] (1.20mg, 0.6mmol, 1.0eq) in DMF (2.5mL) and the reaction stirred at room temperature for 24h after which time over 80% starting material remained.

8.2.2. Reaction of Polyacrylamide [G] 2:1, 1/10. with α -pinene oxide [89] in methanol.

α -pinene oxide (990 μ L, 6.3mmol, 1eq) was added to a stirred solution of polyacrylamide [G] (1.75g, 0.63mmol, 0.1eq) in methanol (26.6mL) and the reaction

stirred at room temperature for 24h to afford campholenic aldehyde [91] (24%), 1,1-dimethoxy-2-[(2,2,3)-trimethyl-3-cyclopenten-1-yl] ethane [125] (8%), *trans*-carveol [92] (9%), 1,7,7-trimethyl-6-*exo*-methoxy bicyclo[2.2.1] heptan-2-*endo*-ol [128] (11%), and *trans*-2-methyl 5(1-methoxy, 1-methylethyl)-2-cyclohexen-1-ol [126] (42%).

Chapter 9. NMR STUDIES.

The maximum field strength of the gradient accessory 0.51T was determined according to standard procedure¹²⁶. The pulse program employed is shown in appendix 3.

9.1 Diffusion Edited NMR: The test system.

Sample Preparation

A solution of the four components, DL-isocitric lactone [161], (S)-(+)-*o*-acetylmandelic acid [162], methyl isobutyrate [163], and *t*-butyl propionate [164] in CDCl₃ was prepared so that the concentration of each individual component in the mixture was 10mM. A second solution with the four components and quinine [165] was prepared at the same concentrations.

Pulsed Field Gradient NMR studies on the test system.

Normal 1D spectra of all the samples were obtained before PFG experiments were performed. PFG NMR spectra were acquired using an LED pulse sequence (appendix 3).

The three variables listed below were changed in order to find the pulse field gradient conditions in which all the peaks in the 4 component mixture were suppressed after 64 scans were acquired. The best conditions found are listed below:

Diffusion delay (d2):	40ms
Gradient pulse width (p16):	2ms
Gradient field strength (cnst21):	50%

The five component sample was then run under the same conditions and the differences between the spectra were noted. The spectra are illustrated in chapter 7.

9.2 Diffusion measurements at pD 5.

10mM solutions of each peptide [153], [154], and [155] and also the TSA [151] in D₂O were prepared. The pD was adjusted to 5 using NaOD and DCl. Samples mixtures containing 1 peptide and the imprint molecule [151] were also made up so that the

concentration of each component was 10mM and the pD was adjusted to 5 using the same method as above.

A series of 22 1D ^1H NMRs were obtained for each of the above 7 samples. The conditions are shown in appendix 3. All parameters were fixed apart from the field gradient strength which was incremented according to a logarithmic scale from 3 to 66% (100% = 0.51T). A graph of $\text{Ln}I$ (I = integral intensity) against the square of the gradient strength was obtained for each resolved peak. The value for the slope of this graph CD was used to calculate the value of the observed translational diffusion rate for each compound, using the average over all resolved peaks. The results are tabulated in chapter 7. Measurements were taken with the following fixed variables: Temperature 300K, d3 40ms, d1 12s, d6 0.05ms, NS 64, d2 30ms, p11 -6db, p16 2ms.

The *N*-methyl resonance, a singlet at 3.2ppm, from the TSA [151] is particularly clear from the rest of the spectrum and can be easily integrated affording a low error. Using this peak for the plot of Ln integral intensity against gradient strength squared the values tabulated in chapter 7 table 11 were obtained.

9.3 Diffusion measurements at pD 7.

10mM solutions of peptide [155], TSA [151] and a 1:1 mixture of [155]:[151] in D_2O were prepared. the pD was adjusted to 7 using NaOD and DCl. A series of 22 1D ^1H NMRs were obtained for each of the three samples, using the same NMR parameters as described previously for the experiments at pD 5. The field gradient was incremented according to a logarithmic scale from 3 to 66% (100% = 0.51T) and a graph of $\text{Ln}I$ (I = integral intensity) was obtained. Using the peak at 3.2ppm, a singlet assigned to the *N*-methyl resonance, from the TSA [151] for the plot of Ln integral intensity against gradient strength squared the values tabulated in chapter 7 table 12 were obtained.

APPENDIX 1

APPENDIX 1

Calculation of the ratio of (1*R*, 5*R*)-*trans*-carvyl amine [93] to α -methyl benzylamine [111] bound in competitive binding study

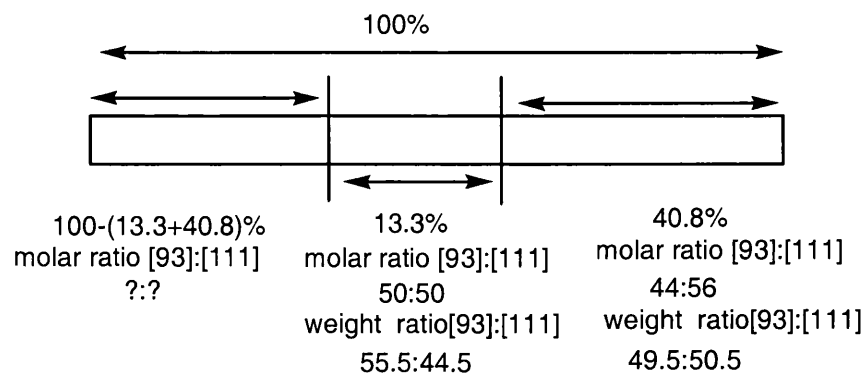
Experimental Extract:

Competitive binding study of polymer [D] Loading 1/15, crosslinker-monomer 2:1.

The polymer was regenerated according to the general method . The amount of DCM (8.0mL) absorbed by the polymer was determined. (1*R*, 5*R*)-*trans*-carvyl amine [93] (53.3mg, 0.35mmol, 1eq) and α -methyl benzylamine [111] (42.7mg, 0.35mmol, 1eq) were used in the competitive binding study. The ratio of the amines left in solution (1*R*, 5*R*)-*trans*-carvyl amine [93]: α -methyl benzylamine [111] was 44:56 (total weight 39.2mg). The ratio of the amines extracted from the polymer was (1*R*, 5*R*)-*trans*-carvyl amine [93]: α -methyl benzylamine [111] 57:43.

MIP	[D]*
initial weight of [93] /mg, 1eq	53.3
initial weight of [111]/mg, 1eq	42.7
total weight at the beginning of the experiment/mg %	96.0 100%
total weight remaining in solution after 15h/mg	39.2 45%
molar ratio [93]:[111] in solution after 15h	44:56
solvent absorbed by polymer/mL	8.0
% bound due to non specific binding	$100 \times (8.0/60) = 13.3\%$
Molar ratio [93]:[111] extracted from polymer	57:43

The percentage weight bound can be easily calculated from the % remaining in solution and the percentage bound non specifically.



The unknown ratio bound [93]:[111], x:y can be calculated using the information above and the weight of each compound at the beginning of the experiment.

(1*R*, 5*R*)-*trans*-carvyl amine [93] bound :

$$= 53.3 - [(0.133 \times 0.555 \times 96.0) + (0.408 \times 0.495 \times 96.0)]$$

$$= 26.8\text{mg} \quad (0.178\text{mmol})$$

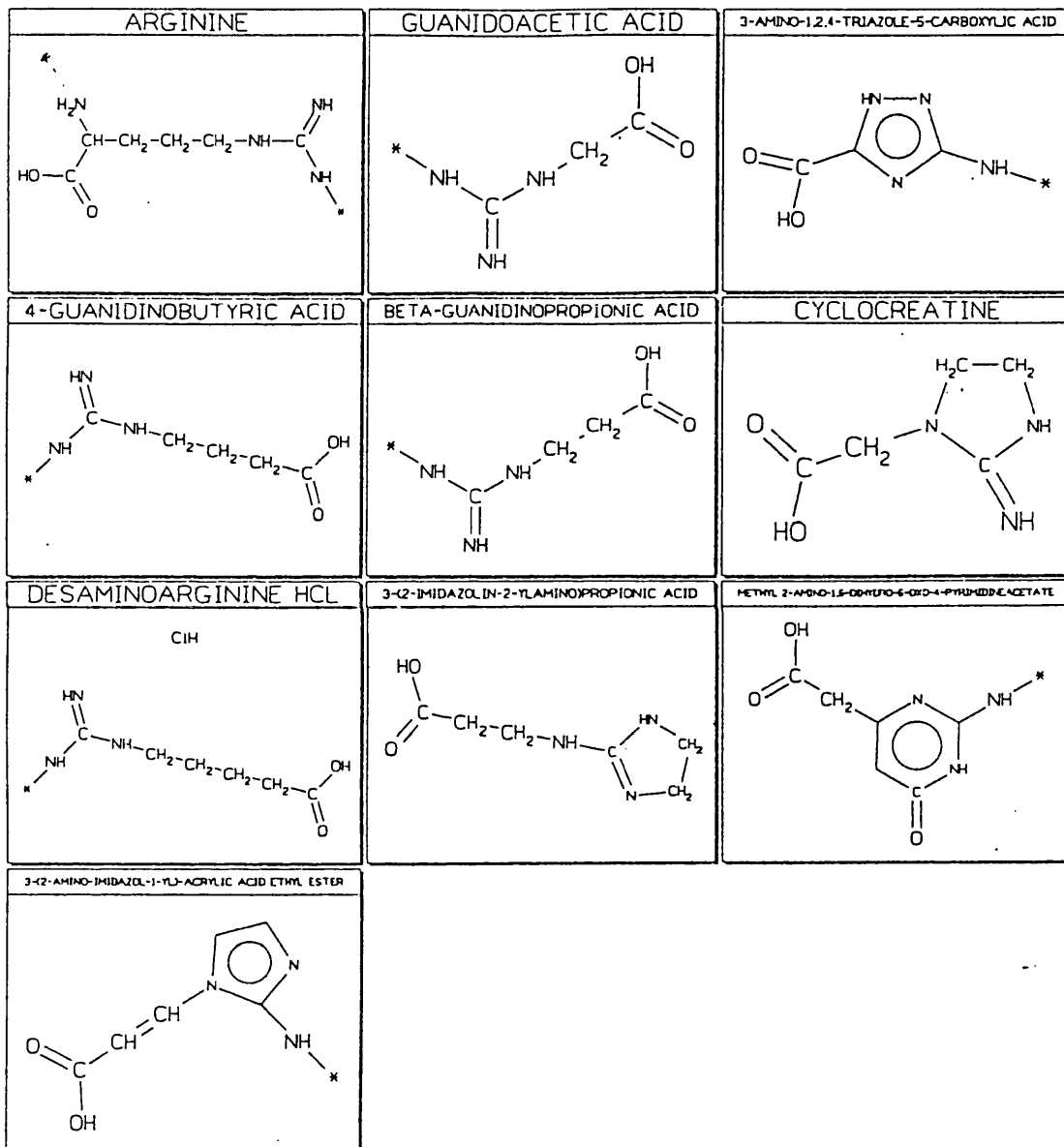
α -methyl benzylamine [111] bound :

$$= 42.7 - [(0.133 \times 0.445 \times 96.0) + (0.408 \times 0.505 \times 96.0)]$$

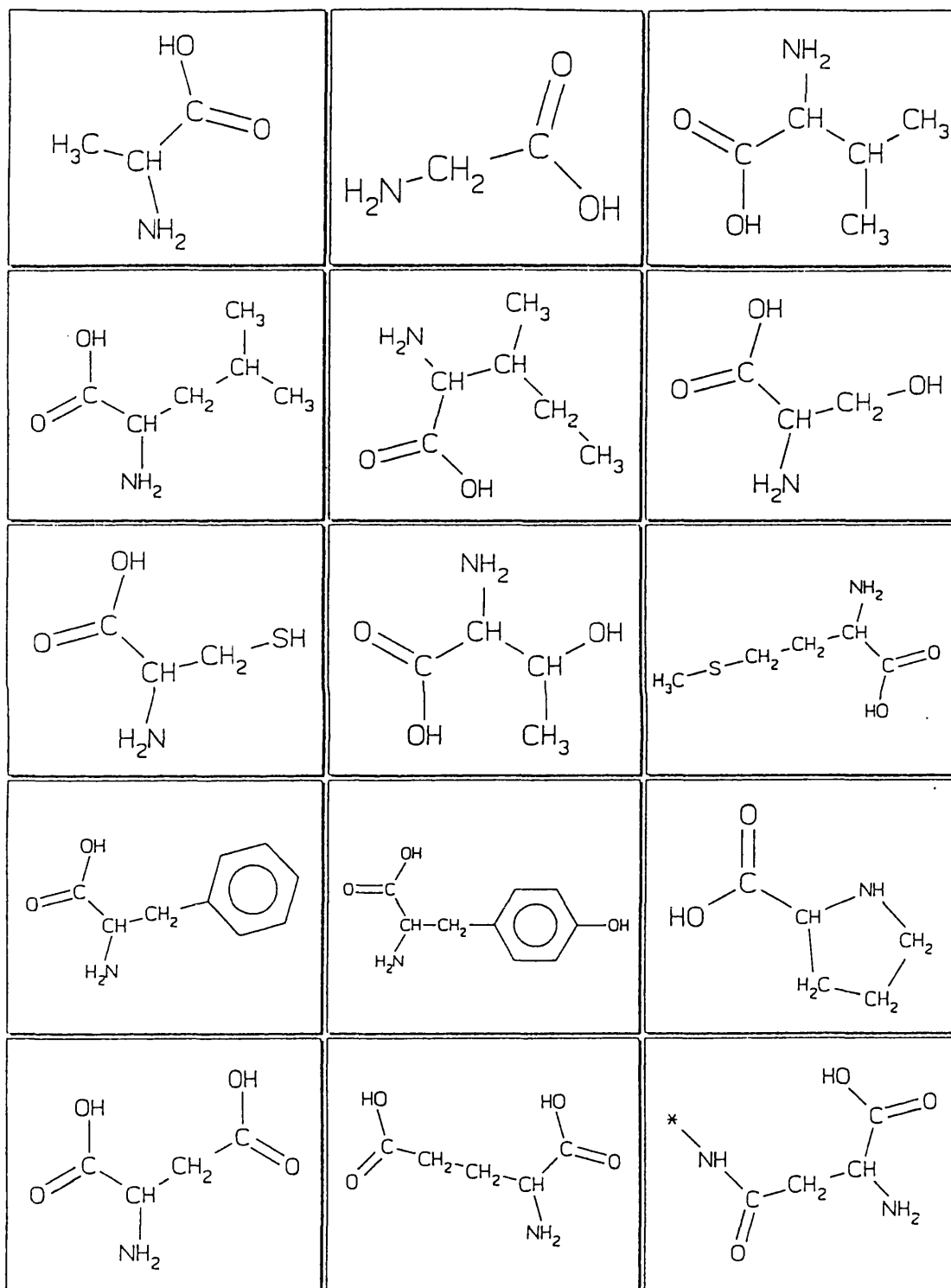
$$= 17.2\text{mg} \quad (0.142\text{mmol})$$

Therefore: Molar ratio bound [93]:[111] 56:44

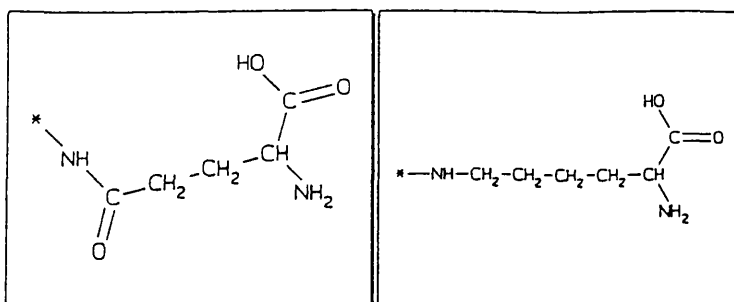
APPENDIX 2

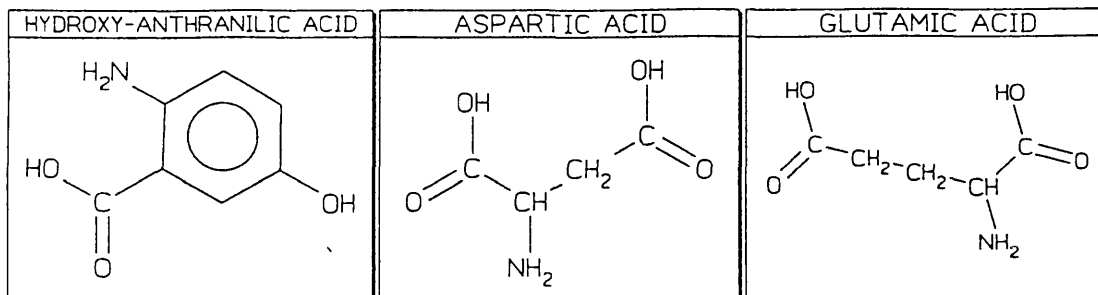
aa₁ Library members

aa₂ Library members

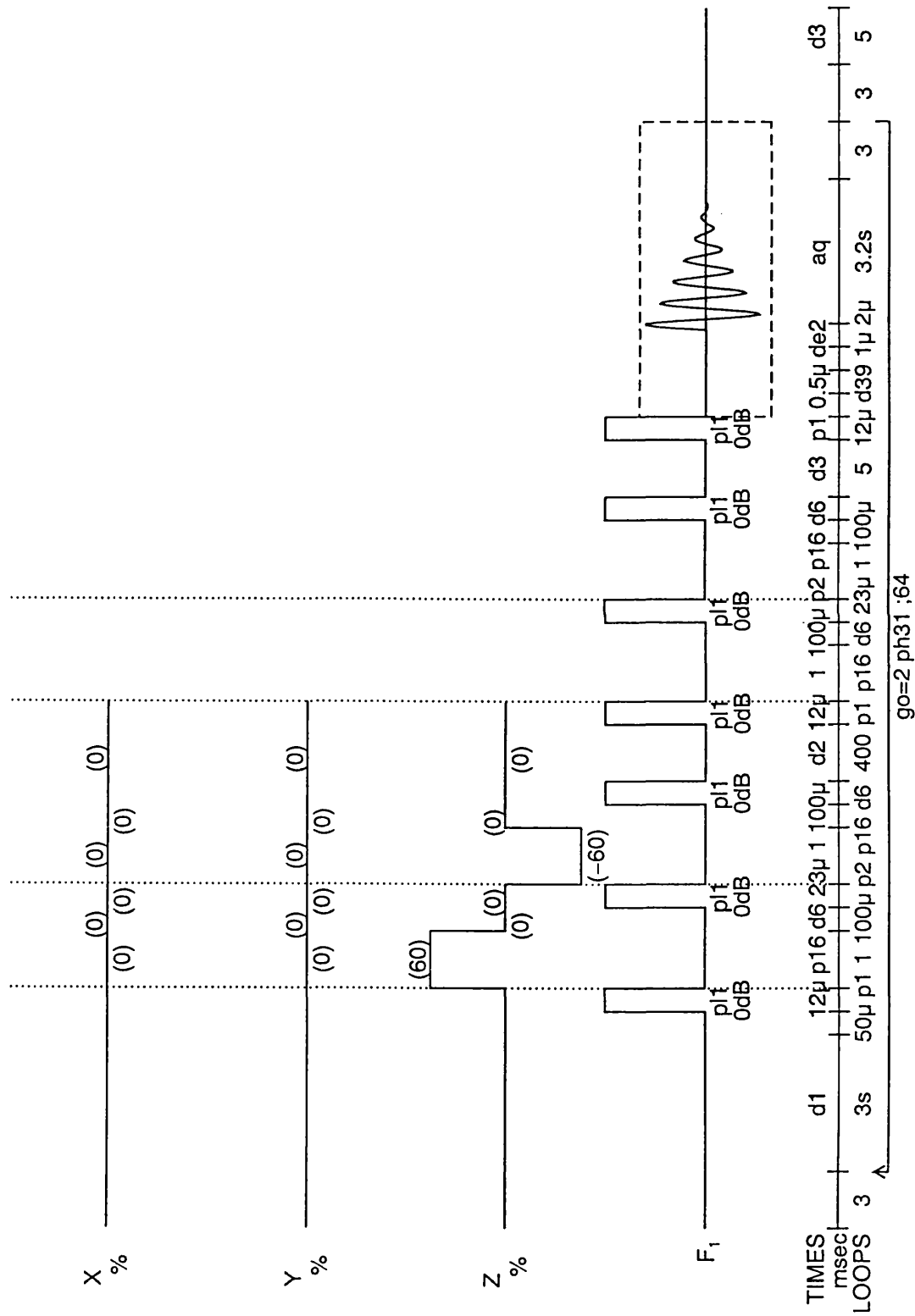


aa₂ Library members



aa₃ Library members

APPENDIX 3



REFERENCES

REFERENCES

1. Pauling, L., *J. Am. Chem. Soc.*, **1940**, 62, 2643.
2. Breslow, R.; Dong, S. D., *Chem. Rev.*, **1998**, 98, 1997.
3. a) Schultz, P. G.; Lerner, R. A., *Science*, **1995**, 269, 1835. b) Schultz, P.G.; Lerner, R. A. *Acc. Chem. Res.*, **1993**, 26, 391.
4. Menger, F. M., *Biochemistry*, **1992**, 31, 5368.
5. Mader, M. M.; Bartlett, P. A., *Chem. Rev.*, **1997**, 97, 1281.
6. Lemieux, R. U., *Acc. Chem. Res.*, **1996**, 29, 373.
7. Dunitz, J. D., *Science*, **1994**, 264, 670.
8. Williams, D. H.; Searle, M. S.; Mackay, J. P.; Gerhard, U.; Maplestone, R., *Proc. Natl. Acad. Sci. USA*, **1993**, 90, 1172.
9. Fersht, A. R.; Shi, J-P.; Knill-Jones, J.; Lowe, D. A.; Wilkinson, A. J.; Blow, D. M.; Brick, P.; Carter, P.; Waye, M. M. Y.; Winter, G., *Nature*, **1985**, 314, 235.
10. Street, I. P.; Armstrong, C. R.; Withers S. G., *Biochemistry*, **1986**, 25, 6021.
11. Teague, S. J.; Davis, A. M., *Angew. Chem. Int. Ed. Engl.*, **1999**, 38, 736.
12. Garcia-Tellado, F.; Goswami, S.; Chang, S-K.; Geib, S. J.; Hamilton, A. D., *J. Am. Chem. Soc.*, **1990**, 112, 7393.
13. Fan, A.; Van Arman, S. A.; Kincaid, S.; Hamilton, A. D., *J. Am. Chem. Soc.*, **1993**, 115, 369.
14. Rockwell, A.; Melden, M.; Copeland, R. A.; Hardman K.; Decicco, C. P.; DeGrado, W. D., *J. Am. Chem. Soc.*, **1996**, 118, 10337.
15. Ma, J. C.; Dougherty, D. A., *Chem. Rev.*, **1997**, 97, 1303.
16. Kirby, A., *Angew. Chem. Int. Ed. Engl.*, **1996**, 35, 707.
17. Hruby, V. J.; Li, G. G.; Haskwell-Luevano, C.; Shenderovich, M.; *Biopolymers*, **1997**, 43, 219.
18. a) Breslow, R.; Schmuck, C., *J. Am. Chem. Soc.*, **1996**, 118, 6601. b) Breslow, R.; Anslyn E., *J. Am. Chem. Soc.*, **1989**, 111, 8931.
19. Breslow, R.; Zhang, B., *J. Am. Chem. Soc.*, **1992**, 114, 5882.
20. Breslow, R.; Zhang, X.; Huang, Y., *J. Am. Chem. Soc.*, **1997**, 119, 4535.
21. a) Diederich, F.; Habicher, T., *Helv. Chim. Acta.*, **1999**, 82, 1066. b) Diederich, F.; Mattei, P., *Helv. Chim. Acta.*, **1997**, 80, 1555.

-
22. Diederich, F.; Jiminez, L.; Chang, S.-W. T., *Helv. Chim. Acta.*, **1993**, *76*, 2639.
23. Kang, J.; Santamaria, J.; Hilmersson, G.; Rebek Jr., J., *J. Am. Chem. Soc.*, **1998**, *120*, 7389.
24. Lauschat, S., *Angew. Chem. Int. Ed. Engl.*, 1996, *35*, 289.
25. Rebek Jr., J., *Acc. Chem. Res.*, **1999**, *32*, 278.
26. a) Kang, J.; Rebek Jr., J., *Nature*, **1997**, *385*, 50. b) Kang, J.; Hilmerson, G.; Santamaria, J.; Rebek Jr., J., *J. Am. Chem. Soc.*, **1998**, *120*, 3650.
27. see 15 for leading references.
28. a) Sanders, J. K. M.; Anderson, H. L.; Walter, C. J., *J. Chem. Soc., Chem Commun.*, **1993**, 458. b) Marty, M.; Clyde-Watson, Z.; Twyman, L.J.; Nakash, M.; Sanders, J. K. M., *J. Chem. Soc., Chem. Commun.*, **1998**, 2265.
29. Tramontano, A.; Janda, K. D.; Lerner, R. A., *Science*, **1986**, *234*, 1566.
30. Pollack, S. J.; Jaobs, J. W.; Schultz, P.G., *Science*, **1986**, *234*, 1570.
31. Hilvert, D.; Hill, K. W.; Narel, K. D.; Auditor, M.-T. M., *J. Am. Chem. Soc.*, **1989**, *111*, 9261.
32. Li, T.; Janda, K. D.; Ashley, J. A.; Lerner, R. A., *Science*, **1994**, *264*, 1289.
33. Hasserodt, J.; Janda, K. D.; Lerner, R. A., *J. Am. Chem. Soc.*, **1997**, *119*, 5993.
34. Hasserodt, J.; Janda, K. D.; Lerner, R. A., *J. Am. Chem. Soc.*, **1996**, *118*, 11654.
35. Li, T.; Janda, K. D.; Lerner, R. A., *Nature*, **1996**, *379*, 326.
36. Romesberg, F. E.; Flanagan, M. E.; Uno, T.; Schultz, P.G., *J. Am. Chem. Soc.*, **1998**, *120*, 5160.
37. Driggers, E. M.; Cho, H. S.; Lui, C. W.; Katzka, C. P.; Braisted, A.C.; Ulrich, H. D.; Wemmer, D. E.; Schultz, P. G., *J. Am. Chem. Soc.*, **1998**, *120*, 1945.
38. Zhou, Z. S.; Flohr, A.; Hilvert, D., *J. Org. Chem.*, **1999**, *64*, 8334.
39. Stewart, J. D.; Liotta, L. J.; Benkovic, S. J., *Acc. Chem. Res.*, **1993**, *26*, 396.
40. Barbas, C. F.; Heine, A.; Zhong, G.; Hoffmann, T.; Gramatikova, S.; Bjornestedt, R.; List, B.; Anderson, J.; Stura, E. A.; Wilson, I. A.; Lerner, R. A., *Science*, **1997**, *278*, 2085.
41. a) Morris, A. J.; Tolan, D. R.; *Biochemistry*, **1994**, *33*, 12291. b) Lai, C. Y.; Nakai, N.; Chang, D.; *Science*, **1974**, *183*, 1204.
42. Gao, C.; Lavey, B. J.; Lo, C-H. L.; Datta, A.; Wentworth Jr., P.; Janda, K. D., *J. Am. Chem. Soc.*, **1998**, *120*, 2211.

-
43. a) Yu, J.; Choi, S. Y.; Lee, S.; Yoon, H. J.; Jeong S.; Mun, H.; Park, H.; Schultz, P. G., *J. Chem. Soc., Chem. Commun.*, 1997, 1957, b) Frederiksson, U. B.; Fagerstam, L. G.; Cole, A. W. G.; Lundgreb, T.; "Protein A-Sepharose C1-4B Affinity Purification of Ig G Monoclonal Antibodies" Pharmacia, Uppsala, Sweden, 1986.
44. a) Cormack, P. A. G.; Mosbach, K. *Reac. and Func. Polymers*, **1999**, *41*, 115. b) Wulff, G. *Angew. Chem. Int. Ed. Engl.* **1995**, *34*, 1812.
45. Beach, J. V.; Shea, K. J., *J. Am. Chem. Soc.*, **1994**, *116*, 379.
46. Matsui, J.; Nicholls, I. A.; Karube, I.; Mosbach, K., *J. Org. Chem.*, **1996**, *61*, 5414.
47. Robinson, D. K.; Mosbach, K., *J. Chem. Soc., Chem. Commun.*, **1989**, 969.
48. Ohkubo, K.; Urata, Y.; Hirota, S.; Honda, Y.; Sagawara, T., *J. Molecular Catalysis*, **1994**, *87*, L21.
49. Toorisaka, E.; Yoshida, M.; Veza, K.; Goto, M.; Furusaki, S., *Chem. Lett.*, **1999**, 387.
50. Wulff, G.; Gross, T.; Schonfeld, R., *Angew. Chem. Int. Ed. Engl.*, **1997**, *36*, 1962.
51. Liu, X-C.; Mosbach, K., *Macromol. Rapid Commun.*, **1997**, *18*, 609.
52. Liu, X-C.; Mosbach, K., *Macromol. Rapid Commun.*, **1998**, *19*, 671.
53. Ye, L.; Ramstrom, O.; Mansson, M-O.; Mosbach, K., *J. Molecular Recognition*, **1998**, *11*, 75.
54. Nagayusa, T.; Tanaka, T.; Sakiyama, T.; Nakanishi, K., *Biotechnol. Bioeng.*, **1994**, *43*, 1108.
55. Bystrom, S. E.; Borje, A.; Akermark, B., *J. Am. Chem. Soc.*, **1993**, *115*, 2081.
56. Alexander, C.; Smith, C. R.; Whitcombe, M. J.; Vulfson, E. V., *J. Am. Chem. Soc.*, **1999**, *121*, 6640.
57. Suh, J.; Hah, S.S., *J. Am. Chem. Soc.*, **1998**, *120*, 10088.
58. a) Bryant, R. A. R.; Hansen, D. A.; *J. Am. Chem. Soc.*, **1996**, *118*, 4598. b) Rudzicka, A.; Wolfenden, R.; *J. Am. Chem. Soc.*, **1996**, *118*, 6105.
59. Jang, B. B.; Lee, K-P.; Min, D-H.; Suh, J., *J. Am. Chem. Soc.*, **1998**, *120*, 12008.
60. Liu, J.; Luo, G.; Gao, S.; Zhang, K.; Chen, X.; Shen, J., *J. Chem. Soc., Chem. Commun.*, **1999**, 199.
61. Ohya, Y.; Miyaoka, J.; Ouchi, T., *Macromol. Rapid. Commun.*, **1996**, *17*, 871.

-
62. a) Gordon, E. M.; Kerwin, J. F. *Combinatorial Chemistry and Molecular Diversity in Drug Design*, John Wiley&Sons, 1998. b) Wilson, S. R.; Czarnik, A. W. *Combinatorial Chemistry: Synthesis and Applications*, John Wiley&Sons, 1997.
63. Menger, F. M.; West, C. A.; Ding, J., *J. Chem. Soc., Chem. Commun.*, **1997**, 633.
64. Menger, F. M.; Eliseev, A. V.; Mingulin, V. A., *J. Org. Chem.*, **1995**, *60*, 6666.
65. Menger, F. M.; Ding, J.; Barragan, V., *J. Org. Chem.*, **1998**, *63*, 7578.
66. a) Gilbertson, S. R.; Wong, X., *Tetrahedron Lett.*, 1996, *37*, 6475. b) Gilbertson, S. R.; Wong, X., *J. Org. Chem.*, **1996**, *61*, 434.
67. Krueger, C. A.; Kuntz, K. W.; Dzierba, C. D.; Wirschun W. G.; Gleason, J. D.; Snapper, M. L.; Hoveyda, A. H., *J. Am. Chem. Soc.*, **1999**, *121*, 4284.
68. a) Jandeleit, B.; Schaefer, D. J.; Powers, T. S.; Turner, H. W.; Weinberg, W. H., *Angew. Chem. Int. Ed. Engl.*, **1999**, *38*, 2494. b) Bein, T., *Angew. Chem. Int. Ed. Engl.*, **1999**, *38*, 323. c) Shimazu, K. D.; Snapper, M. L.; Hoveyda, A. H., *Chem. Eur. J.*, **1998**, *4*, 1885. d) Gennari, C.; Nestler, H. P.; Piarulli, U.; Salom, B., *Leibigs Ann./Recueil*, **1997**, 637.
69. Reviews and leading references on *in vitro* evolution: a) Bornscheuer, U. T., *Angew. Chem. Int. Ed. Engl.*, **1998**, *37*, 3105. b) Kuchner, O.; Arnold, F. H., *Tibtech*, **1997**, *15*, 523.
70. Reetz, M. T.; Zonta, A.; Shimossek, K.; Liebeton, K.; Jaeger, K-E., *Angew. Chem. Int. Ed. Engl.*, **1997**, *36*, 2831.
71. Pederson, H.; Holder, S.; Sutherland, D. P.; Schwitter, U.; King, D. S.; Schultz, P. G., *Proc. Natl. Acad. Sci. USA*, **1998**, *95*, 10523.
72. Lui, D.; Schultz, P., *Angew. Chem. Int. Ed. Engl.*, **1999**, *38*, 36.
73. Taylor, S. J.; Morken, J. P., *Science*, **1998**, *280*, 267.
74. For a general text: Gaussorges, G. "Infrared Thermography" Chapman & Hall, London, 1994.
75. Cooper, A. C.; McAlexander, L. H.; Lee, D.-H.; Torres, M. T.; Crabtree, R. H., *J. Am. Chem. Soc.*, **1998**, *120*, 9971.
76. Reetz, M. T.; Becker, M. H.; Kuling, K. M.; Holzworth, A., *Angew. Chem. Int. Ed. Engl.*, **1998**, *37*, 2647.
77. a) Davies, M.; Bonnat, M.; Guilier, F.; Kilburn, J. D.; Bradley, M., *J. Org. Chem.*, **1998**, *63*, 8696. b) Lowik, D. W. P. M.; Weingarten, M. D.; Broekema, M.;

- Brouwer, A. J.; Liskamp, R. M. J.; Still, W. C., *Angew. Chem. Int. Ed. Engl.*, **1998**, *37*, 1847. c) Bonnat, M.; Bradley, M.; Kilburn, J. D., *Tetrahedron Lett.*, **1996**, *37*, 5409. d) Still, W. C., *Acc. Chem. Res.*, **1996**, *29*, 155. e) Wennemers, H.; Yoon, S. S.; Still, W. C., *J. Org. Chem.*, **1995**, *60*, 1108.
78. Polyakov, V. A.; Neelen, M. I.; Nazapack-Kandlousy, N.; Ryabov, A. D.; Eliseev, A. V., *J. Phys. Org. Chem.*, **1999**, *12*, 357.
79. Cousins, G. R. L.; Poulsen, S.-A.; Sanders, J. K. M., *J. Chem. Soc. Chem. Commun.*, **1999**, 1575.
80. Huc, I.; Lehn, J.-M., *Proc. Natl. Acad. Sci. USA.*, **1997**, *94*, 2106.
81. Lehn, J.-M., *Chem. Eur. J.*, **1999**, *5*, 2455.
82. Giger, T.; Wigger, M.; Audetat, S.; Benner, S. A., *Synlett*, **1998**, 688.
83. a) Rowan, S. J.; Lukeman, P. S.; Reynolds, D. J.; Sanders, J. K. M., *New J. Chem.*, **1998**, 1015. b) Rowan, S. J.; Sanders, J. K. M., *J. Chem. Soc. Chem. Commun.*, **1997**, 1407.
84. Hamilton, P. G.; Feeder, N.; Teat, S. J.; Sanders, J. K. M.; *New J. Chem.*, **1998**, 1019.
85. Swann, P. G.; Casanova, R. A.; Desai, A.; Frauenhoff, M. M.; Urbancic, M.; Somczynska, U.; Hopfinger, A. J.; Le Breton, G. C.; Venton, D. L., *Biopolymers*, **1996**, *40*, 617.
86. For a recent review on thermodynamically driven selection in combinatorial chemistry: Ganesan, A., *Angew. Chem. Int. Ed. Engl.*, 1998, *37*, 2828.
87. Hioki, H.; Still, W. C., *J. Org. Chem.*, **1998**, *63*, 904.
88. Eliseev, A. V.; Nelen, M. I., *Chem. Eur. J.*, **1998**, *4*, 825.
89. Wulff, G., *Angew. Chem. Int. Ed. Engl.*, **1995**, *34*, 1812.
90. Sherrington, D. C., *J. Chem. Soc. Chem. Commun.*, **1998**, 2275.
91. Dunkin, I. R.; Lenfeld, J.; Sherrington, D. C., *Polymer*, **1993**, *34*, 77.
92. Cheikh, R. B.; Chaabouni, A.; Laurent, A.; Mison, P.; Nafti, A., *Synthesis*, **1983**, 685.
93. Andersson, H. S.; Karlsson, J. G.; Piletsky, S. A.; Koch-Schmidt, A.-C.; Mosbach, K.; Nicholls, I. A., *J. Chromatog. A.*, **1999**, *848*, 39.
94. a) Kempe, M.; Mosbach, K., *J. Chromatog. A.*, **1995**, *694*, 3. b) Ekberg, B.; Mosbach, K., *TIBTECH*, **1989**, *7*, 92.

-
95. Fischer, L.; Muller, R.; Ekberg, B.; Mosbach, K., *J. Am. Chem. Soc.*, **1991**, *113*, 9358.
96. Six, Y.; Motherwell, W. B., unpublished results.
97. Shea, J. K.; Sasaki, D. Y., *J. Am. Chem. Soc.*, **1989**, *111*, 3442.
98. Wilson, K.; Renson, A.; Clark, J. H., *Chem. Lett.*, **1999**, *61*, 51.
99. Kunkeler, P. J.; van der Waal, J. C.; Bremmer, J.; Zuurdeeg, B. J.; Downing, R. S.; van Bekkum, H., *Catalysis Lett.*, **1998**, *53*, 135.
100. Salakhutdinov, N. F.; Barkhash, V. A., *Russian Chem. Rev.*, **1997**, *66*, 343.
101. Joyasree, J.; Narayanan, C. S., *Bull. Chem. Soc. Jpn.*, **1995**, *68*, 89.
102. Kaminska, J.; Schwegler, M. A.; Hoefnagel, A. J., *Recl. Trav. Chim. Pays. Bas.*, **1992**, *111*, 432.
103. a) Piletski S. A.; Andersson, H. S.; Nicholls, I., *J. Molecular Recog.*, **1998**, *11*, 94.
b) Dauwe, C.; Sellergren, B., *J. Chromatog. A*, **1996**, *753*, 191.
104. Nicholls, I., *J. Molecular Recog.*, **1998**, *11*, 79.
105. Li, T.; Hilton, S.; Janda, K., *J. Am. Chem. Soc.*, **1995**, *117*, 3308.
106. Abe, I.; Rohmer, M.; Prestwich, G. D., *Chem. Rev.*, **1993**, *93*, 2189.
107. Janda, J. D.; Shevlin, C. G.; Lerner, R. A., *Science*, **1993**, *259*, 490.
108. Na, J.; Houk, K. N., *J. Am. Chem. Soc.*, **1996**, *118*, 9204.
109. Gray, A. P.; Platz, R. D.; Henderson, T. R.; Chang, T. C. P.; Takahashi, K.; Dretchen, K. L., *J. Med. Chem.*, **1988**, *31*, 807.
110. Freytag, H., 'Methoden der Organischen Chemie (Houben Weyl)' Georg Thieme Verlag, Stuttgart, 1958, 1/11, p190.
111. Shvo, Y.; Kaufman, E. D., *Tetrahedron*, **1972**, *28*, 573.
112. Shvo, Y.; Kaufman, E. D., *J. Org. Chem.*, **1981**, *46*, 2148.
113. Eliseev, A. E., *Current Opinion in Drug Discovery and Development*, **1998**, *1*, 106.
114. Dowden, J.; Edwards, P. D.; Flack, S. S.; Kilburn, J. D., *Chem. Eur. J.*, **1999**, *5*, 79.
115. For a review: Stilbs, P., *Progress in N. M. R. Spectroscopy*, **1987**, *19*, 1.
116. Lin, M.; Shapiro, M. J., *J. Org. Chem.*, **1996**, *61*, 7617.
117. Lin, M.; Shapiro, M. J.; Wareing, J. R., *J. Am. Chem. Soc.*, **1997**, *119*, 5249.
118. Hajduk, P. J.; Oejniczak, E. T.; Fesik, S. W., *J. Am. Chem. Soc.*, **1997**, *119*, 12257.
119. Chen, A.; Johnson Jr., C. S.; Lin, M.; Shapiro, M. J., *J. Am. Chem. Soc.*, **1998**, *120*, 9094.

-
120. Bleicher, K.; Lin, M.; Shapiro, M. J.; Wareing, J. R., *J. Org. Chem.*, **1998**, *63*, 8486.
121. Shapiro, M.; Chen, A., *J. Am. Chem. Soc.*, **1999**, *121*, 5338.
122. Shapiro, M. J.; Lin, M.; Versace, R.; Petter, R. C., *Tetrahedron Asymm.*, **1996**, *7*, 2169.
123. a) Motherwell, W. B.; Roberts, J. S., *J. Chem. Soc., Chem. Commun.*, **1972**, 328. b) House, H. O.; Lee, L. F., *J. Org. Chem.*, **1976**, *41*, 863.
124. Johnson Jr., C. S., *J. Magnetic Resonance, Series A*, **1993**, *102*, 214.
125. Lin, M.; Jayawickrama, D. A.; Rose, R. A.; DelViscio, J. A.; Larive, C. K., *Analytica Chimica Acta*, **1995**, *307*, 449.
126. Braun, S.; Kalinowski, H.-O.; Berger, S., '100 and More Basic NMR Experiments: A Practical Course.' V.C.H., 1996.
127. Shea, K. J.; Stoddard, G. J.; Shavelle, D. M.; Wukui, F.; Choate, R. M., *Macromol.*, **1990**, *23*, 4497.
128. Yu, C.; Mosbach, K., *J. Org. Chem.*, **1997**, *62*, 4057.
129. Yu, C.; Mosbach, K., *J. Molecular Recognition*, **1998**, *11*, 69.
130. Takano, S.; Inomata, K.; Ogasawara, K., *Chem. Lett.*, **1992**, 443.
131. Sen, S. E.; Roach, S. L.; *Synthesis*, **1995**, 756.
132. Coates, R.; Ho, Z.; *J. Org. Chem.*, **1996**, *61*, 1184.
133. Lopez, L.; Mele, G.; Fiandanese, R., *Tetrahedron*, **1994**, *50*, 9097.
134. Ravindranath, B.; Srinivas, P., *Tetrahedron*, **1983**, *39*, 3991.
135. Ohkuma, T.; Ikehira, H.; Ikayira, T.; Noyori, R., *Synlett*, **1997**, 467.
136. Sarin, V. K.; Kent, S. B. H.; Tam, J. P.; Merrifield, R. B., *Analytical Biochem.*, **1981**, *117*, 147.
137. Kaiser, E.; Colescott, R. L.; Bossinger, C. D.; Cook, P.I., *Analytical Biochem.*, **1970**, 595.
138. Grob, C. A.; Renk, E., *Helvetica Chimica Acta*, **1954**, *194*, 1672.
139. Koperina, A. W.; Klutcharova, M., *Bull. Chem. Soc. Fr.*, **1945**, 773.
140. Baldwin, J. E.; Kruse, L.I., *J. Chem. Soc., Chem Commun.*, **1977**, 233.